

CATALYSIS OF COAL GASIFICATION AT ELEVATED PRESSURE

W. P. Haynes, S. J. Gasior, and A. J. Forney

Bureau of Mines, U.S. Department of the Interior, Pittsburgh, Pa.

INTRODUCTION

The gasification of coal with steam and oxygen under elevated pressure is an essential step in the Bureau of Mines Synthane process for converting coal to synthetic pipeline gas. Use of a suitable catalyst or additive in the gasification step could conceivably improve the gasification of coal. Earlier investigators have catalyzed the gasification of coke and carbon with various additives and have demonstrated that some benefits would result from the catalysis of gasification at atmospheric pressure. Vignon (1), for example, showed that the percentage of methane in water gas made from coke can be increased significantly by addition of lime to the coke. Neumann, Kroger, and Fingas (2) demonstrated the feasibility of improving the gasification of graphite at 450° to 1,000° C through addition of K₂O, CuO, and other salts. Continuation of the studies by Kroger and Melhorn (3) indicated that addition of either 8 pct Li₂O or (8 pct K₂O + 3 pct Co₃O₄) to low-temperature coke increased steam decomposition at temperatures of 500° to 700° C. More recently, Kislykh and Shishakov (4) studied the effect of Fe(CO)₅, (Fe₂O₃ + CuCl₂), K₂CO₃, and NaCl upon fluid-bed gasification of wood charcoal at 750° C and atmospheric pressure. They found that sodium chloride was the most effective additive, accelerating gasification by 62 pct and increasing steam decomposition 2.5-fold.

The work on catalysis reviewed thus far does not include gasification at elevated pressures nor the use of volatile coals. The bench-scale work now reported compares the catalytic activity of various additives in the gasification of volatile coals with steam under pressure and studies other process parameters of interest such as gasification temperature, type of contact with the catalyst, degree of gasification, and repeated use of a catalyst. Results of pilot plant gasification tests using additives are also reported.

Bench-Scale Studies

The gasification tests were conducted in two bench-scale reactor units, units A and B. The units were essentially the same; each unit contained an electrically heated reactor constructed of a 21-in-long section of 3/4-in, schedule 160 pipe of type 321 stainless steel. The coal-additive charge was contained in the middle 6 in of the reactor to minimize the spread of bed temperatures. Alumina cylinders filled the void space at each end of the reactor. Three thermocouples were located in the 6-in reactor zone, 1/2 in, 3 in, and 5-1/2 in from the top of the zone. The maximum temperature occurred at the middle thermocouple and was considered the nominal temperature of the reaction. The top and bottom bed temperatures were generally within 35° C of the maximum temperature.

During a gasification test, the coal charge was gasified by steam, which was introduced by saturation of the nitrogen carrier gas.

Figure 1 shows a schematic flowsheet of a reactor unit and its auxiliary equipment: high-pressure gas supply, silica gel and charcoal purifiers, calibrated capillary meter as feed gas flow indicator, gas saturator to humidify the feed gas, condenser and trap for liquid product collection, and gasometer for metering and collecting of total product gas. Reactor pressure was controlled by a back-pressure regulator. Temperature of the gas saturation was controlled within $\pm 0.6^\circ \text{C}$ by a chromel-alumel thermocouple control system.

Analyses of dry product gases were done by mass spectrometer as well as gas chromatography. The liquid product about 95 pct water, was drained and weighed.

Coal Used

The coal charged in all the tests discussed in this report was a single batch of high-volatile bituminous coal (Bruceton, Pa.) that had been pretreated at 450°C with a steam-air mixture to destroy its caking quality. The pretreated coal was crushed and sieved to a particle size of 20 to 60 mesh. Proximate and ultimate analyses of the pretreated coal are shown in table 1 below, in weight percent:

TABLE 1. - Analyses of pretreated coal used for feedstock

Proximate		Ultimate	
Moisture	1.5	Hydrogen	3.9
Volatile	22.4	Carbon	74.3
Fixed carbon	65.5	Nitrogen	1.5
Ash	10.6	Oxygen	8.7
		Sulfur	1.0
		Ash	10.6

Standard Gasification Tests for Screening Additives

Standard gasification tests were conducted in units A and B to determine the effect of various additives upon rate of carbon gasification, rate of gas production, and other gasification parameters.

In unit A, the standard gasification tests using various catalysts were made at the selected operating conditions of 850°C , 300 psig, and 5.8 g/hr steam feed carried by $2,000 \text{ cm}^3 \text{ N}_2/\text{hr}$. The coal charge was 10 g plus 0.5 g of catalyst. All catalysts were either powders or crystals that were admixed with the coal except in the case of experiment 203. In experiment 203, a metal tubular insert was flame-spray coated with about 10 g of unactivated Raney nickel, then inserted in the coal bed. In experiment 200, the Raney nickel catalyst powder was activated or approximately 65 pct reduced by treatment with 2 pct sodium hydroxide solution. In the reduced activated state, the catalyst was dried, mixed with coal, and charged into the unit under an inert atmosphere of nitrogen.

Reaction time, at the desired reaction temperature, was held constant at 4 hrs. An additional heat-up time of about 40 min was needed to reach the desired reaction temperature. Steam flow was not started until bed temperature exceeded 200°C . Conditions in unit B were the same as in unit A except that the steam rate was slightly lower at 5.0 g/hr.

Generally, tests were conducted in triplicate or higher replication. The average deviations in carbon gasification rate determinations generally ranged from 1 to 5 pct.

The experimental results of the screening tests conducted in unit A are presented in tables 2a and 2b; and for unit B, are presented in tables 3a and 3b. The specific gas production rates and gasification rates presented are based on the approximate 4-hr reaction time at 850° C. The results indicate that methane production rates as well as carbon gasification rates can be increased significantly by admixing certain compounds with the coal feed.

The rate of carbon gasification for the uncatalyzed coal was about 10 pct higher in unit A than in unit B (experiment 167 vs 300). The slightly higher steam rate in unit A is suspected as the cause of the higher reaction rate. Because of this difference in absolute rates, the percent increases achieved in gasification rates and gas production rates due to additives were related only to rates obtained in the gasification of the uncatalyzed coal in the same unit. Shown in table 4 are the relative effects of 40 additives upon the production of methane and hydrogen; and shown in table 5 are their relative effects upon the production of carbon monoxide and the gasification of carbon. The additives are listed in decreasing order of percent increased production. The corresponding reactor unit used (either A or B) is also listed.

Table 4 shows that at standard test conditions, all the additives listed except $ZnBr_2$ increased methane production and that all the tested additives increased hydrogen production significantly. The sprayed Raney nickel catalyst increased methane production by 24 pct and was the most effective material for promoting methane production. The next three materials ranking highest in promoting methane production were $LiCO_3$, Pb_3O_4 , and Fe_3O_4 with respective methane increases of 21, 20, and 18 pct.

A comparison of the methanation activity of zinc oxide with that of zinc bromide indicates that the anion group of a catalyst can exert significant influence on the activity.

As shown in table 4, the alkali metal compounds proved to be among the best promoters of hydrogen production. The percent increase in hydrogen produced was 105, 83, 55, and 53 pct, respectively, with the addition of KCl , K_2CO_3 , $LiCO_3$, and $NaCl$. The sprayed Raney nickel was the third most effective promoter of hydrogen production yielding a hydrogen increase of 63 pct.

Table 5 shows that the alkali metal compounds K_2CO_3 , KCl , and $LiCO_3$ gave the greatest increase in carbon monoxide production as well as in carbon gasification; the increases ranged from 40 to 91 pct. The compound $NaCl$ provided a significant increase of 31 pct in carbon gasification but was much less effective in increasing the production of carbon monoxide (7-pct increase).

As shown in tables 2b and 3b, the unit heating values of the total product gases generally decreased as a result of mixing additives with the coal but, since the total gas make was increased, the total amount of fuel value produced as product gas increased.

Two methods of applying catalyst--by admixing with the coal or by coating the surface of an insert or carrier--may be compared in the case of unactivated Raney nickel catalyst (experiments 203 and 197).

TABLE 2a. - Specific rate of gas production when using various catalysts (Series A)

Test conditions - Unit A: Charge, 10 g pretreated Bruceton coal, 0.5 g catalyst; feed, 5.8 g H₂O/hr + 2000 std cc N₂/hr; approximately 4-hr duration; 300 psig; 850° C

Catalyst	Expt. No.	No. of test	Total dry gas production rate, N ₂ -free bases, std cc/hr/g coal charged	Specific production rate of constituent gases, std cc/hr/g coal charged							
				H ₂	CO	CO ₂	CH ₄	C ₂ H ₄	C ₂ H ₆	C ₃ H ₈	C ₃ H ₆
No catalyst	166	6	331	166	49.7	70.2	43.7	0.06	0.93	0.24	0.12
Raney nickel, unactivated:											
Sprayed	203	6	453	271	53.7	72.3	54.2	.12	.80	.22	.05
Mixed	197	3	414	216	52.1	95.5	49.1	--	1.19	.18	--
Raney nickel, activated											
Mixed	200	3	442	243	47.9	104.5	45.31	.10	0.84	.13	--
NaCl	209	3	471	254	53.0	115.5	47.6	.33	.55		
KCl	212	3	615	340	90.1	137.3	46.7	.07	.64	.33	.03
ZnO	215	3	440	232	52.2	104.4	50.0	.05	.92	.13	.13
NiCl ₂ ·6H ₂ O	216	3	442	237	51.7	103.6	48.4	.14	.82	.18	.16
NiSO ₄ ·6H ₂ O	217	3	420	220	48.0	102.9	48.0	.21	.78	.23	.05
K ₂ CO ₃	218	3	578	309	95.0	126.4	46.2	.31	.72	.22	.06
ZnBr ₂	219	3	418	224	53.9	96.2	42.6	.18	.79	.10	.08
SnO ₂	224	3	395	213	37.7	98.1	44.0	.15	.65	.33	.28
Fe	225	3	367	193	39.1	88.3	45.4	.09	.95	.38	.24

TABLE 2b. - Specific rate of liquid production, carbon gasification, and gaseous heating value production when using various catalysts (Series A)

Test conditions - Unit A: Charge, 10 g pretreated Brucecon coal, 0.5 g catalyst; feed, 5.8 g H₂O/hr + 2000 std cc N₂/hr; approximately 4-hr duration; 300 psig; 850° C

Catalyst	Expt. No.	Product liquid, g/hr/g coal charged	Carbon gasification rates, g/hr/g coal charged	Unit heating value N ₂ -free product gas, Btu/SCF	Gaseous heating value produced, Btu/hr/cu ft coal charged
No catalyst	167	.478	89 x 10 ⁻³	353	57,700
Raney nickel, unactivated:					
Sprayed	203	.472	98 x 10 ⁻³	359	80,254
Mixed	197	.501	106 x 10 ⁻³	336	68,712
Raney nickel, activated:					
Mixed	200	.489	107 x 10 ⁻³	322	70,258
NaCl	209	.506	117 x 10 ⁻³	318	74,032
KCl	212	.480	148 x 10 ⁻³	307	93,250
ZnO	215	.490	112 x 10 ⁻³	330	71,718
NiCl ₂ ·6H ₂ O	216	.493	110 x 10 ⁻³	328	71,716
NiSO ₄ ·6H ₂ O	217	.498	108 x 10 ⁻³	328	68,163
K ₂ CO ₃	218	.494	144 x 10 ⁻³	312	89,011
ZnBr ₂	219	.454	104 x 10 ⁻³	324	66,783
SnO ₂	224	.507	98 x 10 ⁻³	326	63,700
Fe	225	.517	94 x 10 ⁻³	339	61,500

TABLE 3a. - Specific rate of gas production when using various catalysts (Series B)

Test conditions - Unit B: Charge, 10 g pretreated Brucecon coal, 0.5 g catalyst; feed, 5.0 g H₂O/hr plus 2000 std cc N₂/hr; approximately 4-hr duration; 300 psig; 850° C

Catalyst	Expt. No.	No. of tests	Total dry gas production rate, N ₂ -free bases, std cc/hr/g coal charged	Specific production rate of constituent gases, std cc/hr/g coal charged							
				H ₂	CO	CO ₂	CH ₄	C ₂ H ₄	C ₂ H ₆	C ₃ H ₈	C ₃ H ₆
No. catalyst	300	3	297	147	37.7	69.9	40.8	0.18	0.72	0.20	0.24
Ca(OH) ₂	301	3	345	180	32.0	86.2	45.4	.09	.63	.12	.19
Ni ₂ O ₃	302	3	359	189	43.9	80.9	42.8	.07	.74	.73	.50
NiO	303	3	373	194	52.0	82.0	43.9	--	.94	.22	.29
Ni	304	3	366	189	53.6	76.6	46.2	.17	.46	.29	.27
Fe ₃ O ₄	305	3	380	195	60.3	78.0	45.6	.15	.49	.27	.22
CuO	306	3	385	201	56.3	79.9	46.8	.12	.52	.17	.07
MnO ₂	307	3	375	193	45.7	90.2	44.9	.10	.79	.10	.15
BaO	308	3	395	202	48.9	97.1	45.5	.13	.73	.15	.13
ZrO ₂	309	3	377	192	57.8	80.0	46.2	.12	.88	.05	.12
SrO	310	3	392	203	48.2	91.3	47.6	.15	.76	.15	.15
Bi ₂ O ₃	311	2	390	200	63.9	80.4	44.4	.19	.72	.15	.04
Sb ₂ O ₅	312	2	391	201	63.6	79.7	45.9	.19	.45	.15	.15
MgO	313	3	384	199	48.4	87.7	47.7	.18	.72	.30	.23
PbO ₂	314	3	400	210	52.7	89.1	47.7	.08	1.00	.18	.23
MoO ₃	315	3	380	202	45.0	86.6	45.5	.03	1.09	.30	.13
TiO ₂	316	3	380	197	48.9	85.7	47.2	.33	0.68	.13	.23
CrO ₃	317	3	378	194	52.5	84.4	46.1	.07	.79	.07	.15
LiCO ₃	318	3	439	228	64.9	95.9	49.2	.19	.57	.27	--
V ₂ O ₅	319	3	367	188	47.7	83.5	45.9	.12	.71	.20	.12
Cr ₂ O ₃	320	3	374	184	58.6	83.0	47.4	.57	.57	.10	.12
Pb ₃ O ₄	321	3	400	205	57.2	87.3	49.1	.13	.72	.15	.13
B ₂ O ₃	322	3	394	203	61.0	79.0	47.4	.05	1.59	1.32	.08
Al ₂ O ₃	323	3	380	196	54.6	82.2	46.7	.15	0.61	0.13	.09
CoO	324	4	383	201	48.6	87.0	45.4	.25	.43	.17	.7
Cu ₂ O	325	6	385	203	53.1	84.4	44.1	.28	.42	.14	.13

TABLE 3b. - Specific rate of liquid production, carbon gasification, and gaseous heating value production when using various catalysts (Series B)

Test conditions - Unit B: Charge, 10 g pretreated Brunetton coal, 0.5 g catalyst; feed, 5.0 g H₂O/hr plus 2000 std cc N₂/hr; approximately 4-hr duration; 300 psig; 850° C

Catalyst	Expt. No.	Product liquid, g/hr/g coal charged	Carbon gasification rates, g/hr/g coal charged	Unit heating value N ₂ -free product gas, Btu/SCF	Gaseous heating value produced, Btu/hr/cu ft coal charged
Ne catalyst	300	0.464	81 x 10 ⁻³	350	51,300
Ca(OH) ₂	301	.447	88 x 10 ⁻³	339	57,700
Ni ₂ O ₃	302	.439	92 x 10 ⁻³	344	60,960
NiO	303	.422	97 x 10 ⁻³	340	62,700
Ni	304	.413	96 x 10 ⁻³	349	63,100
Fe ₃ O ₄	305	.396	100 x 10 ⁻³	345	64,800
CuO	306	.418	99 x 10 ⁻³	344	65,500
MnO ₂	307	.406	98 x 10 ⁻³	333	61,700
BaO	308	.417	104 x 10 ⁻³	328	64,050
ZrO ₂	309	.405	99 x 10 ⁻³	344	64,200
SiO	310	.417	101 x 10 ⁻³	337	65,200
Bi ₂ O ₃	311	.415	102 x 10 ⁻³	340	65,500
Sb ₂ O ₅	312	.414	102 x 10 ⁻³	343	66,200
MgO	313	.391	100 x 10 ⁻³	342	64,900
PbO ₂	314	.397	103 x 10 ⁻³	339	67,000
MoO ₃	315	.438	96 x 10 ⁻³	339	63,800
TiO ₂	316	.364	99 x 10 ⁻³	342	64,200
CrO ₃	317	.398	99 x 10 ⁻³	340	63,400
LiCO ₃	318	.364	113 x 10 ⁻³	334	72,400
V ₂ O ₅	319	.402	96 x 10 ⁻³	341	61,900
Cr ₂ O ₃	320	.394	102 x 10 ⁻³	345	63,700
Pb ₃ O ₄	321	.410	105 x 10 ⁻³	342	67,600
B ₂ O ₃	322	.399	104 x 10 ⁻³	355	69,200
Al ₂ O ₃	323	.424	99 x 10 ⁻³	342	64,300
CoO	324	.355	98 x 10 ⁻³	336	63,800
Cu ₂ O	325	.363	98 x 10 ⁻³	336	63,900

TABLE 4. - Increase in the production of methane and hydrogen

Catalyst	Unit	Increase in CH ₄ , pct	Catalyst	Unit	Increase in H ₂ produced, pct
Raney nickel, unactivated spray	A	24	KCl	A	105
LiCO ₃	B	21	K ₂ CO ₃	A	83
Pb ₃ O ₄	B	20	Raney nickel unactivated spray	A	63
Fe ₃ O ₄	B	18	LiCO ₃	B	55
MgO	B	17	NaCl	A	53
PbO ₂	B	17	Raney nickel activated mix	A	46
SrO	B	17	NiCl ₂ ·6H ₂ O	A	43
TiO ₂	B	16	PbO ₂	B	43
Cr ₂ O ₃	B	16	ZnO	A	40
B ₂ O ₃	B	16	Pb ₃ O ₄	B	39
CuO	B	15	SrO	B	38
ZnO	A	14	B ₂ O ₃	B	38
Al ₂ O ₃	B	14	Cu ₂ O	B	38
Ni	B	13	CuO	B	37
ZrO ₂	B	13	BaO	B	37
Sb ₂ O ₅	B	13	Sb ₂ O ₅	B	37
CrO ₃	B	13	MoO ₃	B	37
V ₂ O ₅	B	13	CoO	B	37
Raney nickel unactivated mix	A	12	Bi ₂ O ₃	B	36
BaO	B	12	ZnBr ₂	A	35
MoO ₃	B	12	MgO	B	35
NiCl ₂ ·6H ₂ O	A	11	TiO ₂	B	34
Ca(OH) ₂	B	11	NiSO ₄ ·6H ₂ O	A	33
CoO	B	11	Fe ₃ O ₄	B	33
NiSO ₄ ·6H ₂ O	A	10	Al ₂ O ₃	B	33
MnO ₂	B	10	NiO	B	32
NaCl	A	9	CrO ₃	B	32
Bi ₂ O ₃	B	9	MnO ₂	B	31
NiO	B	8	ZrO ₂	B	31
Cu ₂ O	B	8	Raney nickel unactivated mix	A	30
KCl	A	7	Ni ₂ O ₃	B	29
K ₂ CO ₃	A	6	Ni	B	29
Ni ₂ O ₃	B	5	SnO ₂	A	28
Raney nickel activated mix	A	4	V ₂ O ₅	B	28
Fe	A	4	Cr ₂ O ₃	B	25
SnO ₂	A	1	Ca(OH) ₂	B	22
ZnBr ₂	A	-3	Fe	A	16

TABLE 5. - Increase in production of carbon monoxide and gasification of carbon

<u>Catalyst</u>	<u>Unit</u>	<u>Increase in CO produced_pct</u>	<u>Catalyst</u>	<u>Unit</u>	<u>Increase in carbon gasi- fied, pct</u>
K ₂ CO ₃	A	91	KCl	A	66
KCl	A	81	K ₂ CO ₃	A	62
LiCO ₃	B	72	LiCO ₃	B	40
Bi ₂ O ₃	B	69	NaCl	A	31
Sb ₂ O ₅	B	69	Pb ₃ O ₄	B	30
B ₂ O ₃	B	62	BaO	B	28
Fe ₃ O ₄	B	60	B ₂ O ₃	B	28
Cr ₂ O ₃	B	55	PbO ₂	B	27
ZrO ₂	B	53	Bi ₂ O ₃	B	26
Pb ₃ O ₄	B	52	Cr ₂ O ₃	B	26
CuO	B	49	Sb ₂ O ₅	B	26
Al ₂ O ₃	B	45	ZnO	A	26
Ni	B	42	SrO	B	25
Cu ₂ O	B	41	NiCl ₂ ·6H ₂ O	A	24
PbO ₂	B	40	MgO	B	23
CrO ₃	B	39	Fe ₃ O ₄	B	23
NiO	B	38	CuO	B	22
BaO	B	30	ZrO ₂	B	22
TiO ₂	B	30	TiO ₂	B	22
CoO	B	29	CrO ₃	B	22
MgO	B	28	Al ₂ O ₃	B	22
V ₂ O ₅	B	27	NiSO ₄ ·6H ₂ O	A	21
MnO ₂	B	21	MnO ₂	B	21
MoO ₃	B	19	CoO	B	21
Ni ₂ O ₃	B	16	Cu ₂ O	B	21
SrO	B	15	Raney nickel		
Raney nickel, un- activated spray	A	8	activated mix	A	20
ZnBr ₂	A	8	NiO	B	20
NaCl	A	7	Raney nickel		
Raney nickel, un- activated mix	A	5	unactivated mix	A	19
ZnO	A	5	Ni	B	19
NiCl ₂ ·6H ₂ O	A	4	MoO ₃	B	19
NiSO ₄ ·6H ₂ O	A	-3	V ₂ O ₅	B	19
Raney nickel			ZnBr ₂	A	17
activated mix	A	-4	Ni ₂ O ₃	B	14
Ca(OH) ₂	B	-15	Raney nickel, un- activated spray	A	10
Fe	A	-21	SnO ₂	A	10
SnO ₂	A	-24	Ca(OH) ₂	B	9
			Fe	A	6

Admixing of the catalyst with the coal provides better contact between coal and catalyst than does the insertion of catalyzed surfaces into the bed of coal. The superior contact achieved by admixing the catalyst and coal is proven by the higher specific rate of carbon gasification obtained by the admixed Raney nickel (unactivated) in experiment 197 over that of sprayed Raney nickel (unactivated) in experiment 203 (tables 2a and 2b). This is further confirmed analytically by the larger amount of carbon left in the residue in the case of the sprayed Raney nickel catalyst.

Table 2a indicates that the Raney nickel (unactivated) catalyst was more effective in promoting methane production when sprayed on a surface than when it was admixed with the coal charge. Apparently, the process of methane synthesis from CO and H₂ was more effectively promoted by the sprayed Raney nickel (unactivated) catalyst. Another possible reason for the greater production of methane in the case of the sprayed Raney nickel (unactivated) catalyst is that the poorer contact between coal and catalyst resulted in less reforming of methane and other hydrocarbons. Hydrogen production was also greater when the sprayed Raney nickel (unactivated) catalyst was used than when Raney nickel (unactivated) was admixed with the coal.

Effect of Temperature and Steam Rate

Gasification experiments similar to the standard tests were conducted in unit A, except that the reaction temperatures were varied from 650° to 950° C and steam rates used were 1.16 and 5.8 g/hr. The catalyst used was flame-sprayed Raney nickel 65 pct activated. Also, tests were conducted at 750° C and 1.16 g/hr steam rate with sprayed Raney nickel activated and charged wet and at 850° C, and 5.8 g/hr steam rate with sprayed Raney nickel unactivated.

Results of these experiments are presented in figures 2, 3, 4, 5, and 6, where rates of production of methane, hydrogen, carbon monoxide, carbon gasification, and production of total dry gas, respectively, are shown. At the temperatures and steam rates shown in these figures, the presence of the sprayed Raney nickel insert has resulted in a higher production of nearly all the major gases and in a higher carbon gasification than that achieved without catalysts. One exception is in the case of methane production with the activated sprayed Raney nickel at 850° and 950° C for 5.8 g/hr steam rate (fig. 2), when methane production was greater for the uncatalyzed reaction than for the catalyzed reaction. However, a 6-pct increase in methane production was achieved at 850° C and 5.8 g/hr steam rate when the unactivated sprayed Raney nickel was used as compared to when no catalyst was used (fig. 2). The other exception is in the production of carbon monoxide at 950° C and 1.16 g/hr steam rate (fig. 4). In this case, carbon monoxide production was 5 pct lower for the catalyzed reaction than for the uncatalyzed reaction.

In general, effectiveness of the catalyst decreases as temperature is increased. For example, the increases achieved in carbon gasification and in total gas production due to the use of catalyst became smaller as the reaction temperature increased from 750° to 950° C (Figs. 5 and 6). In the 5.8 g/hr steam rate tests, the carbon gasification rate at 750° C was increased by 0.017 g/hr/g coal charged for a 33-pct increase, whereas at 950° C the increase in carbon gasification was negligible at an increment of 0.001 g/hr/g coal charged. Similarly, total gas production was increased 43 pct at 750° C and 10 pct at 950° C.

As shown by the gas production and carbon gasification rates presented in figures 2 through 6, for reaction temperatures of 750° C and higher, the higher steam feed rate of 5.8 g/hr resulted in significantly higher production rates over that achieved at the lower steam rate of 1.16 g/hr.

Repeated Use of Sprayed Raney Nickel Catalyst

To determine the stability of sprayed Raney nickel catalyst, a single insert flame-sprayed with Raney nickel catalyst was subjected to four gasification tests at 750° C, 300 psig, and a steam rate of 1.16 g/hr. The resulting gas production rates are shown in fig. 7; also shown is the base case, with no catalyst inserted in the bed.

Gas production rates presented in figure 7 indicate that the activity of the sprayed Raney nickel catalyst insert decreased rapidly with use. The gas production of the fourth test (17.8 hr service), was only about 10 pct greater than that obtained when no catalyst was used. An extrapolation of the total gas production rate as a function of accumulated service time on one catalyst insert indicates that the catalyst insert would be completely ineffective after about 20 hrs of operation. Considerable flaking-off of the catalyst is apparent; thus the need is indicated for an effective bonding agent or alloying substance that will increase the physical durability of the catalyst. Sulfur compounds gasified from the coal are also suspected of poisoning the nickel catalyst and resulting in the decline in activity with time.

Effect of Extent of Gasification Time

A series of tests were conducted to determine whether catalysts remain effective as the extent of gasification increases. Sprayed Raney nickel inserts and CaO powder were subjected to the standard test conditions of 850° C, 300 psig, 5.8 g/hr steam rate but with gasification times varying from 2 to 8 hrs. The abridged results presented in table 6 show that although the overall rate of gasification decreases with extent of gasification or with the length of time of gasification, the catalysts tested still generally increased the rate of carbon gasification, and the rate of gas production, as indicated by CH₄ production, over that achieved with no catalyst.

TABLE 6. - Effect of extent of gasification time upon overall effectiveness of catalyst

Unit A. - Temperature, 850° C, N₂ flow, 2000 std cc/hr; steam rate, 5.8 g/hr

Gasification time, hr	CH ₄ production		Carbon gasification	
	2	6	2	6
Rates with no catalyst	53.3 cc/hr/g	28.6 cc/hr/g	0.087 g/hr/g	0.062 g/hr/g
Rates with CaO	56.9 cc/hr/g	30.7 cc/hr/g	.090 g/hr/g	.062 g/hr/g
Increase due to CaO	7 pct	7 pct	3 pct	0 pct
Rates with sprayed Raney nickel catalyst	70.9 cc/hr/g	38.3 cc/hr/g	.093 g/hr/g	.063 g/hr/g
Increase due to Raney nickel	33 pct	34 pct	7 pct	2 pct

Effect of Residues from Catalytic Gasification

The catalytic effectiveness of ash residues (some contain either residual KCl or K_2CO_3) from total gasification operations were tested and compared with the effectiveness of the fresh additive, K_2CO_3 and KCl.

The gasification residues were prepared by nominally complete steam-gasification of coal in a 1-in diameter electrically heated, vertically mounted stainless-steel reactor. The coal charge consisted of 70 g of pretreated Bruceton coal plus 3.5 g of admixed catalyst; the charge was gasified at 950° to 970° C and atmospheric pressure using a steam feed rate of 45 g/hr. The preparatory gasification step was stopped whenever the flow of dry product gas appeared to cease. Carbon and ash content of the pretreated coal and of residues after total gasification and residue analyses are presented in table 7. The ash analyses show that ash from the catalyzed coals contained significantly larger amounts of potassium than did the ash of uncatalyzed coal.

In the standard screening tests conducted in unit A, the amount of residue admixed with the 10-g coal charge was one-seventh of the residue from the total gasification. Thus, a theoretical equivalent of 0.5 g of the original 3.5 g of catalyst was charged with the coal in the standard screening test. Production rates obtained in the standard screening tests are presented in table 8 for the case of plain pretreated coal, for the cases of addition of catalyst-free residue, pure K_2CO_3 and KCl, and for the addition of residues from the total gasification of the coals admixed with K_2CO_3 and KCl.

The results of the tests on residues from total gasification of coal indicate that potassium compounds, K_2CO_3 and KCl, in the residues retained most of their activity in increasing the production of methane, lost part of their capability of increasing hydrogen production, and inhibited carbon monoxide production. The addition of 1.14 g of catalyst-free residue had very little effect on either methane or total gas production (experiment 220 vs 167).

Pilot-Plant Tests

Tests using additives mixed in the coal feed were conducted in the Bureau's 4-in diameter Synthane gasifier system. In this system, coal is first decaeked in a fluidized-bed pretreater and then dropped into the fluidized-bed gasifier for steam-oxygen gasification. The general operation has been described by Forney and others (5).

Ranges of pretreater and gasifier conditions used in this series of tests were as follows:

	<u>Pretreater</u>	<u>Gasifier</u>
Coal rate, lb/hr	17.8 - 21.2	-----
O ₂ feed, scf/lb coal	.31 - .37	2.12 - 3.4
N ₂ feed, scf/lb coal	5.4 - 6.2	-----
Steam feed, scf/lb coal	-----	19.6 - 25.4
Av. temp., ° C	388 515	907 - 945

Pretreater and gasifier pressure was 40 atm.

TABLE 7. - Carbon, ash content, and ash analysis of pretreated Bruceston coal and of residues from total gasification

Gasification conditions: Charge, 70 g pretreated Bruceston coal, 3.5 g of catalyst; water rate, 45 cc/hr
950-970° C, atmospheric pressure

Expt. No.	Carbon and ash content, pct		Mineral analysis of ash, pct									
	Carbon	Ash	Al ₂ O ₃	CaO	Fe ₂ O ₃	Mgo	P ₂ O ₅	K ₂ O	SiO ₂	Na ₂ O	SO ₃	TiO ₂
Charge coal	74.3	10.6	25.9	1.7	10.8	0.9	<0.01	1.7	54.8	1.6	1.6	1.0
Residues:												
No catalyst	1.67	98.9	25.1	1.6	14.4	.8	----	1.9	54.7	1.5	----	----
K ₂ CO ₃	0.47	99.9	19.7	1.1	10.8	.8	----	24.3	41.7	1.6	----	----
KCl	4.7	95.1	22.2	1.3	12.4	.7	----	13.1	48.5	1.4	0.4	----

TABLE 8. - Specific production and gasification rates resulting from addition of potassium compounds and various gasification residues

Standard test conditions:		Unit A: 10 g pretreated Bruceton coal, 0.5 g catalyst (residue charge as indicated); feed 5.8 g H ₂ O/hr + 2000 std cc N ₂ /hr; approximately 4-hr duration; 300 psig; 850° C										
Expt. No.	No. of tests	Residue charged Amt., g	Total dry gas production rate, N ₂ -free basis, std cc/hr/g coal charged	Specific production rate of constituent gases, std cc/hr/g coal charged							C ₃ H ₆	
				H ₂	CO	CO ₂	CH ₄	C ₂ H ₄	C ₂ H ₆	C ₃ H ₈		
No catalyst	167		331	166	49.7	70.2	43.7	0.06	0.93	0.24	0.12	
Catalyst-free residue	220	D-1	1.12	344	180	39.2	79.3	43.9	.07	.81	.33	.21
K ₂ CO ₃	218			578	309	95.0	126.4	46.2	.31	.72	.22	.06
K ₂ CO ₃ residue	221	D-2	1.41	398	205	45.8	98.1	47.6	.27	.72	.12	.30
KCl	212			615	340	90.1	137.3	46.7	.07	.64	.33	.03
KCl residue	222	D-3	1.26	370	175	47.8	94.7	48.6	.22	.72	.19	.24

Expt. No.	Product liquid, g/hr/g coal charged	Carbon gasification rates, g/hr/g coal charged	Unit heating value N ₂ -free product gas, Btu/SCF	Gaseous heating value produced, Btu/hr./cu ft coal charged
No catalyst	167	89 x 10 ⁻³	353	57,700
Catalyst-free residue	220	.449	344	58,500
K ₂ CO ₃	218	.494	312	89,000
K ₂ CO ₃ residue	221	.487	332	65,300
KCl	212	.480	307	93,300
KCl residue	222	.469	336	61,300

To alleviate operating difficulties in the pretreater due to unwanted steam condensation, a nitrogen gas feed was substituted for the steam feed of the pretreater.

The coal feed was Illinois No. 6, River King Mine, 20 x 0 mesh size. Additives used were hydrated lime and dolomite, and additive concentrations used in the coal feed mixtures were 5 and 2 pct by weight, respectively. The analyses and sizes of the additives were as follows:

Hydrated lime: minimum CaO, 72 wt pct
minimum MgO, .05 wt pct
95 pct less than 325 mesh, and

Dolomite : CaCO₃, 55 wt pct
MgCO₃, 44 wt pct
85 pct less than 100 mesh

Results

The effect of the additives upon the percent carbon gasified and percent steam decomposed can be seen in figure 8 for gasification temperature in the 900° to 950° C range. Addition of 5 pct of either hydrated lime or dolomite to the coal resulted in significant increases in carbon gasified. The 5-pct hydrated lime addition resulted in an increase in carbon gasified of about 29 pct at an average gasification temperature of 914° C. Addition of 5 pct dolomite gave a 20-pct increase in carbon gasified at 945° C. These increases compare favorably with the 9-pct increase obtained in the 850° C bench-scale test list using 5-pct addition of hydrated lime.

The 2-pct addition of dolomite did not significantly increase the percent carbon gasification.

Steam decomposition was not significantly increased by either dolomite or hydrated lime at the 2- and 5-pct levels, respectively.

The effect of the additive upon yield of hydrogen and methane in the pilot-plant unit is shown in figure 9. At an average gasification temperature of 914° C, addition of 5 pct hydrated lime in the coal feed increased the hydrogen yield approximately 30 pct from 6.25 to 8.1 scf/lb of moisture-and-ash-free coal feed. A similar increase of 17 pct was obtained by the use of 5 pct dolomite in the coal feed at 945° C average gasification temperature. Such significant increases in hydrogen production were also observed in the bench-scale tests.

The yield of methane was increased significantly by 25 pct at 914° C average gasification temperature through the addition of 5 pct hydrated lime. The use of 5 pct dolomite at 945° C gasification temperature brought no significant increase in methane yield. Failure of catalytic action to increase the yield of methane at the higher gasification temperature (945° C) agrees with the general trend observed on bench-scale tests--that the increase in gas yield due to catalyses decreases with increase in temperature.

The effect of additives upon the yield of carbon monoxide is shown in figure 10. Addition of hydrated lime and dolomite at the 5-pct concentration levels brought respective increases of 23 and 26 pct in yield of carbon monoxide. Figure 11 shows similar increases in product gas yield (CO + H₂ + CH₄), for the same additions.

Addition of dolomite at the 2-pct level failed to bring any significant increase in yields of methane, hydrogen, or carbon monoxide.

Other results in pilot-plant operation due to the use of dolomite and hydrated lime at the 2- and 5-pct concentration levels, respectively, are that higher peak temperatures could be tolerated in the gasifier without incurring excessive sintering. With no additive in the coal, if a local temperature in the gasifier exceeded 1000° C, the operation generally would terminate because of excessive sintering or slagging of the char ash. With the additives in the coal, local temperatures as high as 1045° C were encountered with no adverse effect on operations. A similar elevation in sintering temperature induced by the addition of limestone to the feed coal is reported to be a key feature of the high-temperature Winkler process (6).

SUMMARY AND CONCLUSIONS

The overall results of the bench-scale investigation suggest that the use of suitable additives would improve the coal gasification reaction at elevated pressures. In connection with possible benefits to the Synthane process for making high-Btu gas, it appears that appropriate additives could significantly increase production of methane and hydrogen in the gasification step.

The bench-scale study thus far has shown the following:

1. Alkali metal compounds and many other materials such as oxides of iron, calcium, magnesium, and zinc significantly increase the rate of carbon gasification and the production of desirable gases such as methane, hydrogen, and generally carbon monoxide during steam-coal gasification at 850° C and 300 psig.
2. The greatest yield of methane occurred with the use of an insert flame-sprayed Raney nickel catalyst (unactivated), which has a limited life of activity. Significant methane increase resulted from the addition of 5 pct by weight of LiCO_3 , Pb_3O_4 , Fe_3O_4 , MgO , and many other materials.
3. The increased gasification resulted whether the extent of coal gasification was small or great.
4. At temperatures above 750° C, catalytic effectiveness decreased with further increase in temperature.
5. Residue from total gasification of coal mixed with potassium compounds still contained a significant concentration of potassium (over 10 pct) and was effective as an additive in increasing production of hydrogen and methane.

Operation of the 4-in diameter Synthane pilot-plant gasifier at 40 atm pressure and average temperature of up to 945° C with dolomite and hydrated lime additives at 5-pct concentration has increased product gas ($\text{CO} + \text{H}_2 + \text{CH}_4$) yield significantly and has increased allowable operating temperatures.

REFERENCES

1. Vignon, L., "Water Gas," Ann. Chim. v. 15, 1921, pp. 42-60.
2. Neumann, B., C. Kroger, and E. Fingas., "Die Wasserdampfzeretzung an Kohlenstoff mit Aktivierenden Zusätzen," (Steam Decomposition on Carbon with Activating Additives.) Zeitschrift fur anorg. und allgen. Chemie, Band 197, 1931, pp. 321-338.
3. Kroger, C., and Gunter Melhorn, "The Behavior of Activated Bituminous Coal and Low-Temperature Carbonization and Gasification in a Current of Steam," Brennstoff-Chem., v. 19, 1938, pp. 257-262.
4. Kislykh, V.I., and N. V. Shishakov, "Catalytic Effect on Gasification in a Fluidized Bed," Gaz. Prom. v. 5, No. 8, 1960, pp. 15-19.
5. Forney, A. J., W. P. Haynes, and R. C. Corey, "The Present Status of the Synthane Coal-to-Gas Process." 46th Annual Fall Meeting Society of Petrol. Engrs. of AIME, Preprint - SPE 3586, Oct. 3-6, 1971.
6. Meraikib, M. and F. H. Franke, "Carbon Gasification by the High-Temperature Winkler Process." Chem. Eng. Tech. v. 42, 1970, pp. 834-36.

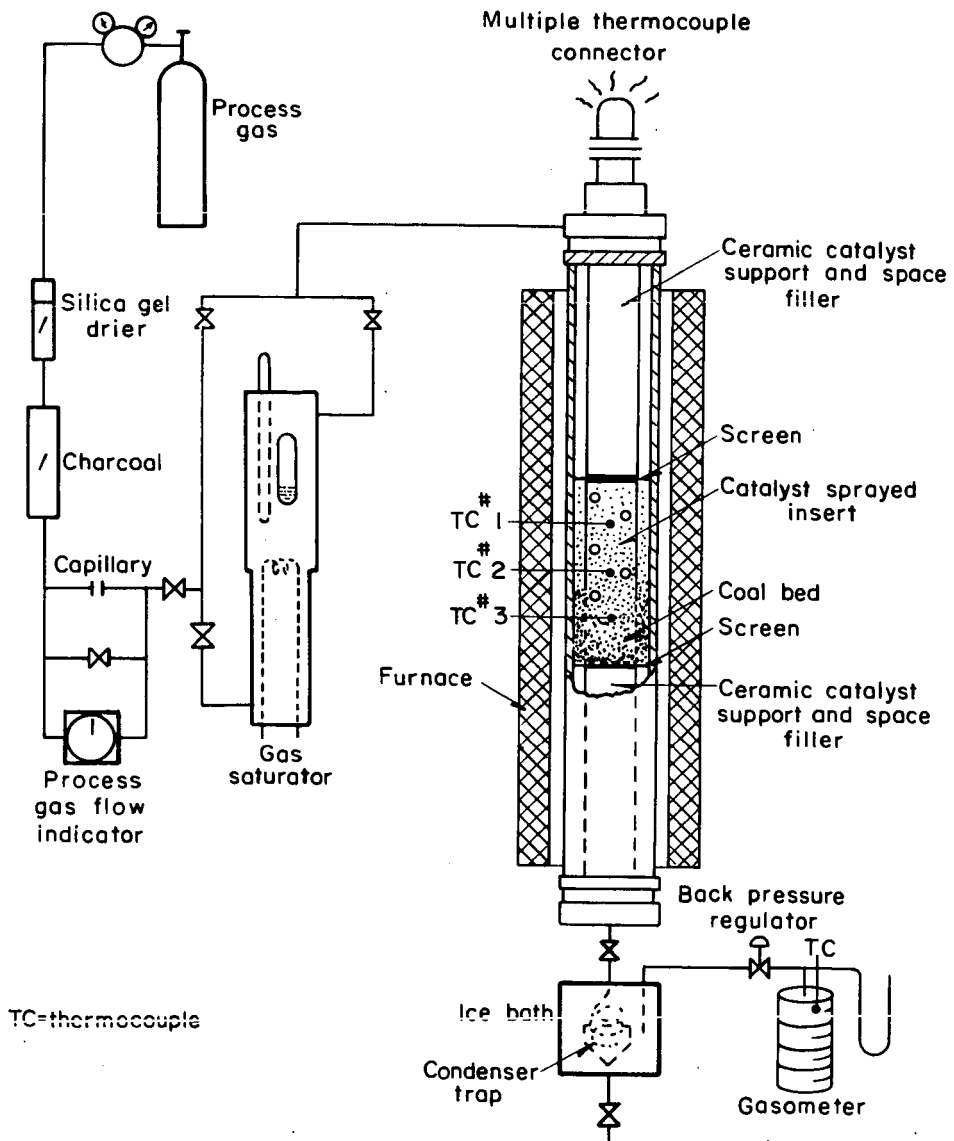


Figure 1.—Apparatus for the catalytic gasification of coal.

L-10298

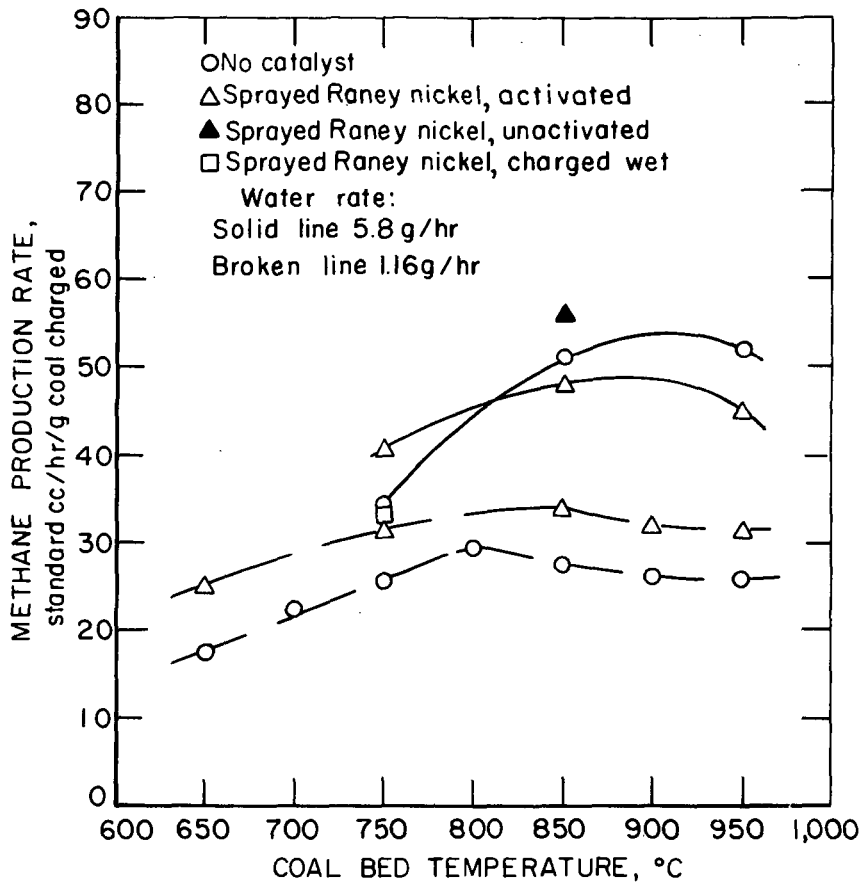


Figure 2—Effect of temperature upon methane production rate using sprayed Raney nickel. Test conditions: pressure, 300 psig; flow, 2,000 standard cc/hour N_2 ; water, 5.8 and 1.16 g/hour.

4-29-68 L-10556

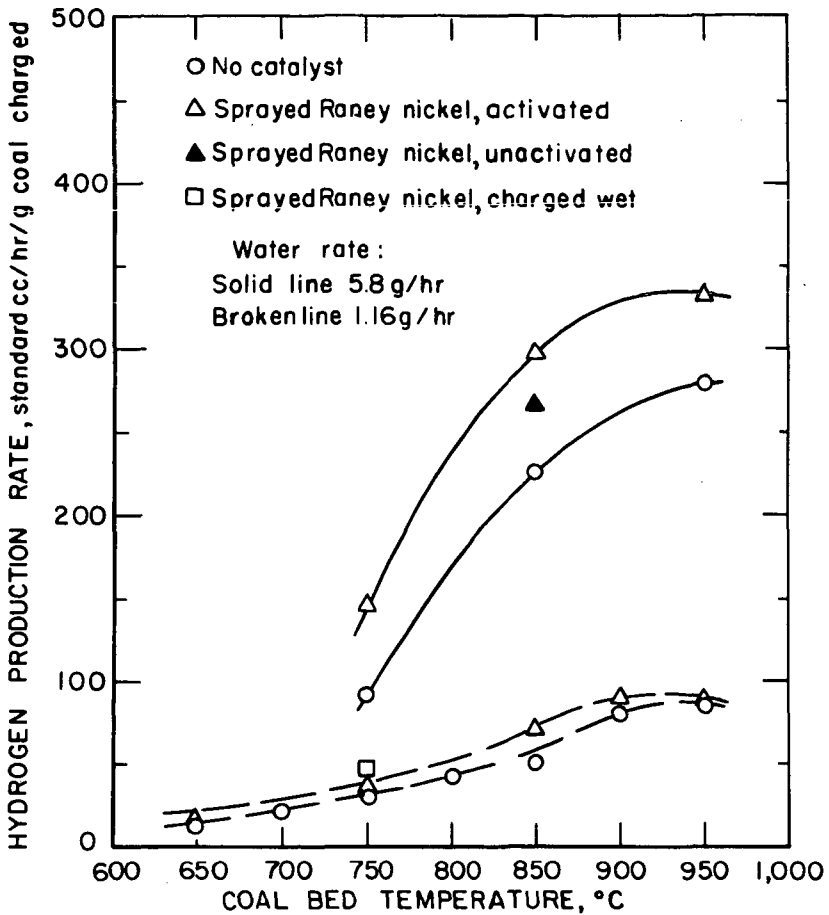


Figure 3. - Effect of temperature upon specific production of hydrogen, using sprayed Raney nickel. Test conditions: pressure, 300 psig, flow, 2,000 standard cc/hour N₂; water, 5.8 and 1.16 g/hour.

4-26-68

L-10551

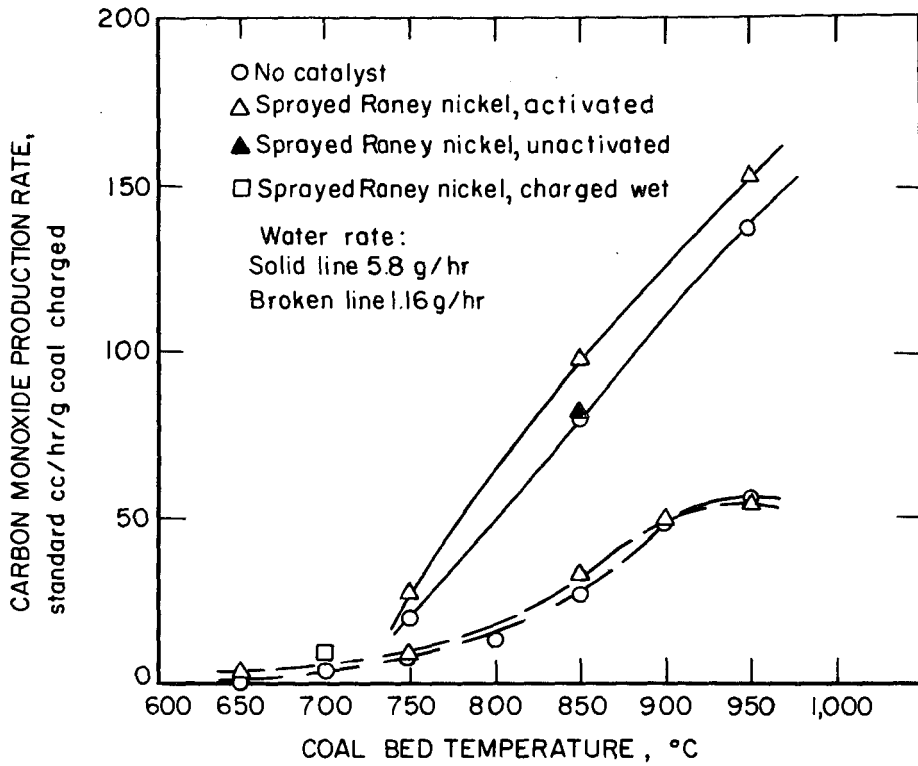


Figure 4.-Effect of temperature upon carbon monoxide production rate using sprayed Raney nickel. Test conditions: pressure, 300 psig; flow 2,000 standard cc/hour N₂; water, 5.8 and 1.16g/hr.

4-29-68 L-10552

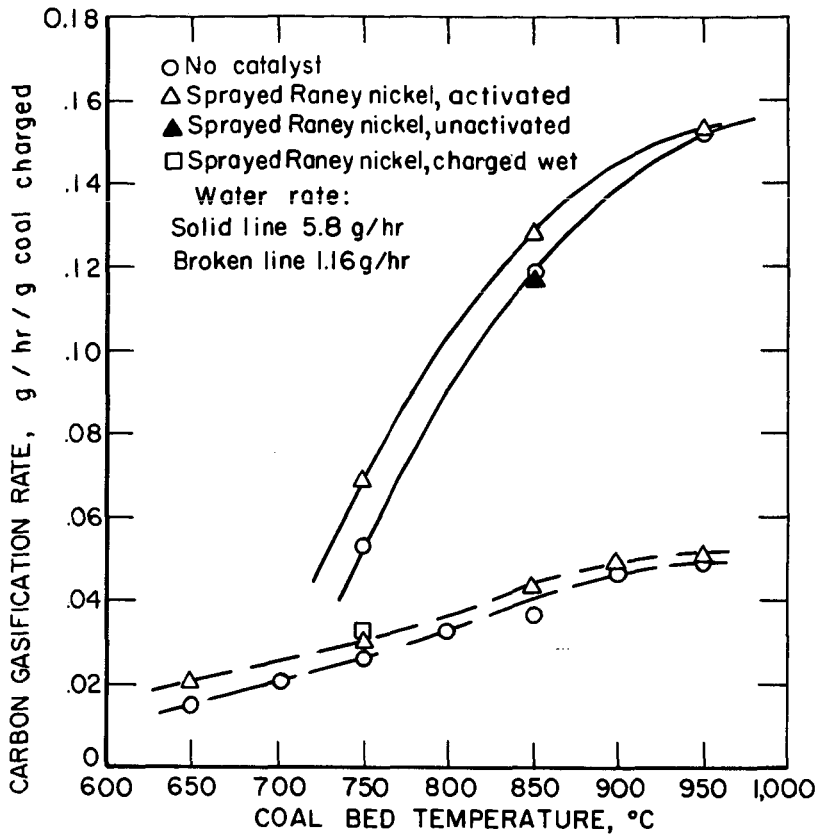


Figure 5.-Effect of temperature upon carbon gasification rate using sprayed Raney nickel. Test conditions: pressure, 300 psig; flow, 2,000 standard cc/hr N₂; water, 5.8 and 1.16 g/hr.

4-30-68

L-10555

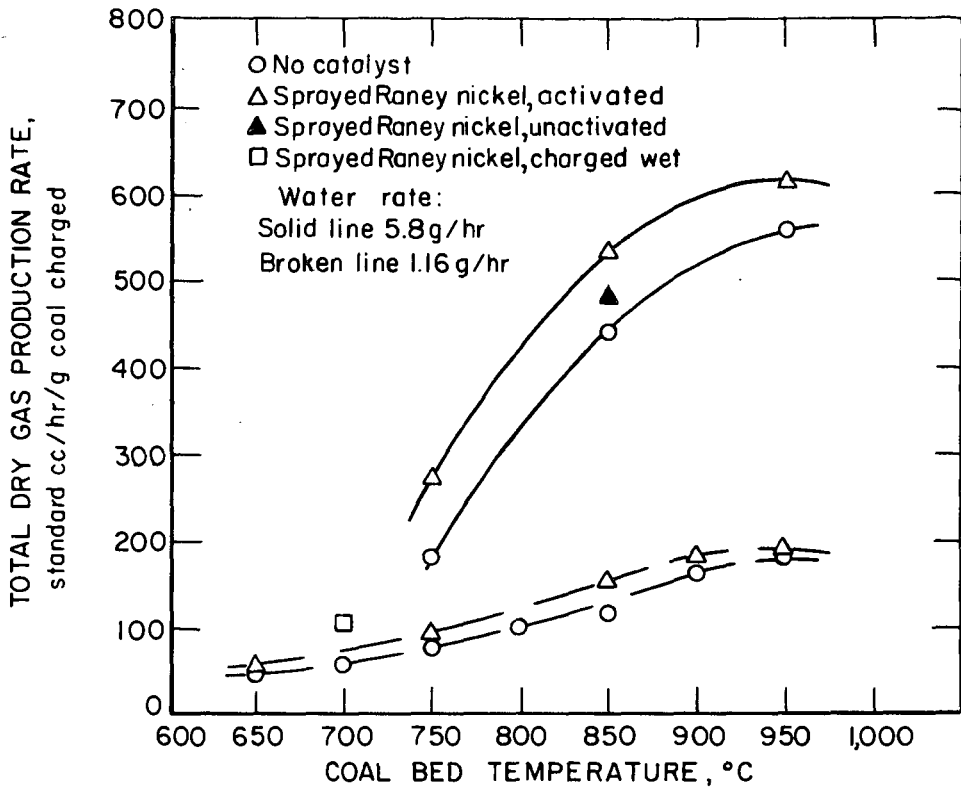


Figure 6. -Effect of temperature upon total dry gas production rate using sprayed Raney nickel. Test conditions: pressure, 300psig; flow 2,000 standard cc/hour N_2 ; water, 5.8 and 1.16 g/hour.

4-29-68

L-10553

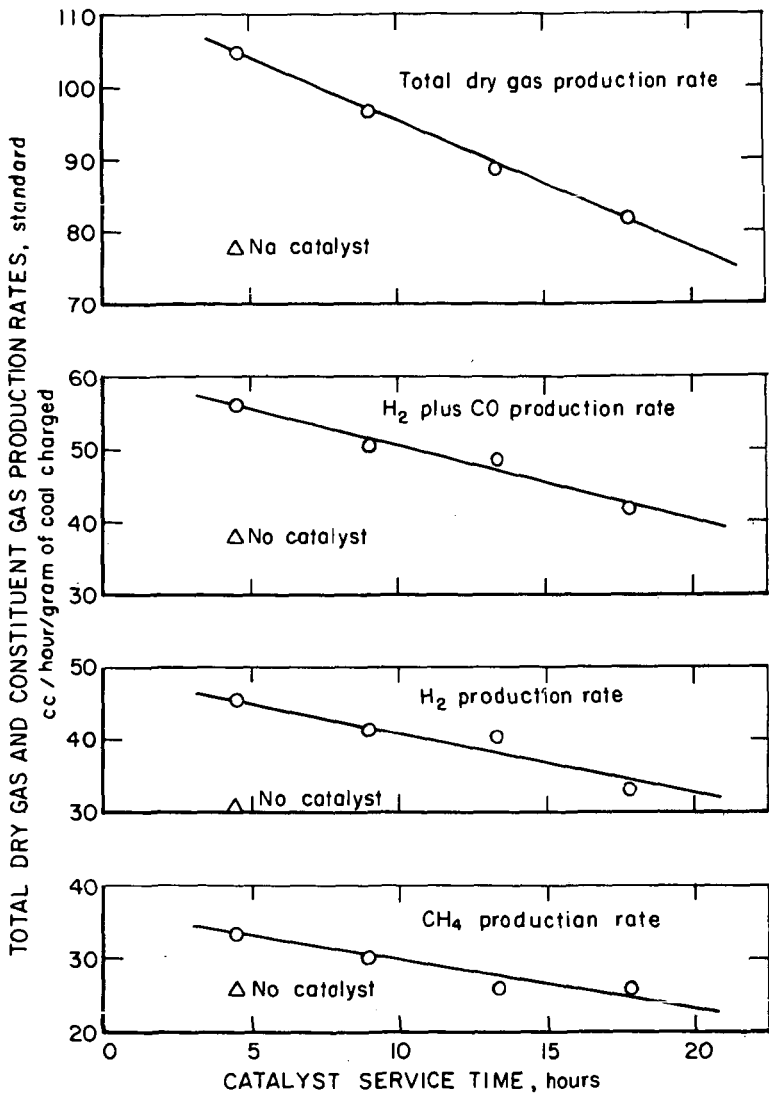


Figure 7.—Effect of catalyst service time upon gas production rates.
 Test conditions: temperature, 750°C; flow, 2,000 standard cc/hour N₂ and 1.16g/hour water.

2-17-71 4-25-68 L-10545

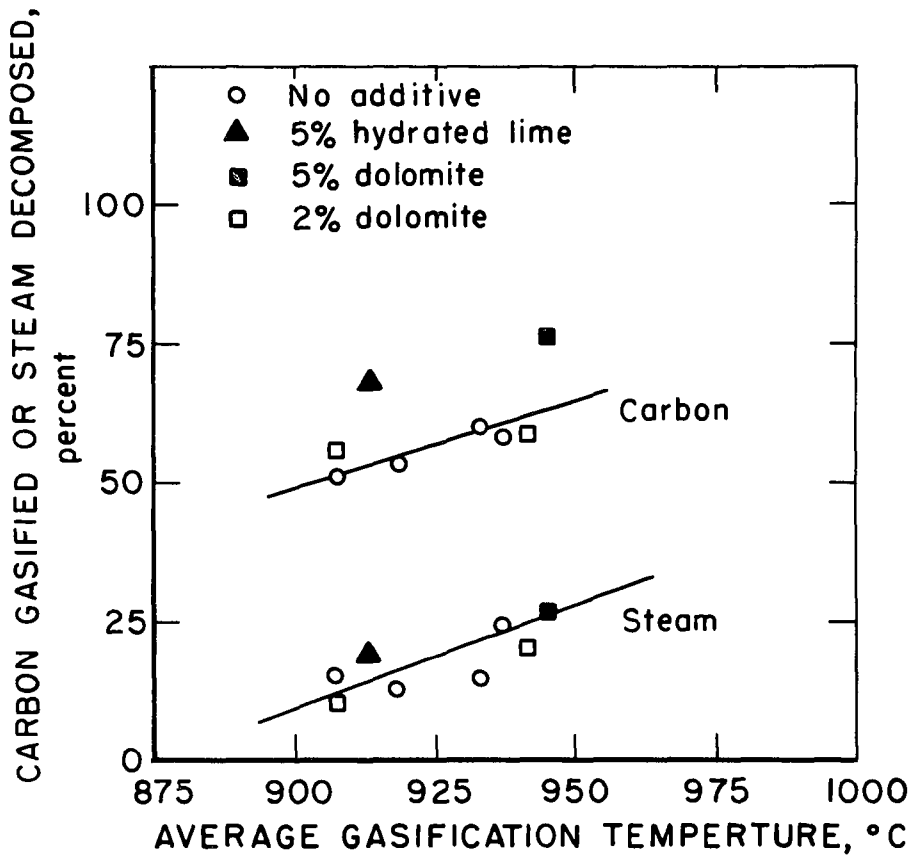


Figure 8— Effect of additives on percent carbon gasified and percent steam decomposition in 4" synthane gasifier operating at 40 atm.

L-13094

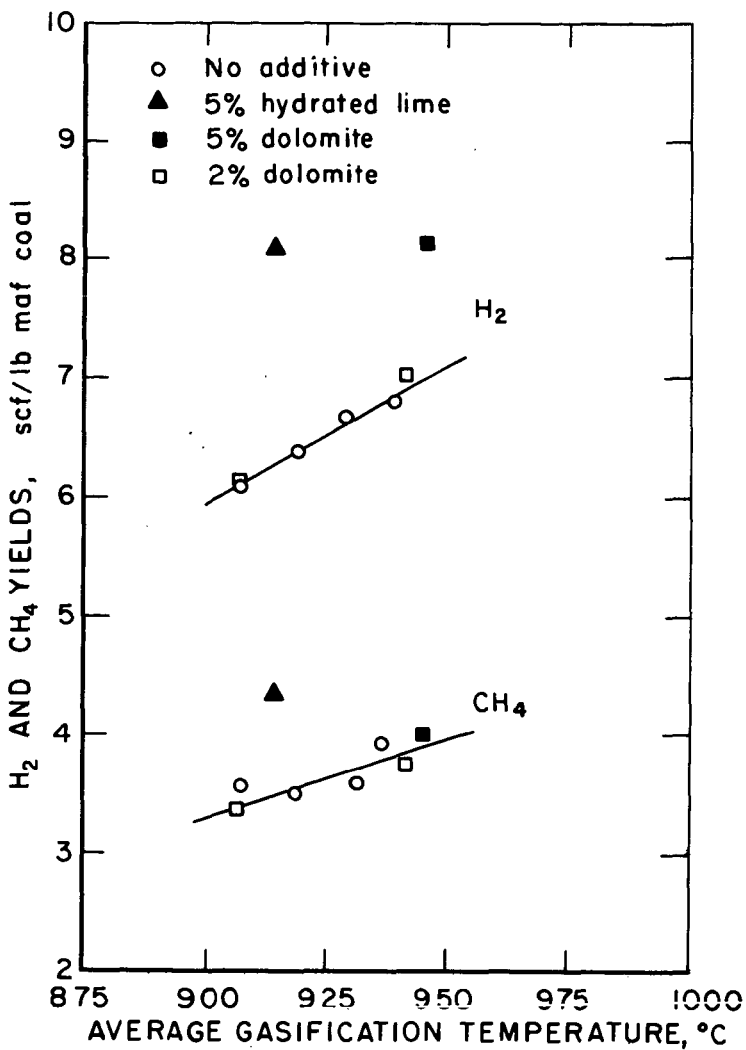


Figure 9—Effect of additives on yield of hydrogen and methane in 4" synthane gasifier operating at 40 atm.

L-13095

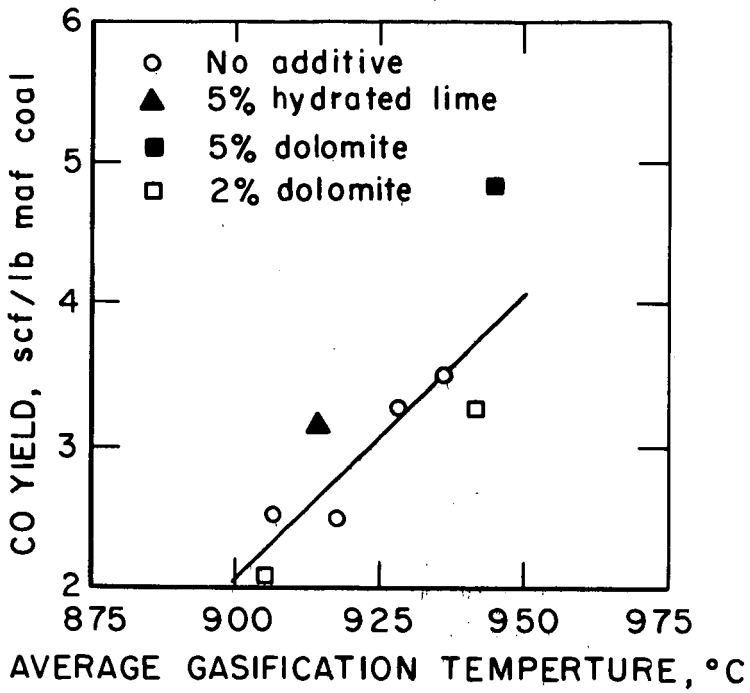


Figure 10- Effect of additives on yield of carbon monoxide in 4" synthane gasifier operating at 40 atm.

L-13096

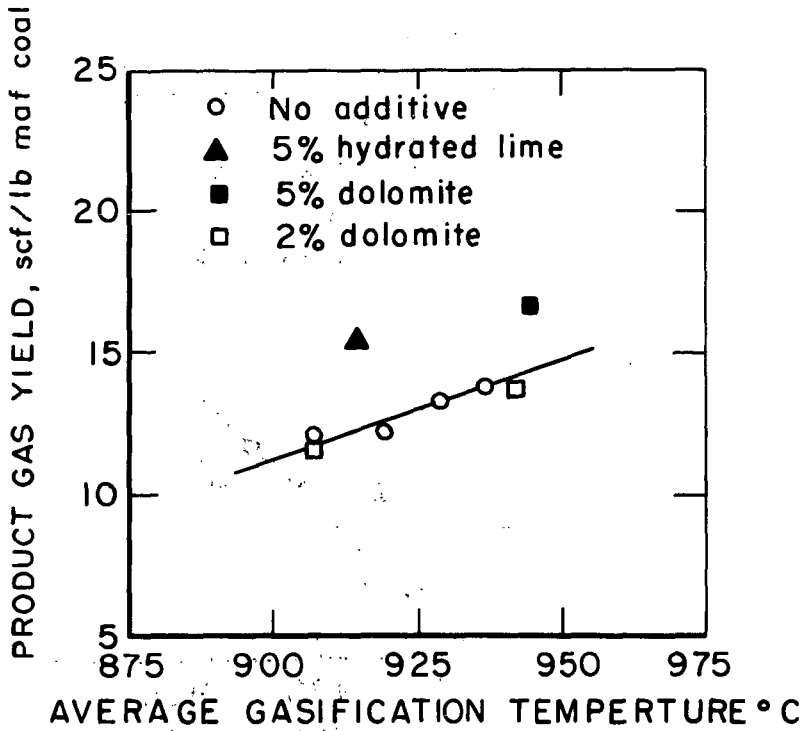


Figure II— Effect of additives on yield of product gas ($\text{CO} + \text{H}_2 + \text{CH}_4$) in 4" synthane gasifier operating at 40 atm. L-13097

Alkali Carbonate and Nickel Catalysis of Coal Steam Gasification

W.G. Willson, L.J. Sealock, Jr., F.C. Hoodmaker,
R.W. Hoffman, J.L. Cox, and D.L. Stinson

Introduction

Considerable work has been carried out on the catalytic effects of various chemicals on the reactions of carbon with steam. This work is of classic importance in the water gas reactions. In addition, many studies have been made to determine active catalysts for the synthesis of hydrocarbons from carbon monoxide and hydrogen. These two reaction systems are usually carried out at vastly different temperatures.

The carbon-steam reactions represented as $C + H_2O = CO + H_2$ and $C + 2H_2O = CO_2 + 2H_2$ are endothermic, and even in the presence of catalysts the operating temperature range of 800-1100°C is usually employed (1). One of the earliest investigations of catalysts for the carbon-steam reactions carried out by Taylor and Neville (2) was at temperatures from 490-570°C. Their most effective catalyst used with steam and coconut charcoal was potassium carbonate, although sodium carbonate also proved effective. Fox and White (2) demonstrated the catalytic effect of impregnating graphite with sodium carbonate over the temperature range of 750-1000°C.

Kröger (3) found that metallic oxides and alkali carbonates or mixtures catalyzed the carbon-steam reactions. Lewis and co-workers (4) stated that if reactive carbons are catalyzed with alkali carbonates reasonable gasification rates are attainable at temperatures as low as 1200°F. A process which uses molten sodium carbonate to catalyze as well as supply heat for the carbon-steam gasification, has been described (5).

In contrast to the carbon-steam reactions, the synthesis of hydrocarbons from carbon monoxide and hydrogen is usually carried out at temperatures below 450°C (6). The most active catalysts were found to be group VIII metals, mixed with various activating materials (7). A method for the direct production of hydrocarbons from coal-steam systems using multiple catalysts in a single-stage reactor has been described by Hoffman (8). Hoffman and co-workers (9) have described the effects of various commercial nickel methanation catalysts in a single-stage reactor. They stated that nickel was chosen for the methanation catalyst since the yield of hydrocarbons was limited essentially to methane.

It has been found in the single-stage reactor that most effective mixed catalysts which produce methane and carbon dioxide from coal-steam systems ($2C + 2H_2O = CH_4 + CO_2$) are potassium carbonate and nickel. In the single-stage reactor with the nickel methanation catalyst, potassium carbonate and coal mixed and charged, it is necessary in order to get effective contact time, to have the coal to nickel catalyst ratio about 1:1. With this in mind it was deemed significant to determine the optimum ratio of potassium carbonate to coal which would give the best methane production.

The principal objectives of this investigation were (1) to determine the optimum ratio of potassium carbonate to coal, holding the nickel catalyst concentration constant, (2) to determine by analytical methods and X-ray diffraction the form and recoverability of the potassium carbonate in the ash, and (3) to determine the amount of potassium that could be recovered economically.

Experimental Systems

Reactor Design: The gasification of coal was carried out in a one-inch (o.d.) diameter, semi-continuous flow reactor described in earlier papers (8,9). Due to the extremely active nature of the nickel catalyst towards oxygen, the re-reduced nickel catalyst had to be stored under nitrogen atmosphere. In addition, the reactor was charged under a nitrogen atmosphere in a glove box.

Feed Materials: The coal used in all runs was a sub-bituminous coal from Glenrock, Wyoming, ground to 60-100 mesh. An analysis of the coal is given in Table I. Certified A.C.S. anhydrous potassium carbonate was used for the alkali catalyst. This catalyst was approximately the same mesh size as the coal. X-ray studies indicate, however, that some of the potassium carbonate had become hydrated, for example $K_2CO_3 \cdot X(H_2O)$. In addition, a commercial nickel catalyst was employed. The nickel methanation catalyst (Ni-3210) containing approximately 35% by weight nickel on a proprietary support was purchased from the Harshaw Chemical Company. The nickel catalyst was reduced with H_2 at approximately 650°C for 12-18 hours and stored under a nitrogen atmosphere.

Table I. Analysis of Glenrock Coal

	Proximate Analysis	
	As Received	Moisture Free
Moisture (wt %)	12.2	----
Volatile Matter (wt %)	39.6	45.1
Fixed Carbon (wt %)	36.1	41.1
Ash (wt %)	12.1	13.8
Heating Value (Btu/lb)	9140	10410

	Ultimate Analysis	
	As Received	Moisture Free
Hydrogen (wt %)	5.1	4.3
Carbon (wt %)	52.7	60.0
Nitrogen (wt %)	0.6	0.7
Oxygen (wt %)	28.6	20.2
Sulfur (wt %)	0.8	1.0
Ash (wt %)	12.1	13.8

Gas Analysis: Product gas volumes were measured by a calibrated wet test meter. Gas compositions were determined with a Beckman Model GC-5 dual column, dual T.C.D. chromatograph. One detector used a helium carrier with

Pora-Pak Q column and other used an argon carrier with a molecular sieve column. Data reduction was aided by an Auto Lab System IV digital integrator equipped with a calculation module.

Analytical Analyses: The potassium remaining in the coal ash was determined with a Perkin-Elmer model 303 atomic absorption spectrophotometer after performing a J. Lawrence Smith ignition on the sample. In order to obtain a total potassium balance it was necessary to recover the potassium that adhered to the nickel catalyst. This was accomplished by digesting the catalyst with acid and determining the potassium by atomic absorption.

The amount of carbonate retained in the ash was calculated from the quantity of carbon dioxide absorbed by ascarite after first scrubbing the gas evolved from the treatment of the ash with a 1:1 hydrochloric acid solution.

In order to determine the amount of potassium that was recoverable by an ambient temperature wash, 1g of ash was washed in 100ml of water for one hour. The amount of potassium in the filtrate was determined by atomic absorption.

X-ray Diffraction: The ground ash was mounted vertically in a General Electric XRD-5 diffractometer. Copper radiation at 50 KVP and 35 MA was used for the analyses. Each scan was started at an angle 2θ of 4° and continued through 70° . The "d" values in angstroms for the recorded X-ray peaks were determined from a copper $K\alpha$ ($\lambda = 1.5418\text{\AA}$) table and compounds were identified from the A.S.T.M. X-ray Powder Data File.

Methodology: Experiments were carried out by charging the reactor with the coal, potassium carbonate and nickel catalyst mixture in a glove box under a nitrogen atmosphere. In those cases where no nickel catalyst was involved the reactor was not charged in the glove box. In all other runs 100g of coal and about 110g nickel catalyst with varying amounts of potassium carbonate were charged. The temperatures on the reactor and super heater were then brought to operating temperatures of approximately 650°C in less than two hours and maintained at the value for the duration of the run. In all cases the length of the run was $7\frac{1}{2}$ hours and approximately 28 ml of water were added. The product gas was monitored for composition every half hour. The reactor pressure was approximately 30 PSIA which is the pressure required to give an adequate sample to the chromatograph.

All runs were repeated until near duplication of two runs was obtained. The criteria for accepting the duplicate runs were based on the total mass balance and the quality of the gas produced. It was decided that a total mass balance of $\pm 4\%$ was sufficient to insure that there were no major leaks to prejudice the results. To insure that the nickel catalyst was properly reduced and had not oxidized during loading in the mixed catalyst runs, only the runs in which the average gas had a heating value of over 800 Btu/SCF (CO_2 free) were used. There were only two cases out of a total of twelve separate runs with the mixed catalyst where the quality of the gas produced was below 800 Btu/SCF. In both cases the runs were repeated a third time and the criteria for acceptance was met. The amounts of methane and gas produced per gram of coal reported in Table II are volume rated average compositions.

Results and Discussion

Table II contains a summary of the runs selected to determine the optimum amount of potassium carbonate to be mixed with the coal and nickel catalyst. Observations obtained with the single-stage reactor indicate that the initial reaction involved is devolatilization of the coal, followed by cracking and hydrogenation of unsaturated compounds in the presence of the nickel catalyst. This is followed by the carbon-steam reaction.

The first run in Table II was made using only coal and steam, and in this run the gas contained about 0.5% ethylene, 0.7% ethane as well as 4 ml of heavy liquids. In all the remaining runs the nickel catalyst was present, and in no case was any hydrocarbon heavier than methane detected. Methane and carbon dioxide were the major components, with hydrogen averaging between 10-14% and the carbon monoxide usually below 2.0% in the product gas. In run No. 2 only the nickel catalyst was employed. It more than tripled the methane production, while it only increased the total gas product by about 20%. This tends to indicate that a substantial quantity of the methane produced is derived from cracking and hydrogenating unsaturated compounds.

Figure 1 shows a plot of total gas production, as well as the methane production versus mass of potassium carbonate charged per 100g of coal. In both cases the dashed line indicates the runs were neither alkali or nickel

Table II Experimental Data for the Gasification Runs *

Run Number	1	2	3	4	5	6	7
K ₂ CO ₃ (g)	0.	0.	15.	20.	30.	45.	60.
Ni-3210(g)	0.	115.	111.	111.	111.	113.	114.
cm ³ CH ₄ /g Coal	51.	185.	225.	281.	266.	232.	234.
cm ³ Gas/g Coal	382.	453.	481.	612.	603.	493.	524.
Total Mass Recovery (wt %)	103.1	97.9	98.9	103.0	98.9	96.0	97.9
Total K Recovery (wt %)	—	—	94.2	105.7	105.9	95.0	98.7
K Recovery by Wash (wt %)	—	—	66.2	79.9	85.8	89.0	90.0
K Insoluble in Wash (g)	—	—	2.9	2.3	2.4	2.8	3.4
CO ₂ Recovery (%)	—	—	97.7	101.2	104.1	101.8	104.8

*All runs were made at ~30 PSIA and an average temperature of ~650°C.

**TOTAL GAS & METHANE
PRODUCTION/g K₂CO₃ CHARGED**

● = Ni-3210 CATALYST

■ = NO Ni OR ALKALI CATALYST

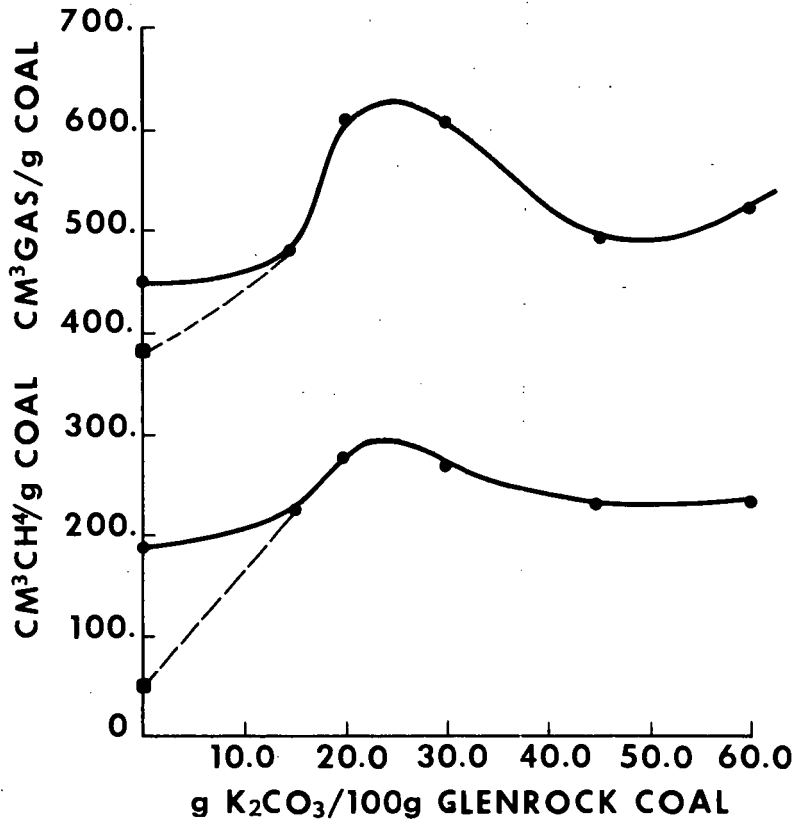


Fig. 1

catalyst were present. These figures show that for the single-stage reactor, using a sub-bituminous coal at about 650°C, the optimum methane as well as gas production is obtained using between 20-25g of potassium carbonate per 100g of coal. Addition of more than 30g of potassium carbonate is detrimental to the methane production as well as total gas production. This decrease in production is readily apparant when the potassium carbonate has been increased to 45g.

Table II also contains the analytical results for potassium recovery and carbonate recovery. The total potassium recovery by the ignition method was satisfactory, giving deviations of $\pm 6\%$. Potassium recovered in the wash solution varied from about 66 to 90%. This shows that between 2.3 - 3.4g of potassium are forming compounds that are insoluble in water at ambient temperatures. It is of interest to note that the least amount of insoluble potassium was obtained when the optimum amount of potassium carbonate was used. The carbonate recovered from the ash was good, giving a deviation of only $\pm 5\%$.

Although the X-ray scan ran from an angle 2θ of 4-70°, the majority of the peaks of interest fell in the range of 20-44°. Table III compares "d" spacings and intensities of X-ray diffraction peaks from 20-44° 2θ for the published data on the hydrated potassium carbonate ($K_2CO_3 \cdot 1 \frac{1}{2} H_2O$) and silicon dioxide, with the potassium carbonate as received and the ashes from the runs containing 0, 20, 45, and 60g of potassium carbonate respectively. The "d" spacings and intensities of the potassium carbonate as received and of the ashes containing potassium carbonate do not correspond exactly to the published anhydrous or hydrated forms of potassium carbonate. For example, the published A.S.T.M. data shows the major peak for $K_2CO_3 \cdot 1 \frac{1}{2} H_2O$ (intensity 100) has a "d" spacing of 2.72Å, whereas the analyzed samples have major peak "d" spacings of 2.77Å for the ashes and 2.79Å for the potassium carbonate as received. It is believed that the analyzed form of the potassium carbonate as well as that in the ash is a partially hydrated compound.

Figure 2 shows the X-ray diffraction pattern for the potassium carbonate as received. Only the peaks with question marks are unidentified peaks. The peaks unlabelled correspond most nearly to those published for $K_2CO_3 \cdot 1 \frac{1}{2} H_2O$. The ash from the reactor run containing no potassium carbonate is shown in figure 3. It displays only silicon dioxide and some unidentified peaks. The ashes from runs using 20, 45, and 60g of potassium carbonate with 100g

Table III. Comparison of d Spacings and Relative Intensities for X-ray Diffraction Peaks from 20°-44° 2θ

K ₂ CO ₃ ·1½(H ₂ O) ASTM 11-655	d(1) I/I ₁	SiO ₂		K ₂ CO ₃ as received		Ash with no K ₂ CO ₃		Ash from 20g K ₂ CO ₃ Run		Ash from 45g K ₂ CO ₃ Run		Ash from 60g K ₂ CO ₃ Run	
		ASTM 5-0490	d I/I ₁	observed values	SiO ₂ unidentifed	observed values	unidentifed	observed values	unidentifed	observed values	unidentifed	observed values	unidentifed
3.86	5	4.26	35	3.86	9	4.26	24	3.86	9	3.86	9	3.86	9
3.46	20	3.46	16	3.46	16	3.51	3.51	3.45	39	3.45	29	3.45	29
3.35	7	3.35	100	3.35	100	3.35	100	3.35	61	3.34	24	3.34	28
3.31	20	3.30	11	3.30	11	3.30	48	3.30	48	3.30	48	3.30	48
3.15	3	3.15	3	3.15	3	3.15	3	3.15	3	3.15	3	3.15	3
3.01	30	3.00	40	3.00	40	3.01	71	3.01	71	3.01	50	3.01	43
2.90	20	2.98	32	2.98	32	2.90	91	2.90	48	2.90	48	2.90	32
2.906	20	2.90	7	2.90	7	2.83	71	2.83	71	2.82	71	2.82	41
2.783	65	2.79	100	2.79	100	2.77	100	2.77	100	2.77	100	2.77	100
2.767	75	2.75	65	2.75	65	2.74	86	2.74	86	2.75	80	2.75	88
2.742	100	2.62	2.62	2.62	2.62	2.57	2.57	2.63	2.63	2.63	2.629	2.63	2.63
2.550	15	2.54	8	2.54	8	2.49	2.49	2.49	2.49	2.49	2.49	2.54	12
2.327	25	2.458	12	2.458	12	2.46	14	2.49	2.49	2.49	2.49	2.54	12
2.304	11	2.33	23	2.33	23	2.38	2.38	2.36	2.36	2.32 B	20	2.33	28
2.267	15	2.30	26	2.30	26	2.32	34	2.32	34	2.31	24	2.31	24
2.259	15	2.282	12	2.282	12	2.26	18	2.26	18	2.26	18	2.26	18
2.228	15	2.26	17	2.26	17	2.26	18	2.26	18	2.26	18	2.26	18
2.183	40	2.237	6	2.237	6	2.23	12	2.23	12	2.23	15	2.23	15
2.128	9	2.18	23	2.18	23	2.18	23	2.18	23	2.18	19	2.18	27
2.11	2.11	2.11	9	2.11	9	2.16	2.16	2.16	2.16	2.16	2.16	2.16	2.16
2.11	2.11	2.11	9	2.11	9	2.08	2.08	2.08	2.08	2.08	2.08	2.11	2.11

(1) Interplanar spacings

(2) Relative intensities

X-RAY DIFFRACTION PATTERN OF
 K_2CO_3 AS RECEIVED

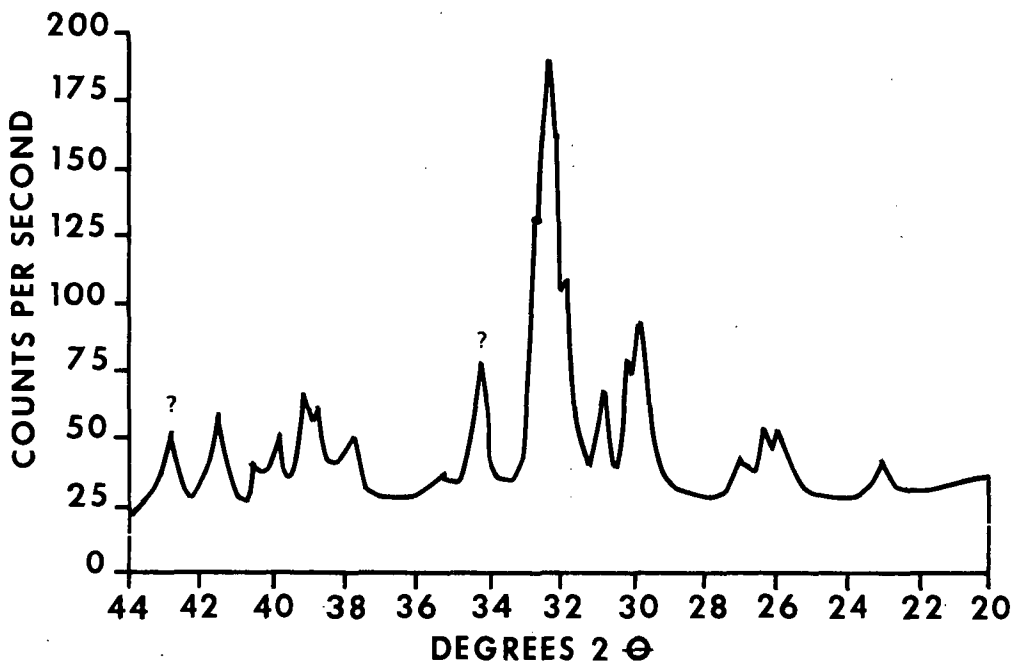
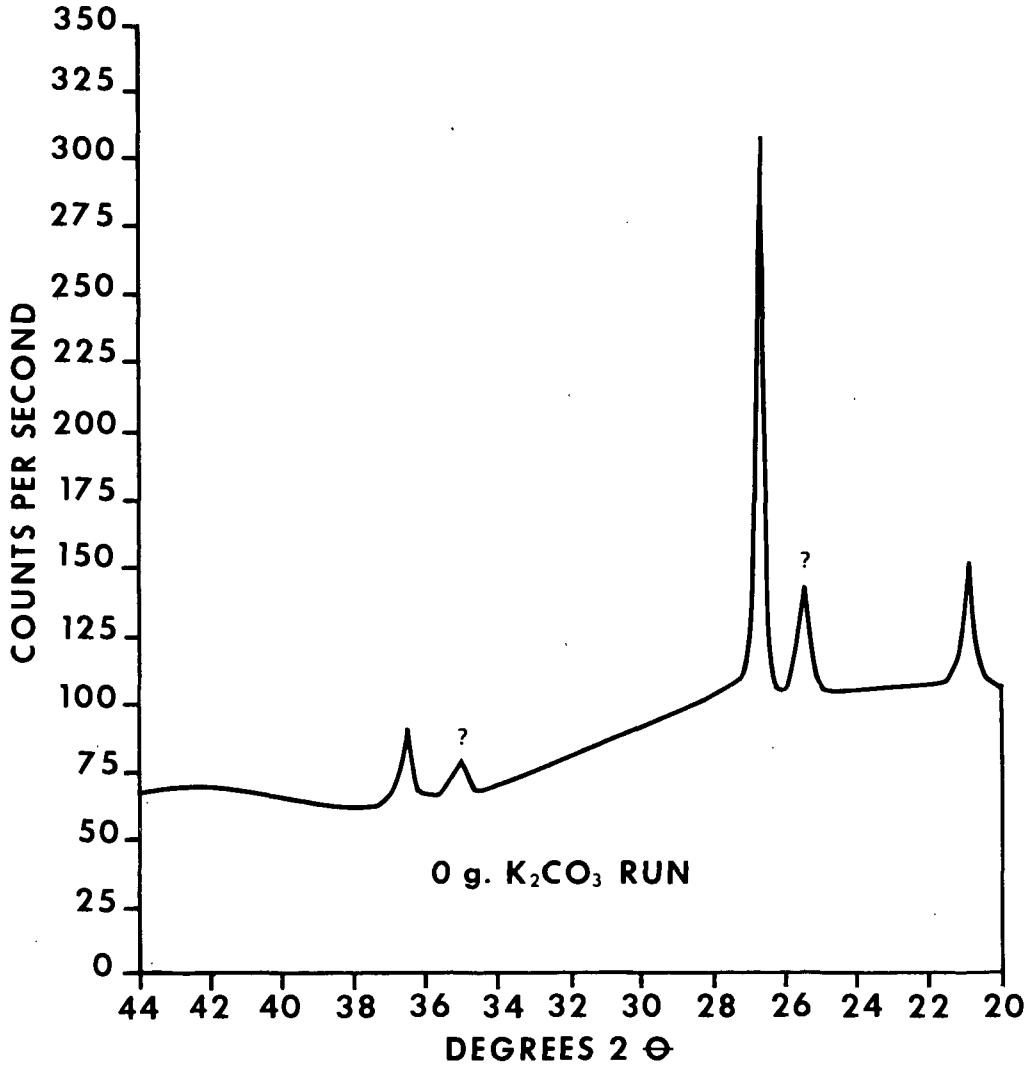


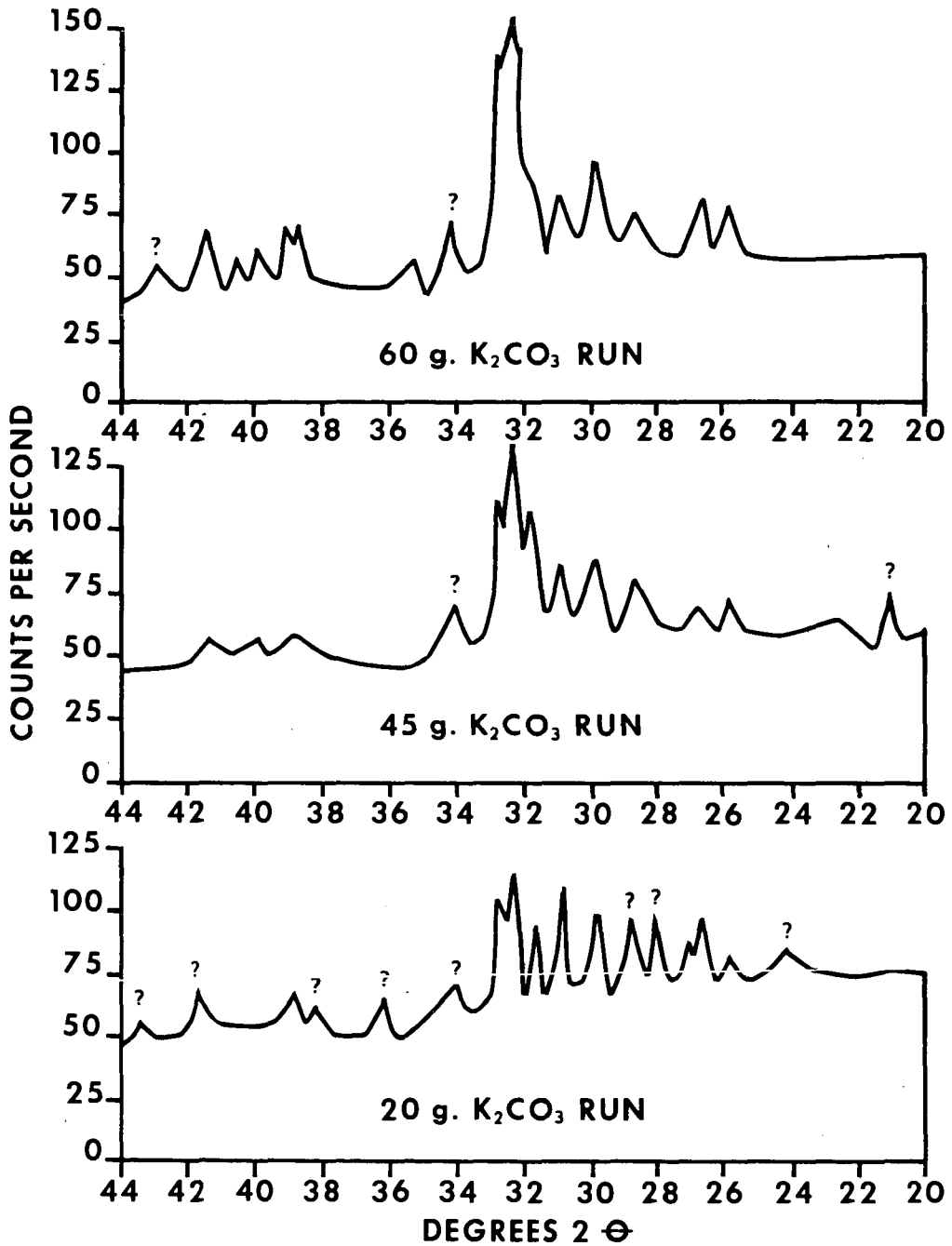
Fig. 2

X-RAY DIFFRACTION PATTERN OF ASH
FROM REACTOR RUN WITH 0 g. K_2CO_3



39 Fig. 3

X-RAY DIFFRACTION PATTERNS OF ASH FROM REACTOR RUNS



40 Fig. 4

of coal charged are shown in figure 4. It indicates that the amount of potassium carbonate remaining in the ash is proportional to the amount charged. This is best observed by noting the changes in the intensities of the major potassium carbonate peaks between $32-33^\circ 2\theta$. Again the peaks that are unidentified are noted with question marks. Comparison of "d" values in table II indicate that the form of the potassium carbonate remains essentially unchanged after the reaction.

Conclusions

The investigations thus far indicate that it is possible in a single-stage reactor, by using a mixed catalyst of potassium carbonate and a nickel catalyst, to react coal and steam principally to methane and carbon dioxide at low pressure and temperatures of approximately 650°C . Under these conditions the optimum amount of potassium carbonate for maximum methane production is between 20-25% the mass of the coal. X-ray diffraction studies indicate that the form of the potassium carbonate remaining in the ash is essentially the same as that charged. At the observed optimum value of 20g of potassium carbonate to 100g of coal nearly 80% of the potassium is recoverable by a one hour wash with water at room temperature.

Selected References

1. Fox, D.A., and White, A.H., *Ind. Eng. Chem.*, 23, 259-266, (1931).
2. Taylor, H.S., and Neville, H.A., *J. Am. Chem. Soc.*, 43, 2055-2071, (1921).
3. Kroger, C., *Angew. Chem.*, 52, 129-139, (1939).
4. Lewis, W.K., Gilliland, E.R., and Hipkin, H., *Ind. Eng. Chem.*, 45, 1697-1703, (1953).
5. Lefrancois, P.A., Barclay, K.M., and Skaperdas, G.T., "Fuel Gasification," 69, 64-80, (1967).
6. Storch, H.H., "Chemistry of Coal Utilization," Volume II, H.H. Lowry, ed., 1797-1800, Wiley, New York (1945).
7. Storch, H.H., *ibid*, 1818-1824.
8. Hoffman, E.J., *Preprints, Div. of Petrol. Chem., A.C.S.*, 16, No. 2, C 20 (1971).
9. Hoffman, E.J., Cox, J.L., Hoffman, R.W., Roberts, J.A. and Willson, W.G., *Preprints, Div. of Fuel Chem., A.C.S.*, 16, No. 2, 64-67, (1972).

CATALYZED HYDROGASIFICATION OF COAL CHARs

N. Gardner, E. Samuels, K. Wilks

INTRODUCTION

The reaction of hydrogen with coal and coal chars to produce gaseous hydrocarbons (hydrogasification) has received considerable attention for at least thirty-five years, since Dent in 1937 first reported on the hydrogasification synthesis⁽¹⁾. The reaction proceeds in two steps. In the initial stage, reaction rates are extremely rapid as the volatile matter and more reactive components of the coal are hydrogenated. Subsequent rapid hydrogenolysis of the higher homologs formed yields methane. In the second stage of the reaction, the structure of the remaining carbon char is more graphitic in character, resulting in a much slower hydrogasification reaction. It is the catalysis of the slow, second stage of the hydrogasification reaction that we have initiated a study of at Case Western Reserve University.

There have been numerous reports and patents on the catalysis of a similar reaction--the liquid phase hydrogenation of coal to liquid and gaseous products. Hydrogenation reactions are generally carried out at high pressures (several hundred atmospheres) and low temperatures (400 to 500°C) where the hydrocarbon products formed are substantially liquid. The ability of tin-halogen compounds, alkali metals⁽²⁾, and many other materials to catalyze the coal hydrogenation reactions is well known. Although the reaction is carried out in conditions where coal has undergone agglomeration and liquifaction,

the method of contacting catalyst and coal particles has a strong influence on reaction rate. For example, the addition of powdered ferrous sulfate to coal particles has almost no effect on the hydrogenation rate⁽³⁾. Impregnation of the coal by immersing it in aqueous solutions of ferrous sulfate, followed by oven drying, resulted in a sharp increase in hydrogenation rate with high productions of asphalt and oil. Impregnated nickelous chloride, stannous chloride, and ammonium molybdate show similar increases in catalytic activity as compared to powders of the same materials⁽⁴⁾.

In contrast to hydrogenation reactions, for the hydrogasification of coal chars, much less is known about the catalytic activity of materials and the dependency of catalyst contacting techniques. Alkali carbonates, one to ten percent by weight, have been shown to catalyze the hydrogasification of coals and cokes at temperatures of 800-900°C⁽⁵⁾. The suggested mechanism was that adsorption of the alkalies by carbon prevented graphitization of the surface. Zinc and tin halides have been shown to be effective hydrogasification catalysts. There is, however, little kinetic information on any of the catalyzed hydrogasification reactions.

There have been extensive studies on the ability of particulate metals and metal salts to catalyze the reactions of graphitic carbon with oxygen and carbon dioxide. For example, colloidal iron on Ticonderoga graphite reduces the activation energy for the carbon-oxygen reaction from 46 kcal/mole to 10 kcal/mole. A seven percent iron deposit impregnated from solution on sugar char reduced the

activation energy from 61.2 kcal/mole to 22.8 kcal/mole for the carbon-carbon dioxide reaction. In addition, dispersions of metals in carbon have been prepared by carbonization of polymers containing metal salts. The dispersions are catalytically active in the gasification reactions of carbon dioxide and oxygen. The mechanism of the substantial reduction in activation energy is not clear although a large amount of superfluous, quantitative information has been obtained. Two types of mechanisms have been proposed, oxygen-transfer and electron-transfer. In the oxygen-transfer mechanism the catalyst is presumed to assist the dissociation of molecular oxygen to chemisorbed atomic oxygen which then reacts with the carbon surface. Electron-transfer mechanisms involve the π electrons of graphitic carbon and the vacant orbitals of the metal catalysts. The catalytic effect presumably results from the altered electronic structure of the surface carbon atoms.

In contrast to the wealth of information on catalyzed hydrogenation of coal, and the catalyzed oxidation reactions of carbon by oxygen and carbon dioxide, little is known about catalyzed hydrogasification reactions as to the ability of materials to serve as catalysts. Also little is known about the kinetics and mechanisms of these reactions. We have initiated a kinetic study of catalyzed hydrogasification reactions using a high temperature, high pressure, recording balance. A thermobalance is particularly useful in gas-solid reactions because the weight of relatively small solid samples can be continuously measured. Direct kinetic analysis of the weight loss curves are straightforward.

II. EQUIPMENT AND PROCEDURES

The high pressure thermobalance is very similar to the balance described by Feldkirchner and Johnson⁽⁶⁾. The thermobalance was designed to operate isothermally at temperatures up to 1000°C and at hydrogen pressures up to 2000 psi. Details of the balance are shown in Figure 1, and a schematic diagram of the system is shown in Figure 2.

The reactor tube was constructed of Haynes 25 superalloy. The mass transducer is a Statham, Model UC 3, attached to a balance arm (Micro-scale accessory UL 5) and has a full scale range of 6 grams.

The sample is lowered into the reaction zone by an electric motor driven windlass at a rate of about one inch per second. The position of the sample in the reactor is obtained by utilizing a potentiometric technique. A small ten turn potentiometer is coupled directly to the windlass. Temperatures in the reactor are measured by stainless steel encased chromel-alumel thermocouples, the closest one to the sample being located 1/4" below the sample. Hydrogen flow rates were controlled ± 5 percent over the range 10 to 40 SCF/hr. Gas analysis was obtained by splitting a portion of the gas product stream to an infrared detector, where methane content was continuously measured, and a gas chromatograph where total gas composition was determined.

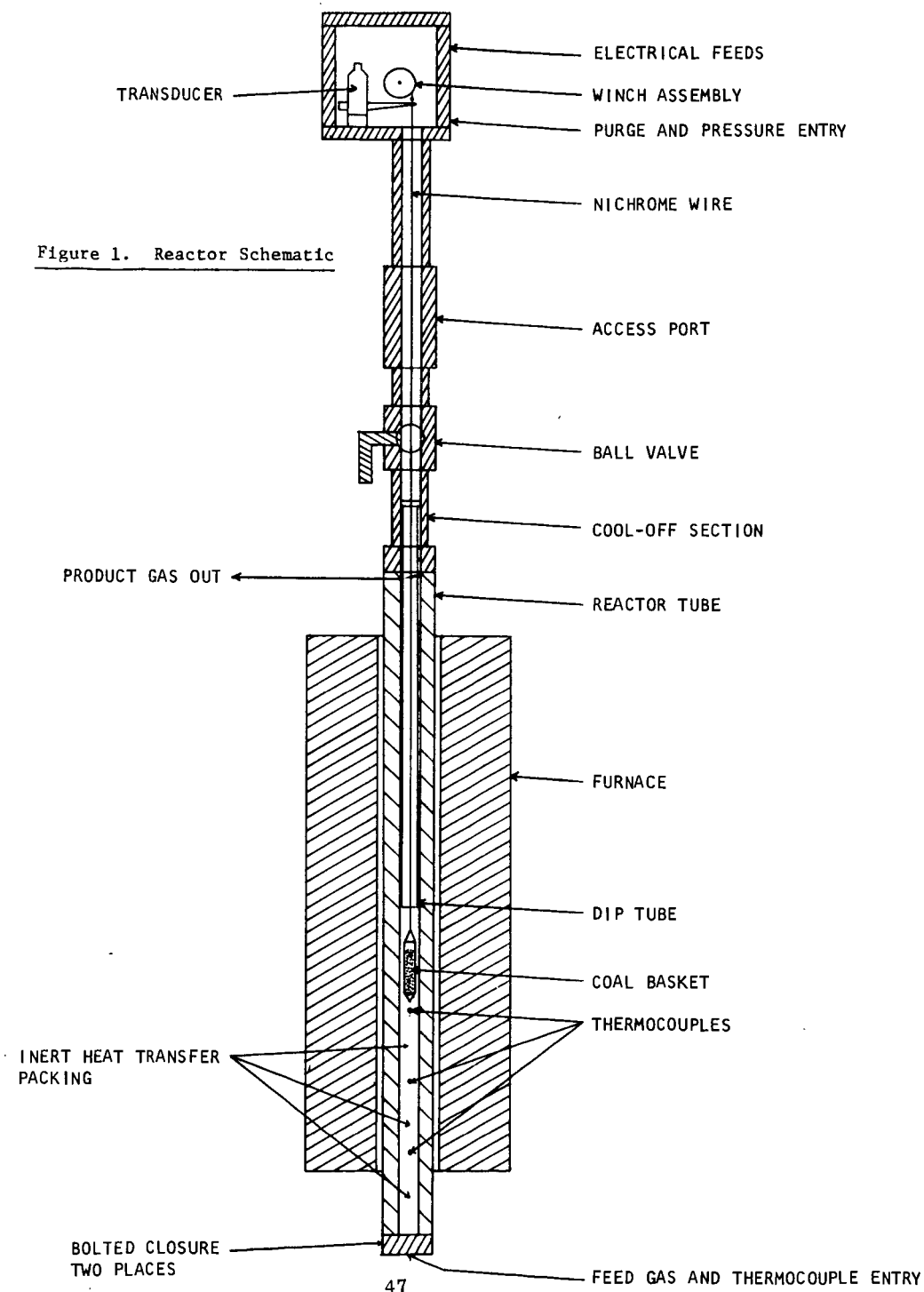


Figure 1. Reactor Schematic

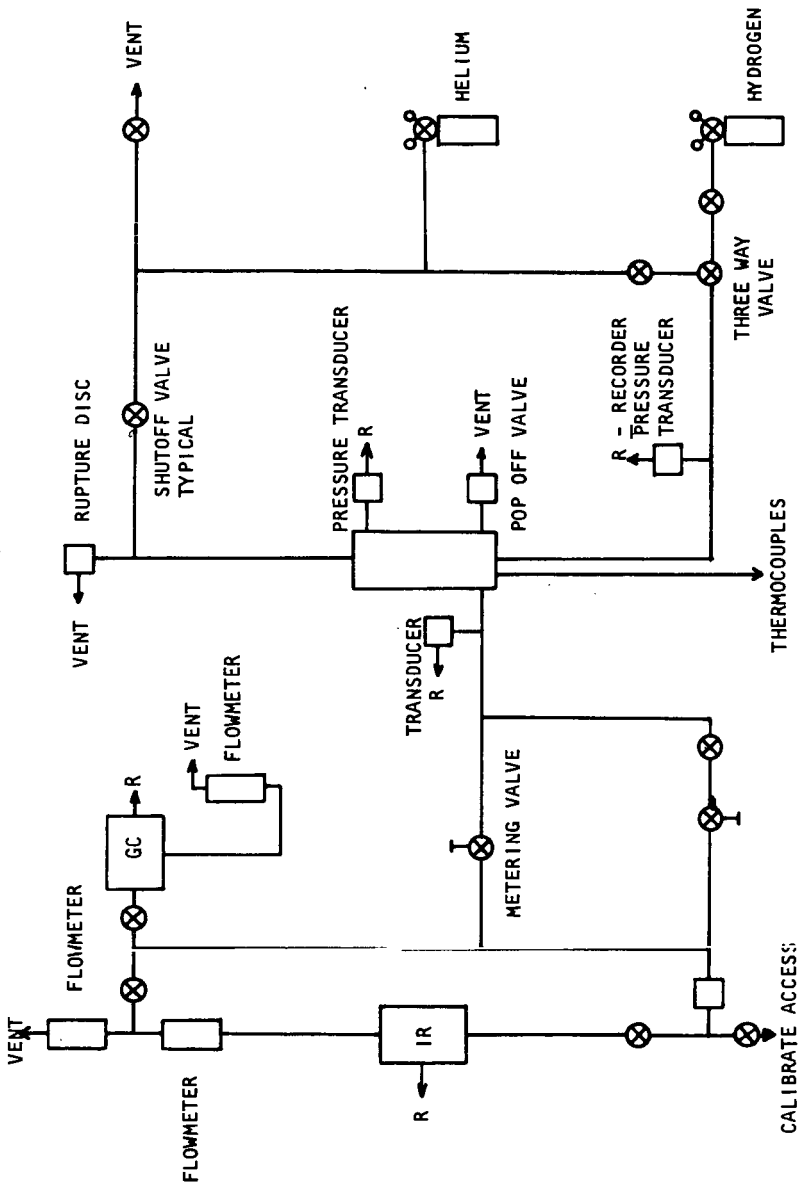


FIGURE 2: SCHEMATIC OF COAL GASIFICATION SYSTEM

All experiments used chars supplied by the Institute of Gas Technology. Char A was a hydrogasified Pittsburgh Seam, Ireland Mine Bituminous coal. Char B was from the same source, but was pre-oxidized (about 1 ft³ of oxygen per pound of fresh coal at 400°C) in an air fluidized bed. An analysis of the two chars is shown in Table I. The char was sized 18 x 35 mesh sieve fraction, U. S. Standard. The sample weight in any given run was 1.5 - 2.5 grams. The sample bucket was constructed of 100 mesh stainless steel screen.

Catalysts were deposited on the char particles by evaporation from solution. Catalysts concentrations were five percent by weight metal. Catalyst distribution on the char was examined by electron microprobe and scanning electron microscopy.

III. RESULTS AND DISCUSSION

Reaction of Non-Catalyzed Chars

Initial runs were performed on both chars to determine non-catalyzed reaction rates. Percent of carbon gasified versus time curves are shown in Figures 3 and 4 for chars A and B, respectively, at 500 and 1000 psi, 950°C. Characteristically, the mass loss curves show high initial reaction rates as the more volatile matter in the char is gasified, followed by a much slower reaction regime where the rate slowly diminishes as the char is consumed. Such phenomena have been previously described by a number of investigators⁽⁷⁻¹¹⁾.

For kinetic analysis of the mass loss data, we propose a model different from those previously discussed. We assume that the reaction rate is given by the following kinetic expression:

$$\frac{dX}{dt} = v_n p_{H_2}^n (1 - X) \exp [-\Delta H^\ddagger / RT] \quad (1)$$

where X = fractional conversion of carbon

v_n = frequency factor

n = order of reaction

ΔH^\ddagger = activation enthalpy for gasification.

In contrast to homogeneous reactions, where activation enthalpies are independent of extent of reaction, hydrogasification activation enthalpies are clearly a function of extent of reaction. One mechanism, postulated by a number of investigators, is based on the carbon structure becoming more graphitic with increasing extent

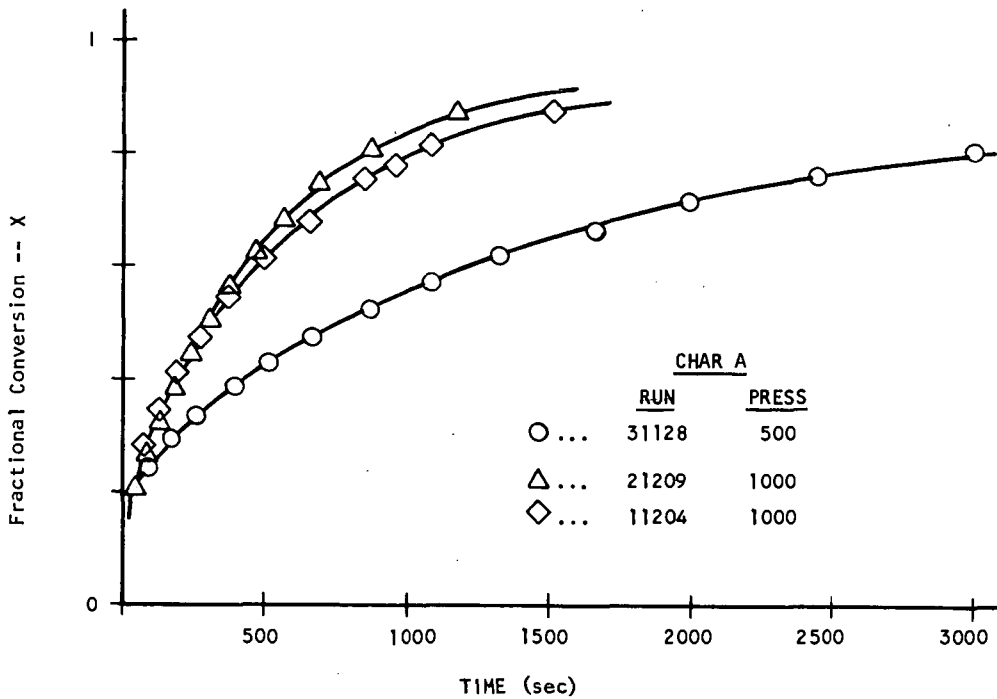


FIGURE 3. NON-CATALYZED HYDROGASIFICATION OF CHAR A AT 500 and 1000 psi, 950°C

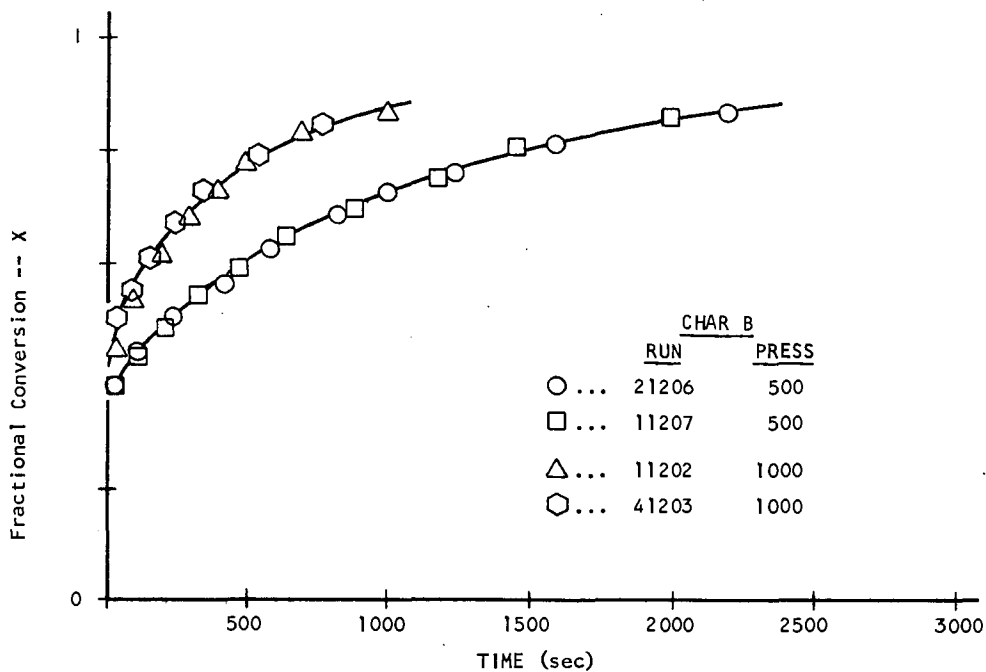


FIGURE 4. NON-CATALYZED HYDROGASIFICATION OF CHAR B AT 500 and 1000 psi, 950°C

of reaction. In the absence of any other information, the simplest function for $\Delta H^\ddagger(X)$ is a linear form

$$\Delta H^\ddagger(X) = \Delta H^0 + \alpha X \quad (2)$$

where

ΔH^0 = initial activation enthalpy

α = factor that determines sensitivity of ΔH^\ddagger to X.

Substituting this expression into equation (1), yields

$$\frac{dX}{dt} = kP_{H_2}^n (1 - X) \exp(-\Delta H^0/RT) \exp(-\alpha X/RT) \quad (3)$$

By lumping the pressure and temperature terms into two constants, Equation (3) can be written in a simpler form in order to test its applicability as a rate expression. Thus,

$$\frac{dX}{dt} = kP_{H_2}^n \exp(-\Delta H^0/RT) \cdot \exp\left(\frac{-\alpha}{RT} \cdot X\right) \cdot (1 - X)$$

and then

$$\frac{dX}{dt} = K \exp(-bX) \cdot (1 - X) \quad (4)$$

where K and b are both constants and equal to

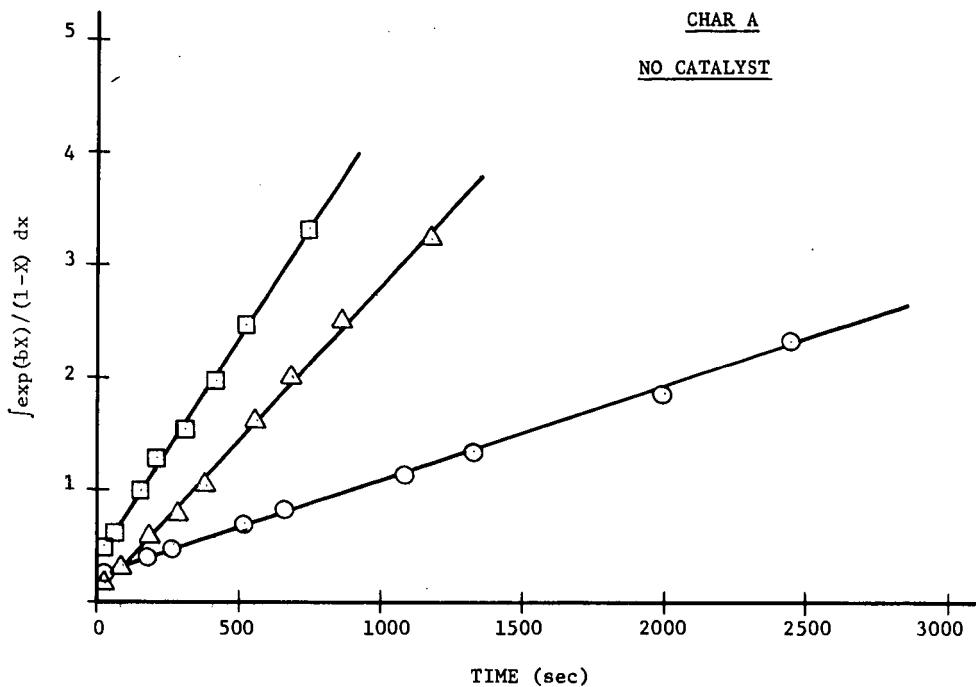
$$K = kP_{H_2}^n \exp(-\Delta H^0/RT)$$

$$b = \alpha/RT$$

Rearrangement and integration of equation (4) gives the final form of the rate expression used to test the kinetic data.

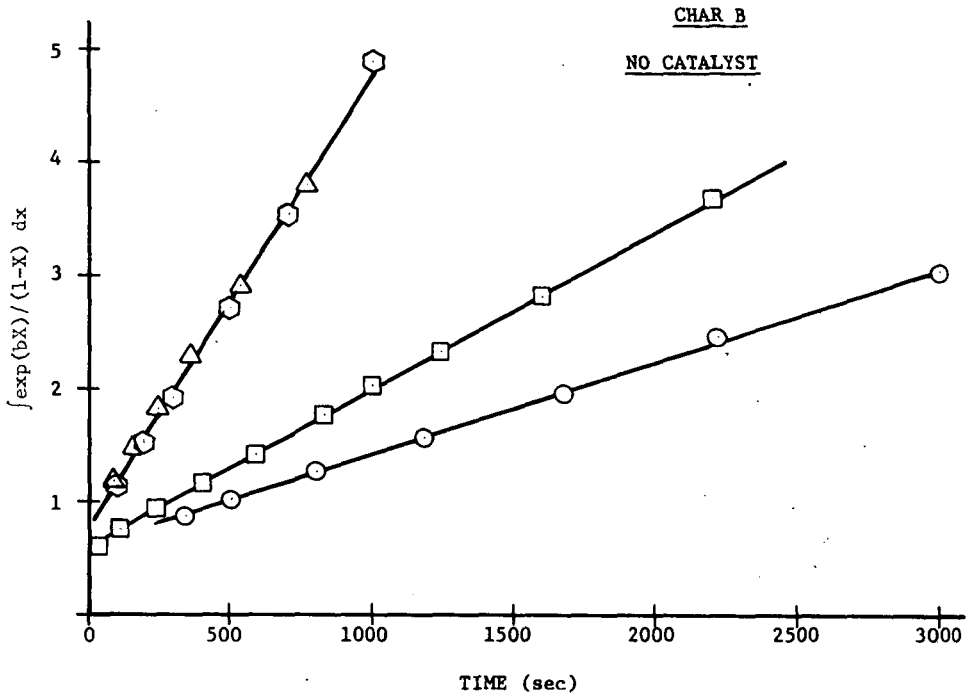
$$\int_0^X \frac{\exp(bX)}{(1 - X)} dX = \int_0^t K dt = Kt \quad (5)$$

Figures 5 and 6 show plots of the integral on the left side of equation (5) versus time for chars A and B, respectively. The parameter b is chosen to minimize the sum of the squares of the



	<u>RUN</u>	<u>PRESSURE</u>	<u>b</u>	<u>K(1/sec)</u>
○...	31128	500	.9	.00081
□...	41121	1000	.8	.00386
△...	21209	1000	.8	.00274

Figure 5. Kinetic Test for the Non-Catalyzed Hydrogasification of Char A at 500 and 1000 psi, 950°C.



	<u>RUN</u>	<u>PRESS</u>	<u>b</u>	<u>K(1/sec)</u>
○ ...	11124	500	1	.000818
□ ...	21206	500	1	.00143
△ ...	41203	1000	1.2	.00386
⬡ ...	11127	1000	0.9	.00399

Figure 6. Kinetic Test for the Non-Catalyzed Hydrogasification of Char B at 500 and 1000 psi, 950°C.

errors of a least square fit to a straight line through the data points. The value of K is then evaluated from the slope of the straight line.

Table II shows the values of b and K determined from Figures 5 and 6.

The values of b are seen to be independent of the hydrogen pressure within experimental error. The ratio of the K values at 1000 and 500 psi, respectively, are for char A, $K_{1000}/K_{500} = 3.27$ and for char B, $K_{1000}/K_{500} = 2.89$. The hydrogen pressure appears in the K term raised to the power n, where n is the order of the reaction. Thus, the hydrogasification reaction order is approximately 1.6 in hydrogen pressure.

The y-axis intercept in Figures 5 and 6 should have been zero. The positive non-zero intercept results from the very rapid first stage of the hydrogasification reaction. For the pre-oxidized char B, the amount of carbon gasified in the rapid first stage of the reaction is greater than that for the hydrogasified char. This effect is due to the pretreatment of the char. In the second, slower part of the reaction, however, the chars behaved almost identically as indicated by similarity in the values of b and K.

Figure 7 shows the fraction of carbon gasified as a function of time for char B at 850 and 950°C, 1000 psi. The values of K and b at 850°C were found to be 2.3 and $.00128 \text{ sec}^{-1}$, respectively. From the variation of K with temperature, the value of ΔH^0 can be estimated to be 29.3 kcal/mole. The activation enthalpy is then given by

TABLE II
 TABULATION OF b AND K VALUES FOR
 NON-CATALYZED CHAR A AND B

Char A (hydrogasified)					
500 psi H ₂			1000 psi H ₂		
Run	b	K	Run	b	K
11122	0.25	0.000974	41121	0.8	0.00386
31128	0.9	0.000810	21209	0.8	0.00274
Average	0.57	0.000892	11204	0.8	0.00212
			Average	0.8	0.00291
Char B (pre-oxidized)					
500 psi H ₂			1000 psi H ₂		
Run	b	K	Run	b	K
11124	1	0.000818	11127	0.9	0.00399
21206	1	0.00143	31209	0.8	0.00290
11207	1	0.00147	41203	1.2	0.00386
31207	0.5	0.00125	11202	1.2	0.00406
Average	0.88	0.00124	Average	1.025	0.00372

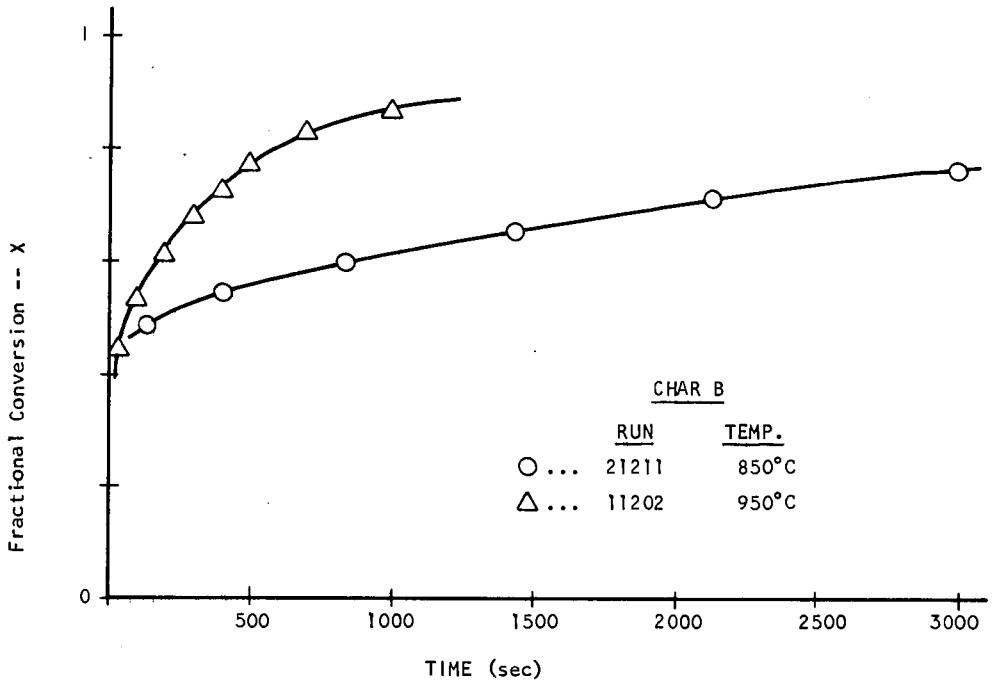


FIGURE 7. EFFECT OF TEMPERATURE ON THE NON-CATALYZED HYDRO-GASIFICATION OF CHAR B AT 850 and 950°C, 1000 psi

the expression,

$$\Delta H^\ddagger \frac{\text{kcal}}{\text{mole}} = 29.3 + 2.43 X \quad (6)$$

for an uncatalyzed char system.

Figure 8 shows a representative composite plot of the carbon fraction converted, the methane rate of production, and the temperature versus time for char B, Run 11128. The concentration of methane in the product stream is proportional to the rate of the hydrogasification reaction, as

$$r = \frac{dP_{\text{CH}_4}}{dt} = \frac{1}{12} \frac{1}{n_c} \left(\frac{dV}{dt} \right) \frac{P_{\text{CH}_4}}{RT} \quad (7)$$

where r = rate (moles/minute/initial gms. of carbon)

n_c = initial moles carbon

P_{CH_4} = partial pressure CH_4 in atms

R = gas constant in L - atm/M - °K

T = temperature, °K

$\left(\frac{dV}{dt} \right)$ = product gas flow rate in liters/minute.

Equation (7) can be integrated numerically. The result is shown in Figure 9.

Although the infrared measurement of methane production leads to qualitative agreement with the direct mass determination, quantitative agreement is not good. This is most probably due to axial dispersion in the gas product stream, which results in a loss of kinetic information, and difficulties in precisely regulating the product stream flow rate, which would lead to cumulative errors.

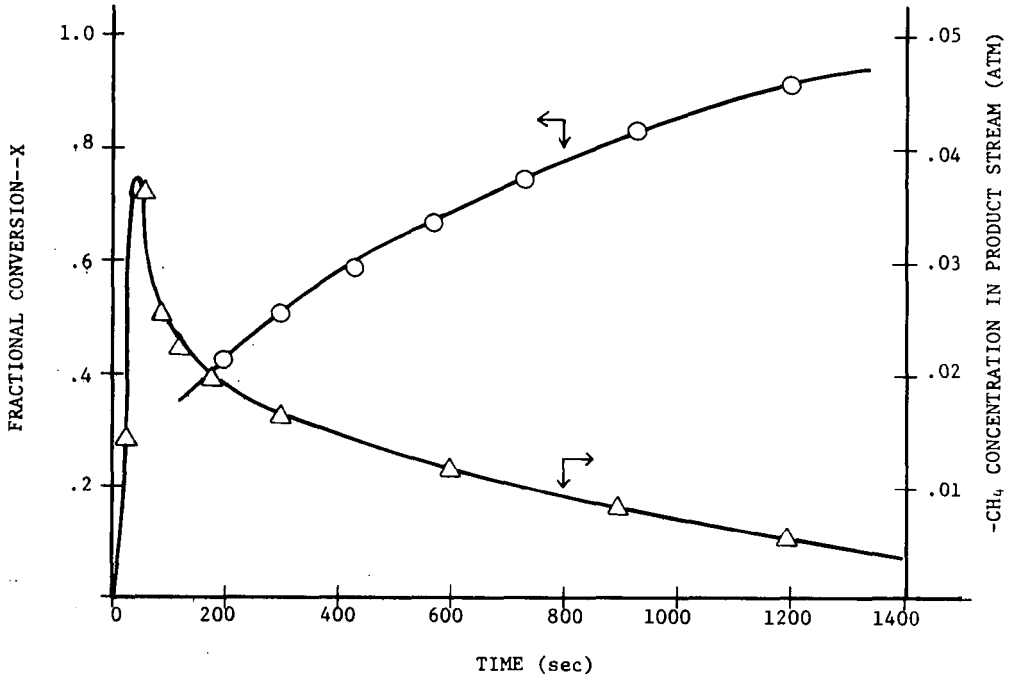
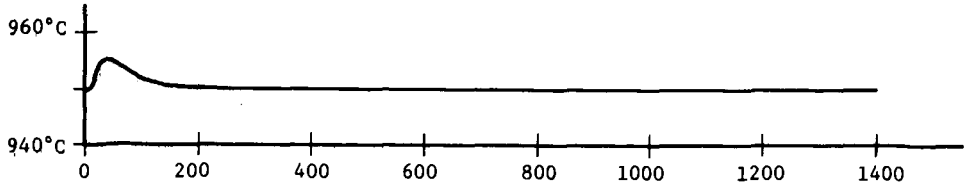


Figure 8. Composite Plot of Rate Data for KHCO_3 Catalyzed Char B, Run 11128, at 500 psi and 950°C .

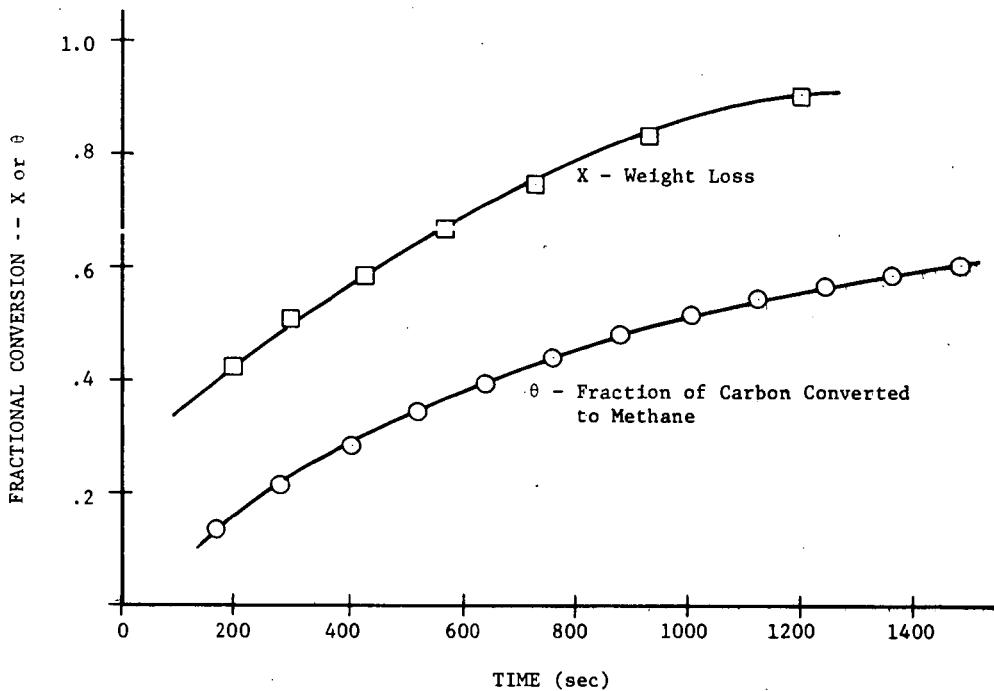


Figure 9. Fractional Conversion of Carbon to Methane for KHCO_3 Catalyzed Char A at 500 psi, 950°C .

The temperature versus time curve shown in Figure 8 indicates a small temperature increase resulting from the exothermic hydrogasification reaction, which diminishes with time. Unfortunately, the actual temperature of the char has not been measured directly.

Reaction of Catalyzed Chars

In this preliminary study we have concentrated on catalysts that have long been known to accelerate the hydrogasification reaction, the alkali metals and zinc salts⁽⁵⁾. Figures 10 and 11 show the percent carbon gasified versus time data for a KHCO_3 catalyst deposited on chars A and B, respectively, at 950°C , 500 and 1000 psi. Figures 12 and 13 show a representative comparison between the carbon converted in catalyzed and non-catalyzed runs on chars A and B, respectively, at 500 psi and 950°C . A substantial catalytic effect is observed. The time to achieve a gasification fraction X is roughly halved by the KHCO_3 catalyst. The kinetic analysis for the parameters b and K are shown in Figures 14 and 15. The kinetic equation (4) is seen to fit the data at high conversions. The evaluation of the b and K parameters for KHCO_3 catalyzed reactions is shown in Table III.

The rate enhancement due to the catalysts is shown by the evaluation of α from the parameter b. Taking -1 to be the average value of b for a catalyzed system, the corresponding value of α is -2.43. This term makes the linear expression for the activation enthalpy decrease with increasing carbon gasification

$$\Delta H^\ddagger \text{ (kcal/mole)} = 29.3 - 2.43 X .$$

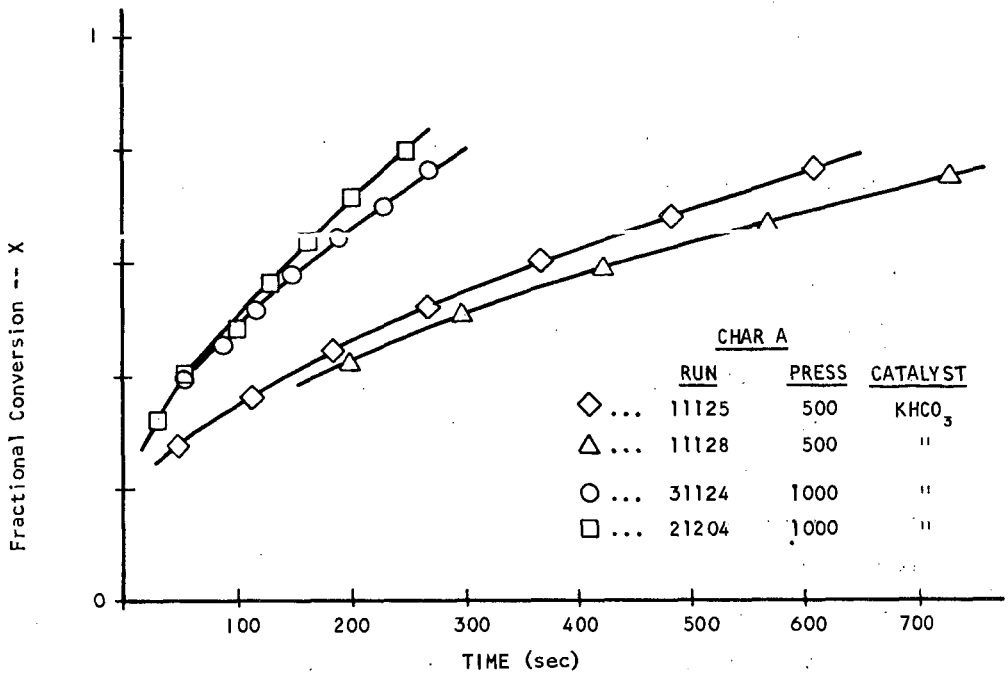


FIGURE 10. CATALYZED HYDROGASIFICATION OF CHAR A AT 500 and 1000 psi, 950°C

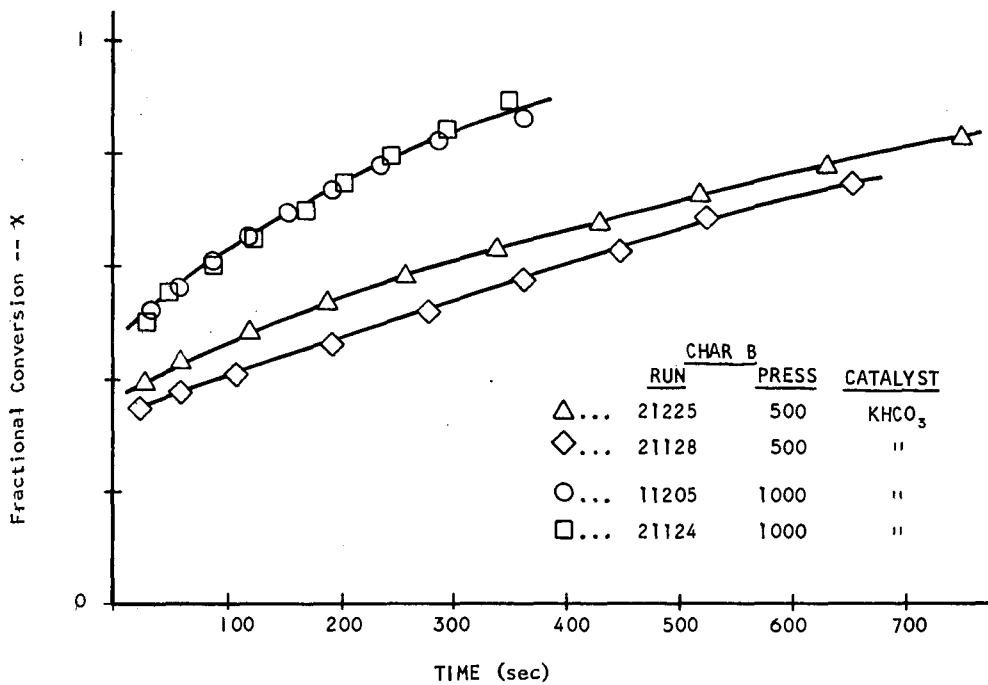


FIGURE 11. CATALYZED HYDROGASIFICATION OF CHAR B AT 500 and 1000 psi, 950°C

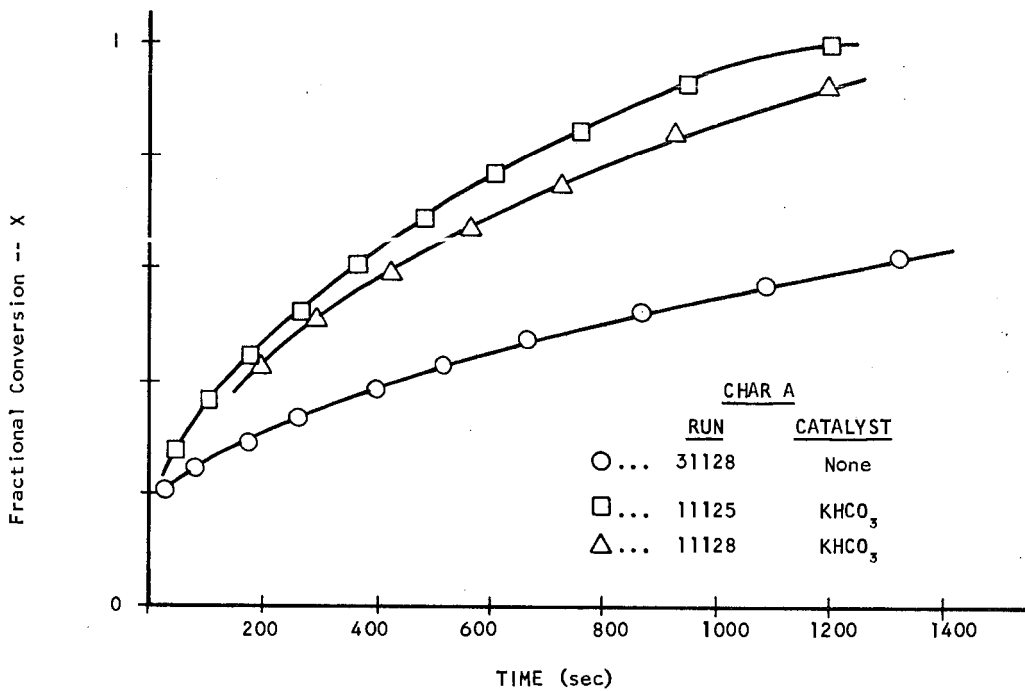


FIGURE 12. COMPARISON OF THE CATALYZED AND NON-CATALYZED HYDROGASIFICATION OF CHAR A AT 500 psi, 950°C

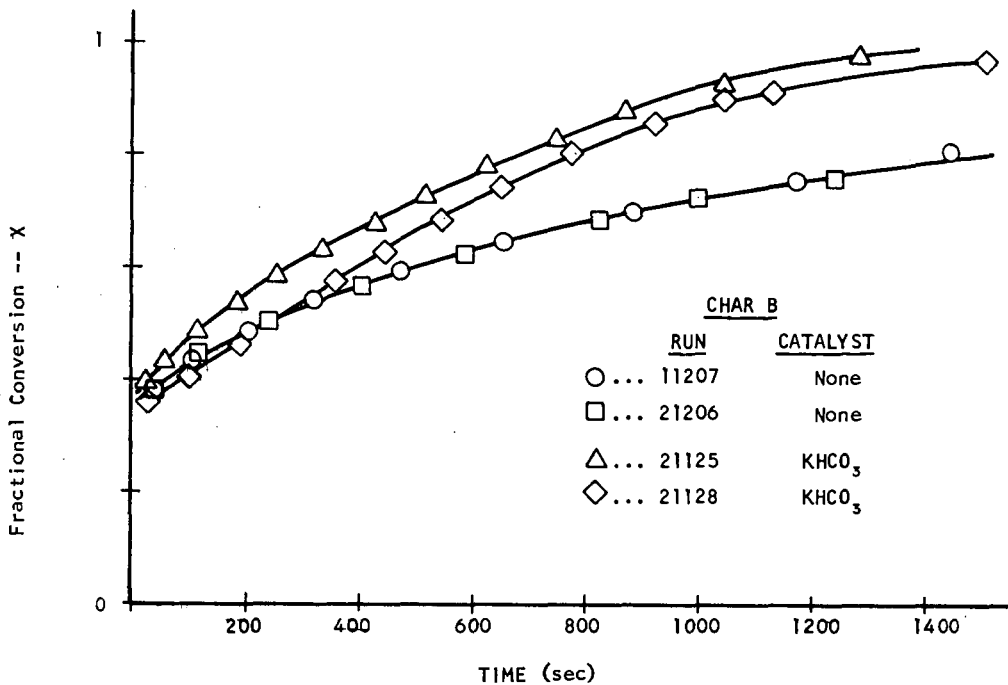
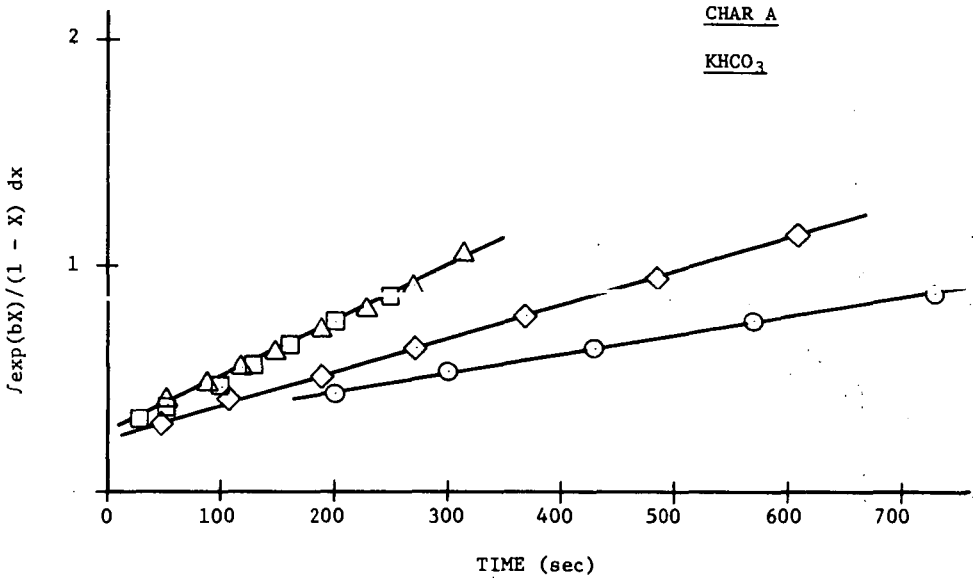
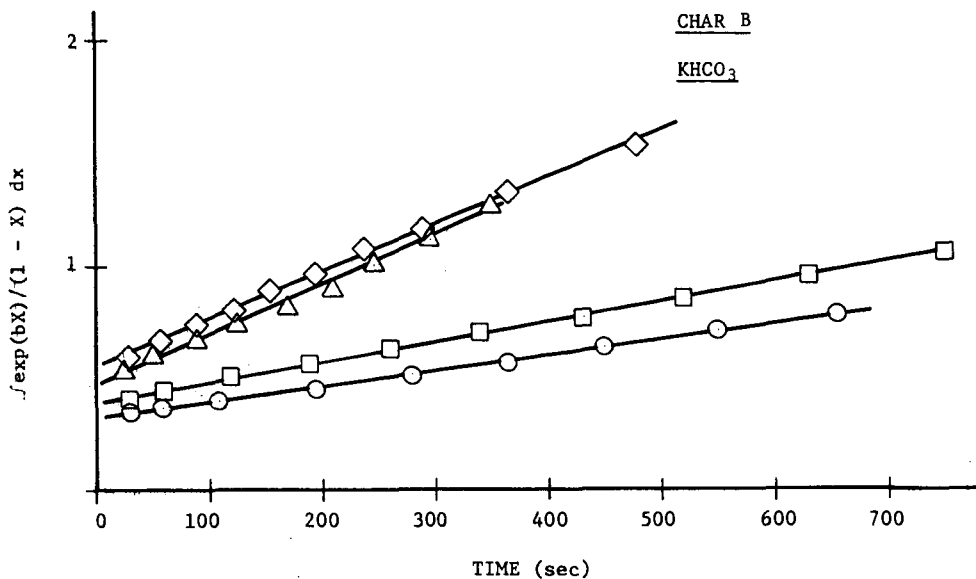


FIGURE 13. COMPARISON OF THE CATALYZED AND NON-CATALYZED HYDROGASIFICATION OF CHAR B AT 500 psi, 950°C



	<u>RUN</u>	<u>PRESSURE</u>	<u>b</u>	<u>K(1/sec)</u>
○...	11128	500	-1.0	.000877
◇...	11125	500	-0.5	.00150
△...	31124	1000	-1.0	.00236
□...	21204	1000	-1.3	.00252

Figure 14. Kinetic Test for the KHCO_3 Catalyzed Hydrogasification of Char A at 500 and 1000 psi, 950°C.



	<u>RUN</u>	<u>PRESSURE</u>	<u>b</u>	<u>K(1/sec)</u>
○ ...	21128	500	-1.3	.000712
□ ...	21125	500	-1.0	.000903
△ ...	21124	1000	-1.0	.00218
◇ ...	11205	1000	-0.75	.00221

Figure 15. Kinetic Test for the KHCO_3 Catalyzed Hydrogasification of Char B at 500 and 1000 psi, 950°C .

TABLE III

TABULATION OF b AND K VALUES FOR
CHAR A AND B CATALYZED WITH KHCO_3

Char A (hydrogasified)					
500 psi H_2			1000 psi H_2		
Run	b	K	Run	b	K
11128	-1.0	0.000877	11208	-0.3	0.00224
11125	-0.5	0.0015	21204	-1.3	0.00252
Average	-0.75	0.00119	31124	-1.0	0.00236
			Average	-0.867	0.00237

Char B (pre-oxidized)					
500 psi H_2			1000 psi H_2		
Run	b	K	Run	b	K
21128	-1.3	0.000712	21124	-1.0	0.00218
21125	-1.0	0.000903	11205	-0.75	0.00221
Average	-1.15	0.000807	Average	-0.88	0.00219

Work has also begun on the catalysts potassium carbonate, K_2CO_3 , and zinc chloride, $ZnCl_2$. These catalysts were also deposited by impregnation at a five percent by weight metal concentration. The K_2CO_3 catalyst behaved very similar to the $KHCO_3$. The weight loss curves for this catalyst at 500 and 1000 psi, $950^\circ C$ are shown in Figure 16. Kinetic analysis of this catalyst produced values of b and K similar to those for $KHCO_3$ (see Table IV).

Microscopy of the Chars

Characterization of the chars is being carried out on the microprobe analyzer and the scanning electron microscope. Features such as particle structure, catalyst distribution, and structural change at the catalyst sites during reaction are of interest.

The scanning electron microscope can take high magnification, high resolution pictures of the char particles, while the microprobe analyzer can be calibrated to scan for any element on the char particle surface.

Presented here will be a cross section of representative photos for each char. Proper interpretation of these pictures is important. The scanning micrographs (scanning electron micrographs) are high quality pictures but are often slightly distorted at low magnification (75-100X). The back scattering electron micrographs (BSE) and x-ray micrographs are all taken on the microprobe analyzer. The BSE micrographs from this instrument are of low clarity because the microprobe was designed to do x-ray analysis. An x-ray micrograph is a scattering of white dots on the picture. If the element

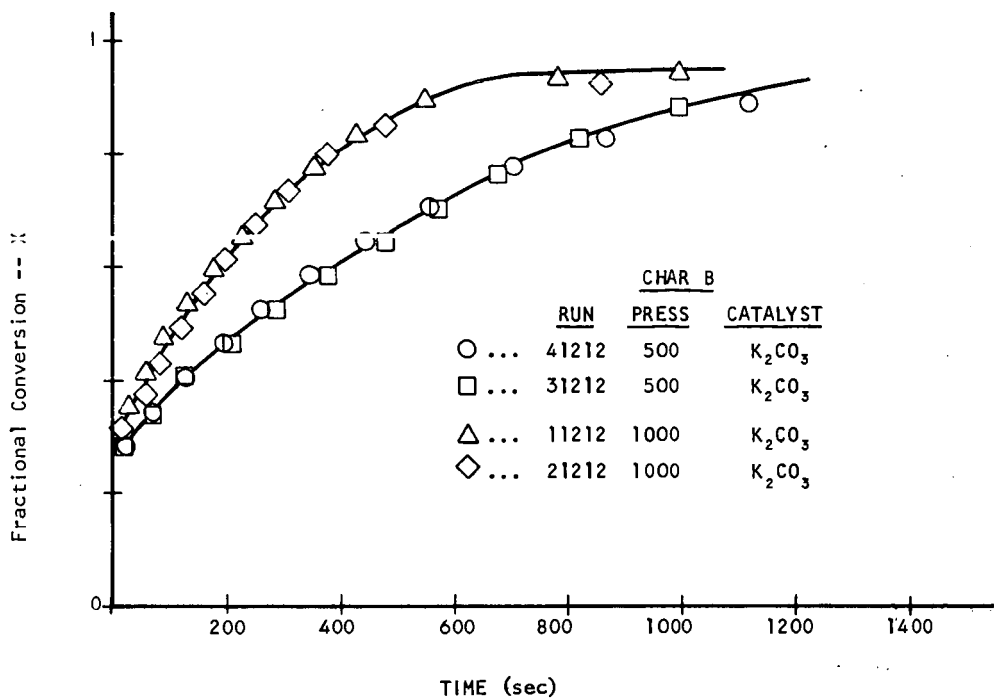


FIGURE 16. CATALYZED HYDROGASIFICATION OF CHAR B AT 500 and 1000 psi, 950°C

TABLE IV
 TABULATION OF b AND K VALUES FOR CHAR A AND B
 CATALYZED WITH OTHER CATALYSTS

Char A (hydrogasified - ZnCl ₂)					
500 psi H ₂			1000 psi H ₂		
Run	b	K	Run	b	K
21214	0.5	0.00160	21208	0.5	0.00492
31214	0.25	0.00140	51208	0.2	0.00301
Average	0.37	0.00150	Average	0.35	0.00397

Char B (pre-oxidized - K ₂ CO ₃)					
500 psi H ₂			1000 psi H ₂		
Run	b	K	Run	b	K
41212	-0.15	0.00155	21212	-0.5	0.00245
31212	-1.2	0.000867	11212	-0.5	0.00248
Average	-0.67	0.00118	Average	-0.5	0.00247

being analyzed is not present, there is an even, but sparse distribution of white dots on the micrograph. (See upper right of Figure 20d where there is no iron present.) This artifact of the analyzer will be referred to as background. The locations where the element being analyzed is present, are then represented by a concentration of white dots. (See also Figure 20d.)

Figure 17a shows a low magnification scanning micrograph of the hydrogasified, KHCO_3 catalyzed char A. This is a representative picture of this type of a char, catalyzed or uncatalyzed. The particle surface is, in general, crumpled but smooth.

Higher magnification micrographs of the center of this particle are shown in Figures 17b and 17c. (See the area circled in Figure 17a.) These are both of the same area on the particle. Figure 17b is a scanning micrograph while 17c is a BSE micrograph. Figure 17d is the iron x-ray superimposed on the BSE of Figure 17c. This shows areas of the particle surface where iron deposits or ash concentrations are located. A close-up of the ash deposit circled in Figure 17b or 17c is shown in Figure 18a.

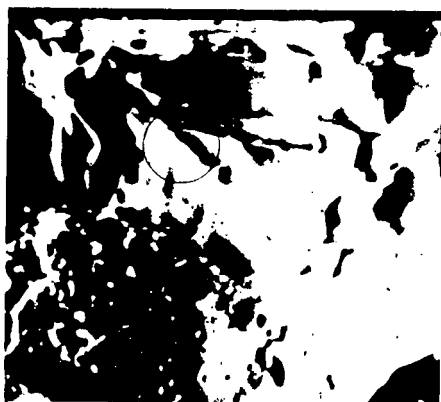
Figure 18b shows a potassium x-ray superimposed on the BSE of Figure 17c, which is KHCO_3 catalyzed char A. The heavy but even concentration of white dots indicates that the catalyst is present in a well-distributed manner. The catalyst must exist on the particle surface in a finely divided state since there are no distinguishable clumps, as noticed in earlier catalytic x-ray analysis.



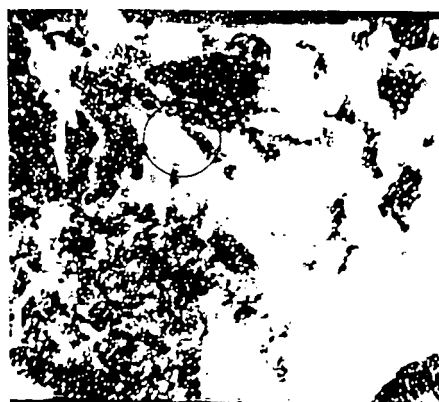
a. Scanning - 75X



b. Scanning - 300X



c. BSE - 200X



d. Iron X-ray on BSE - 200X

Figure 17. Micrographs of KHCO_3 Catalyzed Char A



a. Scanning - 2000X



b. Potassium X-ray on BSE - 200X



c. Cut Particle - Scanning - 100X



d. Cut Particle, Potassium X-ray
on BSE - 200X

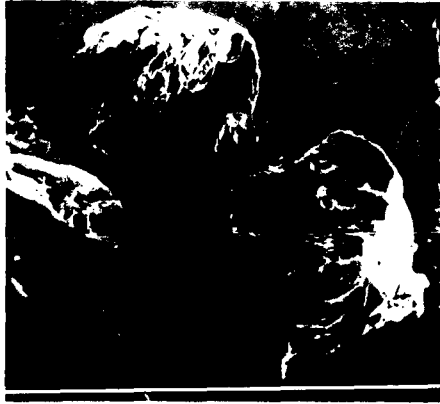
Figure 18. Micrographs of KHCO_3 Catalyzed Char A

The scanning micrograph of a cut particle of char A similar to that in Figure 17a is shown in Figure 18c. The inside of the particle is filled with cavities or cells, somewhat like a sponge. This is very different from the outer surface of the particle. The pretreatment skin⁽¹²⁾, or outer surface, and the resulting inner structure are a direct result of the pretreatment history of the char. A potassium x-ray on a BSE micrograph of the area circled in Figure 18c is shown in Figure 18d. This too shows a heavy catalyst concentration.

The pre-oxidized, uncatalyzed or catalyzed char B appears very similar to char A. Direct comparisons of the same type of outer and inner structure can be drawn from Figure 19a and 19b for char B and Figure 17a and 18c for char A. These are the same chars but have undergone different pretreatment histories.

Direct similarities of ash content can be shown with the scanning micrographs of a particle reacted in hydrogen for eight minutes. Figure 20a and 20b show a portion of an uncatalyzed particle with the close-up of an ash deposit in Figure 20b. This can be verified with the results of Figure 20c and 20d, which are the iron x-ray and BSE micrographs of the same area in Figure 20a. In these same areas lighter concentrations of potassium and silicon have also been found.

The analysis of the KHCO_3 catalyzed char B showed a good distribution, which was similar to that of char A. (See Figure 18b for char A.)



a. Cut Particle, Scanning - 75X



b. Whole Particle, Scanning - 200X

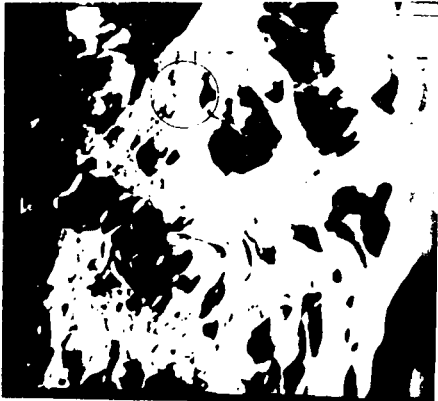
Figure 19. Micrographs of Uncatalyzed Char B



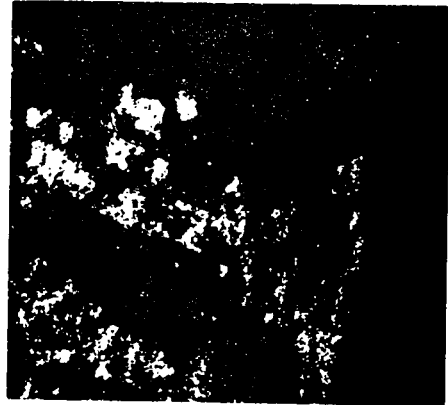
a. SEM - 500X



b. SEM - 2000X



c. BSE - 200X



d. Iron X-ray - 200X

Figure 20. Micrographs of Uncatalyzed Char B

The high iron content is a common characteristic of the two chars and is seen in the x-ray analysis. These chars also have a high sulfur content, which is distributed fairly evenly in the particles. Analysis for zinc and nickel were negative, and slight traces of calcium have been seen in some samples.

IV. CONCLUSIONS

The initial studies of catalysts and contacting systems has begun at Case Western Reserve University. The high temperature, high pressure, recording thermobalance has made direct kinetic analysis of the carbon weight loss curves straightforward.

The data seems to be well represented by the kinetic model proposed in equation (5). Analysis of the fitting parameters for this model show that for the rate dependence on pressure the order of the reaction is about 1.6.

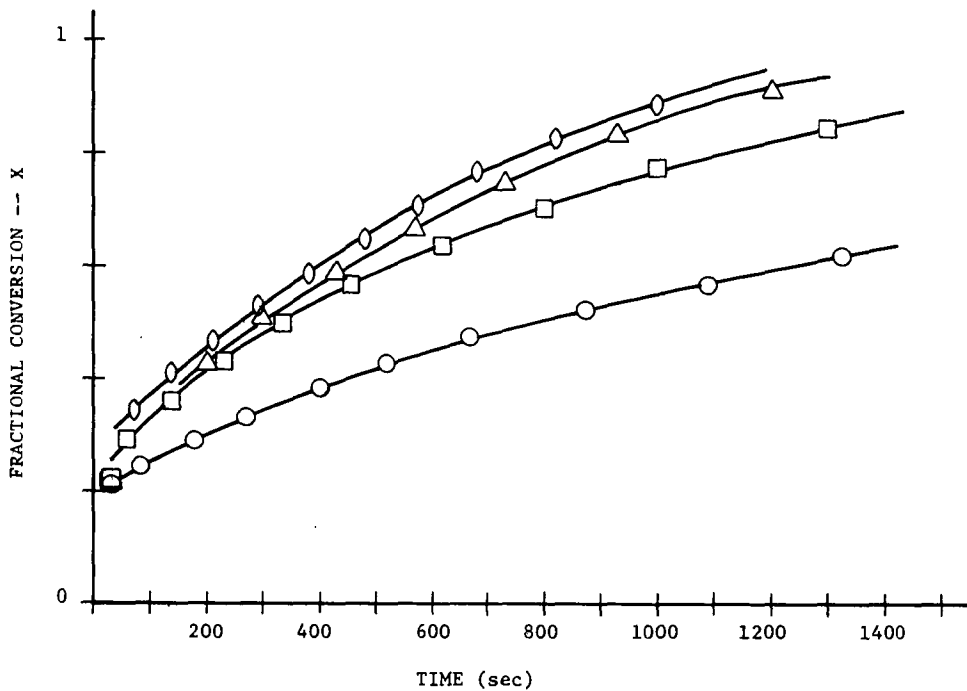
The temperature dependence of the rate constant determines the initial activation enthalpy. The initial activation enthalpy is about 29.3 kcal/mole. Coupling this with the evaluation of the parameter b from the kinetic model we have found the linear form of the activation enthalpy as a function of conversion for a non-catalyzed char. (See equation (6).)

Some information of the relative volatilities of the two chars is discernable from the y-axis intercept in the plots of the kinetic test for our rate expression. This is the portion of the weight loss curves where the rapid first stage of the reaction is taking place. The application of the kinetic model then precedes from the latter part of these curves, which represent the second, slower part of the reaction. Unfortunately, this semi-empirical model leaves us with the lack of a real mechanism. Possibilities of

ash diffusion and/or chemical effects have not been studied in the detail necessary to shed light upon the subject.

The catalytic systems showed substantial slope increases in the weight loss curves (Figure 21). It was found that KHCO_3 and K_2CO_3 exhibited an equivalent catalytic effect which was better than that found for ZnCl_2 (see values of b in Table IV). The net result of the catalytic systems on our kinetic model was to change the value of the parameter b , which changed the value of α in the linear expression for the activation enthalpy. For the KHCO_3 system the value of α for an average value of $b = -.91$ was $\alpha = -2.21$. The catalyst apparently did not affect the value of ΔH° over the course of the reaction.

Microscopy of the char samples is yielding interesting and qualitative information. Characterization of char structure with the scanning electron microscopy has shown the standard pretreatment skin and the celled particle interior. X-ray analysis of the same particles in the microprobe analyzer and the SEM have shown ash deposits on the surface of the char and good catalyst distributions.



	<u>Run</u>	<u>Char</u>	<u>Catalyst</u>
○ ...	31128	A	none
□ ...	21124	A	ZnCl ₂
△ ...	11128	A	KHCO ₃
◇ ...	31212	B	K ₂ CO ₃

Figure 21. Comparison of Various Char-Catalyst Systems at 950°C and 500 psi.

REFERENCES

- (1) Dent, F. J., Blackburn, W. M., and Millett, H. C., *Trans. Inst. Gas Engrs.*, 87, 231 (1937)
- (2) Friedman, S., Kaufman, M. L., and Wender, I., *J. Org. Chem.*, 36, 694 (1971)
- (3) Weller, S., and Pelipetz, M. G., *Ind. & Eng. Chem.*, 43, 1243 (1951)
- (4) Dent, F. J., Blackburn, W. H., and Millett, H. C., *Trans. Inst. Gas Engrs.*, 88, 150 (1938)
- (5) Wood, R. E., and Hill, G. R., *ACS Division of Fuel Chemistry*, Vol. 17, No. 1, Aug. 1972
- (6) Feldkirchner, H. L., and Johnson, J. J., *Rev. Sci. Instr.*, 39, No. 8, 1227, Aug. 1968
- (7) Blackwood, J. D., and McCarthy, D. J., *Aust. J. Chem.*, 19, 797 (1966)
- (8) Moseley, F., and Paterson, D., *J. Inst. Fuel*, 38, 13 (1965)
- (9) Feldkirchner, H. L., and Linden, H. R., *Industr. Eng. Chem.*, 2, 153 (1963)
- (10) Johnson, J. J., *Seminar on Characterization and Characteristics of U.S. Coals for Practical Use*, Pennsylvania State University, 1971
- (11) Hiteschue, R. W., Friedman, S., and Madden, R., *U.S. Bureau of Mines, Reports of Investigation*, Nos. 6027 and 6125, 1962
- (12) Gould, R. F., Ed., *Fuel Gasification*, *Advances in Chemistry Series*, 69, American Chemical Society, 1967

ACKNOWLEDGEMENTS

We gratefully acknowledge the American Gas Association's support under Contract No. BR-75-1.

The thermobalance was made available by Consolidated Natural Gas Service Company, Inc., without which this work would have been impossible.

Special thanks are given to Raymond R. Cwiklinski and Donald C. Grant for their technical assistance.

Liquefaction Study of Several Coals and a Concept
For Underground Liquefaction

Duane R. Skidmore
and
Calvin J. Konya

West Virginia University
School of Mines
213 White Hall
Morgantown, West Virginia

Introduction

In the past, underground coal conversion processes were uneconomical in comparison with cheap energy alternatives or not feasible technically. Some recent changes in technology and economics may have improved the feasibility of underground coal conversion. The selling prices of conventional fossil fuels have been rising because of restricted supply and increasing demand. The price increases should have four effects: (1) the producers of gas and oil are encouraged to find additional sources, (2) the users of these convenient fuels are motivated to restrict their consumption, (3) coal mine operators are inclined toward opening more conventional mines and (4) concepts for alternative energy sources such as underground coal conversion become more attractive for serious engineering evaluation.

The rise of concern for the health and safety of the miners is another factor influencing this renewal of interest in remote coal conversion. Not only have the human costs of conventional mining been large as represented by loss of lives or adverse effects on health but economic costs of industrial accidents have proven considerable. During the summer of 1972 the dreaded pneumoconiosis or "black lung" was the subject of a survivor's benefits bill passed by the U. S. Government in the amount of one billion dollars. The implementation of legislation to protect the health and safety of miners reflects social and economic concern.

The policy alternatives for elimination of energy shortages have been severely restricted by environmental regulations. Surface or strip mining of coal is under severe federal restriction and risks more regulations on the state and federal levels. The spoil banks which result from strip mining, particularly in the eastern United States, have not been reclaimed properly. Siltation of streams has resulted and fish have been killed. Silt has plugged channels and backed up waters to flood areas previously available for recreation and farming. In regions containing high sulfur coal, the streams have become acidic; and additional aquatic life is killed. Public outrage has been predictable.

The need for new technology to extend the coal reserves of the Nation does not and probably should not have a high industrial priority. Domestic coal reserves have been variously estimated but usually are deemed capable of sustaining present total national energy demands for 800 to 4000 years. New technology to utilize coal resources which are presently uneconomical to mine, however, would extend the recoverable energy from a given property and might therefore be worth an intensive research and development effort. The seams of particular interest include those which are low in sulfur and are too deep or too thin for exploitation by presently available methods.

Remote underground coal mines have been developed in northern Europe. As a result, the industry there has become even more increasingly capital intensive. One drawback to this alternative in the United States is that the coal mining industry has had difficulty in borrowing substantial amounts of money for long

time periods at low interest rates. Until the recent shortages of energy became well known and segments of the oil industry entered the coal mining industry, acquisition of equity capital had also been difficult. Some reluctance for stock purchase has been traced to uncertainties over oil import policy and environmental regulations. Furthermore, the European concept requires men underground for equipment maintenance. Finally, some questions have been raised in this country about the acceptability of underground mining for rapid implementation under existing work rules and union contracts.

With the changes in economic and social climate, the United States Bureau of Mines in cooperation with a subsidiary of the Union Pacific Railroad has reopened development work on underground coal gasification.

History

The first reference to underground coal gasification is dated 1868.⁽¹⁾ The most extensive effort occurred in the Soviet Union from the 1930's to about 1960. Premier Stalin had apparently promised the miners some relief from difficult working conditions and had developed underground gasification technology in partial fulfillment of his promise. Some time after Stalin's death, the effort was quietly dropped, probably because extensive oil and natural gas discoveries made underground gasification uneconomical.

The most recent tests in the United States by the Bureau of Mines have defined two main problem areas. The product gas must be confined to the reaction zone and removed under controlled conditions. This implies that an impervious bed of rock must overlay the coal seam. The product gas must be useful for high value energy production. In most circumstances, this would require electrical power generation. Since the gas from underground conversion technology has had low heating value (less than 100 BTU/SCF). The need is obvious for technology to upgrade the product. No previous published work in underground conversion of coal to liquid has been found.

Issues

Underground coal liquefaction concepts include several which are adapted from underground coal gasification. In the blind borehole-backfill system for underground gasification, a simple well is drilled vertically to the coal seam and then horizontally for some distance through the coal. The well is then doubly piped by a smaller diameter pipe within a larger one. Reactants are introduced through the central pipe and products are withdrawn through the outer annulus. The piping system is withdrawn as coal is used up. A void is produced by coal removal and the empty volume is filled with a water or solid waste rock fill material. The blind borehole-backfill system has been recommended for thin coal seams by the USBM report on underground coal gasification.

For somewhat thicker seams, the branched borehole-backfill system has been visualized. The borehole is branched after entering the coal seam so that the reactants can be admitted into the bottom of a seam and products withdrawn from the top. Proper downhole baffling arrangements are required.

Very thick seams lend themselves to the vertical blind borehole-fill system during which the concentric feed and product pipes are withdrawn vertically upward as the coal is produced. Fill from the feed pipe or another piping system readily accumulates in the exhausted volume. Each of the single borehole systems has a multiple borehole counterpart.

Use of a single well for feed reactants and for withdrawal of products obviates the need for connecting separately drilled wells. Boreholes can be connected underground by hydraulic fracturing, explosive fracturing and various modifications of

drilling or electro-linking. Some of these techniques have been successful for gas and petroleum field exploitation and underground coal gasification. Their particular disadvantage for use in underground coal conversion systems lies in the relatively rapid exhaustion of the hydrocarbon reservoir and the need for repeated practice of the linking procedure.

In remote mining schemes, the delivery of hot, hydrogen-donor solvent to the coal is a necessity. The solvent is hydrogenated conventionally and introduced while still hot into the reaction zone underground.

One of the principal problems underground is to maintain the solution temperature in the reaction zone. The total heat to be supplied provides (1) the heat of vaporization for the solvent, (2) the energy to pressurize the solvent vapor in the reaction zone in order to prevent excessive volatilization of the liquid solvent and to activate the solvent for the hydrogen transfer reaction, (3) the activation energy for the coal surface so that the reaction may proceed at an adequate rate, (4) losses to the surrounding rock, and finally (5) losses incurred when the reaction zone has passed and filling or flooding occurs.

The reaction itself is considered to proceed through at least two important thermal stages. First, the coal structure is thermally activated so that pyrolytic cracking or chain breaking of hydrocarbons occurs. Later, hydrogen atoms are released from the donor solvent and added to the coal fragments. Between the first and second phase a gel reaction may occur. During gelation ($\sim 350^{\circ}\text{C}$) the coal and solvent form a viscous composite with high resistance to flow. The advantages of maintaining or establishing low slurry viscosities are obvious so that removal of coal is best effected either before or after the gelation step.

Further Set of Issues Involved

The design of an underground liquefaction process requires definition of (1) the types of coal seam most likely to be leached or liquefied by the physical arrangements suggested above and (2) the solvent or slurry material which would be most effective. Work was undertaken at West Virginia University to define the behavior of different types of coal monoliths exposed to several solvents under conditions possible for achievement underground.

Apparatus and Procedure

The test apparatus was a 750 ml carbon steel autoclave fitted with a Bourdon pressure gauge and a thermocouple well. Closure was effected by a gasket and flange arrangement. Gas inlet and exit lines permitted the autoclave to be flushed with nitrogen. No hydrogen was used. Heat was supplied by a large laboratory Bunsen burner. Reproducibility of heating rate is seen in Figure 1. A final temperature of 270 - 280°C was used for one series of experiments.

Procedure consisted of cutting on a mechanical saw a 1" x 1" x 1 1/4" monolith of the coal type to be tested. Coals included an Oklahoma semi-anthracite, an Illinois #6 sub-bituminous, and an Alabama lignite. Typical chemical analyses are shown in Table 1. After being cut, the coal was carefully placed into the autoclave and 250 ml of solvent was added. Solvents included various cuts of anthracene oil (Table 2), and one commercial motor oil (SAE 30). The autoclave was sealed, flushed with nitrogen, and heated by means of the burner. Figure 2 shows the pressure and temperature for a run with Illinois #6 coal in anthracene oil solvent. Figure 3 shows a similar run with SAE 30 motor oil solvent.

Results

The coal reacted, cracked, crumbled, or dissolved to a greater degree if exposed to reaction conditions for a longer time or at a higher temperature. For a series of runs at the same time and temperature the coals reacted increasingly from semi-anthracite to lignite to sub-bituminous. When different solvents were used the hydrogen donor anthracene oil was more reactive than motor oil. The motor oil was quite unreactive. Recycled anthracene oil lost reactivity.

The coal was observed to fracture at the planes of least resistance which are typified by the joint and bedding planes. The structure of coal which includes bedding and cleavage planes helps in physical breakdown of the sample. As joints and bedding planes open, the fluid is able to penetrate deep into the sample causing rapid disintegrating of the coal.

Interpretation of Reactions

The effects of different solvents upon the rate of the reaction can be interpreted from the work of Severson et al. (2) Coal solubilization most rapidly proceeds in a solvent which has a high boiling point, the ability to donate hydrogen, a relatively high dipole moment, heterocyclic atoms and ring stability. Apparently during one or two cycles, anthracene oil exhausts its available hydrogen and loses the ability to donate until the hydrogen has been replenished. The lack of effect with the motor oil is somewhat more difficult to evaluate unequivocally. The high vapor pressure exhibited at reaction temperature suggests that the solvent will be present in low concentration within the reaction zone. More significantly, the saturated structure of the hydrocarbon makes the motor oil a poor hydrogen releasing solvent.

The gradation in reactivity which was seen with the different coal ranks may be interpreted in the light of suggestions by Wender. (3) Semi-anthracite structures, represented by Wender as analogous to fused carbon ring systems, were visualized as substantially aromatic but with occasional saturated rings. This system was joined by oxygen bridges to adjacent structural units. These were seen as difficult to thermally crack (300 - 375°C) because of extensive opportunities for resonance and as difficult to hydrogenate rapidly for the same reason. The likelihood of easy dissolution was therefore not considered great.

A similar analysis of chemical structures fails to distinguish the solubility of bituminous coal from that of lignite. Earlier work (4,5) has, however, noted that lignite fails to dissolve as extensively or as rapidly as bituminous coal. The lignitic structures in lignite which comprise up to 50 percent by weight of the structure may form a barrier to prevent access by solvent to the internal grain structure.

Hill et al. (6) analyzed the kinetics and mechanism of solution of a high volatile bituminous coal and presented five ways in which the reaction might proceed. These include: (1) dissolving out of included materials, (2) dissolution of the coal structure in the presence of a large volume of solvent, (3) diffusion out of the micropores, (4) hydrogen transfer reactions and (5) solvent imbibition. Applications were discussed for the order of the reaction with respect to the coal and with respect to the solvent. The discussion proceeded on the assumption that little swelling occurred. This assumption was not verified in the present work where gross volume increases of about three times were observed in the case of the Illinois Seam #6 sub-bituminous coal.

The tentative conclusion based on application of the theories of Wender and of Hill to the present research is that the coal imbibes solvent and swells. The

swelling is accompanied by a close association of coal and solvent and a transfer of hydrogen to the cohesive structures between the micelles or microplatlets of coal. The cohesive structure is weakened; the coal forms fragments, and the action of gravity or fluid turbulence removes the coal fragments from the immediate vicinity of the coal face.

Implications for Underground Liquefaction

The implications of this proposed mechanism upon the conceptual design of an underground liquefaction process appear significant. The dissolution of coal need not be completed underground; the reaction may begin underground and be completed at the surface. If the vertical borehole scheme is utilized (Figure 4) the process might be as follows. The borehole is drilled through the thick coal seam and a hot, hydrogen donor solvent is introduced into the bottom of the borehole. The solvent is maintained under pressure to reduce solvent vaporization and to limit the reaction zone as much as possible to the bottom of the coal seam. After some coal has reacted and has fallen from the face of the seam, the recovery step is begun. Solvent, now a slurry medium, under turbulent flow conditions is introduced to suspend coal fragments and carry the fragments to the surface. After significant void volume is produced, the solvent volume would become too great for economy. Water would be introduced to flood the void and to float the solvent upward against the unreacted segment of the coal seam. The loosened coal could be collected periodically in the turbulent stream as before or could be collected continuously with water as the slurry medium. At the surface the coal fragments would be separated by filtration from the water slurry medium or if, in a solvent slurry, would be admitted into the pretreatment step of the complete liquefaction process at the surface.

Host Rock

The host rock would be of special importance in this conceptual design. The host rock would necessarily be impervious to loss of vapor from the solvent or to seepage outward of hydrogen donor solvent and water flood. Moreover, the host rock should be unreactive when exposed to the thermal shocks and high thermal gradients. Some shales may react with hot water or solvent. After swelling and spalling the shale particles would be carried away with the coal and contribute to a high level of waste mineral matter in the subsequent process. Considerable disadvantage is apparent in this case since disposal of mineral waste can be inconvenient and expensive. Possibly, the carbon content of the host rock could be extracted to pay for the disposal of the additional mineral matter. More likely initial tests would be performed on coal seams with unreactive host rock.

Surface Subsidence and Seismic Effects

Surface subsidence and minor seismic shock effects are experienced with most mining techniques. In the present concept their abatement can be planned. The process would be designed to include access wells so placed as to permit coal pillars to remain and to support the roof. Secondary beneficial effects include the reduction of solvent leakage and restriction of the areas into which coal fragments might fall and from which coal particles could be recovered.

Summary

Even in the absence of hydrogen several coal types undergo a swelling and spalling reaction early in their liquefaction reaction with hydrogen donor solvents.

The coals increase their reactivity in the order semi-anthracite, lignite, and sub-bituminous. Increased temperature and reaction time increase the extent of reaction. To utilize these observations a concept is presented which may lead to an underground coal liquefaction process.

TABLE 1
COAL ANALYSES

Oklahoma (Semi-anthracite)

Moisture %	-	S	0.6
Volatile Matter	17.3	H	4.2
Ash	7.6	C	83.8
Fixed Carbon	-	N	1.2
Heating Value (Btu/ #)	15,570		92.4

Illinois Number 6 (Sub-bituminous)

Moisture %	14.7	S	4.5
Volatile Matter	37.2	H	4.4
Ash	15.7	C	66.1
Fixed Carbon	47.1	N	1.2
Heating Value (Btu/ #)	9980	O	8.1

Alabama (Lignite)

Moisture %	37.8	S	1.1
Volatile Matter	40.8	H	4.3
Ash	11.1	C	64.5
Fixed Carbon	-	N	1.0
Heating Value (Btu/ #)	8,010		18.0

TABLE 2
 FRACTIONATION OF CRUDE ANTHRACENE OIL IN NITROGEN ATMOSPHERE

	<u>Boiling Range</u> °C	<u>Volume</u> ml	<u>%</u> <u>By Volume</u>
Light Ends	Ambient - 300°C	48	38.7
Middle Fraction	300°C - 400°C	58	46.7
Heavy Ends	400°C+	<u>18</u>	<u>14.6</u>
		124	100.0

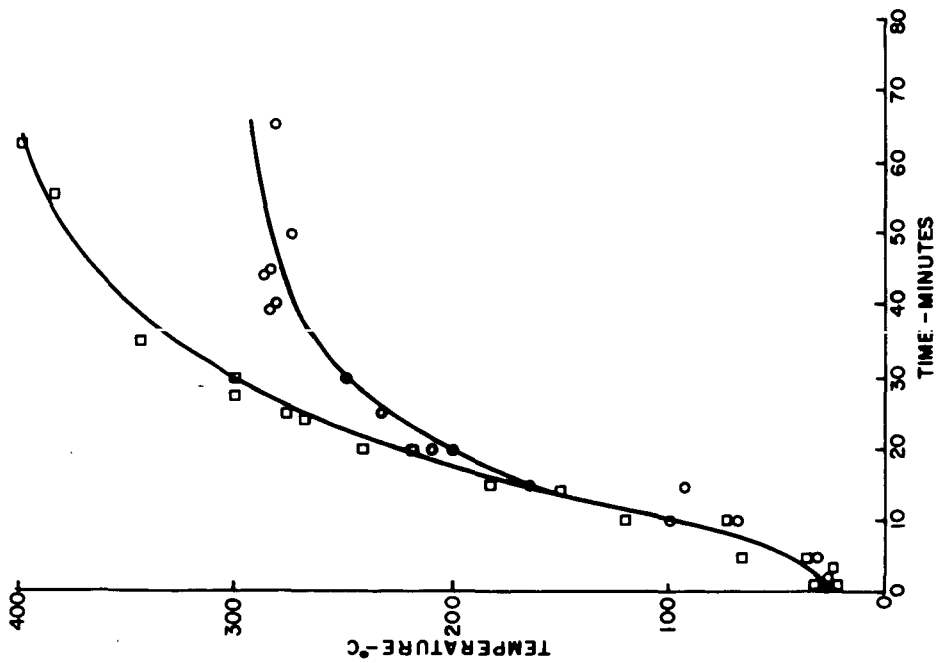


FIG. 1 - THE RELATIONSHIP OF TEMPERATURE AND TIME FOR SIX RUNS.

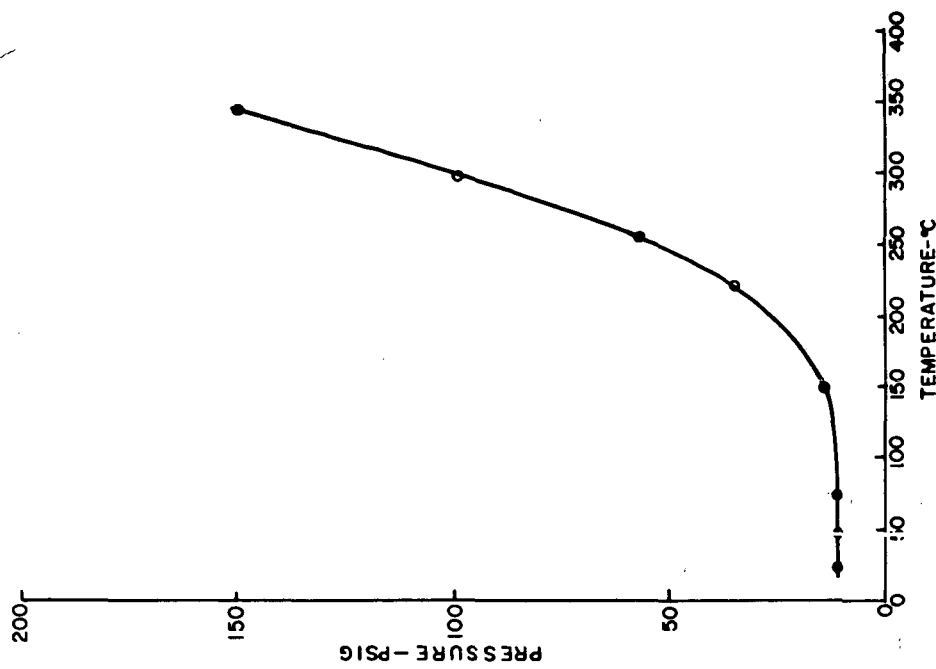


FIG. 2 - THE RELATIONSHIP OF PRESSURE AND TEMPERATURE FOR ANTHRACENE OIL SOLVENT AND ILLINOIS NO. 6 COAL.

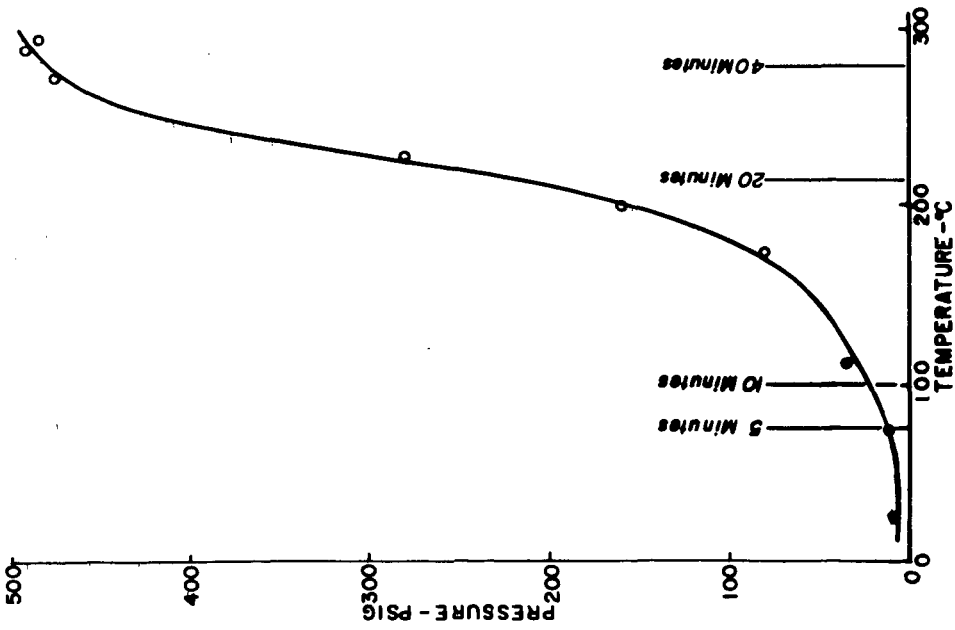


FIG. 3- THE RELATIONSHIP OF PRESSURE AND TEMPERATURE FOR SAE 30 MOTOR OIL SOLVENT AND ILLINOIS NO. 6 COAL.

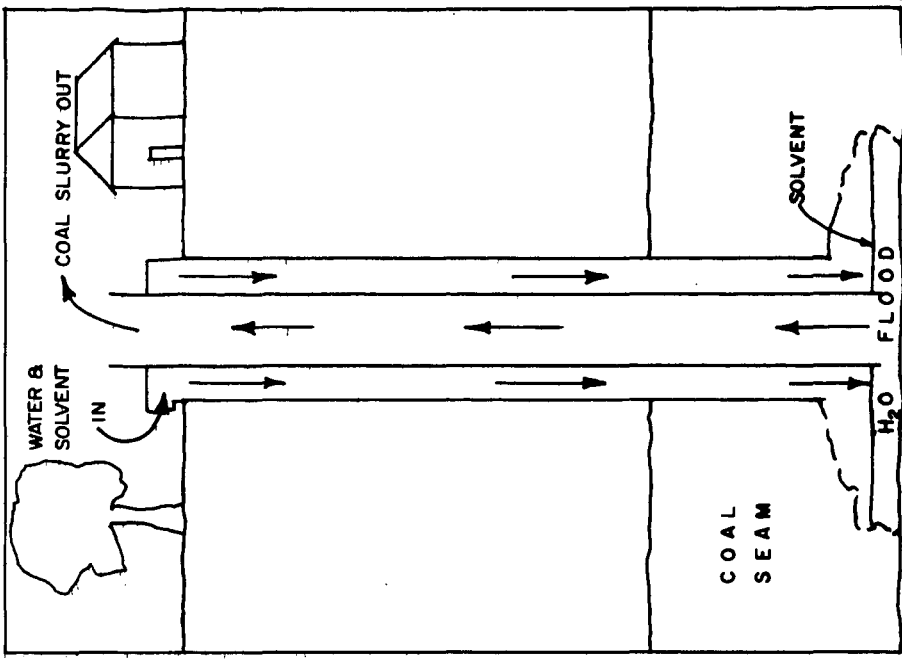


FIG. 4- VERTICAL BLIND BOREHOLE SYSTEM FOR UNDERGROUND COAL MINING AND LIQUEFACTION.

Bibliography

1. A Current Appraisal of Underground Coal Gasification. Report to the United States Bureau of Mines, C-73671, December, 1971.
2. Severson, D. E., Skidmore, D. R., and Gleason, D. S. Solution - Hydrogenation of Lignite in Coal-Derived Solvents. Transactions of the AIME, SME, 247, No. 2, 133-136, 1970.
3. Wender, I., Characteristics of Coal Behavior in Chemical Reactions. Unpublished report.
4. Bull, Willard C., Summary Report of O.C.R. Contract. Pittsburgh and Midway Coal Mining Company, 1965.
5. Appell, H. R., Wender, I. and Miller, R. D. Solubilization of Low Rank Coal With Carbon Monoxide and Water, Chemistry and Industry (London), 1703, 1969.
6. Hill, George R., Hariri, Hassan, Reed, R. I. and Anderson, Larry L., Kinetics and Mechanism of Solution of High Volatile Coal, "Coal Science", ACS Advances in Chemistry Series, No. 55, 1966.

THERMAL SYNTHESIS AND HYDROGASIFICATION
OF AROMATIC COMPOUNDS

H. N. Woebcke, L. E. Chambers, P. S. Virk

In order to synthesize low sulfur fuels from coal, the Stone & Webster Coal Solution Gasification Process employs the stepwise addition of hydrogen to coal. Enough hydrogen is added in the first step to convert the coal to liquids, which are then hydrogasified to methane, ethane and aromatic liquid products.

Since both these steps involve reactions of aromatic type molecules, the possible chemical pathways involved for their thermal reactions have been studied, along with the kinetics of some of the limiting cases.

Available data show that aromatics are formed by pyrolyzing any of the simple paraffinic hydrocarbons. Formation appears to proceed through the production of olefinic intermediates.

It was felt that a tool in evaluating the relative rate of decomposition of simple aromatics would be their respective delocalization energies, which can be calculated from simple orbital theory. Available kinetic data showed this to be true.

Of the aromatics studied - benzene, diphenyl, naphthalene, phenanthrene, chrysene, pyrene, and anthracene - the rate of decomposition was found to increase in that order. Anthracene decomposes almost 800 times as rapidly as benzene. Further, it was found that the kinetics for the intermediate compounds are ordered inversely with respect to their delocalization energies.

A further consequence of the relation between delocalization energy and kinetics is that the rate of aromatic decomposition should be independent of the hydrogen partial pressure, or the character of the products. Data showed the rate of decomposition of benzene to be independent of hydrogen partial pressure, from 0.1 to 100 atmospheres.

At high hydrogen partial pressures, benzene decomposes primarily to methane, a probable intermediate being cyclohexadiene.

At low hydrogen partial pressures, coke is the final product. The intermediate in this case is probably diphenyl, with coke formation proceeding through stepwise reactions involving diphenyl rather than the progressive addition of benzene molecules. It appears that the conversion of benzene to diphenyl is rapid, and essentially at equilibrium, with the second step, the production of coke from diphenyl, being rate controlling.

Aromatic Synthesis

When pyrolysis is carried out at low pressure - for example, in steam cracking for olefins production, the yield of methane and benzene increases monotonically as severity is increased, until conversion to coke becomes significant.

Early investigations⁽¹⁾ showed that aromatic liquids could be produced from all simple olefins and paraffins. Maximum aromatic yields of 5 wt % were obtained from methane by pyrolysis at 1,050 C for 10 seconds,

(1)

while propane gave a yield of 12% at 850 C. In general, olefins were found to give higher yields of aromatic liquids than paraffins and at lower temperature. For example, at 10 seconds residence time, propylene yielded 19% aromatics at 800 C, compared to 12% at 850 C already noted for propane.

Most investigators concluded that aromatics formed from paraffins during pyrolysis involved, as a preliminary step, the formation of olefins, all olefins from C₂ to C₄ playing a significant role in the synthesis.

Studies also showed that nitrogen acted as a true diluent, reducing the rate by reducing the partial pressure of the reactants. Oxygen enhanced the formation of aromatics from olefins, while hydrogen inhibited aromatization. Since the formation of aromatics proceeded through olefins, it is reasonable to assume that this was a result of the hydrogenation of the olefinic intermediates.

An interesting observation was that reactions leading to the maximum aromatic yield from different light paraffins and olefins generally produced a liquid having about the same composition, i.e.,

40 wt % Monocyclic Aromatic
20 wt % Dicyclic
10 wt % Tricyclic

As conversion progressed beyond peak aromatic conversion, coke was formed, presumably from aromatic precursors.

Figure 1 shows data of Kunugi and Kinney and Crowley relating methane and aromatics yield with ethylene conversion. The data of both investigators form a smooth curve, the former limited to low conversions.

Figure 2 presents similar information for propylene. For both olefins, aromatics and methane production are linear with conversion up to the point of maximum aromatics production. This is shown more clearly on Figure 3 which is a replot of data from the first two figures.

Cracking data for naphtha obtained from the Stone & Webster bench scale pyrolysis unit show this same characteristic relationship. Here a somewhat unanticipated result is that the relationship between methane and aromatics yield is essentially independent of pressure, over a very wide range of pressure conditions.

Some further insight on the effect of hydrogen partial pressure on the formation of aromatics can be found in the work of Moignard⁽²⁾ et al. These experimentors found that under conditions selected for the conversion of light paraffinic hydrocarbons to methane and ethane, there was still a significant production of aromatics. In view of the presumption that aromatics are produced from olefins, this suggested that the hydrogenation of the intermediates to paraffins was not rapid enough to inhibit aromatic formation. Using methane formation as a guide to cracking severity, it is interesting to compare Moignard's data for a light paraffinic naphtha, with other noted earlier.

This is shown on Table 1 (Slide 5). As indicated, the presence of hydrogen does significantly reduce the relative yield of benzene to methane.

Aromatic Decomposition

The remainder of this study was limited to noncatalytic reactions involving relatively small aromatic molecules. Some of the compounds studied are shown on Table 2 (Slide 6). The largest, chrysene, has a hydrogen content of 5.3 wt %, compared to benzene with 7.9 wt % H₂.

The detailed chemical pathway(s) for aromatic molecule hydrogenolysis is unknown, but it is convenient to consider it composed of three steps:

1. Aromatic Ring Destabilization
2. Breakdown to Fragments
3. Fragment Reactions

These are described in turn.

Aromatic Ring Destabilization

The above demarcation stems from the well-known chemical premise that aromatic compounds owe their unusual stability to a delocalization of pi-electrons among the ring molecular framework. To get aromatic molecules to react, the "delocalization energy" must be overcome. Since this energy is large, of the order of 40 kcal/mol, initial destabilization of the aromatic ring is invariably the rate determining step. This argument predicts that the reactivity of all aromatic compounds should be ordered inversely to their delocalization energy. These energies can be computed from simple molecular orbital theory.

Some indication of how this agrees with observation is given in Table 3 (Slide 7), which shows the relative rates at which methyl radicals attack some of the compounds of interest. Notice that all the rates are ordered according to the delocalization energy. The same pattern is observed for a wide variety of reactions, such as free radical attack, nitration and sulfonation. Further, note that benzene and anthracene represent the extremes of reactivity.

A second consequence of the initial destabilization step being rate determining is that, since the further course of reaction exerts little influence on the overall rate, a given aromatic molecule should react at a rate essentially independent of the products being formed. This implies, for example, that rates of benzene decomposition during hydrogenolysis and pyrolysis be comparable even though the products - methane and coke - are strikingly different. This second consequence, while qualitatively true, is not quantitatively as well obeyed as the first.

Breakdown to Fragments

Possible pathways for aromatic decomposition are illustrated on Figure 5 (Slide 8).

The destabilized aromatic ring is a short-lived species which will either revert to the original stable aromatic ring or suffer a breakdown to various fragments. In the latter event, some of the fragments will be nonaromatic and hence subject to more conventional reaction pathways. For example, the destabilized benzene nucleus may go to cyclohexadiene,

or it may go to phenyl, pentadienyl or allyl radicals, which will further pyrolyze or be hydrogenated. For aromatics with multiple rings, e.g., anthracene, the initial breakdown products are very likely to contain smaller aromatic rings, e.g., benzene, in addition to nonaromatic fragments.

Fragment Reactions

The nonaromatic fragments formed from aromatic ring breakdown can undergo a great variety of reactions, among which are: (a) Molecular Reactions, such as simple fission (pyrolysis) or hydrogenation-dehydrogenation reaction; (b) Concerted electrocyclic reactions, for example, fission and rearrangements; (c) Free radical chain reactions such as hydrogenation/dehydrogenation, and polymerization.

The complexity of possible fragment pathways can be reduced by certain generalizations.

Molecular fissions have high activation energies about equal to the strength of the bond being broken. As a result, larger hydrocarbons break much faster than the very smallest. Among the paraffins, the order of stability is methane, ethane, propane, butane, and the approximate fission rate constant for ethane is 0.01; that for butane. Likewise, alkyl benzene or other aromatics containing side chains will tend to lose these much faster than the aromatic nucleus is destabilized.

Electrocyclic reactions, which are concerted, are usually much faster than molecular reactions which involve bond breaking or making.

Free radical chains, when operative, can be much faster than molecular pathways. In our case, at the high temperatures required for hydrogenolysis, free radicals will abound.

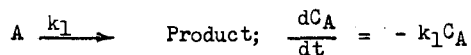
It is probably reasonable to suppose that the hydrogen-olefin-paraffin chain pathways are so fast that equilibrium prevails among these components.

Rate and equilibrium data indicate that the segments of the pathway from benzene fragmentation to ethane formation are expected to be fast relative to benzene destabilization and ethane pyrolysis. A further point to note is that whereas the ring destabilization step (1) is expected to be essentially unaffected by hydrogen, the subsequent product pathways (steps 2 and 3) - whether hydrogenolysis to gas or pyrolysis to coke - should be quite strongly influenced by hydrogen concentration. Finally, multiple-ring aromatics will break down into both nonaromatic and aromatic fragments, of which the former will decompose further by the reactions of step (3), while the latter will tend to lose side chains and go to benzene, the stablest aromatic, which will then further react via the pathway of Figure 5 (Slide 8).

Data Analysis

The essential theoretical hypothesis that aromatic reaction rates are controlled by the ring destabilization step can be tested by comparing the rates of hydrogenolysis and pyrolysis. If the hypothesis is true, the rates of decomposition of a given aromatic compound should be identical for either process. Further, reaction rates and their associated activation energies should correlate with the delocalization energy of that compound.

Sources of experimental information for the aromatic compounds of interest to us are listed in Table 4, along with associated reaction conditions. In each case, the data were processed by the usual simple methods to yield first order rate constants k_1 , sec^{-1} as a function of temperature for the initial decomposition of the aromatic:



It should be noted that the assumption of first order kinetics was not generally verifiable from the data and consequently the precision of these inferred rate constants is not especially good; but the rates are probably of the right order of magnitude in all cases.

Results obtained for benzene and anthracene, theoretically expected to be the extreme cases, are presented on Figure 6 (Slide 9).

Benzene Decomposition Rates

It is apparent that, while the data of separate investigators can each be fitted with straight lines of somewhat different slopes, all the data are adequately described by the single heavy line shown. This indicates that the rates of benzene decomposition during hydrogenolysis and pyrolysis are essentially the same over a rather wide range of experimental conditions. In particular, the insensitivity to hydrogen pressure, which varies from 0.1 atm to 100 atm, is noteworthy. The experimentally observed equality among benzene decomposition rates suggests a common rate-determining step which, in turn, lends support to the thought that aromatic ring destabilization, common to both hydrogenolysis and pyrolysis reactions, is rate-determining.

Benzene Decomposition Products

Some further insight into the reaction pathway can be obtained from the reported reaction products. In the presence of substantial hydrogen, the lowest temperature data (Lang, 900 F) show diphenyl as the sole product, whereas the higher temperature data (Schultz, 980-1,200 F, Dent, 1,100-1,500 F) indicate mainly methane and some ethane as products, with the mole ratio C_2/C_1 tending to unity at benzene conversions below 5%, while approaching zero at high benzene conversion. The diphenyl product suggests either a destabilized ring breakdown to a phenyl fragment or a concerted hydrogen elimination from two benzene molecules. It is also interesting because it represents net dehydrogenation of the benzene for purely kinetic reasons even though thermodynamic equilibrium strongly favors gasification.

None of the above authors report coke (carbon) formation, nor do they mention any hydrogenated C_6 liquid products. However, hydrogen balances on Schultz's data reveal that the empirical formula C_6H_n of the C_6+ components does change from $n=6$ to $n=8$ as benzene conversion proceeds from 0 to 50%, indicating at least some direct hydrogenation of the C_6 ring. In the absence of much hydrogen (pyrolysis), the gaseous reaction products are principally hydrogen and methane. The H_2/CH_4 mol ratio is variable, about 2-4 in Dent's experiments (1,100-1,450 F, 50 atm N_2) and 8-30 in Kinney's case (1,450-2,000 F, 1 atm N_2). Dent also reports small amounts of ethane ($C_1/C_2=1$) at the temperatures of 1,100-1,300 F while Kinney detected traces of acetylene.

Dent makes no mention of coke or condensed products, but Kinney reported diphenyl and carbon (coke) as the major products of benzene pyrolysis and showed further (as shown on Figure 7, Slide 10) that the diphenyl/carbon product ratio decreased in the presence and increased in the absence of coke packing, even though the packing did not appreciably affect the overall benzene decomposition rate. The implications concerning the benzene to diphenyl to coke pathway are, first, that both ring destabilization and breakdown are probably noncatalytic, homogeneous gas phase steps and, second, that the carbon formation reaction is catalyzed by the product, coke, and probably does not involve further benzene participation.

Anthracene Decomposition

The two sources of anthracene decomposition data are Dent and Kinney. For benzene, the coincidence between decomposition rates during pyrolysis and hydrogenolysis also supports the notion that ring destabilization is rate-determining.

Decomposition products from anthracene pyrolysis noted by Kinney were mainly carbon, with the carbon formation catalyzed by coke. Product gases were mainly hydrogen and methane, $H_2/CH_4 = 10$, with traces of acetylene. The hydrogenolysis products noted by Dent were mainly methane and ethane and small aromatic rings, benzene, and naphthalene. No carbon formation was reported. Dent reports only the fraction of anthracene converted to gas. It appears likely that the breakdown of a destabilized anthracene ring, in the presence of

hydrogen, leads to one benzene molecule as a fragment. The gas associated with this initial anthracene breakdown contains methane and ethane in the mol ratios $C_1/C_2 = 3.5$ at 1,200 F and 5.3 at 1,300 F. This does not yield any clear clues about the nonaromatic fragments except, perhaps, that a 4-carbon species (which would give $C_1/C_2 = 2$) may be involved. The change in C_1/C_2 ratio with temperature is too large to be explained by simple ethane pyrolysis with methyl radical hydrogenation.

Other Aromatic Molecules

Decomposition rate data for some of the other aromatic molecules of interest are shown on Figure 8 (Slide 11). Substantially all of the points lie between the anthracene and benzene limits and reasonably straight lines can be drawn to represent the variation of decomposition rate constant vs. temperature for each of the molecules.

Decomposition products observed were as follows:

Diphenyl: During hydrogenolysis at 930 F, 200 atm H_2 , benzene was the sole product. The products of pyrolysis, besides coke, are not clear because the diphenyl results are derived from the benzene pyrolysis data of Kinney.

Naphthalene: During hydrogenolysis at 1,160 F and 200 atm H_2 , Schultz reports methane, ethane and small amounts of propane in the gas with the molal $C_1/C_2 = 1$ at low conversions. Benzene was detected in significant amounts, and traces of toluene and ethylene were also found.

Hydrogen balances indicate some direct hydrogenation of the C₁₀ ring as well, but no coke formation was reported. During pyrolysis, Kinney found the gaseous products are mainly hydrogen and methane with traces of acetylene at 1,500-1,800 F in N₂ at 1 atm. The principal product was solid carbon, and traces of condensation products like 2-2' binaphthyl and perilene were also detected. The binaphthyl is, of course, analogous to diphenyl and suggests an analogous pathway to coke.

Chrysene: Orlow found with 70 atm H₂ that the hydrogenolysis reaction products (by weight) were 25% methane, 35% coke, with the remaining 40% containing phenanthrene, naphthalene, benzene, and various hydrides of each. The pyrolysis products were hydrogen and methane with traces of acetylene in the gas, and solid carbon.

Correlation

The experimental decomposition rate constant data can be fitted by the straight lines shown to yield Arrhenius expressions of the form

$$k_1 = A \exp (-E^*/RT)$$

for each molecule. Values of these Arrhenius parameters, the frequency factor A and activation energy E*, are collected in Table 4 (Slide 12), effectively summarizing the available data.

According to Molecular Orbital theory, the activation energy should be proportional to the delocalization energy, i.e., a plot of E* (experimental) vs. delocalization energy (calculated) should have all molecules lying on the line between the origin and the benzene coordinates. Figure 9 (Slide 13), an arithmetic plot of activation energy vs. delocalization

energy, shows a trend in accord with theory. Anthracene and benzene, the two cases with most data, are in especially good agreement.

Effect of Hydrogen

While it appears that the rate-determining aromatic ring destabilization step is essentially unaffected by hydrogen, the products of decomposition most assuredly are. Increasing hydrogen concentration switches the decomposition pathway from pyrolysis, which leads primarily to solid carbon (coke), to hydrogenolysis, where the product is gas, mainly methane. Understanding how hydrogen concentration controls the crossover between pathways is of interest. However, since the detailed pathway is not explicitly defined, we will focus only on a few aspects expected to be important. Much of the following discussion refers to benzene decomposition, since this case has the most data.

Thermodynamic Equilibrium

It is of interest to examine the equilibrium concentration of H_2 , CH_4 , and C_6H_6 dictated by the following reaction:

	K_p at 1,340 F	
	(a)	(b)
(1) $C_6H_6 + 9 H_2 \longrightarrow CH_4$	10.5	-4
(2) $C_6H_6 \longrightarrow 6C + 3H_2$	16.57	+2
(3) $CH_4 \longrightarrow 2H_2 + C$	1.011	1

where (a) is the exponent to the base 10 and (b) is the power of the pressure term in atmospheres

Calculations for this system show that carbon can always form before benzene has reached gasification equilibrium.

Further, at atmospheric pressure, carbon formation can occur at very low benzene conversions, unless very large excess of hydrogen is used.

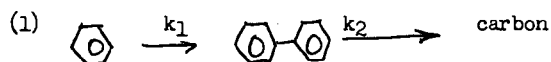
At a fixed hydrogen to benzene ratio, increasing the total pressure favors gasification and retards carbon deposition, based on equilibrium considerations.

A study was therefore made of the effect of total pressure, hydrogen to benzene ratio in the feed, and benzene decomposition on the gross heating value of the product gas. The study was limited to conditions at which ratios of hydrogen to methane in the product gas would be in excess of that required to inhibit the presence of carbon at equilibrium. The results are presented on Figure 10 (Slide 14).

Note that a 15% decomposition of benzene, the maximum heating value that can be obtained at 1,400 F is about 800 Btu/SCF, while at 1,500 F the GHV would be reduced to about 600 Btu/SCF - under conditions where no carbon could exist at equilibrium. The principal curves, i.e., those relating benzene conversion with GHV of product gas, are those for constant pressure and hydrogen to C_6H_6 ratio in the feed. The H_2/C_6H_6 ratios selected for plotting at any given total pressure were those leading to maximum product GHV for a given benzene conversion.

Carbon Formation

Coke is the terminal product of the aromatic pyrolysis pathway and it is of some interest to explore the formation mechanism. Insight into this process is provided by the benzene pyrolysis data of Kinney (1954) in a flow reactor. The diphenyl concentration vs. time behavior reported by Kinney is characteristic of an intermediate in a sequential reaction $A \rightarrow B \rightarrow C$ wherein A (benzene) decreases and C (carbon) increases, both monotonic with time, while the intermediate B (diphenyl) increases at small times and decreases at long times. It is also instructive to compare results at the same temperature, 1,800 F, with and without coke packing as shown in Figure 7 (Slide 10). This further suggests that carbon formation proceeds through a sequence of reactions in series

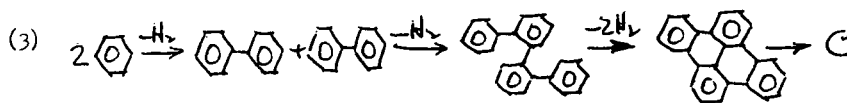


The first reaction is unaffected by coke, whereas the second is catalyzed by coke. Removal of catalyst would slow down the second reaction, thus increasing the intermediate diphenyl concentration as observed.

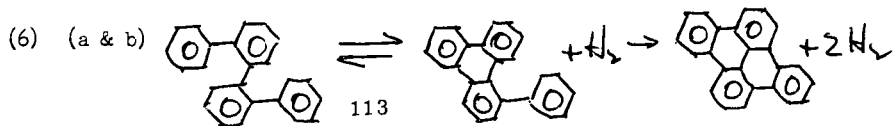
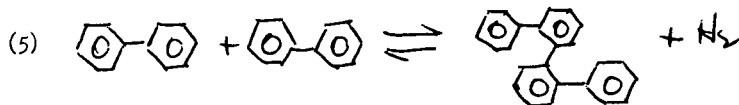
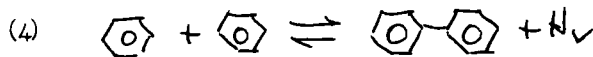
In regard to the molecular reactions leading to carbon, the literature contains many references to a benzene-by-benzene addition with hydrogen elimination (2).

Some of the intermediate products, e.g., diphenyl-benzenes and triphenylene have indeed been detected in the tarry residue resulting from benzene pyrolysis. However, if (2) were the main pathway to carbon, it would

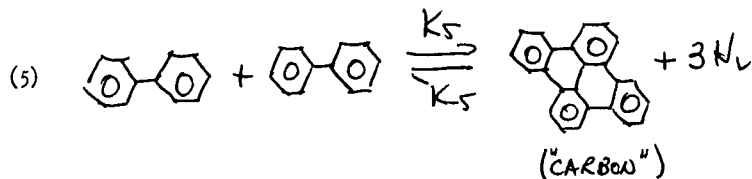
essentially involve benzene in every step and so carbon formation should be very high order in benzene. Catalytic effects enhancing carbon formation should strikingly increase the benzene decomposition rate (and vice-versa). This is not the case as noted above. Further, reactions with benzene in every step would face the maximum benzene delocalization energy barrier compared to reactions between more condensed species with less DE than benzene. Thus, although the concentrations of the condensed species would undoubtedly be lower than benzene, the adverse effect of lower concentration on overall reaction rates could easily be offset by the lower activation energies, and hence higher rate constants, of the more condensed molecules. A plausible alternative scheme for the main pathway to carbon formation is therefore of the form



which involves 1,2,4.... benzene nuclei rather than the 1,2,3.... sequence of (2). According to the above scheme, since the bigger molecules are more reactive, the overall rate should be controlled by the first few steps, namely,



Qualitatively, we can let \bar{C} approximate carbon and since reactions (6) (a) and (b) are intra-molecular hydrogen eliminations which one would expect to be fast compared to the bimolecular hydrogen elimination steps (4) and (5), the reactants of (5) can, in effect, be considered to yield the products of (6b). The essential components of the alternative benzene carbon pathway are thus



of which (4) is a homogenous gas-phase reaction, unaffected by coke, whereas (5) can be catalyzed by coke product.

Kinney's data for benzene pyrolysis to carbon may be modeled by a scheme of two sequential reactions (4) and (5) simplified such that (a) both reactions are kinetically limited in the forward directions and (b) reaction (4) is at equilibrium while (5) is kinetics controlled. Case (b) is the more plausible for the bulk of the data, but some of the experimental trends at low conversions at the lower temperatures are qualitatively as predicted for case (a). A combination of cases (a)

and (b), in which both forward and backward reaction rates are considered for (4) while (5) is assumed kinetics controlled in the forward direction, would probably describe all of Kinney's data adequately.

Finally, we consider the effect of hydrogen on carbon formation. The overall equilibrium, discussed earlier, shows that increasing hydrogen/hydrocarbon ratios and increasing total pressure both retard carbon formation and enhance gasification. Kinetically, however, we have to recognize that there exist at least two types of routes to carbon, namely, by surface reaction and by gas-phase reactions. It is not obvious how these combine. The carbon formation model formulated above is primarily a homogeneous gas phase model and its sensitivity to hydrogen must recognize that the gas-phase route is only one of several possible parallel pathways to carbon. The presence of substantial hydrogen will tend to enhance the back reactions for both (4) and (5) and, clearly, the forward kinetics only, scheme (a), will not be adequate. The maximum conceivable carbon formation that can occur is when reaction (4) is at equilibrium (this gives the maximum diphenyl concentration) and reaction (5) is not retarded by products (even though hydrogen is a product). This, of course, is precisely scheme (b) considered above.

KINETICS OF AROMATIC HYDROGASIFICATION SUMMARY OF EXPERIMENTAL DATA FOR AROMATIC HYDROGENOLYSIS AND PYROLYSIS

Compound	Run Conditions				Reactor			
	Source	Type	Temp, K	Press Atm	HC Mol Fr.	Diluent	Type	Residence, Sec
Benzene	1	H	873-1,123	50	0.10	H ₂	F	60
	1	P	873-1,073	50	0.10	N ₂	F	60
	2	H	800-973	200	0.15	H ₂	B	1,000
	3	P	1,073-1,373	1	0.10	N ₂	F	2-40
	4	H	758	250	0.35	H ₂	B	10 ⁴
Diphenyl	3	P	1,073-1,373	1	0.05	N ₂	F	2-40
	4	H	773	200	0.05	H ₂	B	2x10 ⁴
Naphthalene	2	H	838-958	200	0.10	H ₂	B	1,000
	3	P	1,073-1,273	1	0.02	N ₂	F	2-40
Anthracene	1	H	923-1,073	50	0.04	H ₂	F	60
	3	P	1,073-1,273	1	0.01	N ₂	F	1-40
Chrysene	3	P	1,073-1,273	1	0.005	N ₂	F	2-40
	5	H	723	70	0.13	H ₂	B	10 ⁵

- Sources:**
1. Dent, F.J., 43rd report of the Joint Research Committee, British Gas Council, (1939)
 2. Schultz, E.B. and M.R. Linden, Ind. Eng. Chem. **49**, 2011, (1957)
 3. Kinney, C.R. and E. Delbel, Ind. Eng. Chem. **46**, 548 (1954)
 4. Lang, K. and F. Hoffman, Brenstoff-Chemie **10**, 203 (1929)
 5. Orlow, N.A. and N.D. Lichatschew, Ber., **62B**, 719 (1929)

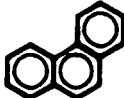
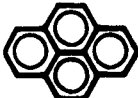
Abbreviations: H- Hydrogenolysis P- Pyrolysis B- Batch F- Flow

Table 1
(Slide 5)

<u>Investigator</u>	<u>Feedstock</u>	<u>Cracked At Press. H₂</u>		<u>Pounds C₆H₆ Per Pound CH₄</u>
Kunugi, et al	C ₂ H ₄	1	No	1.4
Kunugi, et al	C ₃ H ₆	1	No	1.4
Stone & Webster	(Paraffinic	1	No	0.7
Moignard, et al	(Naphtha	10	Yes	0.14

MODEL AROMATIC MOLECULES

KINETICS OF AROMATIC HYDROGASIFICATION

RINGS	NAME	STRUCTURE	FORMULA	T _b , F
1	BENZENE		C ₆ H ₆	176
2	NAPHTHALENE		C ₁₀ H ₈	424
	DIPHENYL		C ₁₂ H ₁₀	491
3	ANTHRACENE		C ₁₄ H ₁₀	646
	PHENANTHRENE		C ₁₄ H ₁₀	643
4	PYRENE		C ₁₆ H ₁₀	740
	CHRYSENE		C ₁₈ H ₁₂	827

KINETICS OF AROMATIC HYDROGASIFICATION REACTIVITY TO METHYL RADICAL ATTACK

<u>COMPOUND</u>	<u>DELOCALIZATION ENERGY</u>	<u>EXPERIMENTAL REACTION RATE RELATIVE TO BENZENE⁽¹⁾</u>
BENZENE	1.155	1
DIPHENYL	1.032	5
NAPHTHALENE	0.904	22
PHENANTHRENE	0.899	27
CHRYSENE	0.833	58
PYRENE	0.755	125
ANTHRACENE	0.632	820

(1) Data from Levy and Swarc, J.A.C.S. 77 1949 (1955)

KINETICS OF AROMATIC HYDROGASIFICATION

ARRHENIUS PARAMETERS FOR AROMATIC DECOMPOSITION RATES

<u>COMPOUND</u>	<u>A</u> Sec ⁻¹	<u>E*</u> Kcal/Mol	<u>T^{1/2}(1,000 °K)</u> Half-life, Sec
BENZENE	4.4x10 ⁸	52.6	499
DIPHENYL	1.6x10 ⁷	43.1	118
NAPHTHALENE	4.5x10 ⁵	36.8	171
CHRYSENE	3.4x10 ⁵	33.5	43
ANTHRACENE	1.8x10 ⁵	30.7	20

Note: $k_1 = A \exp(-E^*/RT)$

$$T^{1/2} = \text{half-life} = (0.693/k_1)$$

PYROLYSIS OF ETHYLENE

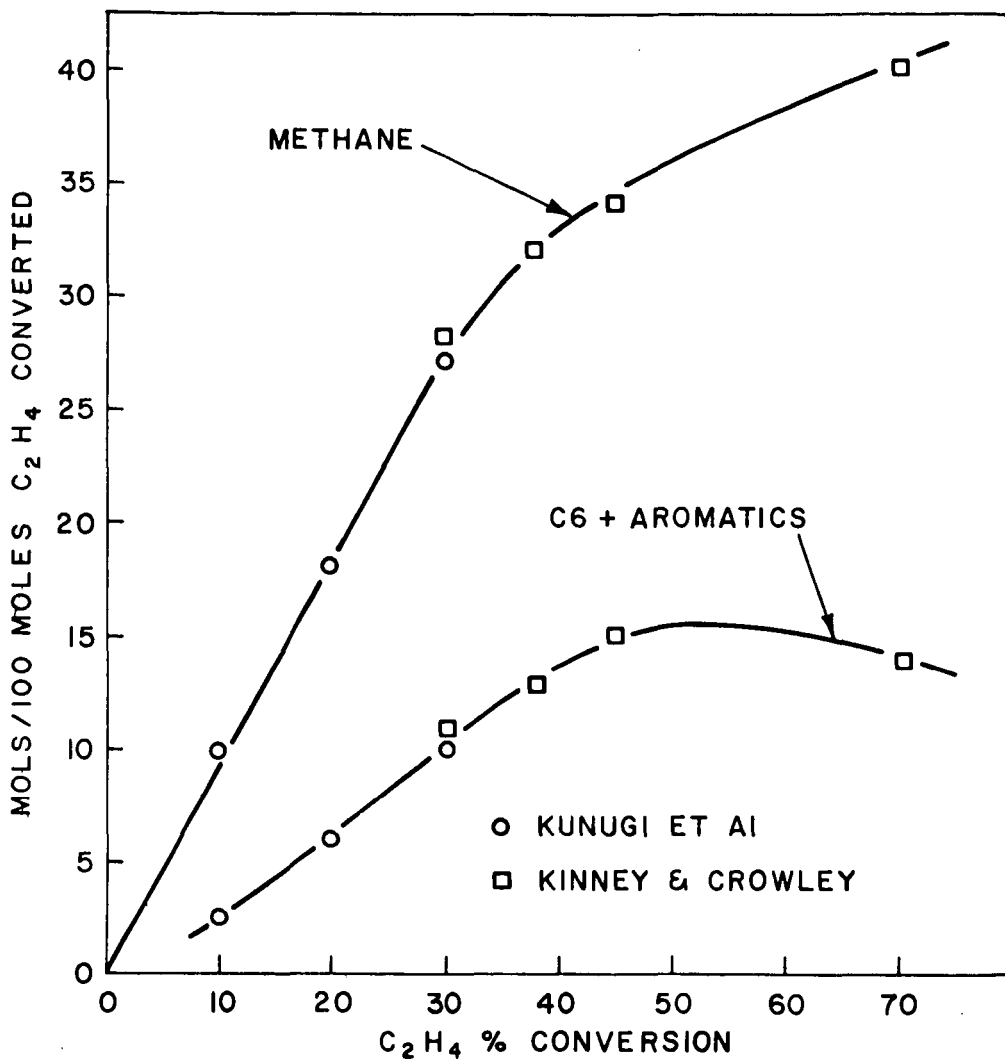
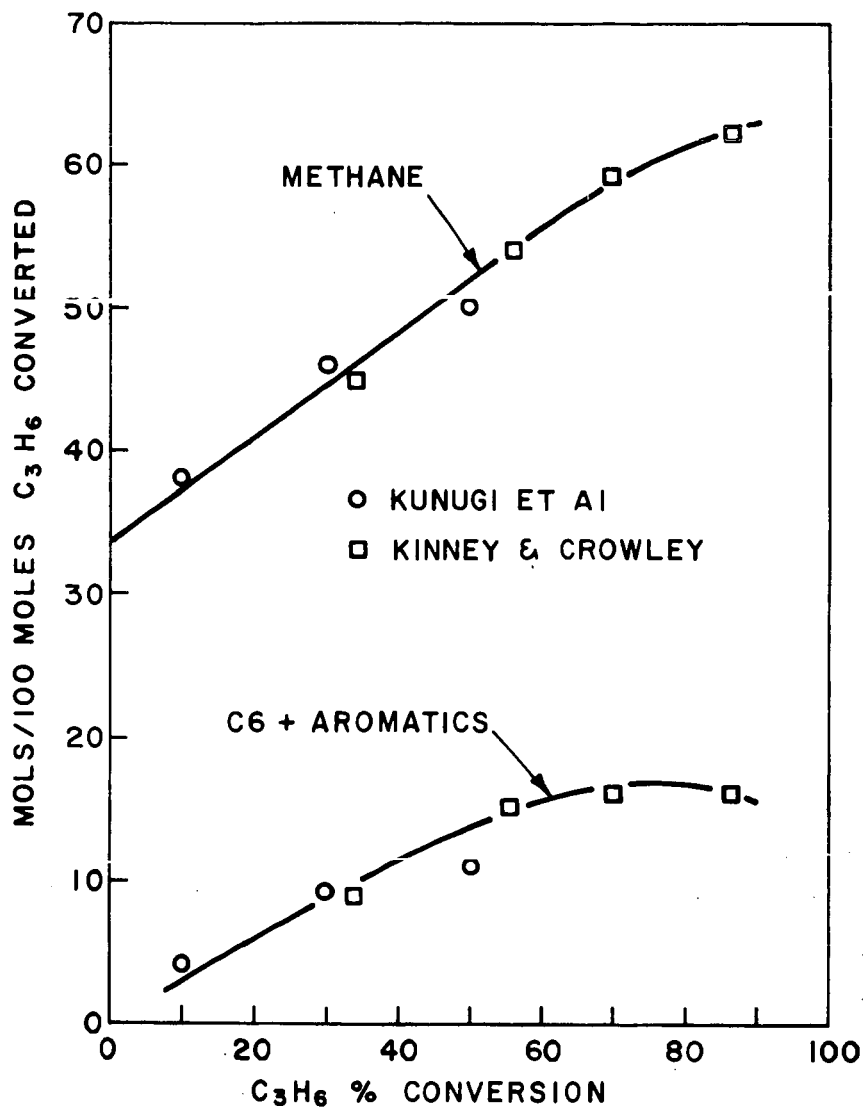


Figure 2
(Slide 2)

PROPYLENE PYROLYSIS



ETHYLENE & PROPYLENE PYROLYSIS (YIELDS AS % FEED CONVERTED)

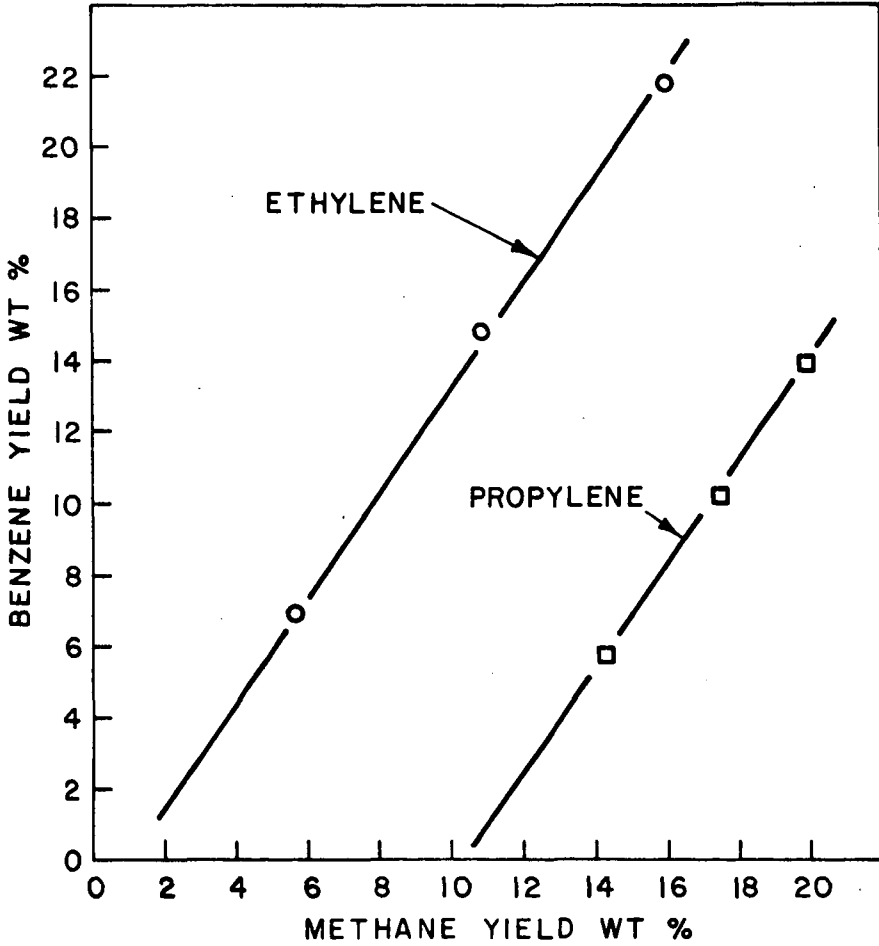


Figure 4
(Slide 4)

NAPHTHA PYROLYSIS

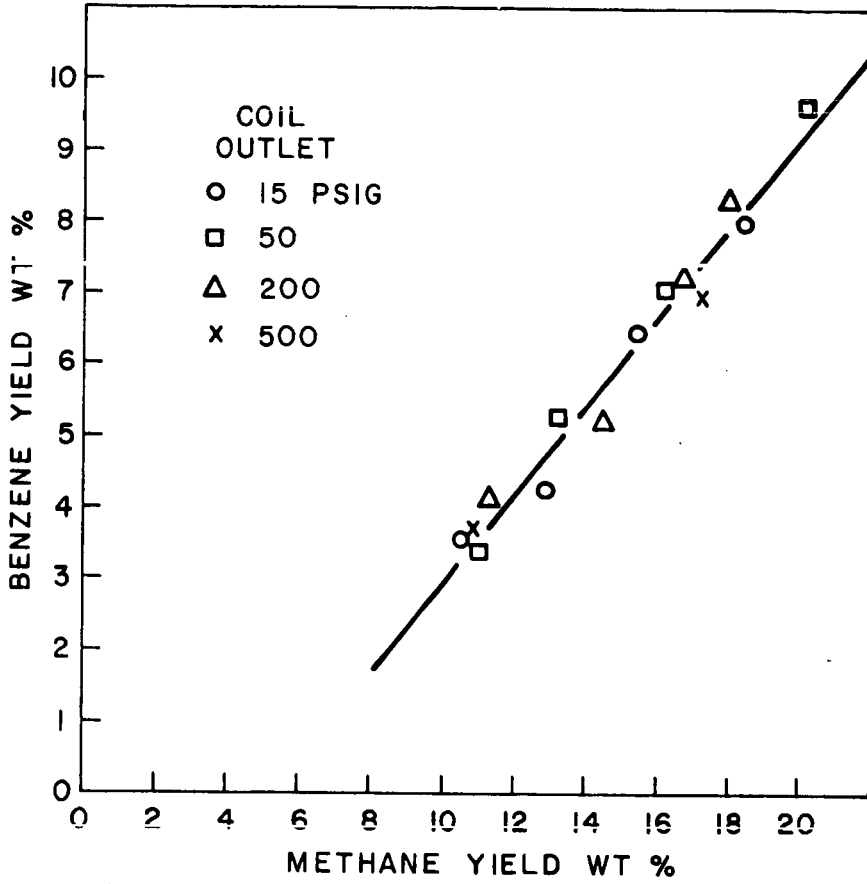
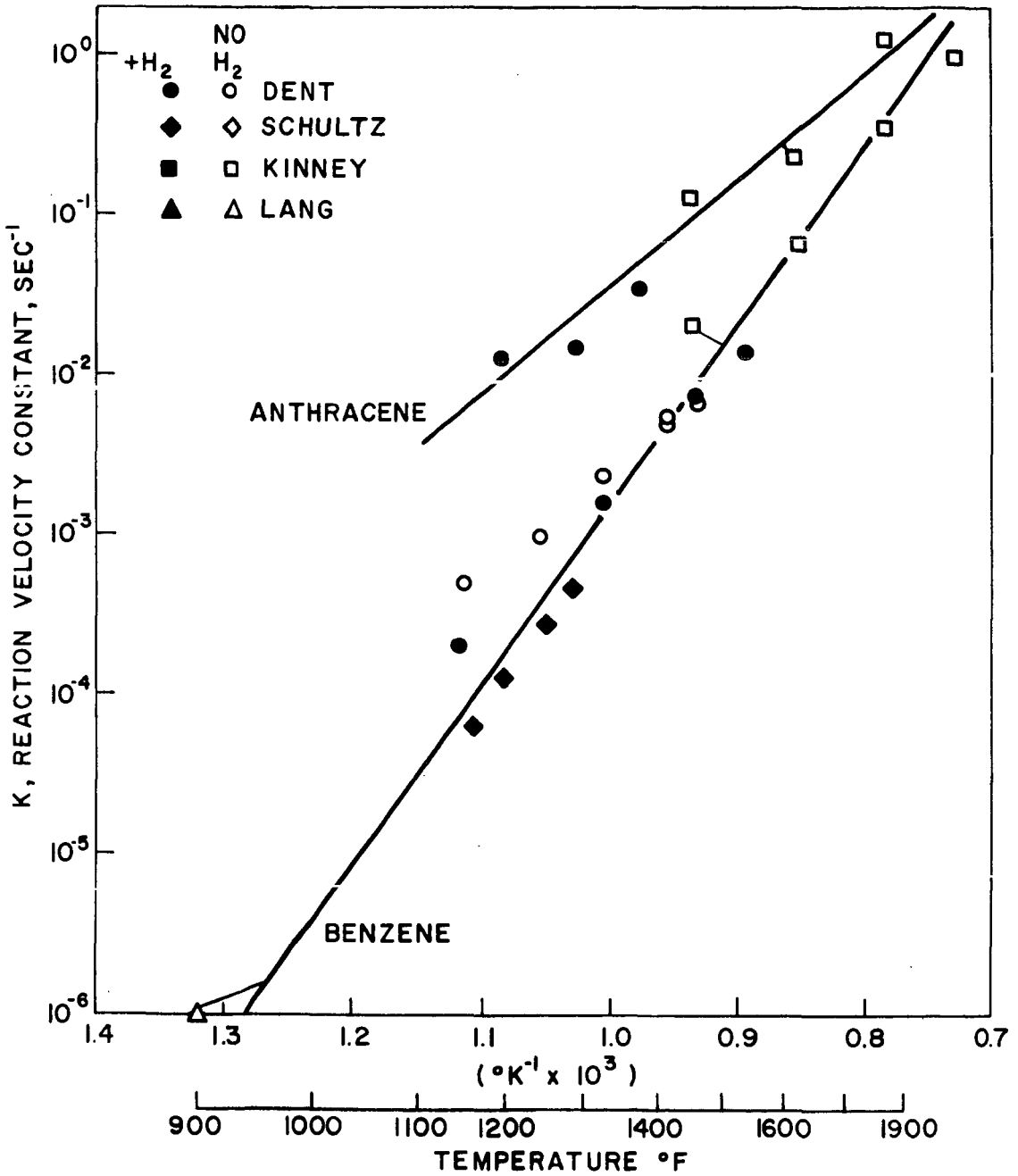
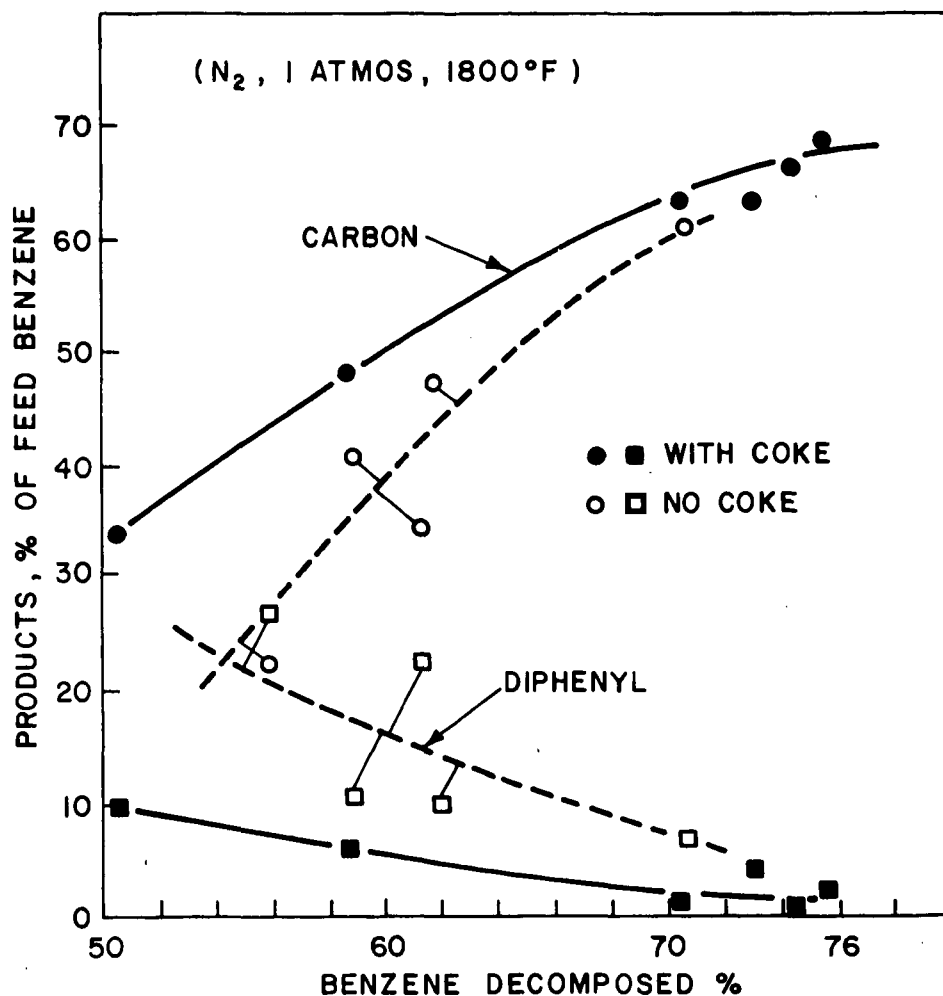


Figure 6
(Slide 9)

RATES OF DECOMPOSITION FOR BENZENE AND ANTHRACENE

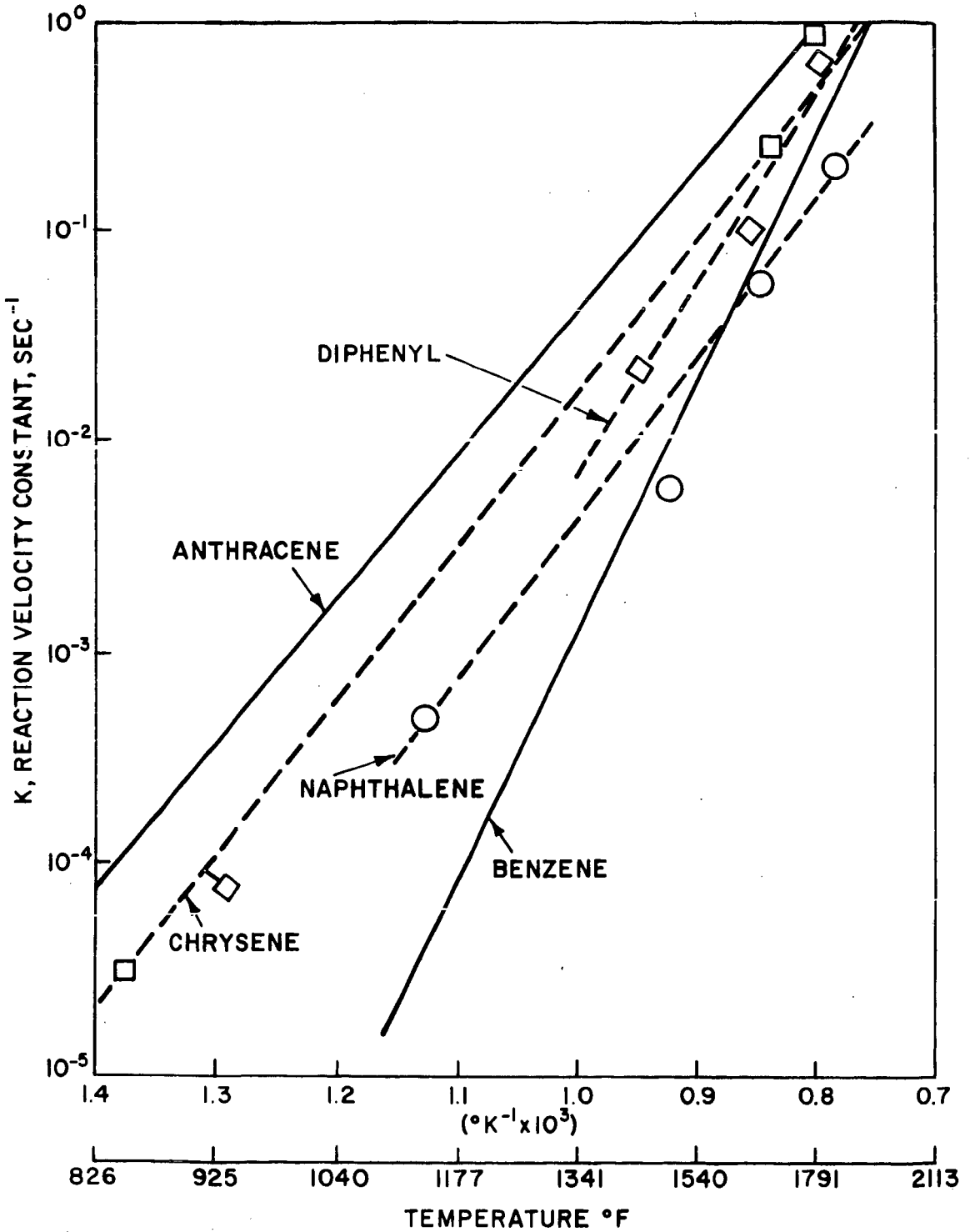


EFFECT OF COKE ON PRODUCT DISTRIBUTION FOR BENZENE PYROLYSIS



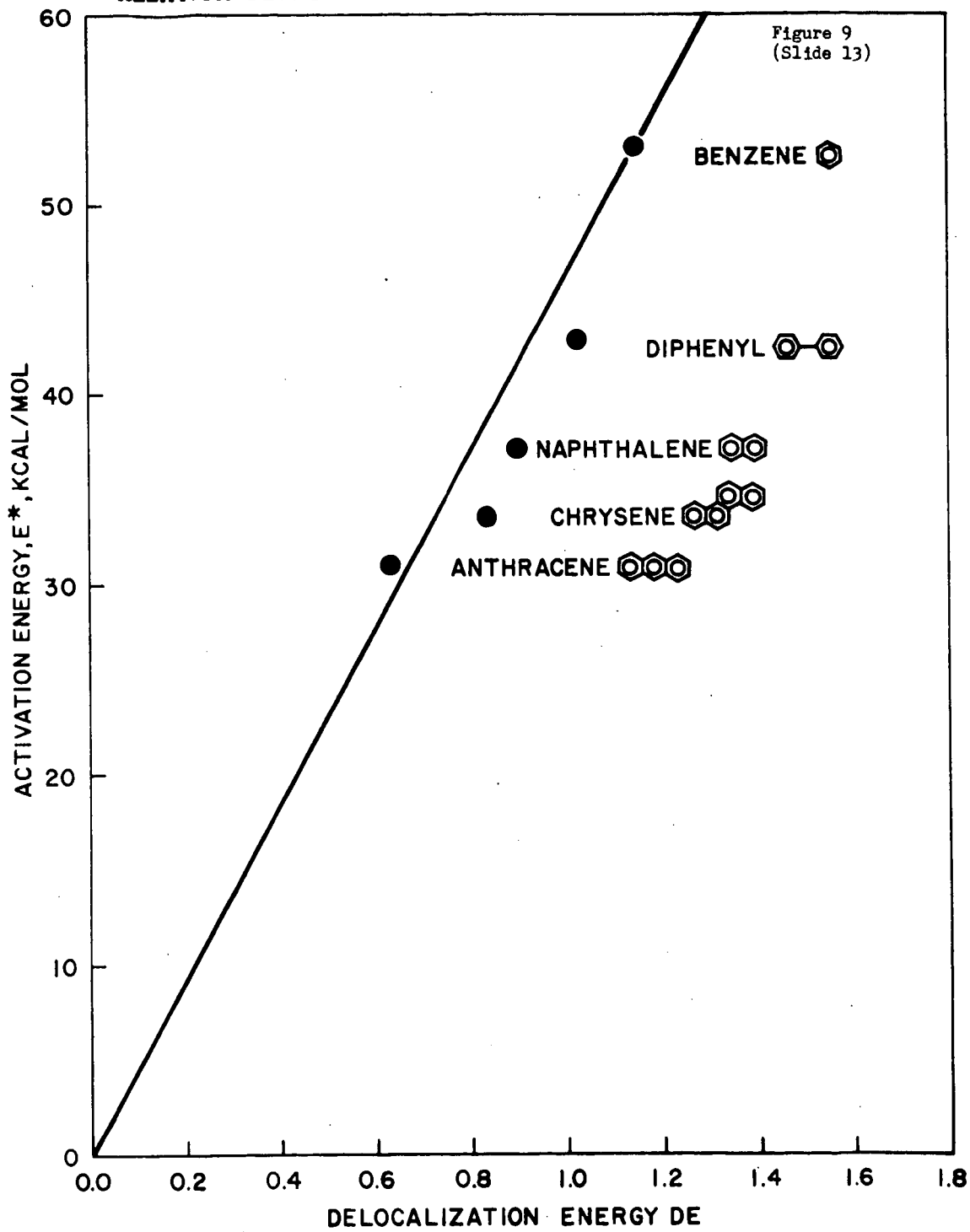
DECOMPOSITION RATES FOR SELECTED AROMATICS

Figure 8
(Slide 11)



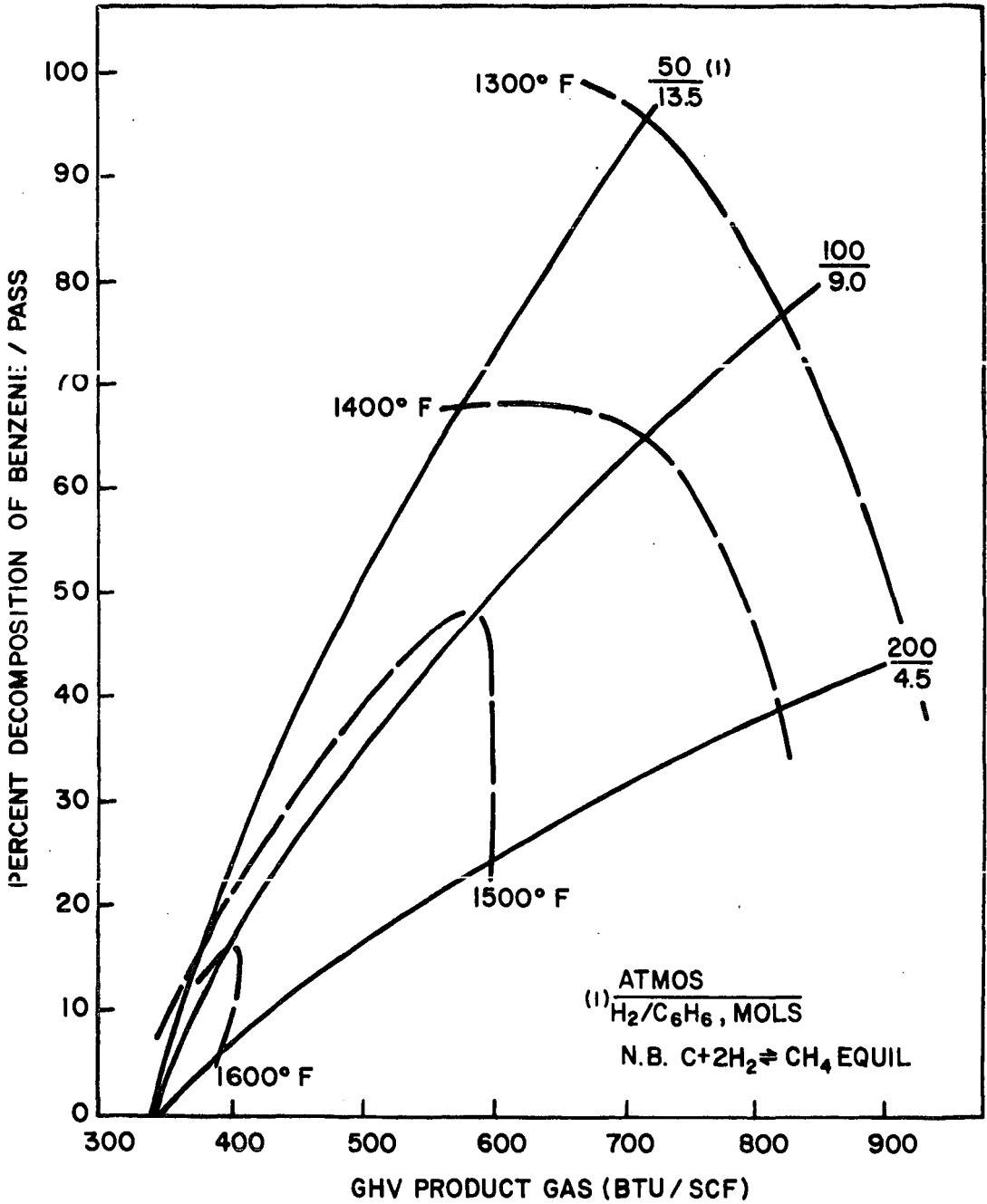
RELATION BETWEEN ACTIVATION AND DELOCALIZATION ENERGIES

Figure 9
(Slide 13)



EFFECT OF OPERATING VARIABLES ON GASIFICATION OF AROMATICS

Figure 10
(Slide 14)



Removal of H₂S On Oxidized Iron

N.J. Kertamus

Babcock & Wilcox Research Center

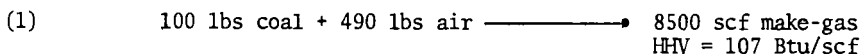
1.0 INTRODUCTION

This paper summarizes tests made by the Babcock and Wilcox Company to remove H₂S from a fuel gas generated from the gasification of coal with air. Reported specifically are:

- (a) Results from bench top tests aimed at yielding information necessary for design purposes.
- (b) A descriptive mechanism that explains H₂S removal and regeneration.
- (c) A hardware design based on these results.

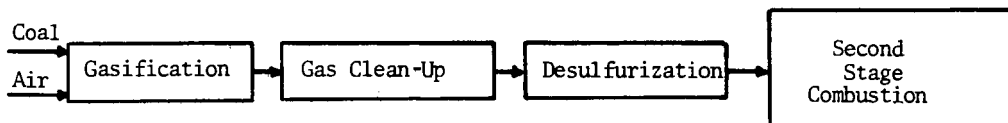
2.0 BACKGROUND

Air-blown gasification of coal in an entrainment or suspension type gasifier represents combustion with substoichiometric air to generate a product gas that contains chemical heat in the form of CO and H₂ diluted with N₂. This so-called 'make-gas', after gas clean-up, is burned in a second stage combustion device to generate electric power. For example, gasification of a typical bituminous coal with 50 percent stoichiometric air is represented by



Sulfur present in the coal winds up largely as reactive H₂S in the make-gas. The concentration depends on the sulfur concentration in the parent coal. Figure 2.1 illustrates the approximate H₂S concentration that would be obtained in air-blown gasification of a typical bituminous coal as a function of heating value of the gas produced and the percent sulfur in the coal being gasified. The H₂S levels illustrated in Figure 2.1 assume complete gasification of coal and no char product.

For electric power production the process concept is:



Justification for air-blown gasification of coal in terms of electric power production stems from the facts that:

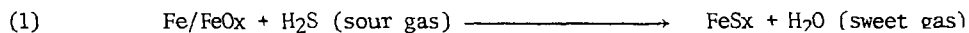
- (a) Sulfur is concentrated in the make-gas as H₂S.
- (b) H₂S is more reactive than SO₂.
- (c) After gas clean-up and desulfurization, the make-gas represents a high quality fuel gas that could have application as a gas turbine fuel.

3.0 APPROACH - BABCOCK AND WILCOX

The approach taken by Babcock and Wilcox is to remove H₂S from the make-gas by reaction with iron oxide at a comparatively high temperature. The objective is to minimize the amount of cooling needed between the gasifier and the second stage combustion device.

The use of iron oxide to remove H₂S is not a new or unique approach. Historically hydrated iron oxide has been used for decades in oxide boxes to remove H₂S from coke oven gas. At the present time, work is being done by the Bureau of Mines on a concept that removes H₂S with a sintered material made from iron oxide and fly ash. Our concept is different in as much that we start out with carbon steel and generate, on the surface of the carbon steel, an FeOx scale that is used as the desulfurization agent. In terms of the mechanism of sulfur removal, it is likely that both the Bureau of Mines' and our concepts are alike.

Briefly, the concept removes H₂S by:



At some point in time all of the available iron oxide scale is converted to the sulfide scale, At that point the system is regenerated with air, as follows:



The overall process accomplishes two things:

- (1) It concentrates sulfur at 0.4% volume percent in the make-gas to 10-13 volume percent SO₂ in the regenerant gas.
- (2) It provides SO₂ in the rich regenerant gas that is either (a) oxidized and recovered as H₂SO₄ or (b) reduced to elemental sulfur.

4.0 OBJECTIVES

In our earlier work reported previously, a one-foot diameter gasifier was coupled to an iron grid desulfurization system. The desulfurization system was operated at temperatures in excess of 1200F. Because material problems exist at these temperatures, our experiments emphasized desulfurization at temperatures from 1200 down to 675F.

A second objective was aimed at understanding, in a descriptive sense, the reactions that occur during desulfurization and regeneration on the iron surface.

Our final objective was to design a sulfur removal system that could be coupled to a large scale gasifier.

5.0 EQUIPMENT AND PROCEDURE

Figure 5.1 shows a sketch of the test system. The reaction vessel was a 1-inch ID aluminum tube filled on the bottom side of the bed with inert mullite chips. The chips served to support the test bed and to preheat the make-gas to the desired temperature.

The modified Reich idiometric technique was used to measure H₂S. This technique does not differentiate between H₂S or SO₂; total sulfur is measured. The SO₂ produced in the air regeneration was measured by an ultraviolet detector developed by the Babcock and Wilcox Company.

The synthetic make-gas composition was:

<u>Constituent</u>	<u>Percent (Volume)</u>	
CH ₄	1.0	
CO	12.0	
H ₂	8.0	HHV = 74 BTU
CO ₂	8.0	SCF
H ₂ O	6.0	
H ₂ S	1.0	
N ₂	Bal.	

Each test was started by heating the reactor to the desired temperature with a nitrogen purge. On attaining test temperature, make-gas was started through the unit; this defined zero time. The H₂S concentration of the desulfurized gas was continuously monitored and the absorption bed was considered saturated when the desulfurized make gas reached 0.10 percent H₂S. At that point the bed was regenerated with air at the same conditions of temperature and flow rate as the sulfur absorption.

The sulfur absorbent was designated as low hardness, perma-abrasive, plain carbon-steel shot with the following analysis:

Total carbon	2.5	-	2.8 wt. %	Phosphorous	0.02 - 0.04 wt. %
Graphite carbon	0.5	-	1.25 wt. %	Hardness	32 - 40 (Rockwell C)
Silicon	1.0	-	1.4 wt. %		

6.0 RESULTS

6.1 Desulfurization Results

Figure 6.1 is a plot of the sulfur concentration of the desulfurized make-gas versus time or volume of make-gas passed through the bed. The shape of the curve is typical of all results obtained at temperatures less than 1000F down to the minimum temperature considered, or 675F. In these tests, initially, a sharp sulfur concentration spike occurred. After the sulfur concentration spike the sulfur level dropped to a very low value, then increased with time or volume of make-gas treated. The increasing sulfur concentration was due to the depletion of available iron oxide scale. Arbitrarily, a test was terminated after the sulfur level increased to 0.1 percent, or when the make-gas at that point was 90 percent desulfurized.

The average sulfur concentration of the make-gas was determined by integrating the area under the curve to the 0.1 percent end point. For the case illustrated in Figure 6.1 the average sulfur concentration was 0.05 percent. Although the average sulfur concentration is relatively low (0.05 percent), because of the concentration spike, the instantaneous level at the top of the spike is higher 0.14 percent. What this means is that in the design of a workable desulfurization device, a number of beds staggered with respect to the regeneration cycle should give a product gas that approaches the average sulfur value, or for 675F operation a gas of 0.05 percent sulfur.

In general the magnitude of the concentration spike decreased as the temperature was raised to 1000F. Operation at 1000F and higher eliminated the concentration spike. Figure 6.2 illustrates the sulfur level of make-gas as a function of operating temperature. These results represent:

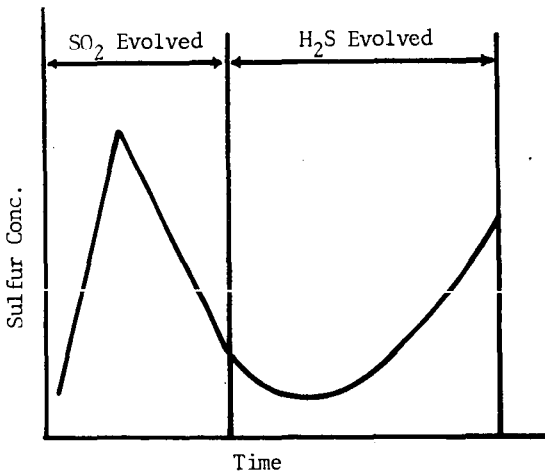
- (a) Operation at space velocities from 2000 to 2500 volumes of gas per volume of bed per hour.
- (b) An end point of 0.1 percent sulfur.

At the same conditions, Figure 6.3 illustrates the sulfur pick-up on a well conditioned surface, namely, the volume of H₂S removed or reacted with the iron oxide scale at 60F and 14.7 psig, based on 100Ft² of iron surface initially charged to the desulfurization unit. The results represented in Figure 6.3 were also determined using an end point of 0.1 percent sulfur for the treated make-gas and space velocities of 2000-2500 vol. gas per vol. bed per hour.

6.2 Descriptive Mechanism

Because of the presence of the unwanted sulfur concentration spike observed during sulfur absorption at temperatures less than 1000F, a series of short tests were made with the objective of defining, in a descriptive sense, the important reactions that govern sulfur removal and regeneration. Some of the pertinent results were:

1. The spike results from SO₂ evolution and not H₂S, even though only H₂S is fed to the bed. This is illustrated below.



- 2 The regeneration temperature determines whether the spike will occur. For example, if regeneration is conducted at a temperature greater than 1000F and the bed is cooled to say 675F for desulfurization, no spike results.
- 3 Pretreating a regeneration bed (low temp) with CO or H₂ eliminates the spike. If, however, the reduced bed is subsequently purged with air SO₂ is evolved.
- 4 Heating and cycling a fresh surface between make-gas and air, in short tests, does not develop a thick scale necessary for desulfurization.
- 5 For short tests the surface is developed by cycling at temperatures around 1450F.
- 6 A high concentration of steam in the make-gas decreases the efficiency of sulfur removal.

The following reactions explain the observed results. In addition thermodynamic calculations suggest these reactions are feasible at temperatures of our system.

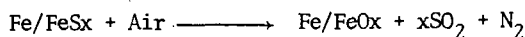
1. Heating in air at temperatures to 1400F develops a thin surface layer of FeOx. Surface not activated.



2. Activation 1450F



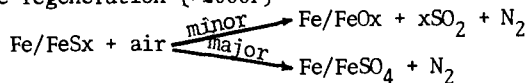
3. High temperature regeneration (>1000F)



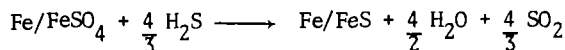
4. Equilibrium sulfur removal



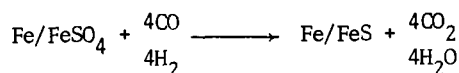
5. Low temperature regeneration (< 1000F)



6. Sulfur concentration spike



7. Prereduction (800F)



7.0 HARDWARE CONCEPT

The hardware concept for sulfur removal and regeneration should:

- (a) Have a large number of compartments at various stages of regeneration to give an average H_2S concentration relatively independent of the regeneration cycle.
- (b) Give a maximum concentration of SO_2 in the regenerant gas.

The hardware that has been designed uses a number of compartments for sulfur removal and the so-called counter-current principle for air regeneration. The desulfurizer uses a modified regenerative type air heater and is referred to as the "regenerative desulfurizer." Figure 7.1 illustrates this concept. The cylindrical unit is segmented into 16 compartments. Each compartment is filled with carbon-steel plates oriented longitudinally with the gas flow. Within each compartment the longitudinally oriented carbon-steel plates will contain about 100 square feet of surface of the carbon-steel plates. The vessel itself will be constructed from high alloy steel.

7.1 Sulfur Removal

Sour H_2S containing make-gas from the gasifier passes downward through 13 of the 16 compartments where desulfurization occurs on the surface of the carbon-steel plates that fill each compartment. The sweet make-gas issues from the base of the unit and is routed to a second stage combustion device.

7.2 Regeneration

The sulfided iron surface is converted back to the oxide in 3 of the 16 compartments shaded in the sketch. The regeneration air passes in and upward in the first compartment to a cross-over, then downward for a second pass, and upward for a third and final pass. At two revolutions per hour each of the 16 compartments is regenerated twice per hour.

Air at 21 percent O_2 enters the first regeneration compartment where it contacts a partially regenerated surface accomplished in the second and third pass down stream. At the end of the first pass the O_2 concentration is well below 21 percent. During the second pass, the O_2 concentration is further reduced while SO_2 increases. Purging the third (most FeS fouled) compartment with a gas containing a minimum concentration of O_2 and a maximum concentration of SO_2 insures a maximum SO_2 concentration of the final regenerant gas. The regenerant gas should contain from 10 to 13 percent SO_2 and up to 4 percent O_2 and nitrogen.

In practice SO_2 in the rich regenerant gas can be:

- (a) oxidized and recovered as sulfuric acid
- (b) reduced to elemental sulfur.

We believe the better approach is reduction and recovery as elemental sulfur. In coal gasification systems, two reductants are available, i.e., make-gas itself ($CO + H_2$) or char. Currently, B&W is actively studying SO_2 reduction using char that will be available from gasification of coal.

8.0 CONCLUSIONS

After a thick layer of iron oxide or sulfide scale is generated on the surface of plain carbon steel, the scale effectively removes more than 95 percent of the sulfur in a make-gas generated from air gasification of coal. The process works at temperatures as low as 675F; however, because of regeneration, operation at temperatures in excess of 1000F is desirable.

Conservative operation of the process should yield SO₂ values of 0.5 - 0.6 lbs per million Btu input, or a value well within the EPA guidelines.

The concept has been demonstrated in bench scale equipment and a hardware design has been developed. The workability of the concept on a large scale, however, has yet to be demonstrated.

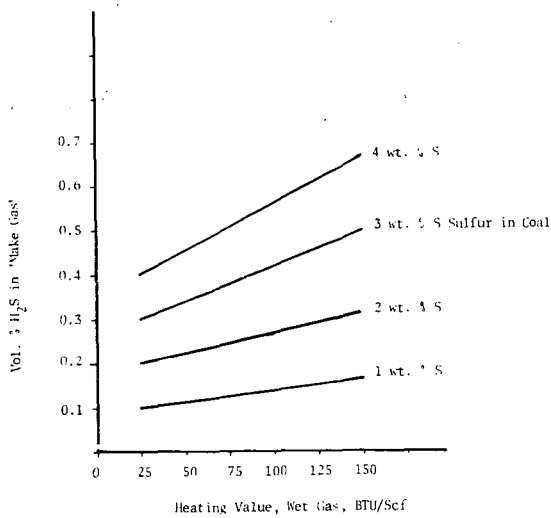


FIGURE 2.1 H₂S CONC. VS. HEATING VALUE COMPLETE GASIFICATION

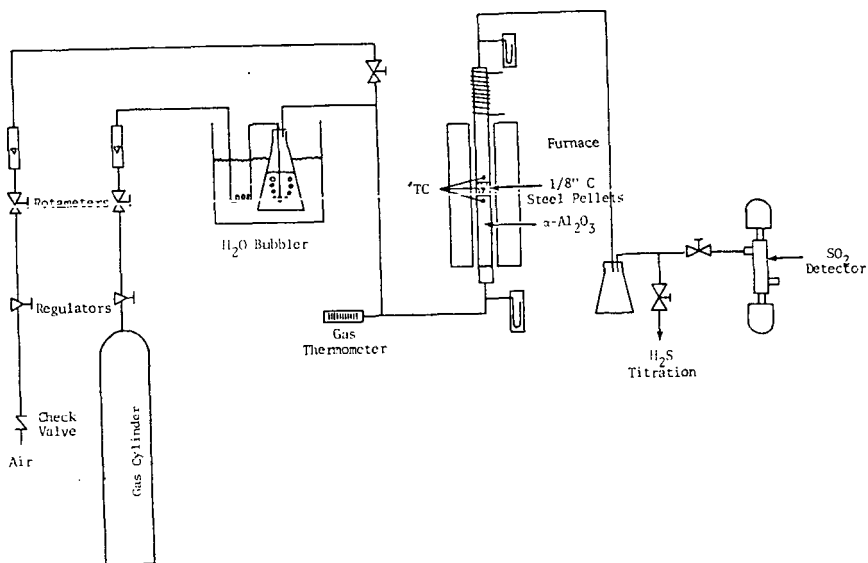


FIGURE 5.1 TEST EQUIPMENT

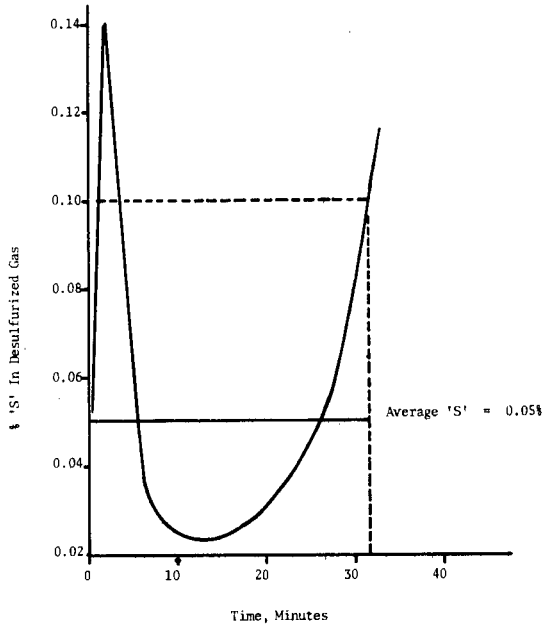
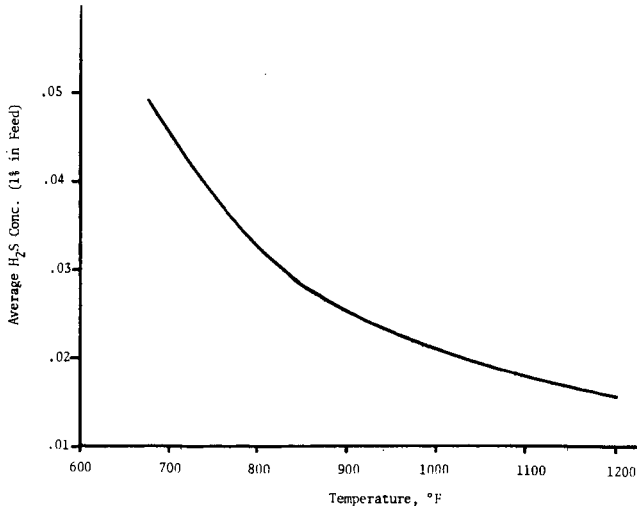


FIGURE 6.1 SULFUR CONC. DESULFURIZED GAS



Space Vel. = 2000-2500 v/v-Hr.
 End Point = 0.10 percent sulfur

FIGURE 6.2 SULFUR CONC. VS. TEMPERATURE

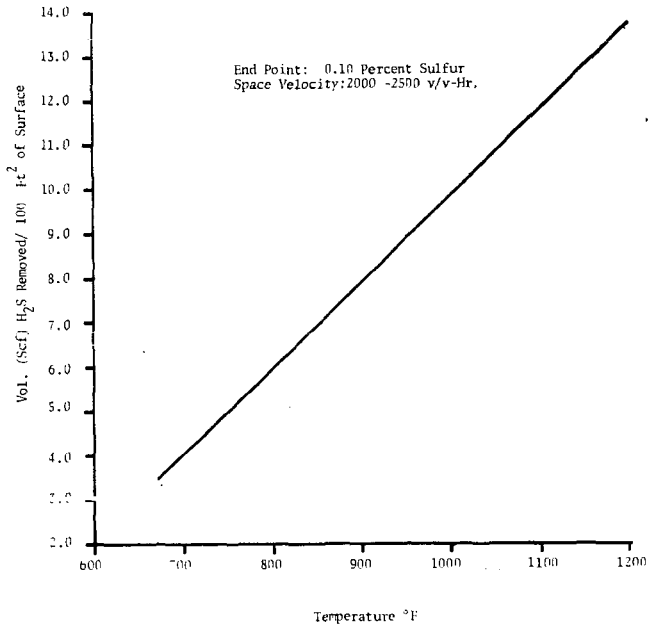


FIGURE 6.3 SULFUR PICK-UP

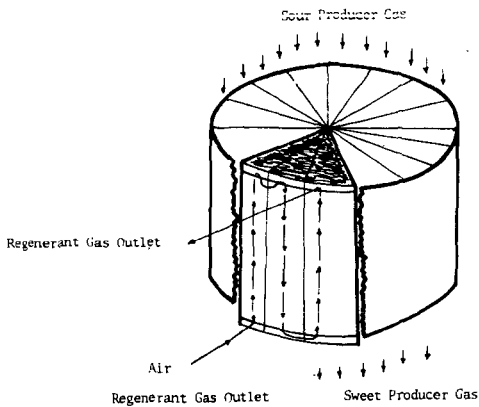


FIGURE 7.1 REGENERATIVE DESULFURIZER

BENFIELD PROCESSES FOR SNG OR FUEL GAS PURIFICATION. D. H. McCrea and H. E. Benson. The Benfield Corporation, 666 Washington Road, Pittsburgh, Pa. 15222

Processes to produce Substitute Natural Gas or fuel gas from liquid hydrocarbons or coal reject excess carbon as CO_2 . In addition, a portion of any sulfur initially in the feed appears in the gas, principally as H_2S . In producing SNG, both CO_2 and sulfur compounds, if present, must be removed. However, it is often advantageous to remove the bulk of sulfur compounds while minimizing CO_2 removal when producing gas for turbine or boiler fuel. While purification methods have not received the coverage of gasification and methanation techniques, purification is an essential step in all gasification processes that can significantly affect overall cost and reliability. This paper discusses the use of Benfield potassium carbonate processes for SNG or fuel gas purification. Process chemistry is described as are means of selective absorption and concentration of H_2 . Benfield systems designed for use in producing SNG from naphtha, from heavier hydrocarbons, and from coal are outlined and their investment and operating costs given. Systems for purification of low BTU fuels are also discussed. Operating data from commercial units are presented.

SYNTHETIC FUEL GAS PURIFICATION

BY THE SELEXOL[®] PROCESS

by John W. Sweny
Allied Chemical Corporation

Processes for production of fuel gases from coal and petroleum come at a time when stringent requirements on sulfur emissions are being imposed. Indeed, part of the demand for these gaseous fuels stems from these requirements, because gases are relatively easy to desulfurize compared to liquids and solids.

The main contaminant to be dealt with is H_2S . After removal H_2S is converted to elemental sulfur, which is harmless and even sometimes profitable. Claus plants get first consideration for H_2S conversion because they are well-known and economical. For high conversion and economy, Claus plants require a feed that is rather rich in H_2S . A feed containing 20% H_2S is considered a satisfactory Claus feed.

Concentrations as high as 20% are difficult to reach when treating synthetic fuel gases. In the production of high-Btu gas from coal, for example, the intermediate gas before methanation usually contains about 0.7 vol % H_2S and 30% CO_2 . If both H_2S and CO_2 are removed to low levels with a non-selective solvent, the

[®]SELEXOL is a Registered Trademark of Allied Chemical Corporation.

Claus gas will be too lean for processing, about 2-3% in H_2S . The low-Btu gases would yield richer Claus feeds than this, but they too will yield gases too lean for economy and high conversion. A typical gas, for example, contains 0.7% H_2S and 8% CO_2 , which would, with a non-selective solvent, yield a Claus gas containing only about 8-10% H_2S .

High Selectivity Required

Thus there is a need for highly selective solvents. Several selective solvents of both physical and chemical type are available but few have enough selectivity to remove H_2S to the very high degree required while holding CO_2 absorption down to acceptable levels. H_2S content of product gases must usually be 4 ppmv or less. If the raw gas contains 0.7% or 7000 ppm, the degree of removal is then at least 99.94%, which may be higher after allowance for shrinkage due to CO_2 absorption. If the Claus gas is to contain 20% H_2S , the amount of CO_2 absorbed can only be four times that of the H_2S , or 2.8% of the original feed gas. Thus, if the original feed gas contained 30% CO_2 , its degree of removal cannot exceed 9.35%; if 8%, 35.0%. The task is then to remove 99.94% of the H_2S while leaving 90.7% of the CO_2 untouched in one example and 65% untouched

in the other.

Chemical solvents can remove acid gases with great efficiency and economy if the concentrations are low, but they cannot, as far as I know, achieve the kind of selectivity for H_2S required for Claus processing of synthetic fuel gases. The 4 commercially available physical solvents, including SELEXOL Solvent, can however achieve the required selectivity. The physical solvents, moreover, can remove certain other sulfur compounds which are non-acidic: COS, mercaptans, organic sulfides, and thiophenes. These must be converted to H_2S before they can be absorbed by chemical solvents. Some physical solvents, including SELEXOL, can simultaneously remove water to the standard specifications for pipeline gas, thus eliminating the need for auxiliary drying units.

Selective Absorption

Absorption systems forming ideal solutions show selectivities in proportion to pure-component vapor pressures, in accordance with Raoult's Law. For example, the vapor pressure of CO_2 at $60^\circ F$ is 752 psia; for H_2S , 230 psia. If the vapor and the liquid form ideal solutions, the relative solubility or selectivity will be $752/230 =$

3.27; that is, under equivalent conditions, H_2S will have 3.27 times the solubility that CO_2 will.

Good selective agents, however, will form non-ideal solutions in which both solutes are solvated, H_2S being more strongly affected than CO_2 . The selectivity for these in SELEXOL Solvent at $60^\circ F$ and 1000 psia is 9.16, about 2.8 times what it would be in an ideal solution. This nine-fold value for selectivity is not constant; it will vary somewhat with temperature, pressure, and composition of the system. Although there are large negative deviations from Raoult's Law, the solvation does not prevent easy desorption. Heats of desorption of H_2S and CO_2 from SELEXOL Solvent are only about $1/4$ of those found with chemical solvents.

Both the vapor phase, since it is under high pressure, and the liquid phase are very non-ideal. Thus many experimental VLE points are required for SELEXOL Solvent. These have been difficult to correlate over the wide ranges of composition, temperature, and pressure encountered in gas purification plants.

The selectivity inherent in the solvent, as expressed by a ratio of K-values, will not be realized unless the

solvent rate is kept low. If the solvent rate is near the minimum required for complete removal of H_2S or COS (i.e., if the Kremser absorption factor is somewhere between 1.0 and 1.5) it will be well below the minimum required for CO_2 removal. In the examples used, only about 15 to 25% of the CO_2 present may be removed, no matter how many contacts are provided in the absorber. CO_2 will be quickly absorbed at the top of the absorber, reaching saturation in the first contact. As the solvent passes downward, absorbing H_2S , through the other contacts, no more CO_2 will be absorbed. In this way a large fraction of the H_2S can be absorbed while holding the absorption of CO_2 to a low level. Absorbers used for selective absorption will therefore have many contacts and low solvent circulation rates, in contrast to the bulk absorbers which will have relatively few contacts and high circulation rates.

The quantity of H_2S in gas from coal and crude oil is low, generally less than 1%. The CO_2 concentration, on the other hand, can be high, as high as 30%. This means that the temperature profile down through the absorber will be dominated by CO_2 rather than by the key component, H_2S .

The high partial pressure of CO_2 will cause substantial absorption to take place at the top, causing a quick rise in temperature at the top contact, followed by a slower rise down through the other contacts as H_2S and smaller quantities of CO_2 are absorbed.

The temperature profile in selective absorption will then normally be irregular, and the assumption of straight-line or equal-percentage variation down the tower cannot be made. At low solvent rates, moreover, the feed gas may further change the profile if the feed temperature is markedly different from absorber temperature.

K-values are sensitive to temperature; for example, the K-values for H_2S in SELEXOL Solvent in methane systems at 1000 psia increase about 15% for each 10°F rise in temperature. Thus, solubility will more than double between a drop from 100°F to 40°F . The temperature profile to be expected must therefore be taken into account in making a satisfactory design, and K-values must be available to permit designing as closely as possible to the temperatures which will prevail down through the tower.

The complete cycle of course, includes flashing, stripping, and heat exchange, which are carried out at a completely different set of pressures, temperatures, and compositions from that for absorption. The K-data required to calculate the results of these operations need to be predicted accurately over a wide range of conditions, which puts a strain on experimental VLE determinations and methods of correlation. Development of reliable K-data is probably the most important single factor in the success of a physical solvent, and offers the most difficult challenge in putting such processes into practice.

High-Btu Synthetic Gas

The SELEXOL process will be used in one of the new coal-gasification processes, the Bi-Gas process originated by the Bituminous Coal Research Corporation and sponsored by OCR and AGA. A demonstration plant is now planned for construction at Homer City, Pa.

To optimize methanation, some coal gasification processes require gas purification at three stages: removal of H_2S from gasifier effluent after CO-shift conversion and two stages of CO_2 removal, one before and

one after methanation. The most important step is H_2S removal. The final product must be H_2S -free, the methanation catalyst must be protected from poisoning, and the CO_2 off-gas must have so little H_2S in it that it can be safely released to the atmosphere. Further, the H_2S removed must be concentrated enough for economical conversion in a Claus plant.

A typical flowscheme for gas purification is shown in Fig. 1. The composition of the feed to the H_2S absorber is:

H_2	-	46.	vol %
CO	-	15.	"
C_1	-	8.	"
CO_2	-	30.	"
H_2S	-	0.7	"

The ratio of CO_2 to H_2S is thus 43/1. H_2S must be removed to a high degree, at least to 4 ppmv (99.94% of that present in feed) to insure that the CO_2 off-gas will contain less than 20 ppmv. This must be done in the presence of a large excess of CO_2 , whose absorption must be suppressed in order to produce a sufficiently rich Claus gas,

something over 20% in H₂S.

This is done by first removing H₂S, using selective absorption and recycling some of the flashed gases. Stripping is with steam, which can be condensed out of the Claus plant feed, giving a mixture of CO₂ and H₂S only. The Claus feed will contain more than 30% H₂S, a concentration well over that required for economical Claus processing.

In the flowscheme shown, only 4 - 4½% of the CO₂ present in feed will be absorbed in the H₂S removal system. This fraction can be varied by altering the number of stages in the absorber, the recycle rate, or the absorption temperature. Thus the costs of H₂S removal can be balanced against the costs of conversion in the Claus plant to bring down the overall costs to a minimum.

Gas leaving the H₂S removal section has essentially the same composition as that entering it, except that H₂S is at 4 ppmv. This gas passes to the CO₂ removal section, where the H₂S concentration will be further reduced to a few tenths of a ppm before methanation.

CO₂ can be removed both before and after methanation to suit any specification of methanator feed. Drying

of the final product to pipeline specification can also be arranged in a SELEXOL Process system, water leaving the system in stripping gas, which can be dry nitrogen coming from the air separation plant required to supply oxygen for gasification.

The CO₂ removal section is very simple. Besides the essential items of absorber, stripper, and pump, it has a flash tank and recycle compressor to keep methane losses very low, and a chiller to counter heat inputs from pumping and warm feed gases. CO₂ removal with SELEXOL Solvent is economical because most of the CO₂ is removed by simple flashing. Indeed, if CO₂ in the product could be 3.0%, regeneration could be by flashing alone. A lower CO₂ specification and a need for drying requires, however, that gas stripping be used.

Low-Btu Synthetic Gas

Another application which the SELEXOL Process seems to fit well is the purification of low-Btu fuel gases from coal. These gases, produced at intermediate pressures, are intended for turbine or boiler fuel. A typical gas from an air blown gasifier would have the following composition:

H ₂	-	15. vol %
N ₂	-	49. "
CO	-	22. "
C ₁	-	4. "
CO ₂	-	9. "
COS	-	.07 "
H ₂ S	-	.7 "

After sulfur removal, this gas is the fuel for gas turbines or boilers. It is important to note that in this example we have shown that COS is contained in the gas. All of the products from coal gasification we have seen have included COS as well as H₂S, in about a 1 to 10 proportion. Complete gas analyses have also shown lesser quantities of CS₂, mercaptans, thiophenes, HCN, aromatics, and olefins. These can all be removed by SELEXOL Solvent without decomposition of the solvent. the solubility of COS, however, lies between that of H₂S and CO₂, so that it is more difficult to produce a concentrate of COS than it is to produce a concentrate of H₂S. It can be successfully done, however, as this low-Btu gas example will show.

We have chosen severe requirements for treating this

gas. Total sulfur, including both H_2S and COS , is to be as close to 1 ppm as possible, while maintaining a Claus gas feed at 15% in total sulfur. The ratio between CO_2 and H_2S is 13 to 1, somewhat more favorable than that for high-Btu gas, but the presence of COS is a serious complication. COS does not harm SELEXOL Solvent and is absorbed by it, but its solubility is somewhat less than that for H_2S , which indicates that relatively higher circulation rates will be required. This will cause a greater absorption of CO_2 , leading to a less-rich Claus feed. In short, if COS becomes the key component, it will be more difficult to produce a satisfactory Claus feed, since the selectivity between COS and CO_2 is about half that between H_2S and CO_2 .

Nevertheless, it is possible to meet these requirements with an efficient absorber and some recycling. The simple flowscheme for this process is given in Fig. 2.

If the concentration of each solute can be 0.5 ppm, the degree of H_2S removal will be 99.9923%, and of COS removal, 99.23%. If COS is removed to the required degree, H_2S will be also, provided that stripping is good enough. Thus, absorption will be controlled by COS and stripping by H_2S . The stripping gas is steam, so that the Claus

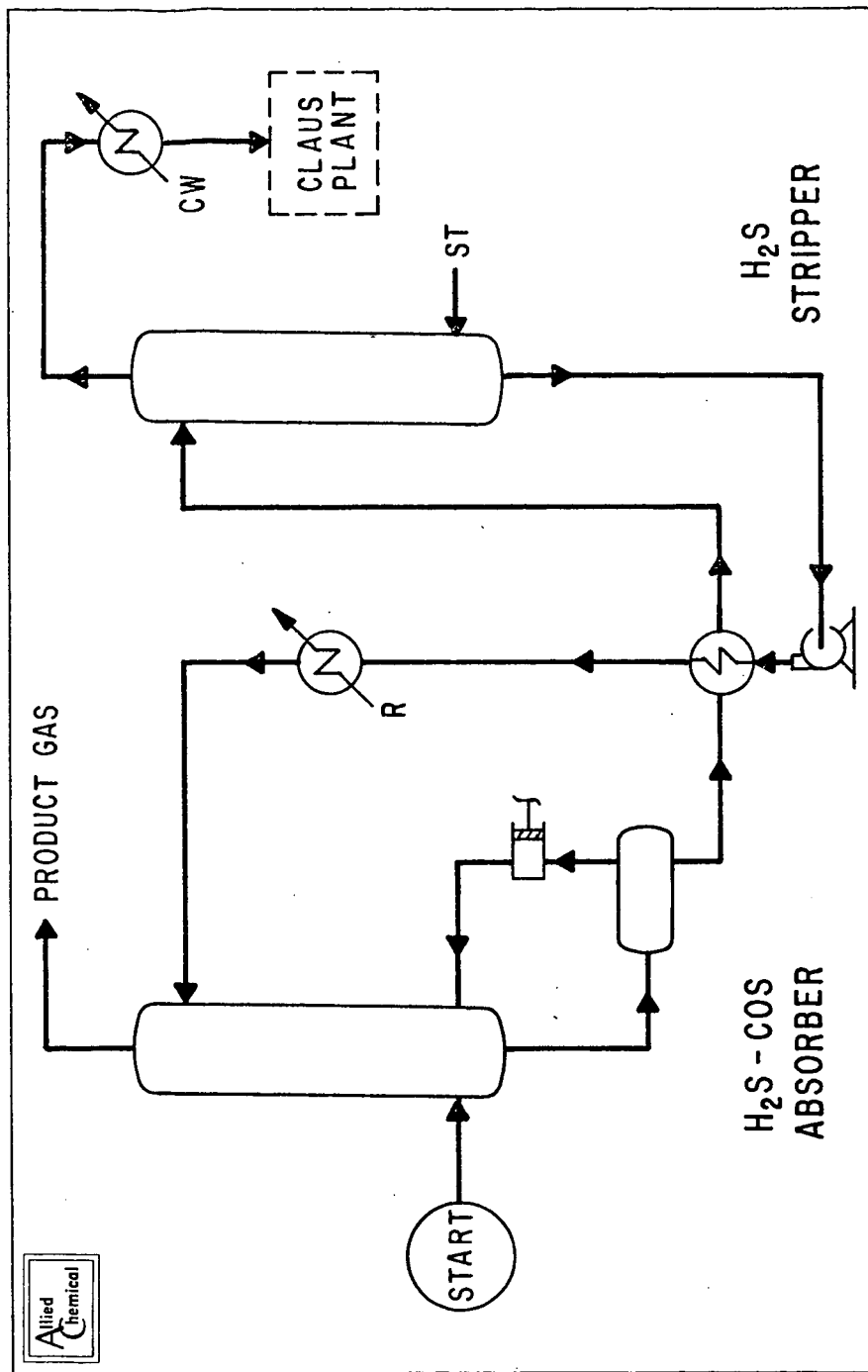


FIG. 2 SELEXOL™ PROCESS FLOW SCHEME FOR LOW-BTU GAS FROM COAL GASIFICATION

gas will consist only of H_2S , COS , and CO_2 . The H_2S - COS content will be over 15% but under 20% because of the lower selectivity between COS and CO_2 .

Conclusion

The trend of anti-pollution regulations governing synthetic fuel gas plants is toward conversion of almost all sulfur in feedstocks to elemental sulfur. The most reliable and economical conversion plant is the Claus plant, which does, however, need reasonably concentrated feeds for efficient operation. Because of high inherent selectivity for H_2S and COS over CO_2 , SELEXOL Solvent can successfully concentrate these sulfur compounds for Claus processing and yet remove them from products sufficiently to satisfy the most stringent requirements.

- - - - -

ACID GAS SEPARATION BY RECTISOL IN SNG PROCESSES

Gerhard Ranke, Linde A. G. 8023 Hoellriegelskreuth, new Munich, Germany
A. B. Munro, Lottebro Corporation

Economical acid gas removal plays an important part in the production of Substitute Natural Gas or of Low-BTU-Gas by coal gasification. Because the removal of H₂S, COS and CO₂ will be carried out under high pressure, a physical absorption process shows lower utility consumption figures and a lower solvent circulation rate than chemical absorption. Desulphurization is especially important. Air pollution standards require that the sulphur content (H₂S, SO₂) in the offgas be as low as possible. The extremely sulphur-sensitive Methanation Catalyst requires that all sulphur in the feedgas be removed down to the PPB-level. Sulphur compounds must be delivered to a Claus-unit at a concentration suitable for elemental-S removal.

Rectisol is most suitable for all these requirements; with a single solvent which is cheap, widely available, and non-corrosive, H₂S and COS are removed down to 1 ppm or, if required, to 0.1 ppm. Final purification of the gas with Zinc Oxide is then feasible. H₂S is concentrated to 20-30% in the H₂S-fraction. CO₂ can be removed to any desired level. The CO₂-offgas contains less than 5 ppm H₂S. CH₄ and H₂ losses can be reduced to less than 1% by means of a recycle compressor.

The process has been in commercial operation for several years for acid gas removal from the crude gas produced by the partial oxidation of residual oil, and meets the air pollution requirements for Los Angeles, California. Actual operating data are given for a plant with 80 MMSCFD throughput.

SYNTHETIC FUEL GAS PURIFICATION USING SHELL TREATING PROCESSES. E. J. Fisch,
C. J. Kuhre, 2525 Murworth, Houston, Texas 77054.

While fuel gas manufacture may initially be based upon gasification of lighter petroleum fractions which are essentially free of sulfur and other impurities, the energy supply industry will eventually turn to gasification of heavier raw materials, coal and crude oil. These materials however, will require more intensive processing, not only because of their lower hydrogen-to-carbon content ratios, but because of their higher contents of impurities, particularly sulfur. Because of society's unwillingness to tolerate even the present level of sulfur emissions, the application of gasification processes to these raw materials will require attendant means of removing the sulfur to acceptable levels in all product streams. Present technology does not offer economical means to adequately desulfurize coal or crude oil prior to gasification. Therefore, sulfur removal will most likely be effected by treating of intermediate or product gas streams. Three gas treating processes developed by Shell for general application for sulfur removal are applicable at one or more points in the manufacture of fuel gases. These are the SULFINOL, ADIP, and SCOT processes. The application of these processes is illustrated by cases for the production of (a) 1000 Btu per cubic foot substitute natural gas, (b) 400-500 Btu per cubic foot gas generated from coal for transportation to power generation units, and (c) 150 Btu per cubic foot gas from crude oil (residue) or coal for power generation via a combined gas/steam turbine cycle.

The Economics of Power Generation
Via the Shell Gasification Process

P. J. Halbmeyer

INTRODUCTION

An SGP-based power station (SGP/PS) is based on the partial oxidation of fuel and differs from a conventional power station (CPS) in the following main aspects:

1. In a CPS the fuel oil is burned with air at atmospheric pressure in a boiler where the heat of combustion is used to produce superheated high-pressure steam.

In an SGP/PS the fuel oil is first partially oxidized with air at elevated pressure, whereby the fuel oil is converted into a raw fuel gas. This gas, after removal of contaminants such as ash and sulphur, is subsequently burned in a combustor and expanded in a gas turbine.

2. In a CPS all electricity is produced by the expansion of steam in turbo-generators.

In an SGP/PS electricity is partly produced by expansion of gas in gas turbo-generators and partly by expansion of steam in steam turbo-generators.

The SGP/PS scheme shows the following interesting aspects:

- a) Recovery of up to 95% of the sulphur in fuel oil as elemental sulphur is possible with conventional, well proven gas treating and sulphur recovery processes.

- b) The high efficiency of electricity generation via the gas and steam turbine cycle compensates for the efficiency loss caused by the processing steps converting the high-sulphur, high-ash residual fuel oil into a clean fuel gas.
- c) No emission of particulate matter.
- d) Low emission of nitrogen oxides because of low flame temperature.
- e) Lower demand for cooling water than in a CPS, since only part of the electricity is raised via the steam expansion (and subsequent steam condensation) cycle.
- f) The operation at elevated pressure results in the use of compact, shop-fabricated, equipment.

The schemes discussed here are all based on the use of residual fuel oil as fuel to the power station. The SGP has been developed with special emphasis on the use of heavy residual fuel oil as feedstock and commercial operation of the SGP units has shown that the reliability and on-stream efficiency of the process is high, even in cases where high-ash fuels are being processed. An on-stream efficiency of 95% can be taken as a realistic figure.

At present close to 100 units with a total throughput exceeding 11,000 tons/d fuel have been, or are being, constructed. A power station based on the above concept but using coal as feedstock has been built in Germany.¹⁾

DISCUSSION

The conversion of the chemical energy of a fuel oil into electricity is usually effected by the following steps (Fig. 1):

- a) Complete combustion of the fuel oil with air at atmospheric pressure.
- b) Recovery of the heat of combustion by the production of superheated, high-pressure steam.
- c) Expansion of the steam through a steam turbo-generator for the production of electricity.
- d) Condensation of the steam and recycle of the condensate in the form of boiler feed water to step b).

In this process the sulphur present in the fuel oil is converted into SO_2 and emitted with the flue gas to the atmosphere unless special equipment is installed for the removal of this SO_2 ²⁾.

An SGP-based power station³⁾⁻⁷⁾ as envisaged here consists of the following steps (Fig. II):

- a) Partial oxidation of the fuel oil with air at elevated pressure (10-20 atm.) for the production of raw fuel gas.
- b) Removal of the sulphur components (mainly H₂S) from the raw fuel gas.
- c) Complete combustion of the clean fuel gas.
- d) Expansion of the combusted gas through a gas expansion turbine, coupled with an electric generator, for the production of electricity.
- e) Cooling of the gas turbine exhaust gas.
- f) Recovery of heat in steps a), c) and e) in the form of high-pressure superheated steam.
- g) Expansion of the steam through a turbo-generator for the production of electricity.
- h) Condensation of the steam and recycle of the condensate in the form of boiler feed water to steps a), c) and e).

Compared with a conventional oil-fired power station the SGP/PS shows three significant new elements. These are:

1. The fuel gas preparation step

In this step the fuel oil is first partially oxidized in a reactor at elevated pressure (15-25 atm.) with air, whereby the oil is converted into a gas with carbon monoxide and hydrogen as the main constituents.

The sulphur of the fuel oil is mainly converted into hydrogen sulphide, which component can subsequently be removed with a conventional gas-treating solvent.

In Fig. III a scheme is given of the Shell Gasification Process (SGP). The main items of the SGP are:

- a) Reactor with combustor/gun assembly.
- b) Waste-heat boiler enabling the production of high-pressure steam.
- c) Gas scrubber to clean the gas of carbon and ash.
- d) Carbon work-up and recycle section.

The operating pressure of these units ranges between atmospheric pressure and around 60 atmospheres. The pressure of the steam raised in the various waste-heat boilers ranges between 30 and 100 atmospheres.

In the case of partial oxidation with air, as envisaged for power station applications, the gas leaving the SGP will have the following composition when starting with a residual fuel oil of 4% wt sulphur:

	% vol. (dry)
H ₂	14.7
CO	22.0
CO ₂	2.5
H ₂ S	0.5
COS	0.03
CH ₄	0.3
N ₂ + A	60.0

This gas is free of soot and ash and is subsequently treated for sulphur removal. Since the gas contains CO₂ as well as the sulphur components H₂S and COS, a number of alternative methods for the removal of the sulphur components and the subsequent conversion of these components into elemental sulphur is to be considered, for instance:

a) Complete removal of COS and H₂S

This is possible by using a mixture of a physical solvent and a chemical solvent such as Sulfinol[®],

which consists of Sulfolane (tetrahydrothiophene 1.1 dioxide) and DIPA (di-iso propanol amine). Such solvent completely removes the H_2S and the COS but at the same time completely co-absorbs the CO_2 . This results in a considerable dilution of the H_2S feed to the subsequent Claus unit, where the H_2S is converted into sulphur. A special design for the Claus unit is therefore required in this case. An overall sulphur recovery of 95% can be obtained.

b) Selective removal of H_2S

This is possible by using a chemical solvent such as di-iso propanol amine (Shell Adip process)⁸, which completely removes the H_2S but only part of the CO_2 and COS . In this way a reasonable H_2S concentration in the feed to the Claus unit is obtained, making the design of the Claus unit simpler but at the cost of a lower overall sulphur removal efficiency, which will be of the order of 85-90%. By incorporating special design features in the sulphur recovery unit (Claus unit), this figure can be increased by up to 5 points.

2. The supercharged boiler

The clean fuel gas, as produced in the gasification/desulphurization section, is burnt in a supercharged boiler at about 10-20 atm. In this boiler the high-pressure saturated steam produced in the waste-heat boilers of the gasification unit is superheated.

The supercharged boiler has the following advantages:

- a) By application of such a boiler the steam conditions are made independent of the gas turbine outlet temperature. This means that the steam superheat temperature can be 540°C instead of 350 to 400°C if the steam is superheated in a non-fired gas turbine exhaust boiler installed downstream of a gas turbine with an inlet temperature of 850 to 950°C (present-day technology for industrial gas turbines). The higher steam superheat temperature results in a higher net efficiency for the power station. A fired exhaust boiler, although superior to a non-fired one, would show higher stack losses as compared with a supercharged boiler.
- b) The high gas pressure and the high heat transfer rates result in a compact boiler, which is fully shop-fabricated.

c) It is expected that the nitrogen oxides emission will be lower than in direct combustion of the gas in the gas turbine combustion chamber.

By controlling both the combustion air dosage and the amount of steam superheated in the boiler, the temperature of the gas leaving the supercharged boiler can be regulated. This gas is sent to the gas expansion turbine.

3. Gas expansion turbine

The incorporation of gas turbines in natural gas (or light distillate fuel) fired power stations is finding increasing application both because of the high efficiencies that can be obtained and/or because the capital cost for such power stations is relatively low⁹). An important aspect of using a gas expansion turbine is that the inlet temperature of such a turbine can be considerably higher (at present 850°C - 950°C) than the temperature at which a steam turbine can operate (550°C), this governed by the fact that steam-raising and superheating at higher temperatures, as well as providing suitable turbine casings for high-pressure/high-temperature steam, meets with great technical problems. The combination of a gas expansion turbine cycle with a steam expansion cycle therefore enables the conversion

of heat into electricity, starting at a very high temperature level, which favourably affects the conversion efficiency.

Another important aspect relevant to the use of gas turbines in power stations is the reliability and availability of the gas turbine. The use of gas turbines in power stations generally has been confined to those power stations that are operated for peak-shaving purposes, for which duty the low capital costs are of advantage and availability is of lesser importance. Recent reports indicate that the availability of the gas turbine cycle can be better than that of the steam turbine cycle⁹⁾ and also that long periods between maintenance are being obtained¹⁰⁾. An example of the increasing confidence in the reliability and availability of gas turbines is their use in high-capital natural gas liquefaction plants¹¹⁾. As already stated, it seems unlikely that a steam temperature above 550°C can be obtained, mainly because of very great material problems encountered in the design of the steam turbine, boiler and superheater. There are, however, promising indications that, through a combination of blade cooling techniques and blade material developments, the allowable inlet temperature of gas turbines will continuously be increased. This means that the efficiency of converting heat into electricity can be expected to gradually

increase for power stations incorporating gas turbines. In Fig. IV a forecast of gas turbine inlet temperature progression, as given by United Aircraft¹²⁾, is presented.

EFFICIENCY OF SGP-BASED POWER STATIONS

The combination of the various elements of an SGP/PS, as described above, together with a conventional steam cycle leads to a power station (Fig. V) where the efficiency loss caused by the clean fuel gas preparation step is compensated to a great extent by the high heat-to-electricity conversion efficiency obtained through the incorporation of the gas turbine. In Table I the effect of the gas turbine inlet temperature on the overall efficiency of the SGP/PS is shown.

Table I
Efficiencies of SGP-based Power Stations^{a)}

Gas turbine inlet temperature, °C	850	1000	1200	1400
Plant efficiency, %	38.5	40.8	43.0	44.7
Percentage power ex gas turbine cycle, %	24	29	35	40
Steam to be condensed, kg/kWh as % of conventional power station %	87	81	74	69

a) The efficiency of a CPS comprising steam turbines with an efficiency equal to those used in the above SGP-based power stations was calculated to be 39.5%.

From this table it can be concluded that at a gas turbine inlet temperature of around 900°C the efficiency of an SGP/PS is equal to that of a conventional oil-fired power station. This means that at 900°C the favourable effect of this high temperature level on the overall plant efficiency has fully compensated for the efficiency losses caused by the fuel gas preparation step.

An interesting aspect is that, since in the SGP/PS electricity is generated both by a gas expansion cycle and by a steam expansion cycle, considerable freedom exists in optimizing towards alternative aspects such as efficiency, capital outlay and cooling water requirement. If, for instance, thermal pollution is an important consideration, the cooling water requirement can be reduced by diverting part of the steam into the gas expansion cycle. In this way electricity generation via the gas expansion cycle is increased, and the cooling water requirement for steam condensation is decreased. This scheme would of course at the same time decrease electricity generation via the steam cycle and would result in consumption of boiler feed water. It has been calculated, for instance, that at 850°C turbine inlet temperature a steam injection into the gas turbine

inlet stream at a rate of 2.5 kg/kg power station oil feed would have the following effects (compare Table I):

Percentage power ex gas turbine cycle would increase from 24% to 36%. Steam to be condensed would be reduced from 87% to 60% (kg/kWh as % of conventional power station). Plant efficiency would be reduced from 38.5% to 37.7%.

ECONOMICS OF SGP-BASED POWER STATIONS

In Table II the economics of an SGP/PS are compared with those of a conventional power station. Some uncertainty exists about the capital cost figures used for the various SGP/PS schemes given.

This aspect is under investigation.

The additional costs incurred in the SGP/PS as compared to the costs of a conventional power station are charged in this table as a "sulphur removal cost" against the fuel oil used. In this way the operation of an SGP/PS can be compared with alternative ways of removing sulphur from fuel oil.

Such an alternative process is, for instance, the hydrodesulphurization of residual fuel oil (the so-called "direct hydrodesulphurization process"). This process results in

desulphurization costs ranging from \$200 to \$360 per ton sulphur removed, depending on crude origin¹³) (for residual oils of certain, high ash content, crude types hydrodesulphurization is not yet feasible).

Table II
Economics of SGP-based Power Stations

Basis: 200 MW unit; 6000 hours annual service period; fuel with 4% wt sulphur; 90% desulphurization.

Operating costs plus a capital charge taken as 20.5% on capital (5% for operating, maintenance and overhead, 0.5% for catalysts and chemicals, 15% for repayment of capital, tax and return on capital).

Sulphur credit: \$20/ton.

Conventional Power Station		SGP-based Power Station			
		I	II	III	IV
Turbine inlet temp., °C		850	1000	1200	1400
Plant efficiency, %	39.5	38.5	40.8	43.0	44.7
Capital US \$ x 10 ⁶ a)	40	48-46.5	48-46	48-45	48-44.5
Cost of sulphur removal ^{b)}					
\$/ton S	approx. 250 ^{c)}	165-134	130-85	96-26	70- -14
\$/barrel/% S	approx. 40 ^{c)}	26-21	20-13	15-4	11- -2

a) The capital figures are taken from a 1970 Shell/Sulzer study^{3, 7}) comparing a 200 MW CPS with a two-stage expansion SGP/PS and escalated for 1972. For Cases I,

II, III and IV two assumptions have been made:

- 1) Capital remains 48 and
 - 2) capital is reduced proportionally with the increase in the gas turbine contribution to power generation.
- b) Calculated on the basis of the difference in price between high-sulphur fuel (for the SGP/PS) and the clean fuel (for the CPS) at a constant electricity price.
- c) Hydrodesulphurization of long residue (cost can be as high as \$360/ton S or \$57/barrel/% S¹³).

From Table II it can be concluded that an SGP-based power station using currently available gas turbines with an inlet temperature of 850°C results in "sulphur removal costs" that are of the order of 60 to 70% of the costs of alternative desulphurization techniques.

A further increase in the gas turbine inlet temperature would result in a substantial reduction of the "sulphur removal costs" of the SGP-based power station.

CONCLUSIONS

Compared with a conventional oil-fired power station, the SGP/PS has the following attractive characteristics:

- 1) Some 90% to 95% of the sulphur in the fuel is not emitted to the atmosphere but is recovered as elemental sulphur. The "sulphur removal costs" compare favourably with the costs of alternative desulphurization techniques.
- 2) No emission of particulate matter.
- 3) Low flame temperatures are applied, which can be expected to result in low emission of nitrogen oxides.
- 4) Reduced cooling water requirements.
- 5) The operation at elevated pressure results in the use of compact, shop-fabricated equipment, which will have a favourable effect on construction time.

References

- 1) Kombiniertes Gas/Dampf-Turbine-Kraftwerk mit Steinkohle-Druckvergasungsanlage im Kraftwerk Kellermann in Lünen by: K. Bund, K.A. Henney and K.H. Krieb, Brennst-Wärme-Kraft 23 (1971) Nr. 6 pp. 258-262.
 - 2) The Shell Flue Gas Desulphurization Process by: F.M. Dautzenberg, J.E. Naber, A.J.J. van Ginneken Chem. Eng. Progr. 67 (August 1971) pp. 86-91.
 - 3) Residual Fuel Oil Based Power Station using Partial Oxidation by: G.J. v.d. Berg, P.J.J. van Doorn and W.A. Aeberli (paper E. 3^a).
 - 4) Gasification of fuels with Gas Desulphurization for thermal power plants by: R. Rudolph and G. Kempf (paper E. 4^a).
 - 5) An Advanced Cycle Power Station System Burning Gasified and Desulphurized Coal by: F.L. Robson and A.J. Giramonti (paper E. 1^a).
 - 6) Method of desulphurization of high sulphurous fuel oil at power station by preliminary gasification under pressure with wet gas cleaning by: S.A. Khristianovich and V.M. Mallennikov (paper E. 2^a).
 - 7) Kraftwerke mit Schwefelfreien Abgas by: G.J. van den Berg, P.J.J. van Doorn and W.A. Aeberli Verfahrenstechnik 5 (1971) Nr. 10 pp. 406-408.
(Ref. 7 is an abstract of ref. 3)
 - 8) Developments in Sulfinol and Adip processes increases uses by: J.P. Klein, Oil and Gas Int. 10 (1970) No. 9 pp. 109-111.
 - 9) Neuzzeitliche Dampf-Kraftwerke, Bericht über die 1971 Steam Plant Convention in 's-Gravenhage. Brennst-Wärme-Kraft 23 (1971) Nr. 6 pp. 367-371.
 - 10) How gas turbine driven centrifugal and power train work for Shell by: C. Dale Davis.
The Oil and Gas J. 66 (1968) March 25th pp. 132-135.
 - 11) LNG from Alaska to Japan by: A.F. Dyer.
Chem. Eng. Progr. 65 (1969) No. 4 pp. 53-57.
 - 12) Advanced Non-Thermally polluting gas turbines in Utility applications by: F.R. Biancardi, G.T. Peters and A.M. Lauterman.
United Aircraft Research Laboratories Report J-970978-8 prepared for the United States Environmental Protection Agency, Water Quality Office, Contract No. 14-12-593; March 1971.
 - 13) The desulphurization of residual fuel oils from Middle East crude oils by: A.J.J. van Ginneken (paper A. 5^a).
- ^a) Ref. 3 to 6 and 13 are papers, as indicated, presented at the "Seminar of the Desulphurization of Fuels and Combustion Gases", United Nations Commission for Europe, Geneva, 16th-20th November, 1970.

FIG. I
BLOCK SCHEME- CONVENTIONAL POWER STATION

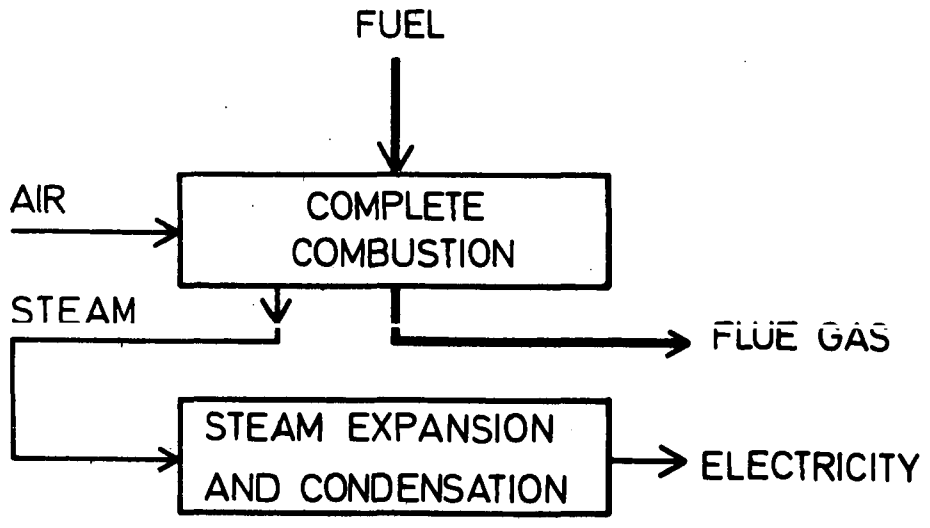


FIG. II
BLOCK SCHEME - PARTIAL OXIDATION BASED POWER STATION

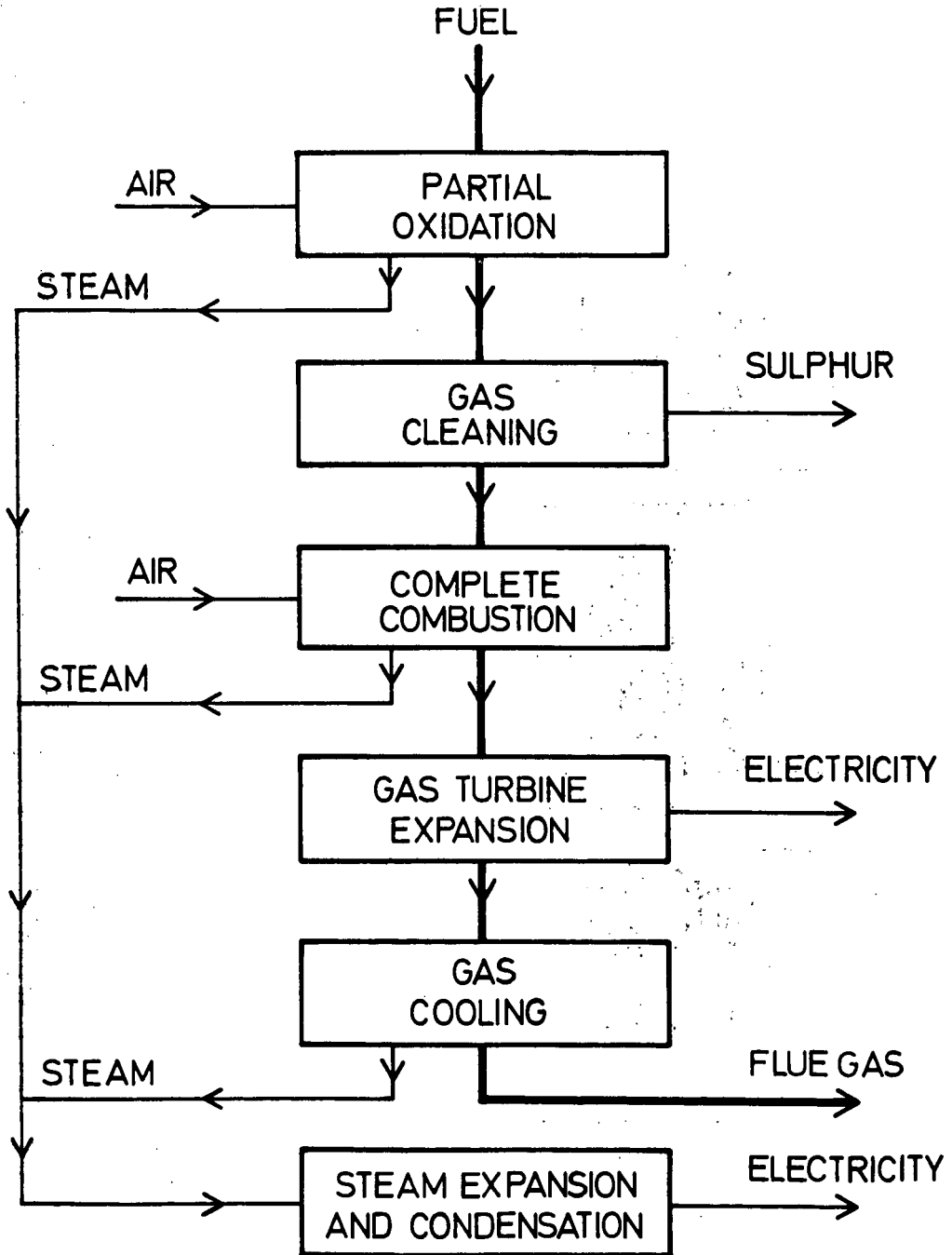


FIG. III
SGP PROCESS WITH CARBON RECYCLE

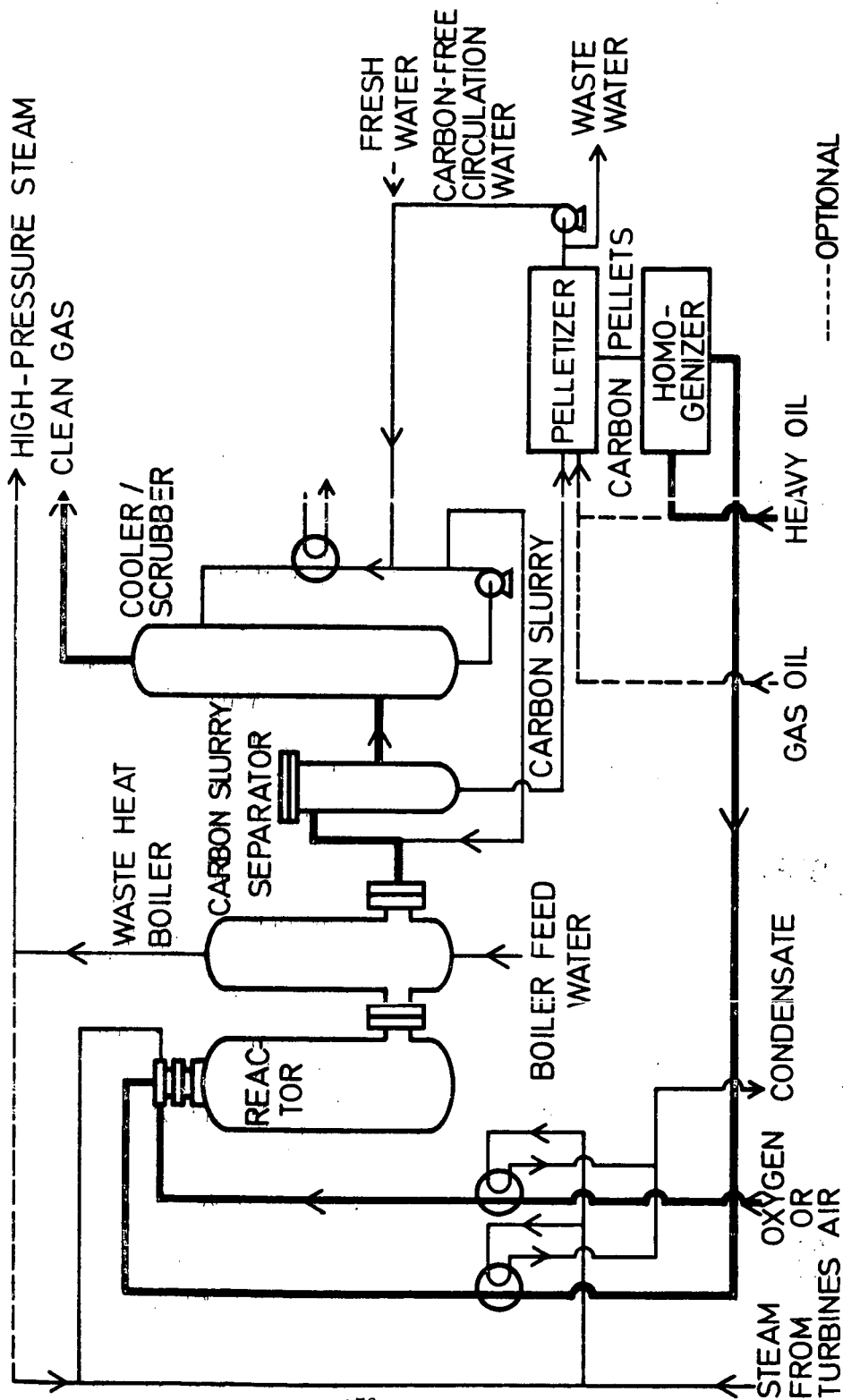


FIG. IV
 ESTIMATED TURBINE INLET TEMPERATURE PROGRESSION 8)
 (UNITED AIRCRAFT ESTIMATE)

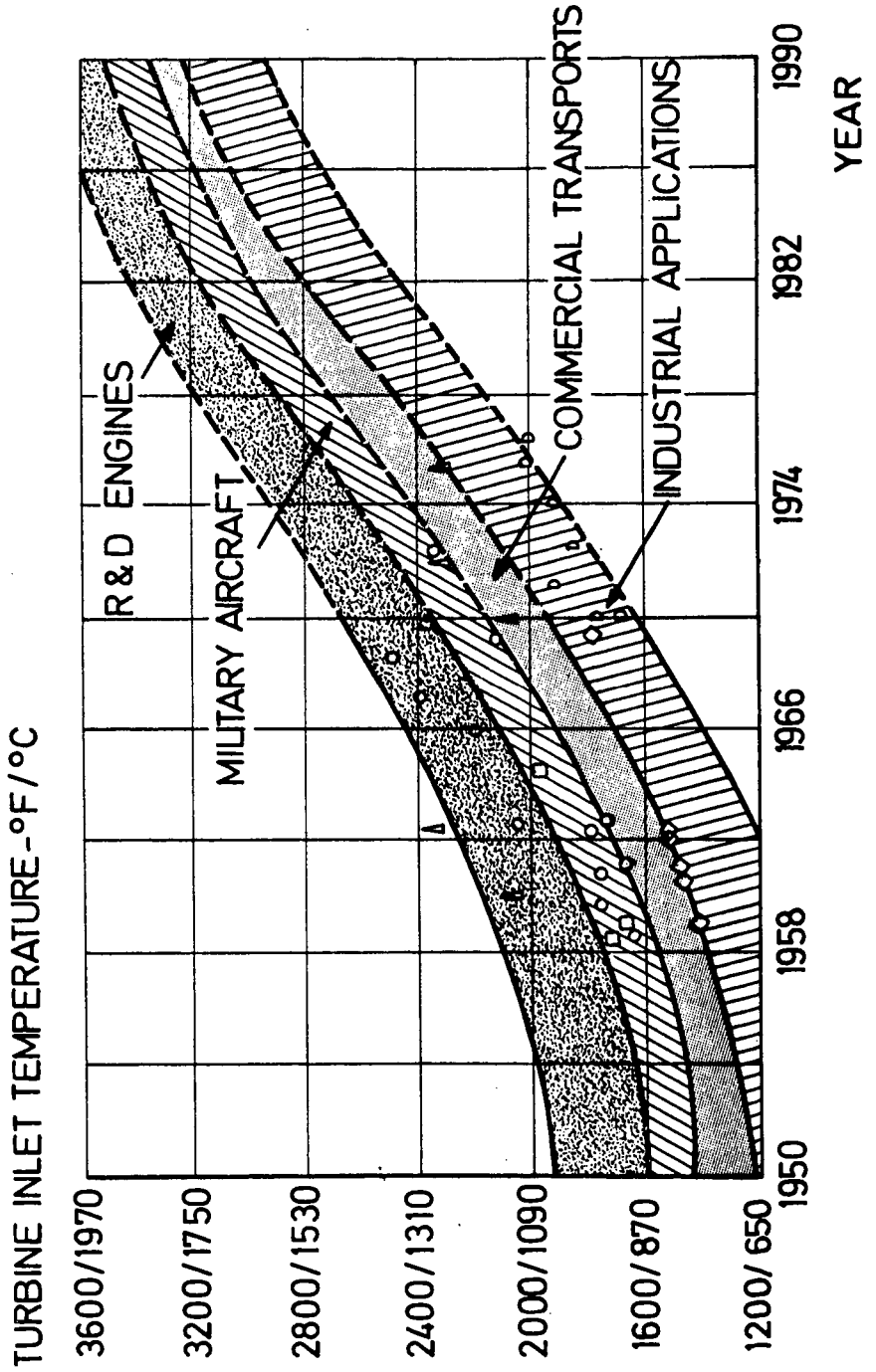
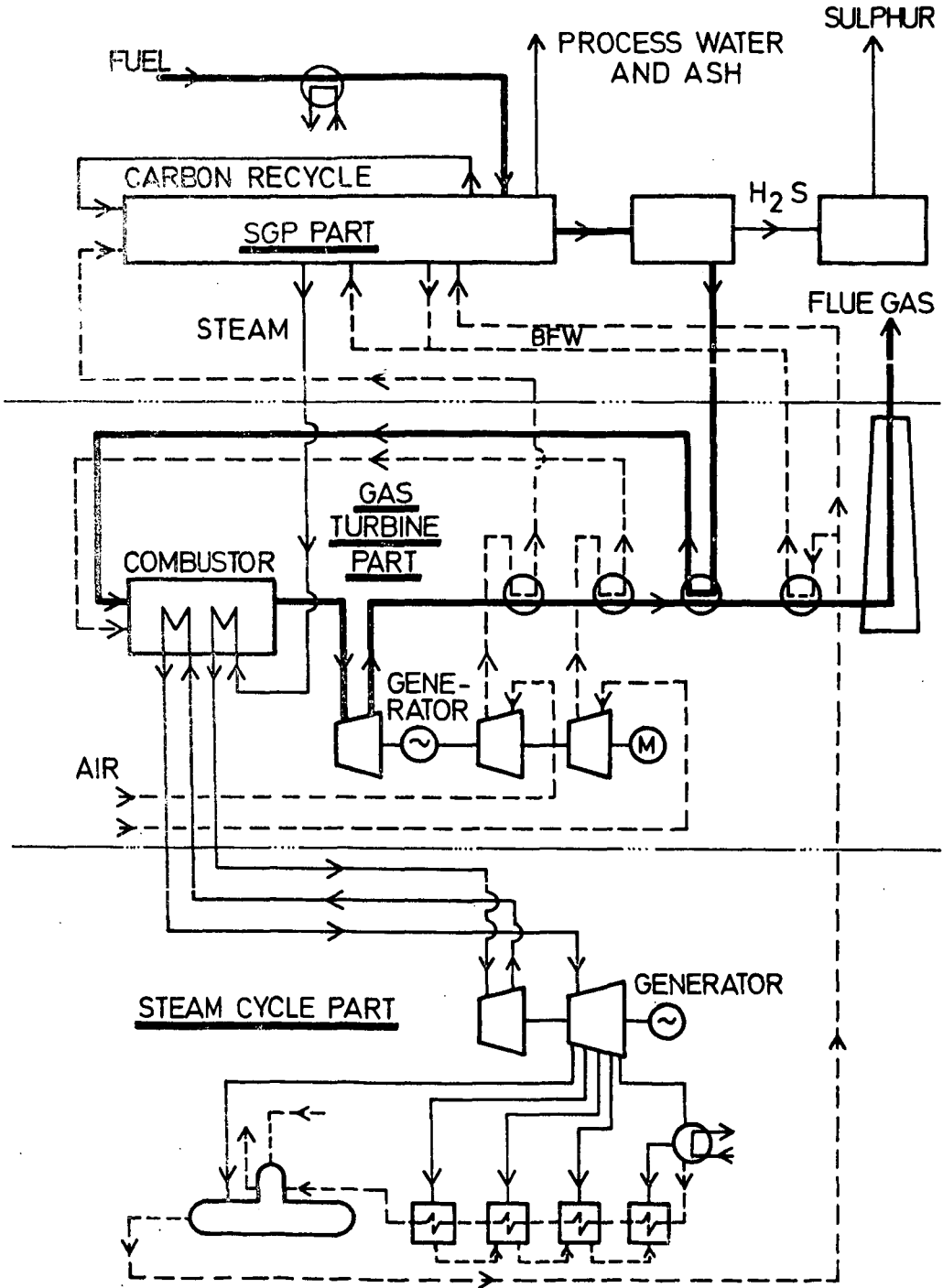


FIG. V
S.G.P.-BASED POWERSTATION



FLUIDIZED-BED COAL GASIFIER AS A LOAD-FOLLOWING CLEAN FUEL SOURCE

J. G. Patel and C. W. Matthews

Institute of Gas Technology
Chicago, Illinois 60616

INTRODUCTION

The electric power generated in the United States is growing at a rate of about 8-10%/yr. The electric load is expected to increase by a factor of 4 in the next 20 years to a total of 6.5×10^6 GWhr. It will take at least 20 years before nuclear energy, which today supplies less than 1% of our electric power, will carry the main burden of our power requirements. Therefore, for the next 15-20 years, most of the demand for electricity will have to be met by fossil fuels, i.e., coal, oil, and natural gas.

Natural gas, which is already in a short supply, will be increasingly assigned to more critical applications than combustion in large power plants. Furthermore, the available supply of natural gas may combat pollution more effectively from an overall standpoint when used for residential and small commercial needs. Coal and oil must, therefore, fill the demand for fuel for electric power generation. The use of oil for power generation must be limited to avoid heavy reliance on politically uncertain oil-producing countries. In addition, our balance of payments problems will balloon with increasing foreign oil purchases. Coal is the most logical answer to meet the growing power demand in the next 2 decades (see Figure 1).³

Coal is one of the largest fuel resources in the United States, but, when burned, it is a primary contributor to the sulfur and particulate pollutants in the atmosphere. One direct way of limiting sulfur emissions from coal combustion is to use low-sulfur coals; however, most are located in areas that do not coincide with the areas of need. When using high-sulfur coals, one alternative is to use scrubbing systems to remove sulfur dioxide produced during combustion. After spending \$300 million on a crash program to develop a scrubbing system, no viable commercial process is yet available. Their efficiency in sulfur dioxide removal is expected to be rather low, in the range of 80-90%.

Coal gasification with gas cleaning before combustion promises the greatest reduction in sulfur emissions. According to the Environmental Protection Agency,¹ a power plant using coal gasification in conjunction with an advanced combined gas turbine-steam turbine cycle promises to have the following benefits:

- Reduction of sulfur oxide emissions up to 99%
- Nitrogen oxide reductions of 90% when compared with present-day coal-fired plants
- A 40-50% reduction in thermal pollution by power stations
- Approximately 20-30% savings in both capital and operating costs over conventional plants
- An important impact on the balance of payments when the system is successfully demonstrated in the U.S. through the foreign sale of complete systems as well as additional royalties from foreign licensees of U.S. turbine manufacturers

- Elimination of the adverse effects of pollution control measures on the coal industry, thus increasing both revenues and employment in the major coal-producing states
- Reassignment of natural gas now supplied to the power industry to higher priority use
- Retention of teams of highly trained turbine designers by the gas turbine industry. These teams are a valuable national resource which might otherwise be dispersed because of the loss of the SST program and a reduction of Department of Defense support.

After a description of the Institute of Gas Technology's coal gasification plant concept for a clean fuel gas, we will show how the fluidized-bed coal gasifier will be able to follow the electric load characteristics of an intermediate-load power plant.

COAL GASIFICATION PLANT FOR UTILITY GAS

The clean gas produced from an air-based coal gasification plant is called utility gas, producer gas, or low-Btu gas. Figure 2 is a process flow diagram for IGT's proposed utility gas coal gasification plant. Values shown are for a nominal coal feed rate of 20 tons/hr.

After the coal feed is crushed to the desired size, single-stage lock hoppers are used to transfer it from atmospheric pressure to the elevated pressure of the gasifier. Steam and air are fed to the bottom of the gasifier. Heat is recovered from the hot raw gases produced in the gasifier and the gas is then cleaned of sulfur at low temperature by a selective hydrogen sulfide removal process. The gas can be scrubbed so that it contains less than 5 ppm of hydrogen sulfide. A small part of the cleaned gas is used to pressurize the lock hoppers.

The main gas stream, after cleaning, is reheated by exchange with hot raw gas from the gasifier. The gas then expands through a gas expander to the optimum pressure level for application to a combined cycle. The gas expander generates some electricity. The gas is cooled by generating steam to about 600° F to meet the gas turbine combustor's requirements. After combustion, the gas expands through the gas turbine, generating a large percentage of the total power output. Part of the energy recovered is used to drive the compressors to supply the gasifier air and the combustor air. Exhaust gas from the gas turbine is reheated by burning gas recovered from the coal feed lock hoppers. Final heat recovery generates steam in the waste-heat boiler for additional power generation. Of the total power generated, about 35% comes from the steam turbine and 65% from the expander-gas turbine.

The hydrogen-sulfide-rich gas from the hydrogen sulfide recovery process goes to a sulfur recovery plant. Ninety five percent of the total sulfur is recovered as elemental sulfur. The Claus plant tail gases still contain about 1% hydrogen sulfide. A process such as the Beavon Process is used to reduce the sulfur content of the tail gas to less than 250 ppm.

GASIFIER

The entire utility gas concept hinges on the coal gasifier's performance. The gasifier and its design concept will not be discussed here because it has been presented elsewhere.⁵ The gasifier must satisfy the following requirements:

- Operate reliably
- Gasify a high percentage of feed carbon
- Accept caking coal as feed
- Be capable of load-following

Figure 3 presents a simplified illustration of the gasifier. A single-stage lock hopper is preferred to transfer coal into the gasifier. This feed system was chosen so that the gasification plant will be simple, reliable, and cheaper. Lock hoppers tend to be attractive for utility gas production as the depressured lock hopper gas can be used without the need for recompression. The gasifier operating pressure has been set at 300 psi in this paper because the maximum operating pressure for commercially demonstrated lock hopper valves is 350 psi. We believe that higher operating pressures may be desirable; however, lock hopper valves to withstand the higher pressures have yet to be developed.

So that the utility gas process can accept the widest variety of coal feed, facilities for destroying caking properties of agglomerating coal are provided within the gasifier. We propose to pretreat at gasifier pressure and feed the hot pretreated char directly into the gasifier. The exothermic pretreatment reaction produces enough heat to generate the steam to satisfy the gasifier's requirements.

The gasifier is designed to gasify coal with air and steam in a fluidized bed. Simultaneously, the coal ash will be selectively agglomerated into larger and heavier particles for removal from the bed. The principle of ash agglomeration and separation which has been used in the gasifier design has been demonstrated both by Godel² and Jequier *et al.*⁴ The gasifier, which we call an ash agglomerating reactor (AAR), resolves the main problem of coal gasification in a fluidized bed rich in carbon—that of selectively removing low-carbon-content ash from the bed. A gas residence time of 10-15 seconds is provided above the fluidized bed so that any tars and oils which may be evolved are thermally cracked to gas and carbon.

Most of the sulfur produced by coal gasification with the gasifier will appear in the form of hydrogen sulfide. Although we selected a low-temperature sulfur removal system, it would be desirable to use a yet-to-be-developed high-temperature sulfur removal system to improve plant efficiency and decrease costs. In combined-cycle plants, a 2% increase in overall power plant efficiency is realized when a high-temperature sulfur removal system is used in place of a low-temperature system as previously discussed.

The combined gas turbine-steam turbine cycle is illustrated in Figure 4. There are many alternative ways that this basic concept can be implemented. The efficiency of combined-cycle systems depends to a major degree on the allowable gas turbine inlet temperature. Gas turbines used today operate around 1800°F. The allowable inlet temperature to gas turbines is projected to increase at 100°F/yr to a maximum of about 3100°F. United Aircraft Research Laboratories⁶ expects ultimate coal gasification-combined cycle thermal efficiencies of 57.7%.

POWER DEMAND REQUIREMENTS

The EPA¹, Division of Control Systems, characterized electrical generating capacity in three categories:

1. Base load. These units are 500 MW and larger and operate at a load factor of 75%. Base-load plants represent about 60% of total electrical generating capacity. Nuclear power plants are expected to fill most of this requirement in the future.
2. Swing or intermediate load. Capacity of these units is from 200 to 500 MW, and their load factor ranges from 40 to 50%. These plants represent about 30% of total capacity. The EPA believes that coal gasification, in conjunction with advanced power cycles, can be applied most favorably in this category.

3. Peak load. This load will probably be satisfied by gas turbines because quick response time is required. Units are less than 200 MW in size and operate at less than a 40% load factor.

If the coal gasification-combined cycle systems are to fill the intermediate load requirement, the coal gasifier must be able to vary its output over wide ranges with rapid response.

One of the large power companies has provided the following typical operating requirements for the upper and lower ends of the swing-load range. To fill the upper end of the range, the gasifier unit would operate 6 days/wk. On weekdays the gasifier would operate at full capacity for 8 hours, at one-third of capacity for 8 hours, and at an output varying from one-third to full capacity for the remaining 8 hours. On Saturday, the gasifier might operate at full capacity for periods up to 12 hours, or in other circumstances, it may operate at one-third capacity for the 24-hour period. The plant would be substantially shut down on Sunday. Desirably, the system would be designed to generate 10% of design output as needed on Sunday. These demands will occur for periods of less than 1 hour.

In the lower part of the range, the gasifier would operate from 6 to 12 hr/day on a random basis during about 3 days of the week. A fuel consumption of up to 5% of the full load requirement during standby periods may be acceptable, although fuel consumption should be as low as possible.

To follow the normal variations in electrical demand, the gasifier should be capable of adjusting at a typical rate of 1% of design capacity per minute. In an emergency situation, almost immediate shutdown is required.

AAR TURNDOWN

The following discussion describes attainable control methods for adjusting the output of a fluidized-bed gasifier without damaging process equipment. The following five possible methods are considered:

1. Change gas velocity in gasifier
2. Adjust gasifier temperature
3. Permit the bed to defluidize (no gas flow)
4. Change gasifier pressure
5. Operate gasifier at a fixed condition and vary the gas flow between the power generating plant and a parallel chemical fuel plant.

The gasifier output can be rapidly changed by adjusting the gas velocity through the fluid bed. The air and steam flows to the gasifier are adjusted while retaining a fixed ratio of steam to air, reactor pressure, and fluid-bed level. As an example, if the design velocity in the gasifier is 1 ft/sec and the minimum practical superficial velocity at the operating temperature is 0.3 ft/sec, a turndown of 3.3 can be obtained.

Another means of turndown is to reduce the coal reaction rates by lowering the gasifier's operating temperature. The temperature is altered by changing the ratio of steam to air entering the bed. Moderate temperature changes that are not made abruptly are satisfactory. Rapid changes over a wide range of temperatures may crack and spall the gasifier's internal insulation, causing both operating and mechanical problems. As the fluidized-bed temperature is reduced, the reaction rates drop off sharply. It is recognized that, in lowering the bed temperature, alterations in the air

and steam flows to the various injection points in the bed will be necessary to minimize changes in the ability to control ash agglomeration. The coal feed rate is adjusted to maintain a constant bed height. A constant superficial gas velocity can be maintained by adjusting the steam and air flow rates. The capability of turndown by this method is shown in Figure 5 for three different superficial gas velocities. The reactor could be turned down tenfold by reducing with the superficial gas velocity to 0.33 ft/sec and the gasifier's operating temperature to 1500°F. Decreasing the superficial gas velocity to one-third of design takes only minutes and gives a turndown to 30% of design. Lowering the reactor temperature to 1500°F at a rate of 100°F/hr (a recommended rate to avoid reactor refractory damage) takes 4 hours and results in a further turndown from 30% to 10% of design. Operating at these conditions, the AAR produces a gas with a heating value of 80 Btu/SCF, as compared to about 135 Btu/SCF under full load conditions. This could be used to fire boilers to produce process plant steam. As the reactor's operating temperature is reduced, the product gas heating value decreases (Figure 6) because less steam reacts with the coal to produce hydrogen and carbon monoxide. Idling conditions could be achieved by reducing the reactor temperature to 1400°F and superficial gas velocity to 0.33 ft/sec. The coal feed rate at these conditions is about 5% of the full load rate. Just enough coal is burned to heat the feed gas (mostly steam) to 1400°F.

For complete shutdown, the gasifier could be cooled to about 1400°F, which would take about 5 hours. The gas and coal flows would then be stopped and the bed allowed to collapse. For restarting, the bed is refluidized by reinjection of air and steam and the temperature slowly raised at a rate of 100°F/hr. For emergency shutdown, the bed is permitted to defluidize at temperature. In the defluidized state, the reactor would cool down at a rate of about 100°F/day. For weekend shutdowns there is no need to supply any heat to the defluidized bed. For longer shutdowns, spurts of air to briefly refluidize and reheat the bed might be injected into the bed to replace the heat lost. With controlled cooling, a hot char bed would not solidify but would maintain a free particulate form that could be refluidized with a minimum of trouble.

The gasifier pressure level can also be changed to obtain a fairly wide range of capacity in a given unit. If the gasifier is designed for 300 psi and the lowest system pressure that can be tolerated is 50 psi, the turndown ratio is 6. Although this may be extreme, one might certainly expect that the 300-psi pressure level could be dropped to 100 psi for a relatively easy-to-obtain turndown ratio of 3. In practice, some process upsets may occur if the pressure is changed too rapidly. Given sufficient time, it should be possible to turn the gasifier down safely by this method. Each incremental change in pressure requires an equivalent incremental change in steam and air injection to maintain a fixed superficial gas velocity in the gasifier.

The fifth way to reduce electrical outputs is to fix the gasifier at constant operating conditions, and, as the electrical load changes, to direct more or less of the gas output to the power-generating equipment. The rest of the gas would flow to a Fischer-Tropsch (F-T) unit designed to accept varying amounts of gas. (The unit need not be very efficient.) A reasonable percentage of the carbon monoxide and hydrogen would be converted to liquid fuels. Unconverted gas from the F-T unit would mix with the main gas flow and be used for immediate power generation. The ash-free, sulfur-free liquid products from the F-T unit would be stored and returned to fuel the power-generating equipment during peakload periods or during periods when the gasifier is shut down for maintenance. If an excess amount of liquid fuel is produced, it can be sold as a raw material for petrochemicals or it could be used as a fuel to supplement petroleum.

Addition of a Fischer-Tropsch unit will add significantly to plant capital costs. However, if no other clean fuels are available to the electric utility for use when the gasifier is shut down for maintenance, or if other fuels are not available for the peaking gas turbines, this addition is an excellent way to supply a clean synthetic liquid from coal.

In the Fischer-Tropsch Process, carbon monoxide is hydrogenated to produce mainly straight-chain hydrocarbons and water or carbon dioxide. Catalysts which may be used are cobalt, nickel, iron, or ruthenium. The purified carbon monoxide and hydrogen-containing gas must have less than 2 ppm of sulfur compounds to minimize catalyst poisoning. Branched-chain hydrocarbons, aliphatic alcohols, aldehydes, and acids are also produced in varying amounts depending on the type of catalyst and the operating conditions. The reaction is exothermic with about 7200 Btu being liberated per pound of oil produced. Optimum temperatures are 340°-400°F for cobalt and nickel catalysts, 390°-620°F for iron catalysts, and 320°-440°F for ruthenium.

The large amount of heat evolved and the relatively narrow range of operating temperatures make the problem of removing the heat of reaction most important in the design of the plant. The presence of substantial amounts of nitrogen in the feed gas should not significantly change the yield of liquids and wax produced per volume of $2\text{H}_2 + \text{CO}$ based on pilot data. Much experience in this type of operation has been gained at Sasol over the last several years.

Interestingly, in processing part of the utility gas through a Fischer-Tropsch unit, if 15% of the reacting carbon monoxide forms methane, the exiting gas heating value is 132 Btu/SCF, assuming a feed gas heating value of 153 Btu/SCF. The difference in gas heating value that will be experienced using various methods for turndown will require sophisticated firing controls in the gas turbine and combustion systems.

Figure 7 shows how the Fischer-Tropsch plant fits in. When the gasifier operation is at design conditions for a high electrical load, only a small amount of gas flows through the F-T unit. As the electrical load decreases, more gas flows through the unit and less goes to the power plant. Finally, all of the gas flows through the F-T unit.

CONCLUSION

The concept of a fluidized-bed reactor as a gas producer for a combined-cycle power plant appears practical. It is possible, as confirmed by the experience of others, to achieve high carbon utilization in such fluidized-bed reactors by rejection of agglomerated, low-carbon ash produced in the gasifier. It is now the opinion of the people in the electric industry that a) such systems should be designed for operation in the intermediate load or swing range and b) to operate satisfactorily they must be capable of load following over a rather wide range.

Several methods which could be used to achieve this flexibility were discussed. It appears at this time that, alone and in combination, these methods will enable fluidized-bed gasifiers to perform satisfactorily under the conditions that will be required by the electric industry. The fluidized-bed reactor concept for coal gasification should find practical application in supplying a clean practical fuel produced from coal for utility use for several decades to come.

REFERENCES CITED

1. Environmental Protection Agency, Control Systems Division, "Coal Gasification/Advanced Power Cycle," December 10, 1971, as Printed on pp. 86-110 of the U. S. Congress, Senate, Hearing Before the Subcommittee on Minerals, Materials, and Fuels and the Full Committee on Interior and Insular Affairs United States Senate, Pursuant to S. Res. 45, A National Fuels and Energy Policy Study, Ninety-Second Congress, First Session on The Developments in Coal Gasification and S. 1846, A Bill to Establish a Coal Gasification Development Corporation, Serial No. 92-15, November 18, 1971.
2. Godel, A., "A New Combustion Technique," Eng. Boiler House Rev. 71, 145-53 (1956) May.
3. Hauser, L. G., Comtois, W. H., and Boyle, R. R., "The Effect of Fuel Availability on Future R&D Programs in Power Generation." Paper presented at the American Power Conference Chicago, April 18-20, 1972.
4. Jequier, L., Longchambon, L. and Van de Putte, G., "The Gasification of Coal Fines," J. Inst. Fuel 33, 584-91 (1960).
5. Matthews, C. W., "A Design Basis for Utility Gas From Coal." Paper presented at the 3rd International Conference on Fluidized Bed Combustion, Hueston Woods State Park, Ohio, October 30-November 1, 1972.
6. Robson, F. L., Giramonti, A. J., Lewis, G. P. and Gruber, G., Technological and Economic Feasibility of Advanced Power Cycles and Methods of Producing Nonpolluting Fuels for Utility Power Stations. Final Report under Contract CPA 22-69-114 for the National Air Pollution Control Administration, U. S. Department of Health, Education, and Welfare, Durham, N. C., by United Aircraft Research Laboratories, December 1970.

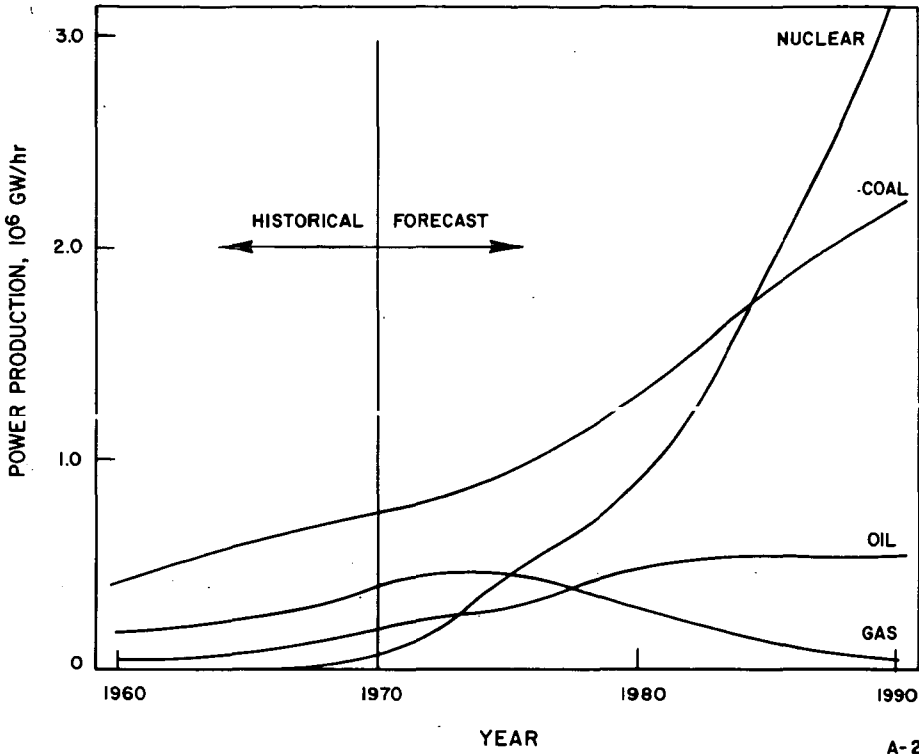


Figure 1. FORECAST OF POWER GENERATION BY FUEL IN THE U.S.

A-23-191

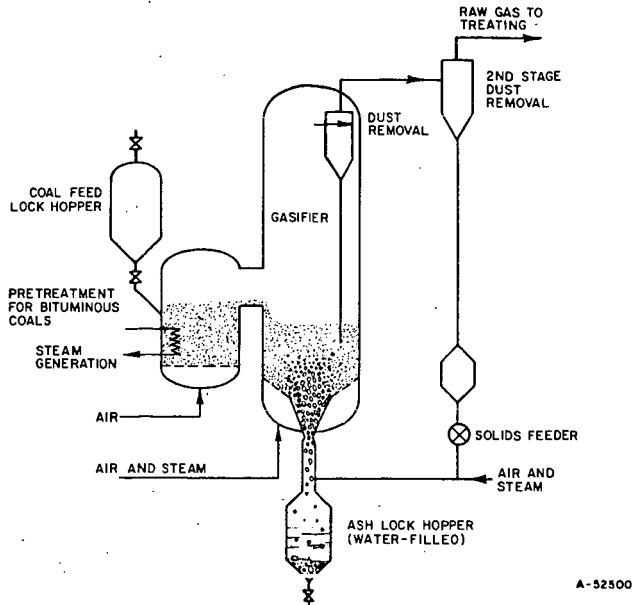


Figure 3. AGGLOMERATING BED REACTOR

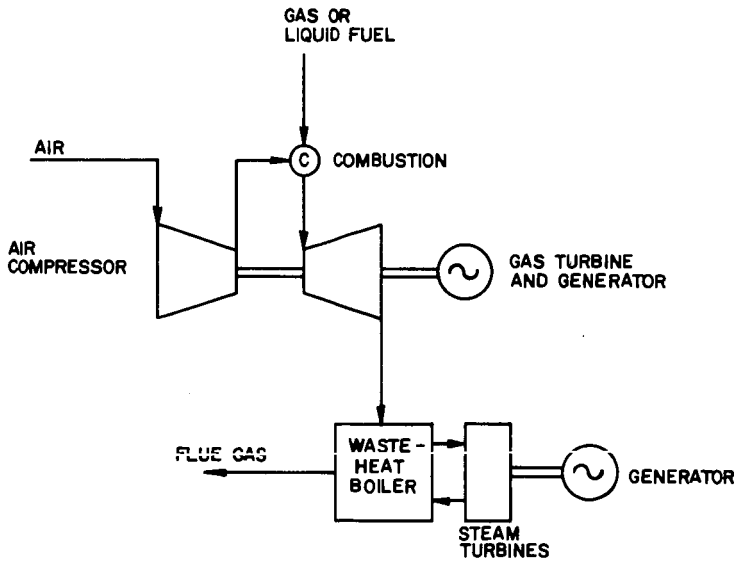


Figure 4. COMBINED-CYCLE POWER GENERATION WITH GAS AND STEAM TURBINES

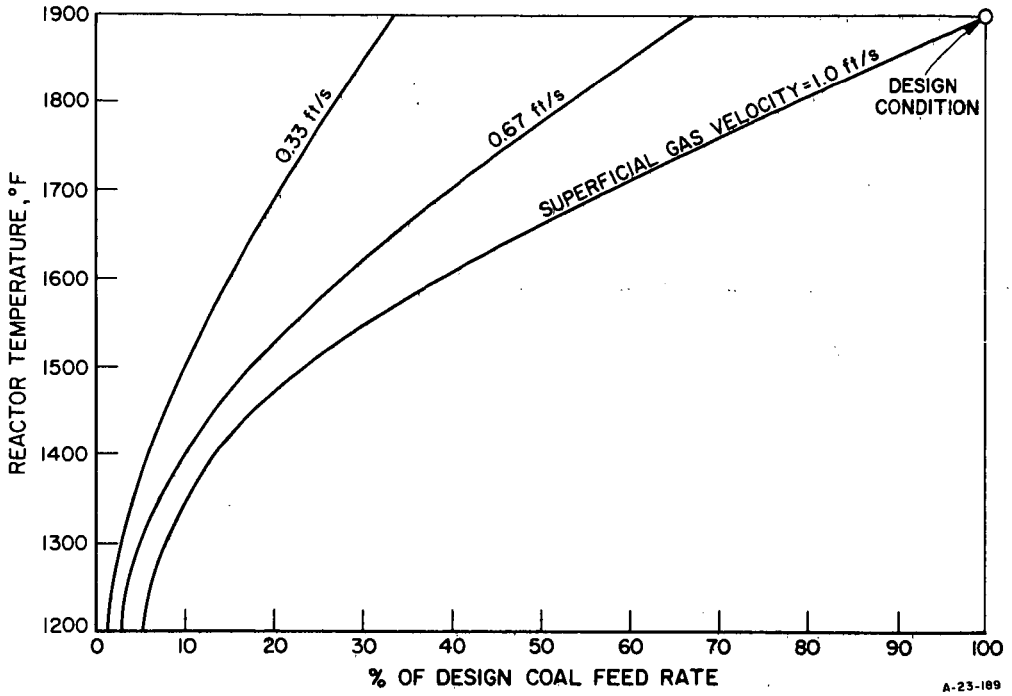


Figure 5. AAR TURNDOWN CAPABILITY

A-23-189

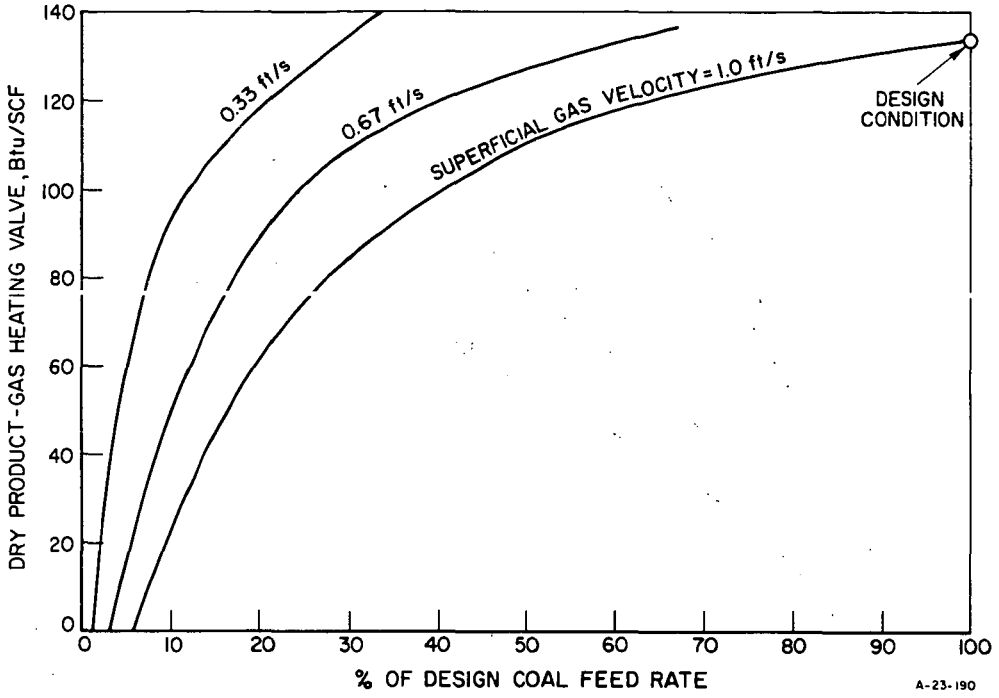
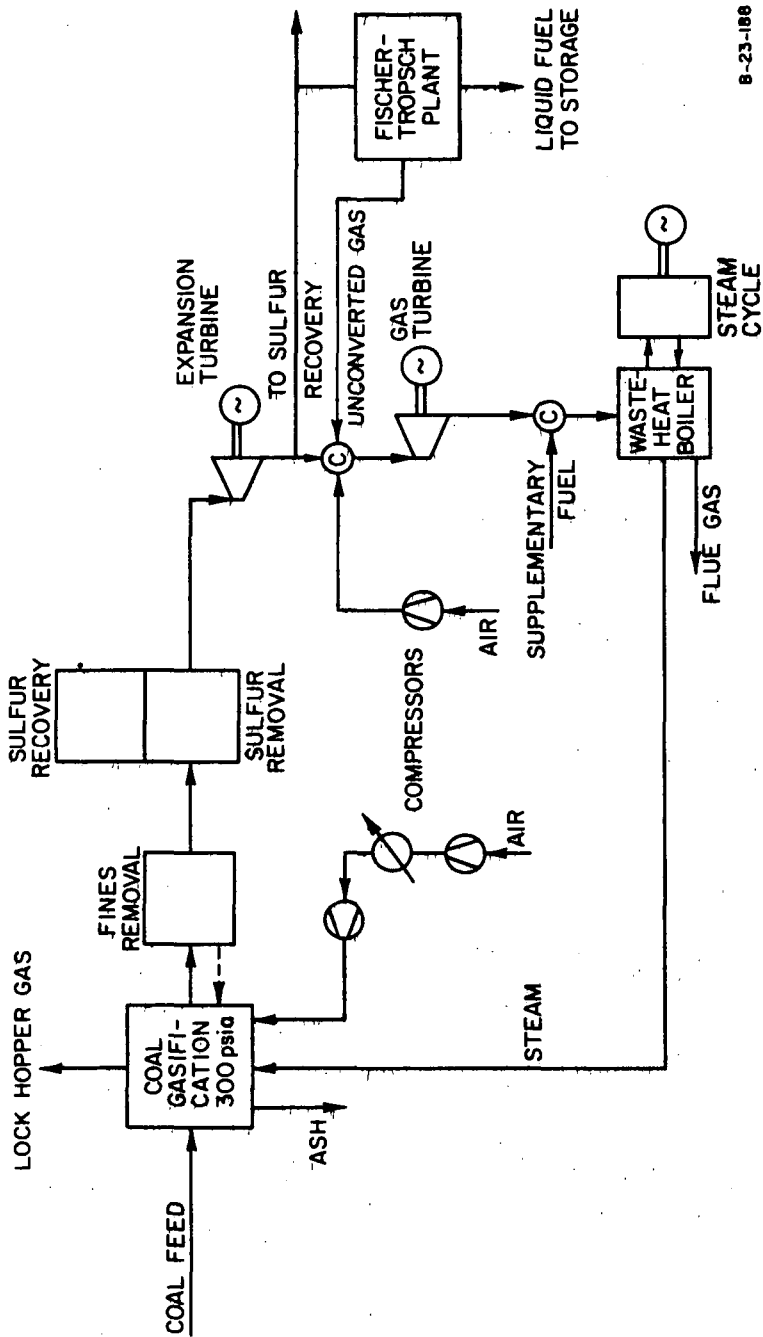


Figure 6. PRODUCT GAS HEATING VALUE AS A FUNCTION OF AAR TEMPERATURE

A-23-190



B-23-186

Figure 7. FISCHER-TROPSCHE PLANT ADDITION TO COMBINED-CYCLE POWER GENERATION BY COAL GASIFICATION

PRODUCTION OF LOW-BTU GAS FROM RESIDUAL OIL IN COMBINATION WITH
ADVANCED POWER CYCLES. A. M. Squires, S. I. Dobner, M. J. Gluckman,
Department of Chemical Engineering, The City College of the City University of
New York, 245 West 104th Street, New York, New York 10025.

An examination of the interface between equipment converting residual oil to low-Btu gas and power-generating equipment which combines gas- and steam-turbine cycles. Examples will be based upon Texaco or Shell "partial oxidation" followed by both conventional gas cleaning at low temperature and hot gas cleaning by means of a panel bed filter charged with half-calcined dolomite. Another example will employ cracking in a coke-agglomerating bed with production of an aromatic liquid and a coke byproduct.

ADVANCED COGAS POWER SYSTEMS FOR LOW POLLUTION EMISSIONS

Albert J. Giramonti
United Aircraft Research Laboratories
East Hartford, Connecticut 06108

ABSTRACT

Analytical studies have been conducted to define commercially feasible, advanced-technology central power stations which would eliminate or significantly reduce utility-caused atmospheric pollution and thermal water pollution. The basic concept investigated represents a combination of (1) advanced cycle, Combined Gas And Steam (COGAS) turbine electric power generation systems based on technology spin-off from the aircraft gas turbine industry, and (2) selected processes for deriving nonpolluting gaseous fuel from high-sulfur residual fuel oil.

The results of these studies clearly indicate that advanced COGAS power systems integrated with fuel gasification systems would be more effective than future fossil steam systems in controlling emissions of ash, sulfur oxides, and waste heat. In addition, preliminary calculations indicate that emissions of nitrogen oxides could be reduced up to several orders of magnitude by using low-Btu gasified fuel compared with emissions caused by the combustion of high-Btu fuels. It appears that advanced gas turbine and COGAS power systems using low-Btu fuels could be fired to higher turbine inlet temperature to improve performance and still emit significantly less nitrogen oxides than when operating at low turbine inlet temperature with high-Btu fuels. Furthermore, prospective COGAS systems could produce electricity at lower cost than could be produced by alternative fossil steam systems with comparable air and water pollution controls. Also, despite the relatively high cost of fossil fuels, advanced COGAS power systems should offer a viable alternative to nuclear power systems for future base-load power generation.

INTRODUCTION

The electric utility industry in the United States is currently the target of numerous regulatory agencies and environmental groups whose goal is the elimination or significant reduction of objectionable emissions such as sulfur oxides, nitrogen oxides, particulate matter, and waste heat. A number of exploratory studies and demonstration projects are being carried out on methods of reducing power station

pollution. While some stack gas cleaning methods show promise, the only proven method currently available for the reduction of sulfur oxides is the use of relatively expensive, low-sulfur fuels. Similarly, the only available methods for the reduction of nitrogen oxides involve combustion modifications. All of these methods have the disadvantage of increasing the cost of generating power because of their high capital and operating costs.

An alternative method of pollution control involves the conversion and cleanup of dirty coal or residual fuel oil prior to combustion. Such fuel treatment would result in a significant increase in the cost of fuel delivered to the power generating system. In order to offset this increased fuel cost, the thermal efficiency of electric power generation should be increased as much as possible by using advanced-cycle power systems.

Several feasibility evaluation studies of advanced-cycle power systems have been conducted by the United Aircraft Research Laboratories, including one for the Environmental Protection Agency (formerly National Air Pollution Control Administration of the Department of Health, Education, and Welfare) reported in Ref. 1 and another for the Connecticut Development Commission reported in Ref. 2. The results of these studies indicate that power systems incorporating advanced-design gas turbines used in conjunction with steam turbines and gasification systems producing low-Btu fuel offer the potential of essentially eliminating the air and thermal water pollution problems of electric utilities while simultaneously producing lower-cost power than is projected for conventional steam systems. Previous papers summarizing the results of these studies have dealt primarily with the design, performance, sulfur emission control, and cost characteristics of advanced-cycle power systems operating on gasified coal (see Refs. 3 and 4, for example). This paper briefly summarizes these same characteristics for advanced-cycle systems operating on gasified residual fuel oil, with emphasis placed on the lowered nitrogen oxide emission characteristics anticipated for gas turbine systems operating on low-Btu gaseous fuels.

ADVANCED COGAS POWER STATIONS

The generic type of power system that shows the most promise for effective pollution control consists of a gasification process producing a clean, low-heat-content fuel gas for use in a Combined Gas And Stream (COGAS) turbine power system. Unlike some present-day COGAS systems in which the gas turbines are essentially air preheaters for the steam boiler, advanced-cycle COGAS systems would utilize large industrial gas turbines operating at high turbine inlet temperature. The technology basis for these gas turbines represents spin-off from the aircraft gas turbine industry. These gas turbines would produce approximately 60% of the net

station electric output, and their exhaust gases would be directed into waste-heat boilers which would generate steam for a steam turbine system producing the remaining 40% or so of the net station output.

Advanced Gas Turbine Technology

By adapting recent and continuing advances in aerospace technology to industrial turbine machinery design, substantially improved large capacity gas turbine power systems with appreciably higher thermal efficiency could result, leading to their widespread use in intermediate-load and base-load power generation applications. These advances in aerospace technology were achieved during extensive research and development efforts on military and commercial aircraft gas turbines and include improvements in materials technology, blade cooling techniques, aerodynamic flow path design, high-heat-release burners, and modular fabrication techniques.

While meaningful improvements in aerodynamic performance are projected for future gas turbines, the most significant future technological advances are expected in the area of turbine inlet temperature. Current industrial gas turbines are limited to turbine inlet temperatures of approximately 1800 F for base-load ratings. Part of the projected increase in turbine inlet temperature will be achieved by the use of improved turbine blade materials. Historically, maximum turbine blade temperatures have advanced approximately 20 F per year because of improvements in materials and coatings. Recently, however, significant increases in turbine inlet temperature approaching 70 to 80 F per year have been achieved in aircraft gas turbines through substantial improvements in turbine cooling techniques in combination with newer materials. Aircraft gas turbine engines beginning commercial operation during the early 1970s will operate at turbine inlet temperatures of approximately 2100 F during cruise and up to 2400 F during takeoff.

By applying the same sophisticated convection-cooled blade design philosophy to industrial engines and by precooling the turbine cooling air before being utilized in the turbine for cooling purposes, it should be possible to begin designing a new 2200 F industrial engine which could be put into commercial base-load operation in the near future. Further improvements in materials, oxidation-resistance coatings, and more advanced cooling concepts should permit base-load operation at turbine inlet temperatures on the order of 2600 F by the early 1980's. A conceptual design for a 100-Mw class simple-cycle gas turbine designed for 2600 F turbine inlet temperature and 20:1 compressor pressure ratio is depicted in Fig. 1. By the 1990's industrial gas turbine inlet temperatures of 3000 F or higher should be in commercial operation.

Waste-Heat Recovery in COGAS Systems

A simplified schematic diagram for an integrated COGAS/oil gasification power station is illustrated in Fig. 2. All the desulfurized fuel gas would be delivered to the gas turbine burner and the main heat recovery boiler would be unfired. In the short term, before turbine inlet temperatures are increased appreciably, it may be desirable for some applications to burn additional fuel in the boiler. This would increase output power and might result in lower emissions of nitrogen oxides per unit of output power. In the long term, however, when turbine inlet temperatures exceed approximately 2200 F, unfired heat recovery systems would result in highest overall efficiency and lowest overall cost.

During operation of an integrated COGAS/oil gasification power system, de-aerated feedwater from the main heat recovery steam cycle would be passed to the fuel gas waste heat boiler and converted into saturated steam at the same pressure as the high-pressure steam raised in the main steam cycle. Some of this high pressure saturated steam could be used to preheat the oil feed to the gasifier and some could be injected into the gasifier. The balance would be returned to the main steam cycle to be superheated along with the steam generated in the main boiler. The resulting superheated steam would be expanded in steam turbines to drive an electric generator and the booster air compressor.

Previous cycle studies (Ref. 1) have demonstrated that when the inlet gas temperature to the main boiler is below approximately 1200 F, single-pressure steam systems would result in stack temperatures in excess of 300 F. By adding a second low-pressure steam cycle, as depicted in Fig. 2, it is possible to extract additional heat from the stack gases and drop the stack temperature to 300 F, thereby improving steam cycle efficiency.

RESIDUAL FUEL OIL GASIFICATION AND CLEANUP SYSTEMS

The availability of clean, desulfurized fuel is an absolute requirement for the type of advanced gas turbines described in the previous section, and processes for producing such clean fuels from high-sulfur coal and oil are expected to become available concurrently with the advanced power systems. Processing high-sulfur residual fuel oil to produce clean, low-sulfur, gaseous fuel involves partial oxidation in a high-pressure reactor vessel to produce a hot, gaseous raw fuel (see Fig. 2). The hot, raw fuel gas would be cooled in heat exchangers and waste heat boilers, water scrubbed to remove carbon and soot particles, and then passed through an absorption system to remove sulfur compounds. The resulting fuel gas composition, after scrubbing and desulfurization, would be approximately 13-16% H₂, 20-25% CO, and 55-60% N₂ (by volume). Smaller concentrations of H₂O, CO₂, CH₄, A, sulfur

compounds, and nitrogen compounds would be present. The heating value of the clean fuel gas would vary from approximately 120 to 140 Btu/scf, depending on operating conditions. The desulfurized fuel gas would then be passed to the power system, and the sulfur compounds would be processed to produce elemental sulfur.

Partial Oxidation of Residual Fuel Oil

The partial oxidation of liquid-hydrocarbons is well-developed technology with numerous plants in operation working on a wide variety of feedstocks. The partial oxidation process was developed for the production of synthesis gas or hydrogen in the early 1950's by Texaco Development Corporation in the United States and Shell Internationale Petroleum Maatschappij N.V. in Europe. Both of these companies have made recent contributions to the technology of noncatalytic partial oxidation of hydrocarbons and have processes for license.

Generally, the partial oxidation process is very flexible in its operating characteristics. When used to produce fuel gas, feedstock (oil), air, and sometimes steam (to increase the hydrogen yield and to help control temperature) would be preheated and mixed before entering the refractory-lined reaction chamber. The oil feed would be converted into desirable products (hydrogen, carbon monoxide, and methane), undesirable products (hydrogen sulfide, carbonyl sulfide, carbon dioxide, and water vapor), diluents (nitrogen and argon), and soot (carbon) which would be recycled to extinction. The relative amounts of carbon monoxide and hydrogen would depend on the air/oil ratio, steam/oil ratio, oil composition, preheat temperatures, and pressure.

Sulfur Removal and Recovery from Raw Fuel Gas

During scrubbing and desulfurization operations, most of the H_2O , 50 to 70% of the CO_2 , and over 95% of the sulfur compounds would be removed from the fuel gas stream. The sulfur originally present in the fuel oil would appear in the raw gas principally as hydrogen sulfide, H_2S , with small but important quantities of carbonyl sulfide, COS . There is a wealth of technological data (see Refs. 5 and 6) available for the removal of H_2S from hydrocarbon gases, largely due to the development of the natural gas industry during the past 30 years.

Two types of chemical-solvent scrubbing systems look very attractive for the removal of sulfur compounds in power generation applications: hot potassium carbonate and amine scrubbing systems. The hot potassium carbonate scrubbing process was developed by the Bureau of Mines for the removal of CO_2 from coal gas to upgrade its heating value. It was discovered that H_2S and COS were also effectively removed. Amine scrubbing systems have been highly developed and are popular methods for removing CO_2 and H_2S from natural gas. These methods are based on employing monoethanolamine (MEA), diethanolamine (DEA), di-isopropanolamine, or other scrubbing solvents.

The desulfurization of fossil fuels usually requires some plan for the disposition of the sulfur compounds which are removed from the raw fuel gas. Various schemes have been developed to recover the sulfur in a form that has economic value. The most important of these schemes, which involve the selective oxidation of H_2S to elemental sulfur, have been classified together as Claus systems. By proper design of the scrubbing and Claus systems (incorporating, for example, multiple stages and improved designs), it is possible to achieve an overall sulfur removal effectiveness of 85 to 96%. By further treating or recycling of the tail gas from the Claus system it should be possible to exceed 98% overall sulfur removal effectiveness.

CHARACTERISTICS OF INTEGRATED COGAS/OIL GASIFICATION POWER STATIONS

Selected characteristics of integrated COGAS/oil gasification power systems corresponding to three levels of technology (present day plus technology projected to be available during the mid-1970's and early 1980's) are presented in Table I. The general requirements and design characteristics for the gasification system, gas turbines, and waste heat recovery steam system are summarized in the table along with selected performance data for the integrated power stations. The net station outputs range from 159 to 309 Mw, and the estimated net station thermal efficiencies range from 32% to 40%. These net station efficiency estimates could possibly be increased as much as 3 points by further cycle optimization combined with the use of higher temperature (1300-1500 F) fuel gas delivered to the gas turbine burner. Higher fuel gas temperature might be feasible in future systems by using high-temperature desulfurization and cleanup or an improved gasifier heat recovery scheme which would regenerate clean, low-temperature fuel gas against raw, high-temperature fuel gas.

Also indicated in Table I are estimated emission rates for sulfur oxides, nitrogen oxides, and thermal heat rejection to the cooling tower circuit. Sulfur emissions would be low because of the desulfurization process incorporated in the gasification system. Nitrogen oxide emissions would be low because of the favorable combustion characteristics of low-Btu gasified fuel as described in the next section.

All conventional power generating equipment (with the exception of simple-cycle gas turbines) reject heat to cooling water. The rates of heat rejection from fossil- and nuclear-fueled steam stations are approximately 4300 and 6600 Btu/kwhr, respectively. COGAS stations would have significantly lower heat rejection rates (as much as 30% lower than fossil and 50% lower than nuclear stations), as noted in Table I, due to their high thermal efficiency and increased heat rejection rate to the atmosphere. The impact of this heat rejection on cooling water supplies could be reduced for all types of power systems by the use of cooling

towers. Wet (evaporative) cooling towers might, under certain circumstances, cause objectionable fogging at ground level, and dry (nonevaporative) towers are very expensive. The environmental and economic impact of using cooling towers for COGAS systems would be significantly less than for the alternative systems because of the reduced heat rejection rate of COGAS systems.

NITROGEN OXIDE EMISSIONS FROM GAS TURBINE POWER SYSTEMS BURNING LOW-BTU FUEL GAS

Oxides of nitrogen are receiving increasing attention as air pollutants. The oxides NO (nitric oxide) and NO₂ (nitrogen dioxide) are commonly lumped together as NO_x. They are easily interconverted in the atmosphere, and their ratio changes depending on the action of sunlight, oxygen, and other oxidizing or reducing agents present. Nitrogen oxides are formed in the hot reaction zones of all air-breathing combustion engines. They are formed primarily as NO, although small quantities of NO₂ and N₂O (nitrous oxide) may also be formed.

Control of NO_x emissions from gas turbines can be accomplished in either of two ways: (1) preventing NO formation by fuel pretreatment and/or by careful design and operation of the burner, and (2) removal of NO_x compounds after combustion from the exhaust gases. This paper deals with the first alternative because removal of NO_x compounds after their formation is likely to prove far more difficult and costly (see Ref. 7).

Nitric Oxide Formation Mechanisms

Two mechanisms are known to contribute to the formation of nitric oxide in combustion systems. The most important mechanism for gas turbines and other systems which burn relatively clean fuels is referred to as the thermal or hot air mechanism. In this mechanism, nitrogen and oxygen from the atmosphere react in the hot combustion zone to form nitric oxide. The second mechanism is important when relatively dirty fuels such as coal and residual fuel oil are burned. Most dirty fuels contain small but significant quantities of organic nitrogen compounds. Because nitrogen-carbon and nitrogen-hydrogen bond energies are so much lower than that for molecular nitrogen, much of the fuel nitrogen becomes oxidized during combustion. Experimental studies (Ref. 8) of the formation of nitric oxide from fuel nitrogen indicate that the formation rates are very rapid, occurring on a time scale comparable to that of the hydrocarbon combustion reactions. This mechanism is strictly fuel dependent and proceeds at lower temperatures than needed for the thermal mechanism.

Fuel nitrogen should not be a problem in systems using gasified fuels. During gasification of dirty fuels, some fuel nitrogen would carry over into the raw fuel gas as combustible nitrogen compounds (primarily ammonia, with smaller concentrations of hydrogen cyanide, pyridine, pyridine bases, and acidic nitrogenous compounds). If retained in the fuel gas, these compounds could result in excessive emissions of nitrogen oxides. Fortunately, considerable literature on the removal of these nitrogen compounds from gaseous streams is available (Ref. 6, for example). Before the advent of synthetic ammonia processes, by-product ammonia from gasification and carbonization processes constituted the most important source of fixed nitrogen. Practically all processes in commercial use for removal of ammonia are based on washing the gas stream either with water or a strong acid. Successful attempts (see Ref. 5) have been made to develop processes for the simultaneous removal of hydrogen sulfide and ammonia, recovering both compounds in the form of ammonium sulfate and elemental sulfur. Most other nitrogen compounds would be eliminated in the normal course of removing ammonia from the gas stream.

The chemical kinetics of NO formation via the thermal mechanism are fairly well understood (Refs. 8 and 9). Three variables of primary importance in NO production are local temperature, residence time, and chemical species concentration. Unfortunately, it is extremely difficult to relate these primary variables to the geometry and operating characteristics of practical gas turbine combustors due to limitations in analytical combustor modeling techniques. Previous investigations of NO formation kinetics (Refs. 10 and 11) have identified several significant simplifying assumptions which appear to apply to gas turbine burners. The most important of these are the following: (a) the NO formation rate is very slow relative to the hydrocarbon combustion reaction rates; and (b) within the uncertainty of known rate constants and present combustor models, it appears that the hydrocarbon chemistry can be decoupled from the kinetics of NO formation, i.e., the concentrations of all species except nitrogen compounds can be assumed to be in thermodynamic equilibrium at the local temperature and fuel/air ratio.

Under these conditions, the elementary reactions of importance in NO formation are:



Reactions (1) and (2) are the principal reactions, with (1) being the rate controlling reaction. Reaction (3) is of minor importance in fuel-rich mixtures.

A simplified kinetic model based on the above reactions was programmed for solution on a digital computer and combined with a program which calculates equilibrium thermodynamic properties and species concentrations. This model can be applied to a steady flow process where the temperature-time-composition histories of the fluid elements in the flow are known.

Before presenting NO emission estimates for gas turbine burners, it is instructive to consider idealized fluid elements in the flow as combustion products of uniform temperature, pressure, and composition (with the exception of nitrogen compounds) and to investigate the increase in NO concentration with time for conditions which are considered to be typical of gas turbine burners. Typical computer results are presented in Figs. 3 and 4. Figure 3 depicts NO concentration vs time estimates for a number of different types of fuels, including a range of low-Btu fuels, all supplied at room temperature. Figure 4 depicts similar results for a single low-Btu fuel supplied at a range of temperatures. The flame temperatures denoted in these figures represent the local temperature in the primary combustion zone of a gas turbine burner and should not be confused with the turbine inlet temperature which would be much lower. The strong dependence of NO formation on temperature and fuel heating value is evident from these figures.

Nitric Oxide Emissions from Gas Turbine Burners

The local temperature, residence time, and species concentrations which govern NO production are controlled by engine operating conditions, the combustor internal flow field, fuel nozzle characteristics, and the air addition schedule to the burner can. Lack of an adequate analytical description of the combustor flow field and the fuel/air mixing characteristics has prevented accurate estimation of the temperature-time-concentration history which is essential for reliable estimation of NO formation. At the present time, several engineering and research establishments, including several groups within United Aircraft Corporation, are attempting to develop comprehensive gas turbine combustor models. The results of this modeling work have been very encouraging and are leading to a better understanding of NO emissions.

A relatively simple three-zone burner model developed by the Combustion Group at Pratt & Whitney Aircraft (Ref. 11) was modified to permit consideration of low-Btu fuel combustion. Results of preliminary NO calculations using this model are presented in Fig. 5. The predicted NO concentrations in the burner exhaust are plotted against the maximum combustion or flame temperature in the primary zone. These calculations were based on a typical burner air and fuel flow distribution for a representative industrial gas turbine. The specific NO emission predictions for CH₄ and JP-5 shown by the individual points in Fig. 5 agree reasonably well with measured data. For low-Btu fuels with combustion temperatures in the 3600 to 4200 F range NO emissions below 10 ppm, and perhaps approaching 1 ppm, appear to be feasible.

The NO emission estimates presented in Fig. 5, although preliminary, are very encouraging and suggest that the use of low-Btu fuels would provide a very effective method of NO control for gas turbines. Furthermore, it seems evident that gas turbines using low-Btu fuels could be fired to high turbine inlet temperature and still emit significantly less NO than low-temperature gas turbines using high-Btu fuels. It should also be noted that these estimates have not taken into account additional NO control techniques such as steam or water injection and off-stoichiometric combustion. Utilization of these techniques, together with low-Btu fuels, might permit even further reduction of NO emissions.

ECONOMICS OF FUTURE POWER GENERATION

Historically, the electric utility industry successfully reduced the cost of generating power by utilizing the latest available technology and taking advantage of economics associated with large-scale generation facilities. This era of decreasing costs of electricity has ended, and we are now on the threshold of a new era with rising costs. This unfortunate situation is a direct result of rapidly rising construction and fuel costs, combined with public demands for effective control of atmospheric and thermal water pollution. Rising costs plague all methods of power generation, both fossil and nuclear. At the present time, nuclear stations are more economical than fossil stations in many parts of the country. But this situation may change as advanced COGAS power stations, incorporating high-temperature gas turbines with fuel gasification and desulfurization systems, become a commercial reality.

The busbar cost of power is the annual owning and operating expense divided by the annual kwhr generated. The annual owning costs include the capital charges due to depreciation, interest, taxes, and insurance; and the operating costs include maintenance, supplies, and fuel. The estimated capital costs for integrated COGAS/oil gasification power stations are summarized in Table II for three levels of gas turbine technology. All costs are presented in terms of estimated mid-1970's dollar value. The total installed capital costs range from \$211/kw to \$303/kw, depending on technology.

Annual owning and operating cost estimates are also summarized in Table II. Maintenance costs for the fuel processing system are based upon guidelines applicable to the chemical process industry, and corresponding costs for the power equipment are based on actual experience and projections. Fuel costs are taken to be 53.4¢/10⁶ Btu for high-sulfur oil in the Northeast. The resulting busbar power cost estimates range from 11.1 to 15.5 mills/kwhr depending on technology.

The power cost estimates presented in Table II are high by today's standards, but cost estimates for alternative methods of power generation with corresponding pollution control measures could be as high or higher, as depicted in Fig. 6. The 1975 EPA and 1973 Connecticut standards could be met by using low-sulfur oil or by adding stack gas cleanup, but doing so would increase the cost of generating power by 15 to 25% relative to a conventional steam station burning high-sulfur (2.6%S) oil. The use of gasified oil in steam or COGAS systems using present-day technology would satisfy the most stringent emission regulations in large cities, but doing so would increase the cost of generating electricity by 30 to 40% (relative to stations burning high-sulfur oil). As technology advances to permit higher turbine inlet temperatures and less costly gasifiers, COGAS systems will be capable of producing lower-cost clean power than alternative fossil steam systems. Furthermore, it appears that COGAS stations based on future gas turbine technology could also compete with future nuclear power generation, despite the relatively high cost of fossil fuels.

CONCLUSION

Advanced COGAS electric power stations consisting of gas and steam turbines integrated with residual fuel oil gasification systems should offer a viable alternative for future base-load generation applications. These stations could improve the environment by essentially eliminating the air and thermal water pollution problems caused by the generation of base-load power, and do so at competitive costs.

Although there are no basic technological problems which have to be solved before COGAS power stations could be built using present-day technology, advanced design and development programs should be energetically pursued to secure the benefits in performance and economy obtainable by advanced technology. Gas turbine technology is expected to increase during future years until turbine inlet temperatures in excess of 3000 F are achieved. COGAS stations designed with these advanced gas turbines, improved heat recovery steam cycles, and improved gasification systems would be very attractive. The eventual use of gasified coal in COGAS stations would further improve the economic potential of these stations.

REFERENCES

1. Robson, F. L. and A. J. Giramonti: Final Report on the Technological and Economic Feasibility of Advanced Power Cycles and Methods of Producing Non-polluting Fuels for Utility Power Stations. United Aircraft Research Laboratories Report J-970855-13 prepared for the US Department of Health, Education, and Welfare, National Air Pollution Control Administration, Contract CPA 22-69-114, December 1970.
2. Giramonti, A. J.: Advanced Power Cycles for Connecticut Electric Utility Stations. United Aircraft Research Laboratories Report L-971090-2 prepared for the Connecticut Development Commission under Research Support Award No. RSA 71-21, January 1972.
3. Robson, F. L. and A. J. Giramonti: The Use of Combined-Cycle Power Systems in Nonpolluting Central Stations. Journal of the Air Pollution Control Association, March 1972.
4. Robson, F. L. and A. J. Giramonti: Nonpolluting Central Power Stations. AAS Paper No. 70-083, printed in Technology Utilization Ideas for the 70's and Beyond, Volume 26 of AAS Science and Technology Series, 1971.
5. Goar, B. G.: Today's Gas-Treating Processes. Oil and Gas Journal, Parts 1 and 2, July 12 and 19, 1971.
6. Kohl, A. L. and F. C. Riesenfeld: Gas Purification, McGraw-Hill, New York, 1960.
7. Robson, F. L., et al.: Final Report on the Analysis of Jet Engine Test Cell Pollution Abatement Systems. USAF Contract F29601-72-C-0049, United Aircraft Research Laboratories Report L-971297-11, October 1972.
8. Bowman, C. T.: Kinetics of Nitric Oxide Formation in Combustion Processes. Fourteenth Symposium (International) on Combustion, Pennsylvania State University, August 1972.
9. Bowman, C. T. and D. J. Seery: Investigation of NO Formation Kinetics in Combustion Processes: The Methane-Oxygen-Nitrogen Reaction. Symposium on Emissions from Continuous Combustion Systems, General Motors Research Laboratories, Warren, Michigan, September 1971.
10. Marteney, P. J.: Analytical Study of the Kinetics of Formation of Nitrogen Oxide in Hydrocarbon-Air Combustion. Combustion Science and Technology, Volume I, pp. 261-469, 1970.
11. Roberts, R., et al.: An Analytical Model for Nitric Oxide Formation in a Gas Turbine Combustion Chamber. AIAA Paper No. 71-715, June 1971.

TABLE I
SELECTED CHARACTERISTICS OF INTEGRATED
COGAS/OIL GASIFICATION POWER STATIONS

	Level of Technology		
	Early 1970s	Mid 1970s	Early 1980s
<u>Fuel Processing System</u>			
Number of Gasifiers	2	2	2
Residual Fuel Oil Flow, lb/hr	93,600	118,000	144,000
Clean Fuel Gas Output, lb/hr	620,000	781,000	954,000
Clean Fuel Gas Temperature, F	95	520	550
Fuel Process Hot Gas Efficiency, %	70	74	76
<u>Gas Turbines</u>			
Number of Gas Turbines	4	2	2
Nominal Output per Gas Turbine, Mw	23	66	94
Compressor Pressure Ratio	13	16	20
Turbine Inlet Temperature, F	1800	2200	2600
Gas Turbine Thermal Efficiency, % (HHV)	30	32	37
<u>Waste Heat Recovery Steam System</u>			
Number of Steam Turbine Generators	1	1	1
Gross Steam System Output, Mw	80	110	136
Throttle Steam Temperature, F	700	870	980
Throttle Steam Pressure, psia	865	1250	1500
Net Steam System Efficiency, %	27	29	30
<u>Integrated Station</u>			
Net Station Output, Mw	159	228	309
Net Station Efficiency, % (HHV oil)	32	36	40
Sulfur Oxide Emissions, lb SO ₂ /10 ⁶ Btu	0.1-0.2	0.1-0.2	0.1-0.2
Nitrogen Oxide Emissions, lb NO ₂ /10 ⁶ Btu	0.004-0.1	0.01-0.1	0.01-0.2
Heat Rejection, Btu/kwhr	4500	3700	3100

TABLE II
COST SUMMARY FOR INTEGRATED COGAS/OIL GASIFICATION POWER STATIONS

Based on Estimated Mid-1970s Dollar Value

	Level of Technology		
	Early 1970s	Mid 1970s	Early 1980s
<u>Capital Costs, 10⁶\$</u>			
Fuel Processing System (96% S removal)	14.6	15.9	16.8
Gas Turbines	8.4	9.5	12.0
Steam System	14.5	18.2	22.1
Miscellaneous Equipment	7.5	9.0	9.9
Interest During Construction (7%/yr)	<u>3.1</u>	<u>3.7</u>	<u>4.3</u>
Total Capital Cost, 10 ⁶ \$	48.1	56.3	65.1
Specific Cost, \$/kw	303	247	211
<u>Owning and Operating Costs, mills/kwhr</u>			
Capital Charges (17%/yr and 70% load factor)	8.5	7.0	5.9
Maintenance, Labor and Supplies			
Fuel Processing System	0.3	0.2	0.2
Gas Turbines	0.8	0.3	0.3
Steam System	0.2	0.2	0.2
Residual Fuel Oil (53.4 \$/10 ⁶ Btu)	<u>5.7</u>	<u>5.0</u>	<u>4.2</u>
Busbar Power Cost, mills/kwhr	15.5	12.7	11.1

FIG. 1. CONCEPTUAL DESIGN OF 100-MW CLASS BASE-LOAD GAS TURBINE

EARLY-1980S TECHNOLOGY

TURBINE INLET GAS TEMPERATURE 2600 F

COMPRESSOR PRESSURE RATIO 20:1

AIRFLOW 300 LB/SEC

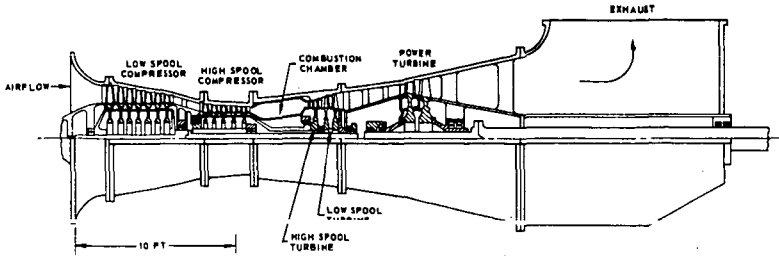


FIG. 2. SCHEMATIC DIAGRAM OF INTEGRATED COGAS/OIL GASIFICATION POWER STATION

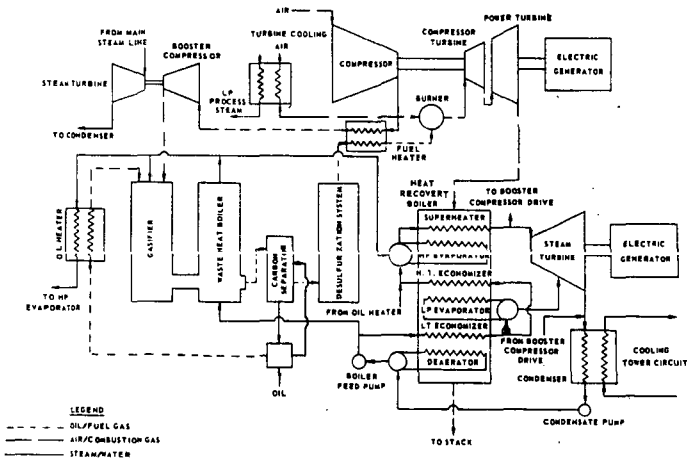


FIG. 3. NITRIC OXIDE FORMATION BY VARIOUS FUELS

PREVAPORIZED, PREMIXED, HYDROCARBON - AIR EQUILIBRIUM
 EQUIVALENCE RATIO = 1.0 AIR TEMPERATURE = 1235 R (775 F)
 PRESSURE = 14 ATM FUEL TEMPERATURE = 540 R (80 F)

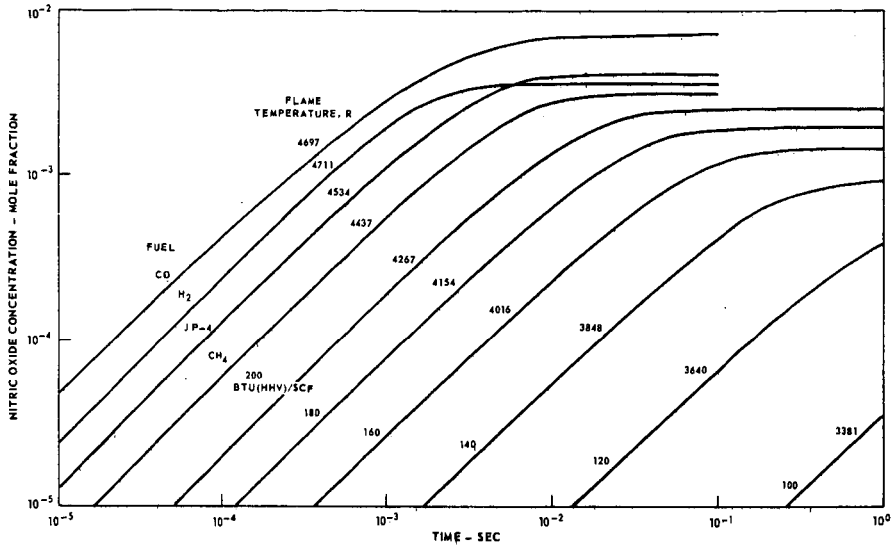


FIG. 4. EFFECT OF GASIFIED FUEL TEMPERATURE ON NITRIC OXIDE FORMATION

PREMIXED, HYDROCARBON - AIR EQUILIBRIUM
 EQUIVALENCE RATIO = 1.0 AIR TEMPERATURE = 1235 R (775 F)
 PRESSURE = 14 ATM

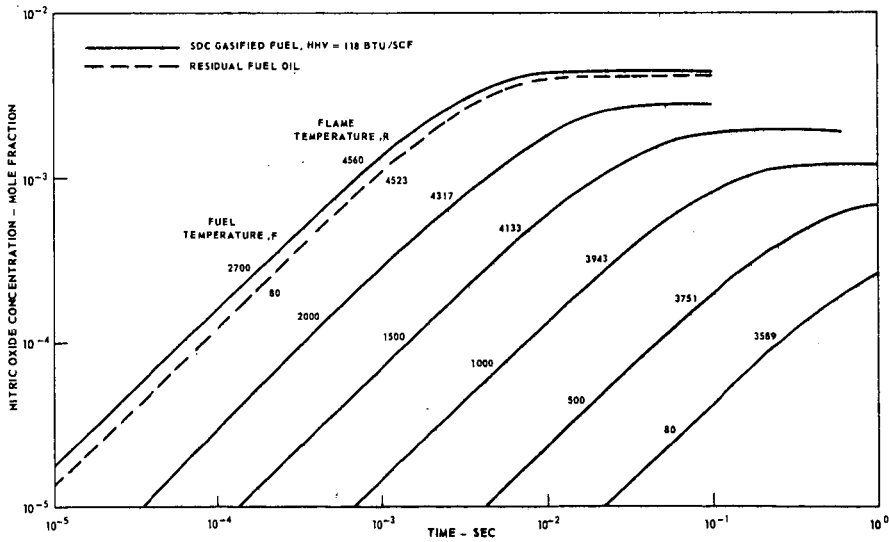
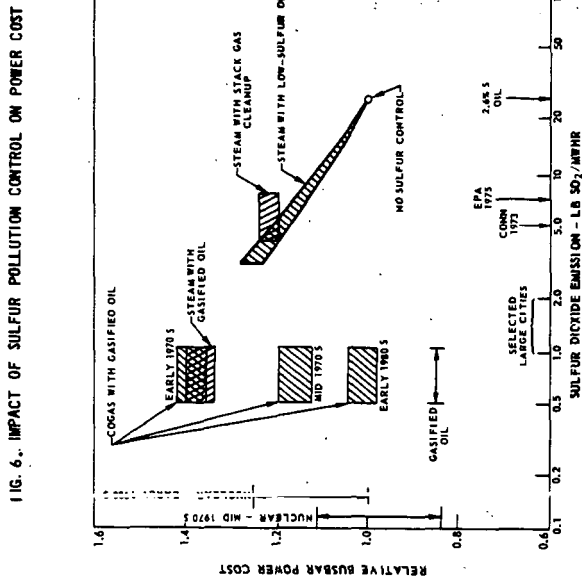
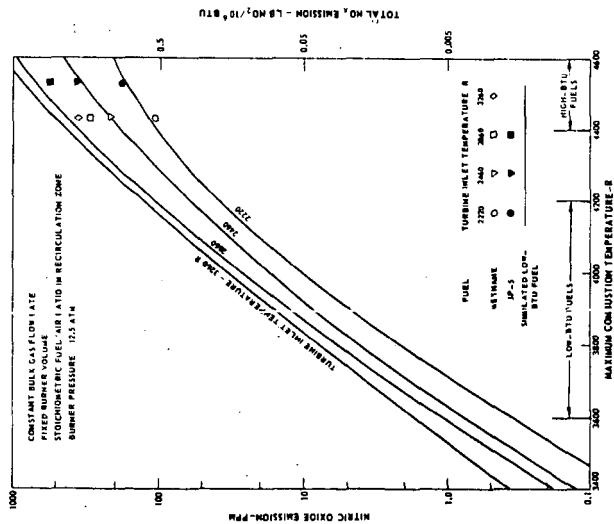


FIG. 5. NITRIC OXIDE FORMATION IN GAS TURBINE BURNER
 BASED ON P3WA THREE-ZONE BURNER MODEL



PREDICTING PERFORMANCE OF A COAL-FIRED AIR-BLOWN GASIFIER

W. L. Sage

Babcock and Wilcox Research and Development Center
Alliance, Ohio

Recent reviews of available energy sources to meet our rapidly escalating needs for electric power over the next 2-3 decades conclude that fossil fuel must supply a major portion. Furthermore, these reviewers stress that coal must be the major source. However, government restrictions on stack emissions (particulates, sulfur and NO_x) severely tax present day approaches. As these restrictions become more binding, it becomes obvious that some new approach to generating electric power by the use of coal must be found. One such approach involves cycles employing coal gasification. Basically two types of cycles have been proposed as near term solutions. The simplest of these employs a conventional steam cycle as illustrated schematically by Figure 1. The second involves operation under pressure using a combination of steam and gas turbines.

Inherent in cycles of these types are:

1. Smaller gas quantities to cleanup.
2. Conversion of the sulfur to H_2S , a more reactive and readily removable form.
3. Two-stage combustion which results in reduced NO_x production.

The combined turbine cycle (Figure 2) also has the potential of improved efficiency over the conventional steam cycle. However, if either of these approaches is to find acceptance in the power industry it must, in addition to meeting limits on stack emissions, also have:

1. Good thermal efficiency
2. Reliability
3. Favorable economics

The key to the success of these cycles is most likely the coal gasifier with gas cleaning running a close second. The ability to accurately predict gasifier performance is essential to designing and locating the various heat absorbers for maintaining a high cycle efficiency. A simple analysis of either cycle leads to the conclusion that the gasifier must be air blown (oxygen would be prohibitively expensive). Not quite as obvious is the lower cycle efficiency attained when steam is used as the gasifying medium. In this case heat is lost because this medium enters as water at ambient temperature and exits as steam at stack temperature.

Figure 3 diagrams the performance of a gasifier. If the three outputs at the bottom of the diagram are assumed to be relatively constant then the relationship between the chemical heating value of the gas (expressed as Btu/scf) and the sensible heat in the gas (expressed as gas temperature) can be calculated based

on a given set of inputs. This relationship is shown in Figure 4 for a specific set of assumptions as given in the figure. Using the coal analysis specified in Figure 4 the heating value of the product gas can be calculated as a function of the fuel heat input per unit of air fed to the gasifier. This is illustrated in Figure 5, where the fuel to air ratio is expressed as Btu input from the fuel per lb of air, and gas heating value is expressed as Btu/scf.

From an analysis of Figures 4 and 5 it becomes apparent that given a specific coal analysis, the preheated air temperature, the amount of heat loss to the enclosure, the unconsumed fuel (solids) heating value and the sensible heat in the discharge residue, the gasifier performance can be reasonably well defined if the heating value of the product gas is known. However, here is where the difficulty exists. Although the concept of air-blown coal gasification is quite old a good theoretical treatment was presented by Gumz¹ in 1950 - no experimental data is given. Limited data has been presented by Lowry² and in a review of gas generators conducted by Bituminous Coal Research, Inc., on an Office of Coal Research project.³ However, this data is very sketchy, incomplete, and in most cases involves the use of saturated air at about 140°F (0.15 lb. steam per lb of dry air).

During the period 1960-1963 the Babcock & Wilcox Company in cooperation with the General Electric Company conducted an intensive test program to develop a combined cycle concept involving coal gasification.⁴ This work covered limited testing of 1-ft diameter suspension and 3 ft x 4 ft fixed bed gasifiers and very extensive testing of a larger 5-ft diameter suspension involving many major modifications of the gasification chamber. All three gasifiers were air-blown using preheated air and all were operated at atmospheric pressure. However, due to limitations of gas cleaning equipment complete gasification was not attained. Essentially complete gasification is considered necessary for the two cycle concepts described earlier. The gasifier arrangement tested is shown schematically on Figure 6 with the equipment arrangement for the larger test unit shown on Figure 7.

Some of the pertinent features of this test unit were the division of the gasifier into separately water-cooled sections for assessment of heat losses. Gas cleanup for solids was accomplished by twin single stage cyclone separators which permitted some carbon carryover with the product gas. However, solids removal was reasonably complete permitting extrapolation to obtain an estimate of the product gas at complete gasification. Also, in an actual process, complete gasification implies total recycling, for a practical gas cleanup system some solid carbon will be entrained in the product gas.

1 Wilhelm Gumz, D. Eng. "Gas Producers and Blast Furnaces", 1950, John Wiley & Sons Inc., N. Y.

2 H.H. Lowry "Chemistry of Coal Utilization" Supplementary volume 1963, John Wiley and Sons.

3 "Gas Generator Research & Development" BCR Report L-156 prepared for Office of Coal Research under Contract No. 14-01-0001-324, March 1965.

4 E.A. Pirsh and W.L. Sage "Combined Steam Turbine - Gas Turbine Super Charged Cycles Employing Coal Gasification" American Chemical Society, Division of Fuel Chemistry Vol. 14, No. 2. at the Symposium of Coal Combustion in Present and Future Power Cycles Toronto, Canada May 1970.

Based on the results of the above test program it was concluded that the most important factor in determining high quality product gas was the heat available for promoting gasification and that this heat available (h_a) can be calculated as follows:

$$h_a \text{ (btu/lb air)} = \text{heat of combustion of fuel at stoichiometric conditions} + \text{sensible heat in the air and fuel stream above } 80^\circ\text{F} \text{ minus the heat losses to the gasification zone.}$$

One problem arises in defining what portion of the gasification zone should be included in defining heat losses. Since gasification reactions are believed to be very rapid, it is believed that only the surface up to or shortly after the start of the gasification zone should be included. Table I lists typical data obtained on the 5 ft diameter gasifier and Figure 8 shows the gasifier configuration pertaining to the test points.

Figure 9, similar to Figure 5, shows the heat available (h_a) lines based on a correlation of about 150 data points obtained on various gasifier configurations. This data is directly applicable to an air-blown suspension type gasifier only. However, with the proper definition of terms, it should be useful for predicting the performance of fluidized or fixed bed gasifiers, but actual experimental data is lacking to verify this.

Figure 9 serves to define operational limits of an air-blown suspension gasifier. For example, assume a gasifier operating with the coal analysis indicated on figure 4, preheated air temperature of 1000°F , a char recycle rate equal to 50% of coal input heating value, and designed to hold heat losses to 10% of input. Then:

Chemical heat @stoichiometric is ⁽¹⁾	1270 Btu/lb air
Sensible heat in air (1000°F)	<u>230 Btu/lb air</u>
	1500
Less 10% heat loss	<u>150</u>
	1350
Gasifier fuel input is ⁽²⁾	3750
Predicted product gas HHV ⁽²⁾	94 Btu/scf

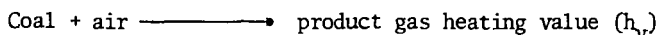
(1) based on coal @1320 Btu/# air and char (C_6H) at 1220 Btu/# air

(2) point located on Figure 9.

Based on these operating conditions the coal feed rate to the gasifier is fixed for a 100% gasification. If the coal feed rate drops then the gas quality drops, or if the coal feed rate is increased then excess char is produced. For the sample cited the exit gas temperature without heat removal would be 3500°F . Hence, steam generating surface must be incorporated in the gasifier and gasifier exit zone to cool the gases to the desired temperature for gas cleanup and sulfur removal.

The case shown has been that somewhat simplified with regard to char recycle rate. Figure 9 indicated that a higher recycle rate would increase product gas quality. However, in actual practice a high excess of char recycle decreases h_a and also imposes a greater heat loss on the gasification zone, since the char has been cooled before collection and recycle. At moderate recycle rates this loss has a major effect on product gas quality but if very high recycle rates are used gas quality will drop.

Figure 9 implies that product gas quality is kinetically and not equilibrium controlled, at least for this gasification process. If the basic reaction is



then

$$\frac{d(h_v)}{dt} = k (\text{coal}) (\text{air})$$

where K is the apparent rate constant of the form $Ae^{-E/RT}$

This indicates that the most important factor in increasing product gas heating value is temperature (T). Actually h_a is very closely related to T . However, the above relationship also indicates that high char recycle rate or the use of steam addition to the gasification zone will lower T and hence lower product gas quality. Limited data obtained during this test program verified this prediction.

Figure 10 shows the basic components of a combined cycle including both the steam turbine and gas turbine. However, if a forced draft fan were substituted for the turbine compressor then the same basic configuration applies to the conventional steam cycle. Although the overall cycle efficiency is not affected by the gasifier product gas quality provided the same boundary conditions are maintained, the location of the various heat traps does have considerable bearing on the gas qualities, and it is essential that the details of such a cycle enable accurate prediction of this value.

Although electric power generation from coal gasification to meet atmospheric pollution limits may have considerable merit, it also creates problems. To cite two of these:

1. Because there are few heat sinks where low level heat can be economically recovered, gas cleanup and sulfur removal should be accomplished at the highest feasible temperature leading to the needs for developing a high temperature gas cleaning system.
2. To obtain the low level heat sinks, regenerative feed-water heating which is essential to high steam cycle efficiency may have to be sacrificed to some degree.

TABLE I

Test	8	27	41	51	53	74	76	121	124
Coal Feed lb/hr	5500	5480	4600	4980	2560	3900	4340	4650	4460
Air Flow lb/hr	22860	24260	21370	24010	15930	19740	22180	25820	19410
Heat in Btu/lb Air	1471	1461	1501	1525	1490	1485	1497	1425	1430
Heat Losses Btu/lb Air	182	162	218	241	325	223	298	181	177
h_a Btu/lb Air	1289	1299	1283	1284	1165	1262	1199	1244	1253
Fuel Input Btu/lb Air	4034	3880	3325	3147	2535	2550	2525	3050	2920
(4) Solids/lb hr	2805	1975	1800	1495	990	1805	1670	3180	2830
(5) Product Gas (Dry)/lb hr	25590	26765	23330	26235	17005	21680	24220	28230	21480
Solids lb/hr	1035	1240	865	680	480	585	620	430	1110
Gas Composition (Vol. %)									
H ₂	8.5	7.8	6.9	5.4	3.8	6.7	5.5	5.5	8.6
CO	16.5	15.9	14.4	14.8	9.0	15.5	13.6	15.0	16.6
CH ₄	0.58	0.45	0.18	0.04	0.2	0	0	0	0.06
CO ₂	8.2	9.2	10.0	9.8	13.3	8.9	10.4	8.9	8.0
N ₂	66.3	66.8	68.6	70.0	73.6	8.1	9.0	8.0	7.5
H ₂ O (% Vol. - Wet)	8.5	9.1	9.4	10.5	8.6	8.1	9.0	8.0	7.5
HHV Btu/Scf Dry	86.7	80.9	70.4	65.6	43.6	71.7	66.2	72.7	82.0

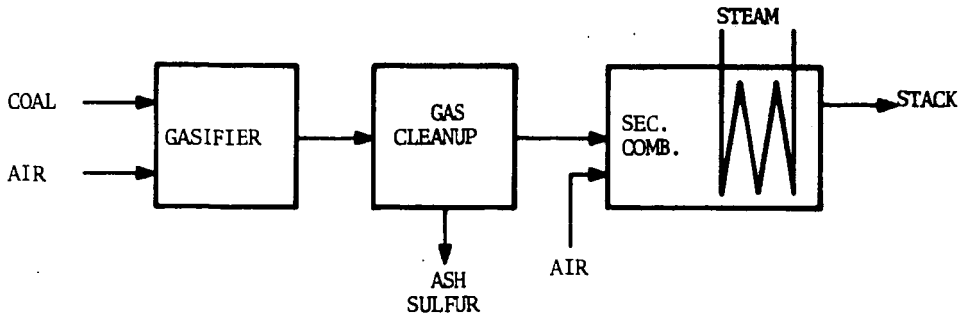


FIGURE 1. STEAM CYCLE

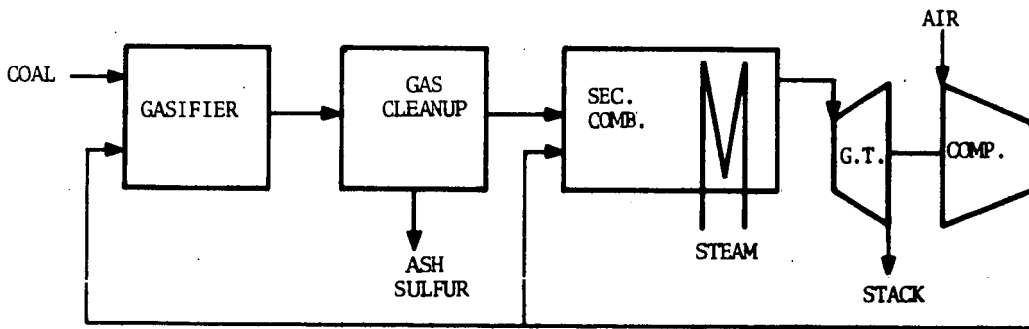


FIGURE 2. COMBINED CYCLE

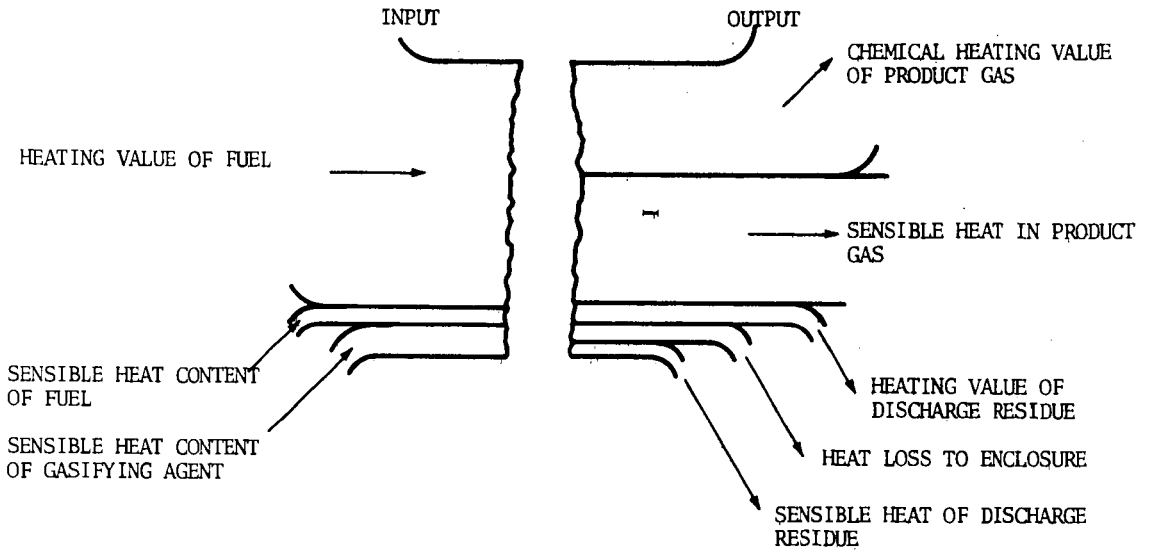


FIGURE 3. GASIFIER HEAT FLOW DIAGRAM

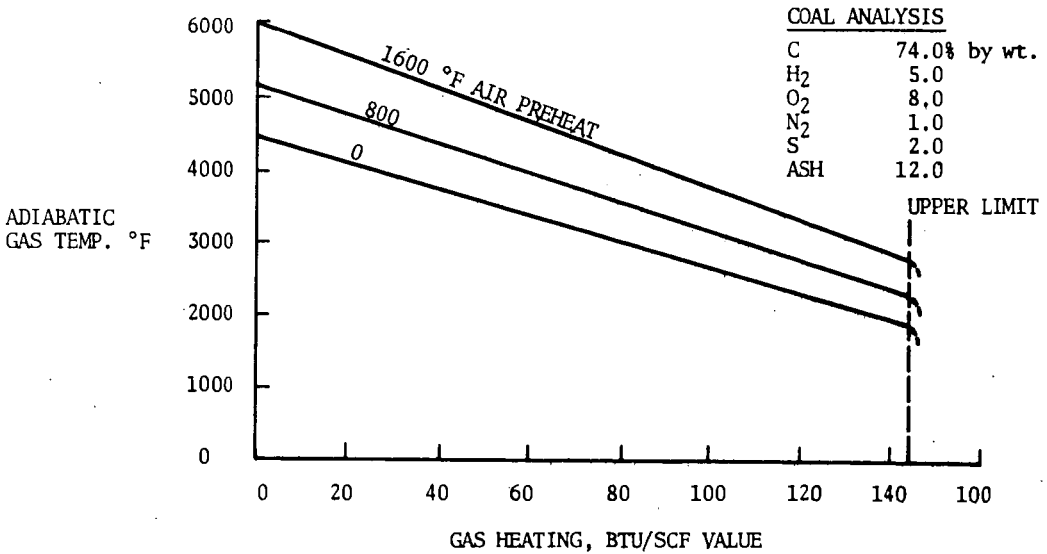


FIGURE 4. GASIFIER ADIABATIC FLAME TEMPERATURE VS. GAS HIGHER HEATING VALUE

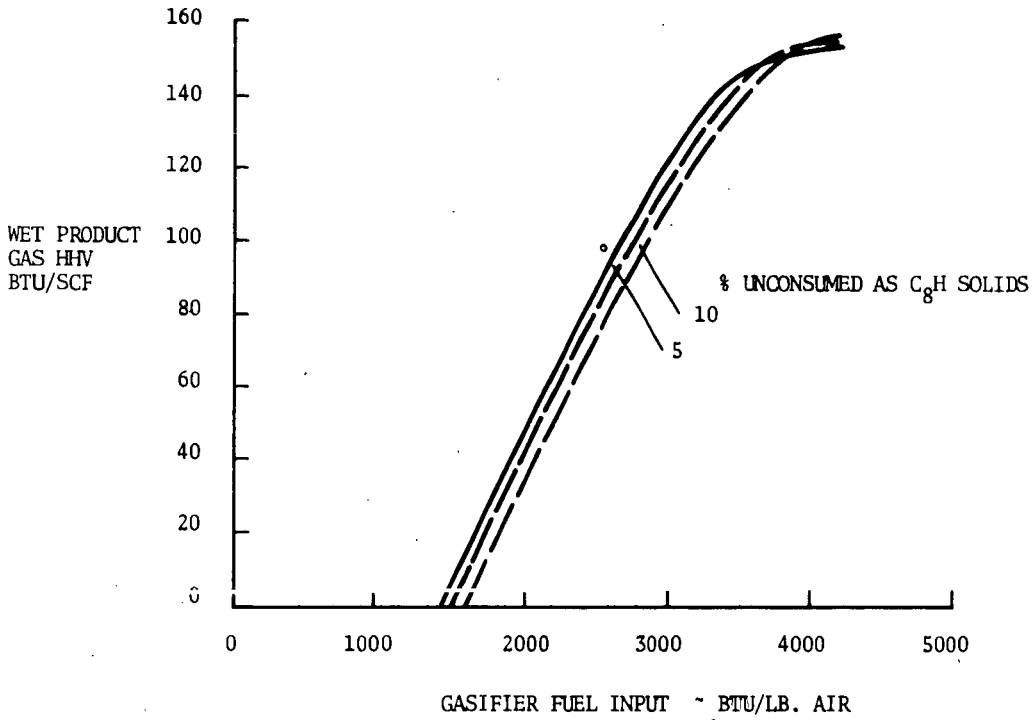


FIGURE 5. PRODUCT GAS HEATING VALUE VS. GASIFIER FUEL INPUT

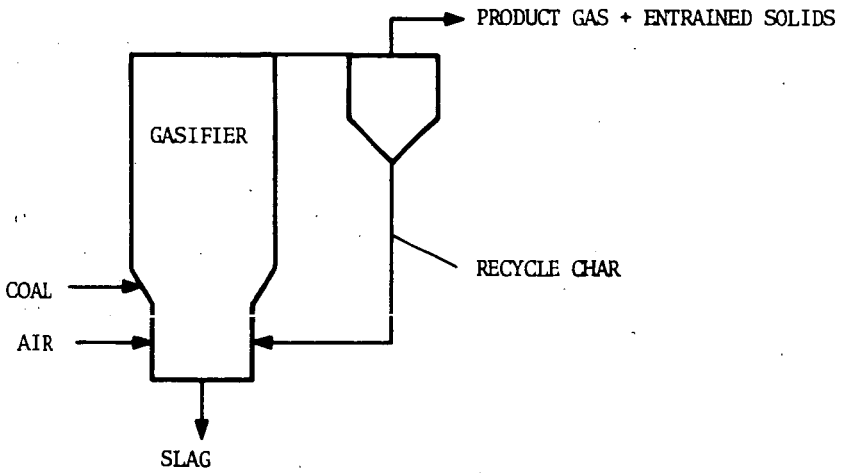


FIGURE 6. AIR-BLOWN SUSPENSION GASIFIER ARRANGEMENT

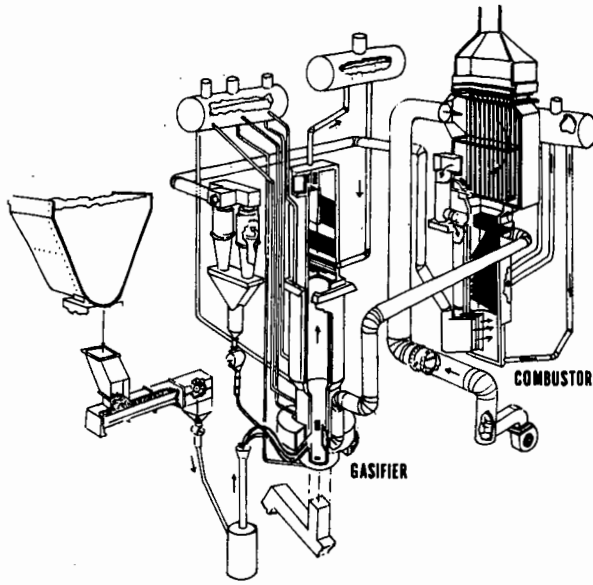


FIGURE 7. ALLIANCE LARGE SCALE GASIFIER

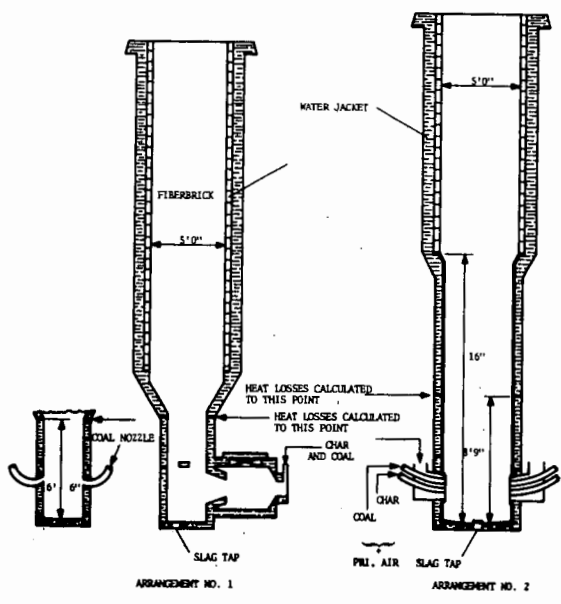


FIGURE 8. GASIFIER ARRANGEMENTS

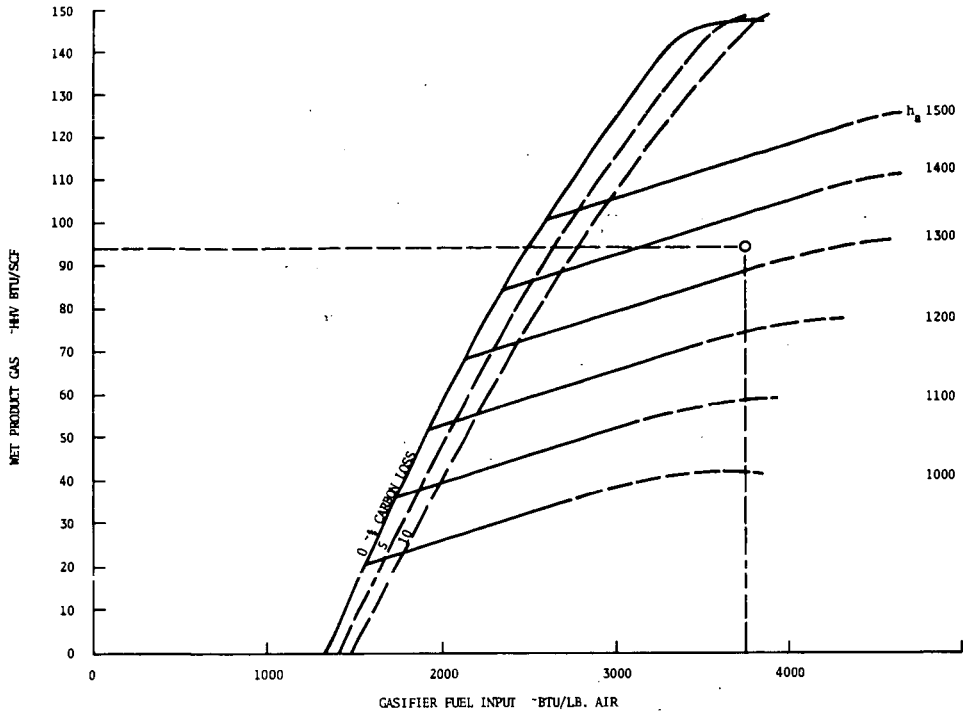


FIGURE 9. PRODUCT GAS HEATING VALUE

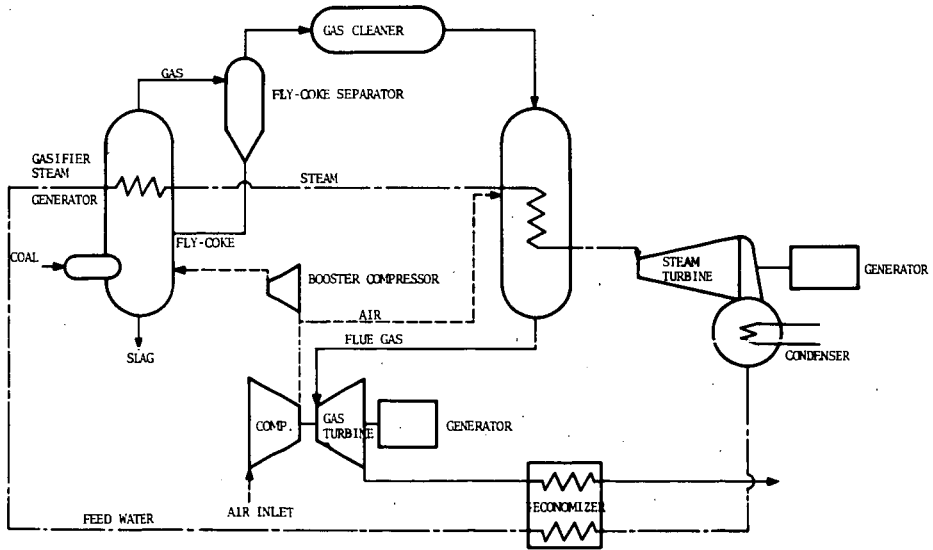


FIGURE 10. COMBINED CYCLE COMPONENT ARRANGEMENT

Microwave Pyrolysis of Coal and Related Hydrocarbons

David M. Bodily, Stanley Chia-lin Che and Wendell H. Wiser

Department of Mining, Metallurgical and Fuels Engineering
University of Utah
Salt Lake City, Utah 84112

INTRODUCTION

The pyrolysis of coal at high temperatures and short reaction times has been investigated by a number of laboratories using a variety of experimental techniques. These techniques include reactions with plasmas¹⁻⁷, flash heating⁷⁻⁹, arc-image furnaces¹⁰, laser irradiation¹¹⁻¹⁴ and microwave discharges¹⁵⁻²⁰. Temperatures of thousands of degrees Kelvin are achieved in a fraction of a second. Gases are evolved and char and tar are produced from the coal. The yields of gaseous products vary with experimental conditions, rank of coal, and reactor design. Major gaseous products from high-temperature pyrolysis are H₂, CO, C₂H₂, CH₄ and HCN. The gaseous products contain higher mole percentages of C₂H₂ and CO and lower percentages of CH₄ than the gaseous products of coal carbonization at 900°C. Temperatures in the reactor vessels are not uniform and differences of thousands of degrees may exist between the center and the walls of the vessel. The composition of the product gas is controlled by kinetics and may vary significantly from thermodynamic equilibrium.

Microwave discharges have been extensively used to study chemical reactions. Blaustein and Fu²¹ have reviewed the reactions of organic molecules in electric discharges. Studies of coal and other carbonaceous materials include direct pyrolysis in a microwave field and reaction with reactive species produced by a discharge. Pyrolysis products include H₂, CO, CO₂, H₂O and hydrocarbons¹⁹. Acetylene is the major hydrocarbon, while CH₄ and C₂H₆ are present in lesser amounts. Quenching of primary reaction products enhances the yield of C₂H₂. Hydrogen and H₂O vapor in the discharge increased the yield of hydrocarbons and of total gas¹⁶.

In this work, coal was subjected to rapid heating in a microwave discharge of argon. Naphthalene, anthracene, methane, ethane and acetylene were also studied.

EXPERIMENTAL

The experimental equipment is shown in Figure 1. The microwave field was generated by Raytheon Model PGM-100 Microwave Power Generator. The frequency of the field was 2450 MHz and the power level was about 200 watts. The microwaves traveled down a wave guide containing a monitor and tuner and were focused by a tapered section. The reaction vessel was constructed of Vycor and quartz. The sample could be suspended in the microwave field or below the field in a discharge generated plasma. The volume of the reaction vessel was 160 ml. Pressures of 20 torr was used for argon discharges.

After irradiation the gases were collected in the trap and analyzed by gas chromatography. A Packard 7401 dual column chromatograph with flame ionization and thermal conductivity detectors was used for analysis. A 1/4 inch by 10 feet column of activated alumina was used for separation of gases. The column temperature was increased at 5°C/min to 250°C. In some cases, chromatographic results were checked by mass spectrometry using a Hewlett-Packard mass spectrometer. The residue from naphthalene pyrolysis was extracted with tetrahydrofuran and analyzed by gas chromatography using 10 foot column of 10% carbowax 20 M supported on chromosorb W.

The coal sample is from the Hiawatha, Utah mine and is a high volatile bituminous coal (47% VM, daf basis). A -60 + 100 mesh sample was used. Mallinckrodt purified naphthalene and Baker grade anthracene were used in these experiments. Matheson ultra purity grade methane and CP grade ethane and acetylene were used. A dry ice-acetone trap was used to remove impurities from the gases.

RESULTS AND DISCUSSION

The gaseous pyrolysis products from coal, naphthalene and anthracene are shown in Table I. The samples were placed in the focus of the microwave field and the bottom of the vessel was immersed in a dry-ice acetone bath. H_2 , CO, and CO_2 were not measured in these experiments. Hydrogen yields have been determined for naphthalene pyrolysis, in which case hydrogen is a major product. Coal and anthracene do not react when the sample is placed outside the microwave field, but within the argon discharge. Naphthalene was found to react in the discharge, but the product yield is different.

The results for coal pyrolysis are in agreement with the observations of other investigators¹⁵⁻²⁰. The yield of C_2H_4 is higher than others have reported.

Naphthalene and anthracene both give high yields of C_2H_2 . Wiley and Veeravagu²² observed over 80 percent yield of C_2H_2 from these compounds in laser pyrolysis. Fu and Blaustein¹⁶ obtained C_2H_2 as the major hydrocarbon product in the reaction of crysene in an argon plasma.

Table I
Gaseous Products From Pyrolysis of Solids

	Coal	Naphthalene	Anthracene
Sample weight, gm	0.196	0.140	0.140
Argon pressure, torr	20	20	20
Reaction time, sec.	15	20	30
Gaseous products			
mole % of hydrocarbons			
CH_4	25.70	6.85	32.75
C_2H_6	1.62	0.40	2.02
C_2H_4	19.91	2.48	8.13
C_2H_2	46.70	83.57	50.28
C_3H_8	0.23	0.06	-
C_3H_6	2.54	0.34	1.14
C_4H_{10}	Trace	0.01	-
C_4H_8	1.60	-	0.32
Butadiene	-	0.12	0.32
Benzene	1.70	5.96	4.58
Toluene	-	0.21	0.46
Liquid Products	-	Naphthalene	Anthracene
		α-methyl naphthalene	α-methyl naphthalene

Sanada and Berkowitz²⁰ attributed the formation of C_2 to C_4 saturated hydrocarbon in the microwave pyrolysis of coal to the non-aromatic structures in the coal. These results indicate that saturated hydrocarbons are produced from totally aromatic molecules.

The yield of hydrocarbon gases from pyrolysis of organic gases is shown in Table II. Methane pyrolysis yielded C_2H_6 , C_2H_4 and C_6H_6 as hydrocarbon products. Acetylene was not detected as a major product from CH_4 or C_2H_6 pyrolysis. Other investigators report^{20,21,23,24} acetylene as a major product and benzene as a minor

product. The presence of benzene was verified by mass spectrometry. Acetylene shows a high yield of aromatic products. Naphthalene also yields little C_2H_2 when reacted with the argon plasma. Acetylene seems to be produced only at the very high temperatures at the focus of the field.

Table II
Products from Pyrolysis of Organic Gases

	CH_4	C_2H_6	C_2H_2
Sample pressure, torr	10	10	10
Argon pressure, torr	20	20	20
Reaction time, sec.	30	30	60
Mole % of hydrocarbons			
CH_4	94.74	0.61	0.18
C_2H_6	2.73	97.63	0.17
C_2H_4	0.14	1.23	0.07
C_2H_2	-	-	96.56
C_3H_8	0.02	0.18	0.08
C_3H_6	-	0.04	0.01
C_4H_{10}	-	0.09	Trace
Benzene	2.33	0.20	0.55
Toluene	-	-	2.38
Unidentified	0.04	0.02	

The yield of products varies significantly with reaction time as shown in figures 2 and 3. Figure 2 is for naphthalene placed at the focus point and figure 3 is for naphthalene placed 5 cm below the focus point.

Griffiths and Standing²⁵ have reviewed the thermodynamics of hydrocarbon gases. Above 900°K the free energy of formation of CH_4 is positive. The free energy of formation of C_2H_2 decreases with temperature and becomes negative at about 4000°K. Acetylene is thermodynamically favored over methane above 1200°K. Although the pyrolysis system is not at thermodynamic equilibrium, thermodynamics influences the formation of H_2 and C_2H_2 at the high temperatures of the discharges.

REFERENCES

1. Bond, R. L., Galbraith, I. F., Ladner, W. R., and McConnell, G. I. T., *Nature*, 200, 1313 (1963).
2. Bond, R. L., Ladner, W. R., and McConnell, G. I. T., *Fuel*, 45, 381 (1966).
3. Bond, R. L., Ladner, W. R., and McConnell, G. I. T., "Coal Science," *Advances in Chemistry Series*, No. 55, American Chemical Society, Washington, D. C., 1966, pp. 650-65.
4. Granger, A. F., and Ladner, W. R., *Fuel*, 49, 17 (1970).
5. Kawa, W., Graves, R. D., and Hiteshue, R. W., U. S. Bureau of Mines, Report Inv. 6829, (1966).
6. Graves, R. D., Kawa, W., and Hiteshue, R. W., *Ind. Eng. Chem., Process Des. Develop.*, 5, 59 (1966).
7. Anderson, L. L., Hill, G. R., McDonald, E. H., and McIntosh, M. J., *Chem. Eng. Progr. Symp. Ser.*, 64, No. 85, 81 (1968).

8. Hawk, C. O., Schlesinger, M. D., and Hiteshue, R. W., U. S. Bureau of Mines, Report Inv. 6264 (1963).
9. Rau, E. and Seglin, L., Fuel, 43, 147 (1964).
10. Rau, E., and Eddinger, R. T., Fuel, 43, 246 (1964).
11. Sharkey, A.G., Jr., Shultz, J. L., and Friedel, R. A., "Coal Science," Advances in Chemistry Series, No. 55, American Chemical Society, Washington, D. C., 1966, pp. 643-49.
12. Karn, F.S., Friedel, R. A., and Sharkey, A. G., Jr., Fuel, 48, 297 (1969).
13. Karn, F.S., Friedel, R. A., and Sharkey, A. G., Jr., Fuel, 51, 113 (1972).
14. Joy, W. K., Ladner, W. R., and Pritchard, E., Fuel, 49, 26 (1970).
15. Fu, Y.C., and Blaustein, B. D., Chem. Ind., 1967, p. 1257.
16. Fu, Y. C., and Blaustein, B. D., Fuel, 47, 463 (1968).
17. Fu, Y. C., and Blaustein, B. D., Ind. Eng. Chem., Process Des. Develop., 8, 257 (1969).
18. Fu, Y. C., Chem. Ind., 1971, p. 876.
19. Fu, Y. C., Blaustein, B. D., and Wender, I., Chem. Eng. Progr. Symp. Ser., 67, No. 112, 47 (1971).
20. Sanada, Y., and Berkowitz, N., Fuel, 48, 375 (1969).
21. Blaustein, B. D., and Fu, Y. C., "Phys. Methods Chem" Weissberger, A., and Rossiter, B. W., Ed., Wiley Interscience, N.Y., 1971, Vol. 1, pt.2b, Chap. XI, pp. 91-208.
22. Wiley, R. H., and Veeravagu, P., J. Phys. Chem., 72, 2417 (1968).
23. Kawahara, Y., J. Phys. Chem., 73, 1648 (1969).
24. Griffiths, P. R., Schühmann, P. J., and Lippincott, E. R., J. Phys. Chem., 73, 2532 (1969).
25. Griffiths, D. M. L., and Standing, H. A., "Coal Science," Advances in Chemistry Series, No. 55, American Chemical Society, Washington, D. C. 1966, pp. 666-76.

This research is sponsored by the Office of Coal Research on contract no. 14-32-0001-1200.

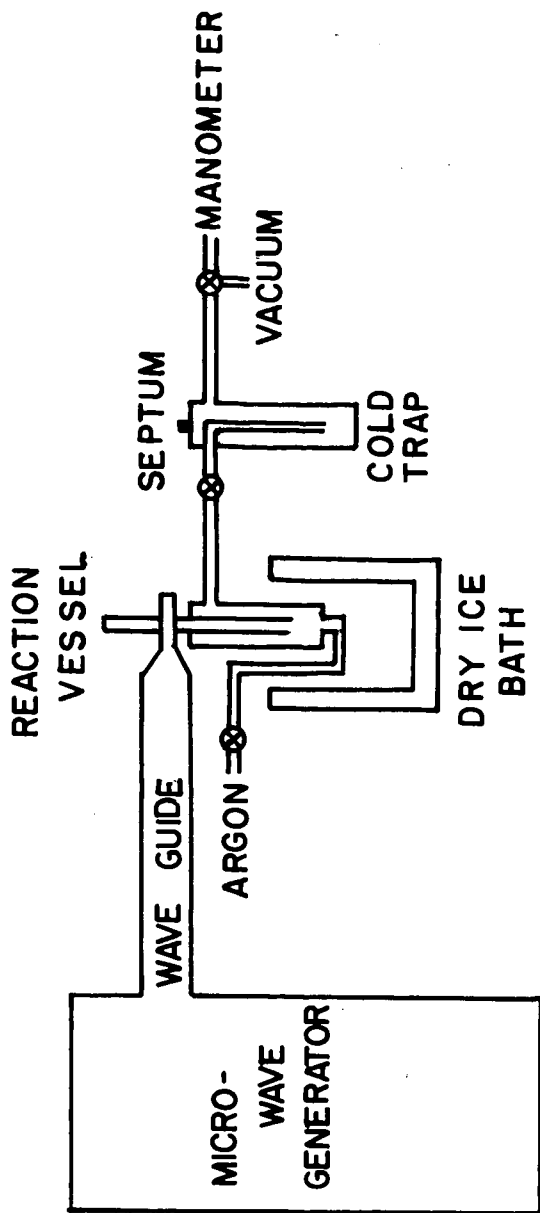


FIGURE 1
MICROWAVE EQUIPMENT

FIGURE 2
HYDROCARBON GASES FROM NAPHTHALENE PYROLYSIS

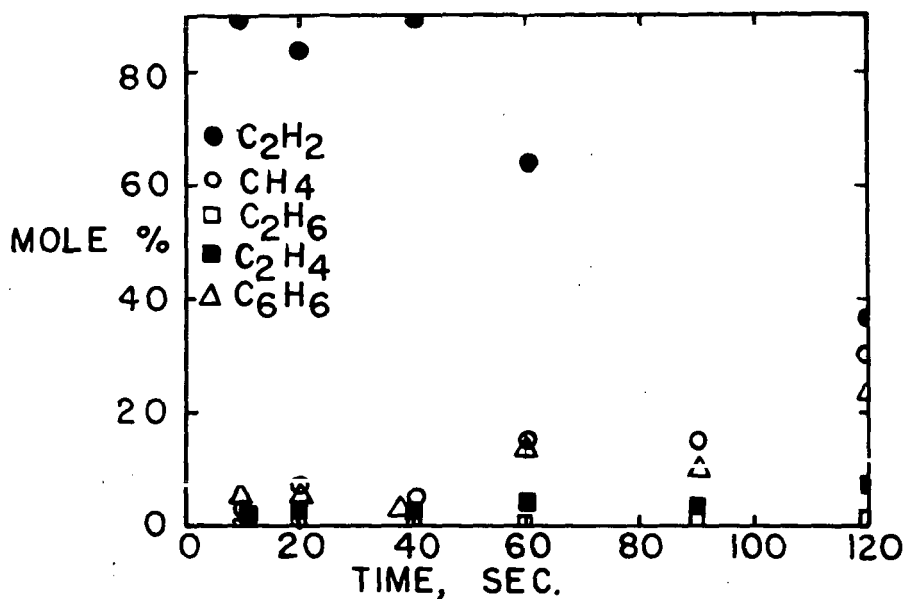
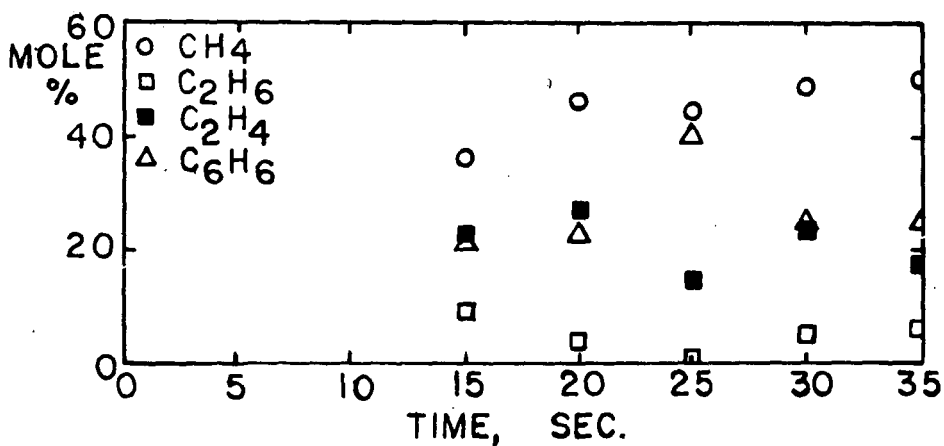


FIGURE 3
HYDROCARBON GASES FROM REACTION
OF NAPHTHALENE IN ARGON PLASMA



Catalytic Activity of Coal Hydrogenation Catalysts

Kanjiro Matsuura, David M. Bodily and Wendell H. Wiser

Mining, Metallurgical and Fuels Engineering
University of Utah
Salt Lake City, Utah 84112

INTRODUCTION

Catalytic hydrogenation of coal has been the subject of extensive investigation for many years. Mills has reviewed recent developments in catalyst systems. Molten halide salts have been shown to be effective catalysts for hydrocracking coal and coal extracts². Zinc chloride and stannous chloride have been found to be effective catalysts for the hydrogenation of coal in a short-residence-time reactor³. This study is part of an investigation of the catalytic processes in coal hydrogenation. A previous paper was concerned with the thermal behavior of coal-catalyst systems⁴. The acidity of hydrogenation catalysts and their catalytic activity for simple reactions are discussed.

EXPERIMENTAL

The acid strength of the catalysts was determined with amine bases. A 0.2 g sample was placed in a test tube with 4.0 ml of a solution containing 0.1 mg of indicator in benzene. The mixture was agitated briefly and color changes were noted. The benzene was distilled over metallic sodium to remove water and the solid catalysts were heated to 150°C for 5 to 6 hours prior to the experiments. Experiments were performed at room temperature.

Surface acidities were determined by back titration of n-butyl amine with hydrochloric acid⁵. About 5 g of sample was added to 25 ml of 0.0963 M solution of n-butylamine in benzene. The suspension was stirred vigorously for 3 hours and filtered to remove the solid catalyst. The amine solution was titrated with aqueous hydrochloric acid using phenolphthalein indicator. The acidity of the sample was calculated from the decrease in the n-butylamine concentration. All samples except $\text{SmCl}_2 \cdot 2\text{H}_2\text{O}$ and $\text{FeCl}_3 \cdot 6\text{H}_2\text{O}$ were heated at 150°C for 6 hours prior to the experiment.

The polymerization of propylene was studied in a 90 ml reaction vessel. About 1.5 - 2.0 g of catalyst was evacuated to 10^{-6} torr in the vessel and heated to 200°C for 3 hours. Propylene was introduced at 400 torr and the temperature was held at 150°C. Changes in pressure were noted. The propylene was purified by alternate condensation and vaporization, with evacuation following condensation.

The isomerization of n-butenes was studied in the system shown in Figure 1. A large vessel was used to eliminate diffusion effects. About 1.5 g of catalyst was evacuated at 150°C for 3 hours. A sample of n-butene or trans-2-butene was introduced to the vessel at a pressure of 300 torr. The reaction was carried out at 100-150°C with periodic sampling of the gas. Gas samples were analyzed by chromatography at room temperature using a 15 ft. column of propylene carbonate on activated alumina and a thermal conductivity detector.

The hydrogenation of ethylene was studied in the apparatus shown in Figure 1. The catalyst was introduced into the vessel and evacuated and heated. A known mixture of hydrogen and ethylene was introduced and the reaction was followed at 130-140°C by periodic sampling and analysis by gas chromatography in the system previously described. A typical composition would be an initial hydrogen pressure of 40 torr and an ethylene pressure of 19 torr.

Reagent grade chemicals were used as catalysis. In some cases, the catalysts were impregnated on Hiawatha, Utah coal (4% V.M., daf basis) from aqueous solution.

RESULTS AND DISCUSSION

The acid strength of various halide catalysts are shown in Table I along with a silica-alumina catalysts (Houdry, 13% Al₂O₃). Zinc chloride shows a slightly higher acid strength with a maximum pKa of 1.5. The other halide catalysts show a maximum pKa of 3.3. The acid strength of the halide catalysts is much less than that of the silica-alumina catalyst. The surface acidities are shown in Table II. The acidities of the halide catalysts are greater than the silica-alumina catalyst. Impregnation of the catalyst on coal decreases the acidity significantly.

Table I
Acid Strength of Catalysts

	Phenylazo Naphthylamine	Dimethyl Yellow	Benzeneazo Diphenylamine	Dicinnamal Acetone	Anthraqui- none
pKa	4.0	3.3	1.5	-3.0	-8.2
Wt. % H ₂ SO ₄ of corresponding acid strength	5X10 ⁻⁵	3X10 ⁻⁴	0.02	48	90
Color Change					
ZnCl ₂	Yes	Yes	Yes	No	No
ZnBr ₂	Yes	Yes	No	No	No
ZnI ₂	Yes	Yes	No	No	No
SnCl ₂ ·2H ₂ O	Yes	Yes	No	No	No
FeCl ₃ ·6H ₂ O	Yes	Yes	No	No	No
SiO ₂ ·Al ₂ O ₃	Yes	Yes	Yes	Yes	Yes

Table II
Surface Acidity of Catalysts
Decrease in n-butylamine
concentration, M moles/l

Catalyst	Decrease in n-butylamine concentration, M moles/l	Acidity, M moles/g
ZnCl ₂	0.0907	4.54
ZnBr ₂	0.0739	3.98
ZnI ₂	0.0590	2.90
SnCl ₂ ·2H ₂ O	0.0844	4.16
FeCl ₃ ·6H ₂ O	0.0847	4.26
SiO ₂ ·Al ₂ O ₃	0.0216	1.02
ZnCl ₂ /coal (12.3%)	0.0545	1.36
ZnI ₂ /coal (12.4%)	0.0398	1.00
SnCl ₂ /coal (12.2%)	0.0313	0.76

The catalytic activity of ZnCl₂, ZnBr₂, and ZnI₂ was determined for the polymerization of propylene. This reaction is catalyzed by Bronsted acids⁶. The catalysts show no activity for this reaction. It is concluded that the halides whose Bronsted acidity is very weak, if present at all, are not responsible for carbonium ion reactions. Bronsted and Lewis acids may catalyze the isomerization of butenes. Zinc chloride and bromide show very little activity for the isomerization of 1-butene or trans-2-butene under the conditions of these experiments. The activity was much less than that of other solid acids such as silica-alumina and BF₃ treated alumina⁷. Zinc chloride and bromide also show no activity for the hydrogenation of ethylene although other solid acids show considerable activity at lower temperatures than those employed in these studies⁸⁻¹⁰.

The metal halide catalysts used in these studies, with the exception of $\text{FeCl}_3 \cdot 6\text{H}_2\text{O}$, show strong catalytic activity for the hydrogenation of coal at short reaction times^{3c}. They all show high acidity, but much lower acid strength than silica-alumina cracking catalysts. They show little activity for the acid-catalyzed reactions of this study. Temperature would be expected to be an important factor. In these experiments, the catalysts were in the solid form. In coal hydrogenation reactions, the temperature is about 500°C and the catalysts are molten.

REFERENCES

1. Mills, G. A., *Ind. Eng. Chem.*, 61, No. 7, 6 (1969).
2. Zielke, C. W., Struck, R. T., Evans, J.M., Constanza, C.P., and Gorin, E., *Ind. Eng. Chem., Process Des. Develop.*, 5, 151, 158 (1966).
3. Wood, R. E., and Hill, G. R., *Preprints Division Fuel Chem., Am. Chem. Soc.*, 17, No. 1, 28 (1972).
4. Bodily, D. M., Lee, H., and Hill, G. R., *Preprints Division Fuel Chem., Am. Chem. Soc.*, 16, No. 2, 124 (1972).
5. Shibata, K., Kiyoura, T., and Tanabe, K., *J. Res. Inst. Catalysis, Hokkaido Univ.*, 18, 189 (1970).
6. Mitsutani, A., "Catalytic Engineering," Vol. 10, Catalysis Society of Japan, Ed., Chijinshokan and Co., Tokyo, 1967, p. 108.
7. Matsuura, K., Suzuki, A., and Itoh, M., *J. Catal.*, 23, 395 (1971).
8. Dent, A. L., and Kokes, R. J., *J. Phys. Chem.*, 73, 3772, 3781 (1969).
9. Tanaka, K., and Blyholder, G., *J. Phys. Chem.*, 1393 (1972).
10. Harrison, D. L., Nichollas, D., and Steiner, H., *J. Catal.*, 7, 359 (1967).

This research is sponsored by the Office of Coal Research on Contract No. 14-32-0001-1200.

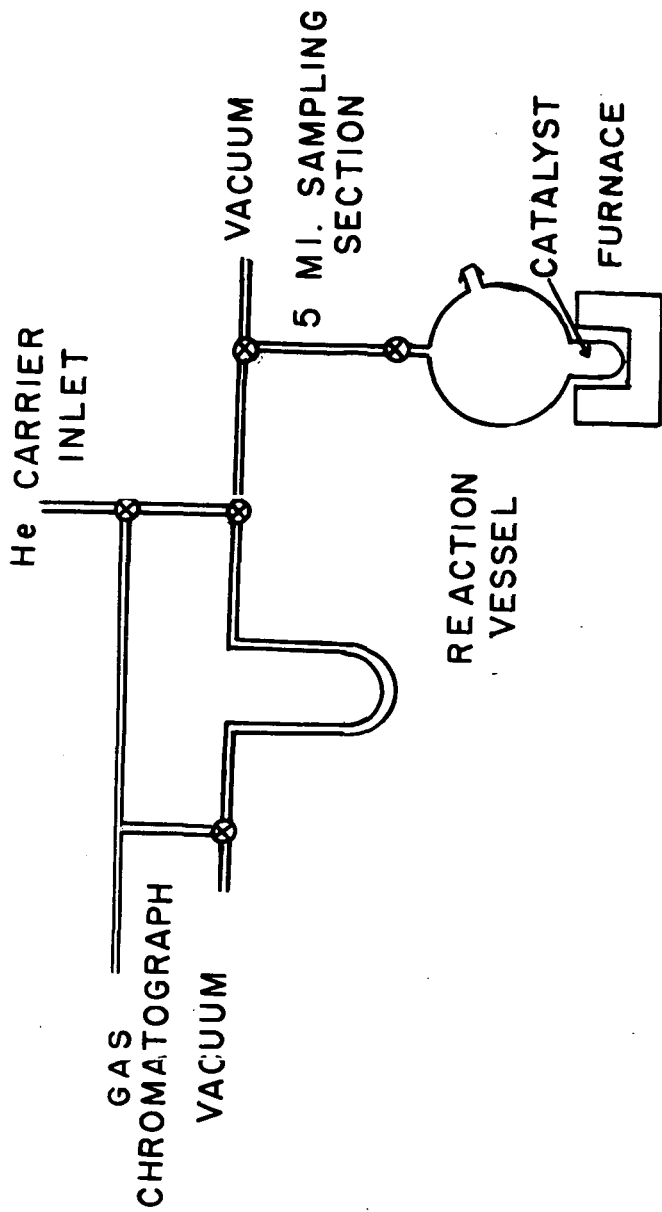


FIGURE 1
REACTION SYSTEM

EVALUATION OF ANALYTICAL TECHNIQUES FOR THE DETERMINATION OF TRACE ELEMENTS IN COAL, FLY ASH, FUEL OIL, AND GASOLINE - Darryl J. von Lehmden, Robert H. Jungers, and Robert E. Lee, Jr., Environmental Protection Agency, National Environmental Research Center, Research Triangle Park, North Carolina 27711.

The Environmental Protection Agency has initiated a program of routine monitoring of fuels and related emissions for elements in trace quantities (at the ppb level). Analytical method comparisons are underway for twenty-six elements to determine optimal analytical schemes for selected fuel and emission matrices. Included in the elements under investigation are mercury, beryllium, lead, cadmium, arsenic, vanadium, manganese, chromium, and fluorine. Methods compared include neutron activation analysis, atomic absorption, spark source mass spectrometry, optical emission spectrometry, anodic stripping voltammetry, and x-ray fluorescence. The results of the evaluation program are evaluated with respect to accuracy and precision. The results from an interlaboratory comparison for trace elements in coal, fly ash, residual fuel oil, and gasoline are used for the evaluation of the various methods employed. The interlaboratory comparison for the twenty-six trace elements showed that for at least seven trace elements in each of the four matrices the reported concentration ranges were greater than one order of magnitude. The large range in reported results points out the need for standard reference materials certified in trace elements which are essential for method evaluation and quality control. A program to provide standard reference materials for trace elements in coal, fly ash, residual fuel oil, and gasoline will be described.

WASTE COAL RECLAMATION

by

Joseph W. Leonard
and
William F. Lawrence

One of the major problems facing the electric power generating industry is the ever increasing demand for energy coupled with a real and vociferous public demand for reduced pollution levels. A partial solution to this dilemma could lie in the redemption of waste coal piles (gob or culm banks) which would result in the production of needed energy while reducing the ecologic and aesthetic problem these banks currently represent. Although this study was based upon banks present in the Monongahela River Drainage Basin in Southwestern Pennsylvania, Northern West Virginia and parts of Maryland, the conclusions to be drawn will be applicable with minor modifications to other coal mining areas of the U. S.

A waste coal pile or culm bank is heterogeneous rather than homogeneous in composition and variation will occur, both horizontally and vertically. Culm bank materials in the Monongahela Basin will generally consist of coal, shale, bone coal, sulfates, carbonates and pyrite (FeS_2) or marcasite (FeS_x). In addition, slag materials may be present if combustion of portions of the bank has occurred. The relative amounts of each constituent will be dependent upon such factors as the market for which the coal was cleaned and the methods of cleaning, the efficiency of the cleaning process, the mining methods and systems employed and such natural factors as the quality of the coal seam. In order to illustrate the effects of the many variables upon the composition of the materials being placed on a culm bank, a hypothetical history of an imaginary culm bank is included. While no such bank may actually have been formed, many of its features can be seen in existing banks. Figure 1 has been prepared to show the major markets for bituminous coal from 1917 to 1956. The history of a mine in its cleaning facility and its resultant culm bank could therefore be as follows:

1917--A coal mine is opened and a picking and screening facility is constructed to help supply an existing market for metallurgical and railroad locomotive fuel and for fuel for industrial and commercial heating plants as well as for household furnaces. Mining is not yet mechanized to any extent, and waste material from the picking and screening facility contains mainly hand picked pieces of rock and coaly material along with the undersize material for which no steady market exists. This fine material is predominately coal and is mixed with the waste rejects and discarded. Due to the method of dumping, the softer, more friable materials tend to be concentrated in the interior of the pile while the harder, higher ash, hand sorted materials accumulate along the edges.

1920--Coal production and coal sales are dropping. In order to retain markets, greater selectivity in mining is employed and the preparation facility is enlarged and improved to produce a higher quality coal. Additional pickers are hired and more rigorous sorting and sizing are initiated. The ash and the sulfur content of the coal being marketed are successfully reduced, and more fine coal is being deposited on the pile.

1923--A new market for intermediate quality coal develops with the construction of an electric power generating station nearby. In addition, gas and oil are beginning to replace lump coal as the common fuel for commercial boilers and household furnaces. A buyers market still exists and the waste material being placed on the pile continues to be high in fine coal content. Due to the need to remain competitive, some machinery is introduced into the mine with the result that less preliminary cleaning and selection occurs during mining. Consequently, more rock, fines, and other dilutant materials are handled at the preparation facility and more material having high ash and sulfur content is discarded to the pile.

1925--The demand for high quality metallurgical and intermediate quality power plant fuel continues to increase. Concentrating units are added to the screening and picking facility. The waste materials reaching the bank now contain less fuel values and are relatively higher in rock and ash constituents than during any previous period.

1929--A major decline in the national economy begins and will continue for several years. In order to sell coal in a declining market, rigorous preparation is practiced, thereby maintaining competitiveness in a seriously oversupplied market. Although growth of the culm bank is limited, a relatively large amount of coal fines improve the fuel value.

1933--The marketing situation for coal is unstable, but the trend appears to be upwards. Additional mechanization takes place in the mine with the result that fluctuating tonnages of high ash and high fuel value material are intermittently being placed on the culm bank.

1940--World War II is approaching, and increasing industrilization is creating a demand for all forms of energy. A seller's market exists and before it peaks in 1943, many existing culm banks will be spot loaded to recover pockets containing high fuel value materials. Material entering the culm bank is high in ash and moderate in sulfur and because of spontaneous combustion and the mining of the richer pockets the bank is becoming increasingly deficient in fuel value.

1945--The advent of the diesel engine signals the beginning of the end of the railroad locomotive market. Also, other domestic markets are declining. Power stations and metallurgical coking ovens are the only growth markets for coal. More advanced cleaning and mining methods continue to be installed at the facility and a high ash, high sulfur and moderate fuel value material is placed on the culm bank.

1950--The power station is modernized and pulverized fuel boilers are installed; moreover, increasing tonnages of clean, high quality metallurgical coal are produced and marketed. More mechanical equipment is introduced into the mine. At the plant, crushers are installed and the cleaning process is made more efficient. As a result of the demands for a high quality metallurgical product and the willingness of the power station to accept a lower cost middling quality fuel, the waste material being place on the bank is very lean in fuel values and has a high ash and sulfur content.

1969--Increasing safety legislation causes more water to be used in the mine and more diluent material to be removed. The ash or mineral content of the coal entering the cleaning plant continues to increase. Much more material enters the culm bank of high ash content and low to to moderate fuel value. Older sections of the bank are being mined to recover previously discarded fuel values as a result of a seller's market.

1972--A major change occurs as a result of air pollution control legislation. Coal is now being sold to utilities on the basis of sulfur content rather than on the traditional BTU value. In order to meet the new requirements, new and more costly methods of concentration are employed and large tonnages of medium ash, high sulfur and high fuel value material are being placed on the bank. In addition, more of the older portions of the pile are being mined for the moderate ash, moderate sulfur fuel values placed there previously.

While this history is of necessity brief and overly simplified and such a culm bank is purely hypothetical, it can serve to illustrate some of the complex inter-acting factors which determine the composition of the material present at any specific location within the pile. It can also serve to illustrate the extreme care which must be taken to obtain representative samples for the pile. The decision to reclaim fuel values from a particular bank should be based on a combination of sample data and a knowledge of the bank's history.

Older piles, formed using simple dumping methods, will often have a profile similar to that shown in figure 2. Such a pile will have general distributional zones which will reflect the different coal associated strata which were being mined. Assuming that the coal materials are relatively softer than the associated rock material, the coal would degrade more rapidly and the resulting finer particles would tend to migrate towards the center of the pile (zone A). This coal material will generally be relatively low in moisture and ash and high in Btu value. The material at the outer edge of the pile will generally be larger in size and will be more prone to combustion resulting in burnt out pockets of slag material.

More recent piles, in which the waste was laid down in layers and then compacted will tend to have horizontal pockets of relatively rich coal material alternating with layers of high ash, high rock content.

Affects Upon Power Plant Operations

It has long been known that materials with very low heating values can be burned. Coal refuse crushed to one-quarter inch size and with as little as 3,000 to 3,500 Btu heating value has been burned in the Office of Coal Research pilot scale fluid-bed column designed and operated by Pope, Evans and Robbins.¹ Coal waste with as little as 5,000 Btu heating value can be burned in specially designed, conventional boilers provided that the wastes are friable enough to permit economical grinding to a fine size.² Boilers designed to burn coal waste must be equipped with oversize ash handling capability since approximately one-half or more of the coal wastes fed to the boiler would remain as ash and would therefore have to be continuously removed.

The direct burning of lean gob piles to produce power is well established from experience in France where anthracite waste banks have been used up as a source of fuel during the past twenty-five years.³ Combustion was achieved using the Ignafuid boiler which burns coal refuse crushed to approximately 1/4 inch. Refuse with a dry ash content as high as 40 percent and heat content as low as 7,500 Btu's was found to provide a satisfactory fuel. Moreover, it is preferable that refuse fed to an Ignafuid installation should contain between 15 to 20 percent volatile matter, less than 5 percent sulfur and have ash with a fusion temperature ranging from 2,000 to 2,600°F.

¹Private communication with John Bishop, Pope, Evans and Robbins, Alexandria, Virginia.

²Private communication with Combustion Engineering Company, Windsor, Connecticut.

³Private communication with Paul A. Mulcey, Consulting Engineer, Dallas, Pa.

Most present coal burning power plants operate with coal having fuel values ranging between 10,000 and 12,000 Btu per pound and with ash contents ranging up to approximately 30 percent. The refuse from most banks can be mixed directly with coal provided that the heating value and ash content of the mixed product meets the Btu design level of the boiler for which the fuel is intended.

Economic Utilization Potential

The attached table is included to provide preliminary information about the size and composition of some randomly selected refuse banks in the Monongahela River Drainage Basin.

Test increments for banks of various sizes are reported in the table under composition on an as received basis. Composition includes volatile matter, fixed carbon, ash, sulfur and Btu values. Because an extensive and long term sampling program would be required to establish the composition of all banks in the area, no conclusions are offered concerning the quality of the total deposit. Nevertheless, it is interesting to note that 8 of the 20 increments contain a volatile matter content of greater than 19 percent while 14 of the 20 increments contain heating values greater than 3,500 Btu with the result that nearly 75 percent of the bank increments meet at least one of these generally favorable characteristics. Had these increments been beneficiated, there is little doubt that considerably more than 75 percent would yield a product with 3,500 Btu and/or 19 percent volatile matter on an as received basis.

While the preceding estimates provide a measure of the relative number of bank increments that might be utilized in new or specially designed boilers, it is equally important to note the relative number of bank increments that might qualify for utilization as a fuel for the already commercially available Ignaf fluid process. Hence, 3 out of 20 bank increments would appear to readily qualify as an Ignaf fluid fuel and, with some beneficiation, as many as 14 out of 20 bank increments might be beneficiated to meet specifications.

Finally, it would appear that the same raw and/or beneficiated 14 out of 20 bank increments could be used in blends with higher grade coal for utilization in existing power stations.

The preceding information strongly infers that a high percentage of coal refuse banks in the Monongahela drainage basin could be burned in new, modified or existing combustion processes to produce useful power with the simultaneous benefit of converting unsightly piles of refuse to greatly reduced quantities of more readily utilized ash.

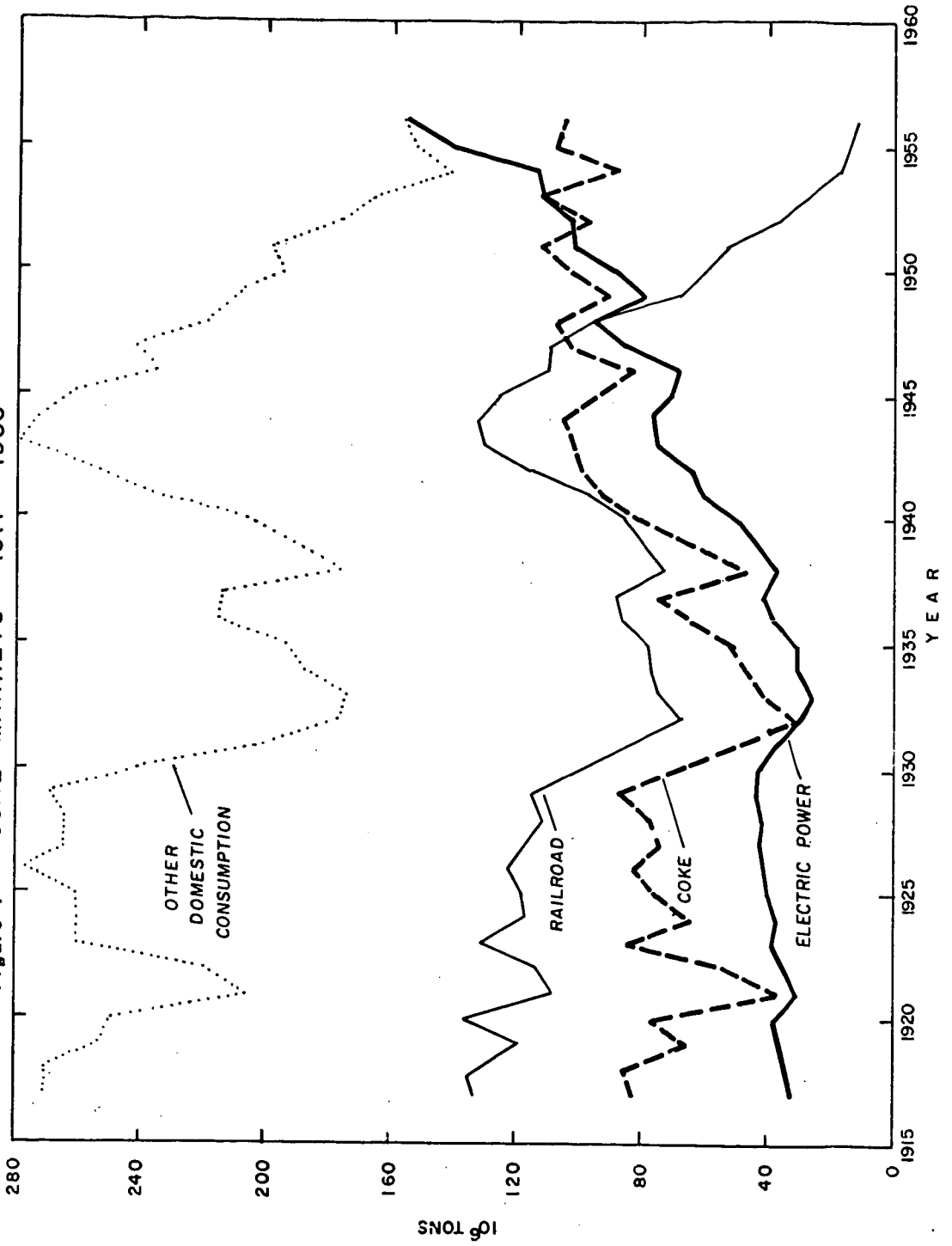
TABLE I

ESTIMATED SIZE AND COMPOSITION OF SOME RANDOMLY
SELECTED COAL WASTE BANKS LOCATED IN THE
MONONGAHELA RIVER DRAINAGE BASIN

Cubic Yards	Size	Acres	As Received Basis			Composition*		Sulfur %	Ash %	Btu
			Moisture	Volatiles Matter %	Fixed Carbon %	Carbon %				
45,733,000		315	9.19	10.17	7.10	73.54	.31	1,589		
8,219,000		102	16.29	16.20	19.21	48.30	2.02	3,943		
7,644,000		39	7.61	12.80	9.50	70.09	.74	2,502		
6,000,000		101	16.14	22.01	33.22	28.63	2.24	7,933		
4,000,000		115	14.38	17.14	16.94	51.54	0.93	4,202		
3,554,000		44	2.41	13.24	8.01	76.34	.69	2,225		
3,000,000		32	19.50	16.16	7.18	57.16	2.23	2,315		
2,800,000		44	8.28	15.97	21.15	54.60	.56	4,321		
2,749,000		42	10.35	14.23	25.46	49.96	.81	4,802		
2,000,000		29	9.08	26.38	41.08	23.46	1.14	9,611		
1,400,000		23	9.60	25.34	23.51	41.55	7.17	6,475		
1,299,000		27	23.62	16.38	9.50	50.50	2.59	2,467		
871,000		6	11.29	14.89	21.18	52.64	0.83	4,547		
700,000		5	9.30	19.41	23.64	47.65	0.78	5,828		
600,000		21	13.80	19.30	24.31	42.59	1.34	5,756		
200,000		5	9.18	15.98	30.21	44.63	.61	6,294		
200,000		4	25.24	19.9	10.33	44.45	2.59	2,689		
176,000		11	12.58	24.66	38.18	24.58	1.09	8,796		
80,000		6	14.98	20.96	26.52	37.54	0.88	6,364		
-		-	12.79	17.80	20.85	48.56	1.51	4,756		

*Composition is based on analyses of some randomly selected increments of weight of refuse obtained from each bank, and should not necessarily be construed to be representative of the entire bank.

Figure 1 - COAL MARKETS 1917 - 1956



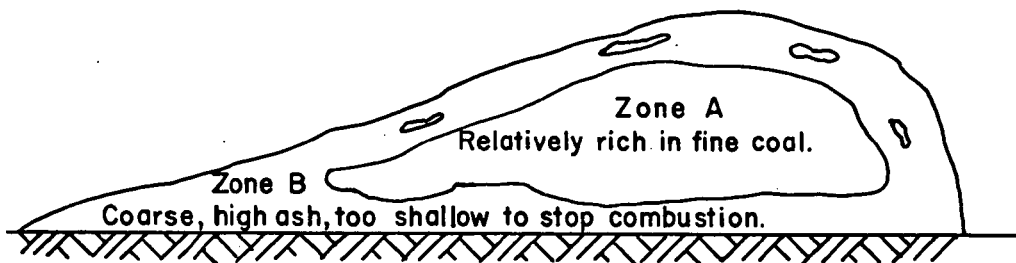


**Figure 2 - PROFILE OF TYPICAL APPALACHIAN GOB PILE
FORMED BY DUMPING RATHER THAN SPREADING
AND COMPACTION.**